BIOCHEMICAL MECHANISM OF APOPTOTIC EXECTUION

KUMIKO SAMEJIMA

A THESIS PRESENTED FOR THE DEGREE OF

DOCTOR OF PHILOSOPHY

UNIVERSITY OF EDINBURGH

October 2000

ACKNOWLEDGMENTS

I really appreciate my supervisor, Bill Earnshaw for giving me the opportunity to work in his laboratory, for great suggestions, a lot of time, and heart-warming support when I needed it. I would also like to acknowledge our wonderful collaborator Dr. Scott Kaufmann at the Mayo Clinic, Rochester MN.

I would like to say thank you to all members of the lab, present and past, who taught me from scratch and the effort for understanding my Japanese-English. I will not forget you all, Richard Adams, Alexandra Ainsztein, Mar Carmera, Carol Cooke, Jeff Craig, Helen Dodson, Francoise Durrieu, Sander Henzing, Damien Hudson, Nadia Korfali, Luis M. Martins, Ciaran Morrison, Anca Petruti-Mot, Sandrine Ruchaud, Tone Shigenobu, Atushi Takahashi, Paola Vagnarelli, Pascal Villa, Peter Warburton, Sally Wheatley, and Chuck Yang. In particular, Stefanie-Kandals Lewis for her advice both in the lab and in baby-care. I am happy with my outcome during my Ph D. I am also sure that we can be proud of our productivity (nine babies from one lab in three years!).

Thank you to the members of the Heck lab and Lewis lab for their support and all the people from ICMB who helped me in the past four years.

I am very grateful for my husband, Itaru, about his suggestion to apply to Bill's lab and his continuous support. I love my baby, Mami. Finally I thank my parents for their love and support over the years.

ABSTRACT

Apoptosis is a major form of physiological cell death characterized by morphological and biochemical changes including nuclear and cytoplasmic condensation, followed by cellular disassembly into membrane-enclosed vesicles, and internucleosomal DNA cleavage. These changes are accompanied by the activation of caspases and DNases.

Cytoplasmic extracts from chicken DU249 cells at various stages along the apoptotic pathway were prepared to analyze changes in nuclear morphology during apoptotic execution. When isolated interphase nuclei were exposed to S/M extracts prepared from morphologically normal cells in the "committed stage " stage of the apoptotic pathway, they became condensed and the DNA was cleaved. These changes were dependent on caspase activity. In contrast, when the same nuclei were exposed to E/X extracts, prepared from morphologically apoptotic cells, they underwent apoptotic changes in a caspase-independent manner. These results suggest that nuclear disassembly is driven largely by factors activated downstream of the caspases at the onset of apoptotic execution. One such factor, the caspase-activated DNase, CAD/CPAN/DFF40, can induce apoptotic chromatin condensation in isolated HeLa cell nuclei in the absence of other cytosolic factors. However, as morphological changes occur even when CAD activity is inhibited, CAD cannot be the sole factor triggered by caspases. Indeed, in this study it was found that DNA topoisomerase IIα

(topo IIα), which is essential both for chromosome condensation and segregation in mitosis, also functions during apoptotic execution. Simultaneous inhibition of topo IIα plus either caspases or CAD completely abolished apoptotic chromatin condensation. Furthermore it was demonstrated that CAD functionally interacts with topo IIα.

The localization of CAD and its inhibitor ICAD in nonapoptotic cells has remained controversial. ICAD exists in two forms, ICAD-L and ICAD-S, which are transcribed from a single gene by alternative splicing. They differ at the C-terminus: 70 amino acids of ICAD-L are replaced by four different amino acids [VGKN] in ICAD-S. CAD is associated with ICAD-L in healthy cells and it has been proposed that a major function of ICAD-L is to sequester CAD in the cytoplasm. In this study it was found that a GFP:ICAD-L fusion protein localized to cell nuclei, while GFP:ICAD-S was distributed throughout the cell. These data are in agreement with the presence of a NLS in the COOH-terminal 20 amino acids of ICAD-L, a region absent from ICAD-S. In addition, GFP:CAD was found mostly in the nucleus. These localization patterns were confirmed by cell fractionation and western blotting for the endogenous protein. Thus these data demonstrate that the CAD/ICAD-L complex should be nuclear in intact cells.

This study presented the first evidence that activities such as CAD and topo II that function downstream of caspases in apoptosis are largely responsible for nuclear disassembly. Furthermore, it is demonstrated that

CAD and topo II which are located in the nucleus in healthy cells, have interactions but work in parallel during chromatin condensation.

CONTENTS

Chapter 4

4. DNA topoisomerase IIα interacts with CAD and is involved in chromatin condensation during apoptotic execution

LIST OF FIGURES

LIST OF TABLES

ABBREVIATIONS

aa	amino acids
AIF	apoptosis-inducing factor
ALPS	autoimmune lymphoproliferative syndrome
aomk	Z-Glu-Lys-Asp-(α-((arylacl)oxy)methyl ketone)
APC	adenomatous polyposis coli
ATP	adenosine 5'-triphosphate
BH	Bcl-2 homology domain
bp	base pair
BSA	bovine serum albumin
c-Flip	cellular Flip
C/D extract	nonapoptotic extract from cells in condemned phase
CAD	caspase-activated DNase
CARD	caspase recruitment domain
caspase	cysteine-dependent aspartate-direcrted protease
Cb1/Cb1-b	cellular homologues of the murine Cas NS-1retrovirus oncogene
cDNA	complementary DNA
CED	cell death abnormal
CIDE	cell death inducing DFF45 like effector
cmk	chloromethyl ketone
CPAN	caspase-activate nuclease
DAPI	4'6'-diamidino-2-phenylindole
dATP	2'-deoxyadenosine triphosphate
DD	death domain
DED	death effector domain
DFF	DNA fragmentation factor
DISC	death-inducing signaling complex
DMSO	dimethylsulfoxide
DNA	deoxyribonucleic acid
DTT	dithiothritol
E/X extract	apoptotic extract from execution phase cells
ECL	enhanced chemiluminescence
EDTA	ethylene diaminetetraacetate
EGTA	(ethylenbis(oxyethlenetrintrilo))tetraacetic acid
ERK	extracellular signal-related kinase
FADD	Fas-associated death domain
FAK	focal adhesion kinase
FLIP	FLICE(caspase-8)-inhibitory protein
fmk	fluoromethyl ketone
GFP	*A. victoria* green fluorescent protein
GST	glutathione-S-transferase
HA	hemagglutinin tag
HEPES	4-(2-hydroxyethyl)-1-piperazine-ethanesulfonic acid
His tag	hexa-histidine tag
HMG	high mobility group

hr	hour(s)
Hrk	harakiri
HRP	horseradish peroxidase
IAP	inhibitor of apoptosis protein
ICAD	inhibitor of CAD
IκB	inhibitor of NFκB
IKK	kinase that regulates IκB
IPTG	isopropyl β-D thiogalactopyranoside
JNK	Jun N-terminal kinase
JNKK	Jun N-terminal kinase kinase
kD	kilo Dalton
M-phase	mitosis
MEK	MAPK/ERK kinase
min	minute(s)
mRNA	messenger ribonucleic acid
MW	molecular weight
$N_2(l)$	liquid nitrogen
NF-κB	nuclear factor kappaB
NLS	nuclear localization signal
NMR	nuclear magnetic resonance
OD_{600}	optical density at 600 nm
PAGE	polyacrylamide gel electrophoresis
PARP	poly(ADP-ribose) polymerase
PBS	phosphate buffered saline
PCR	polymerase chain reaction
Pi 3 kinase	phosphoinositide 3-kinase
PIPES	1.4-piperazinediethanesulfonic acid
PKB/AKT	protein kinase B
PKC	protein kinase C
PMSF	α-phenyl-methylsulfonyl fluoride
PP2A	protein phosphatase 2A subunit Aα
pRB	retinoblastoma protein
prICE	protease resembling ICE (caspase-1)
RasGAP	Ras GTPase-activating protein
RIP	Receptor interacting protein
S-phase	DNA synthesis (replication)
S/M extract	proapoptotic extract from committed phase cells
SDS	sodium dodecyl sulfate
TNF	tumor necrosis factor
Topo I	topoisomerase I
Topo II	topoisomerase II
TRADD	TNFR-associated death domain
TRAF2	TNF receptor accociated factor 2
v/v	volume per unit volume
Z-EK(bio)D-aomk	N-(Nα-benzyloxycarbonylglutamyl-Nε-biotin-yllysyl asparticacid ((2,6-dimethylbenzoyl)oxy)methyl ketone
°C	degrees celcius

Amino acid abbreviations

Amino Acid	3-letter code	1-letter code
Alanine	Ala	A
Arginine	Arg	R
Asparagine	Asn	N
Aspartate	Asp	D
Cysteine	Cys	C
Glutamate	Glu	E
Glutamine	Gln	Q
Glycine	Gly	G
Histidine	His	H
Isoleucine	Ile	I
Leucine	Leu	L
Lysine	Lys	K
Methionine	Met	M
Phenylalanine	Phe	F
Proline	Pro	P
Serine	Ser	S
Threonine	The	T
Tryptophan	Trp	W
Tyrosine	Tyr	Y
Valine	Val	V

Chapter 1

1. Introduction

1.1 What is apoptosis and why is apoptosis research important?

1.1.1 Definition of apoptosis

Apoptosis and necrosis are two major types of cell death. Apoptosis is a physiological process and a major form of programmed cell death and is essential for development, tissue homeostasis, and host defense against viruses (Wyllie, 1980; Raff, 1992; Thompson, 1995; Nagata, 1997). In contrast, necrosis occurs accidentally when cells are exposed to a serious physical or chemical insult. Differential features and the significance of apoptosis and necrosis are summarized in table 1.

During the last decade, apoptosis research has become an exciting area principally because of its essential involvement in many biological processes and systems. In a human body about a hundred thousand cells are produced every second by mitosis, and a similar number die by apoptosis. Apoptosis is characterized by a series of distinct morphological and biochemical changes, including nuclear and cytoplasmic condensation, DNA fragmentation, and alterations in cell membrane composition (Kerr, 1971; Wyllie, 1980). These changes have been observed in almost all cell types, suggesting the presence of a common death pathway.

Table 1. Differential features and significance of apoptosis and necrosis

Apoptosis	
Morphological features	Membrane blebbing, but no loss of integrity Aggregation of chromatin at the nuclear membrane Shrinking of cytoplasm and condensation of nucleus Formation of membrane bound vesicles (apoptotic bodies)
Biochemical features	Tightly regulated process involving activation of enzymatic steps Internucleosomal DNA fragmentation (DNA ladder) Release of various factors (cytochrome *c*, AIF) from mitochondria Activation of caspase cascade Alteration in membrane asymmetry (translocation of phosphatidyl-serine from the cytoplasmic to the extracellular side of the membrane)
Physiological significance	Affects individual cells Phagocytosis by adjacent cells or macrophages No inflammatory response
Necrosis	
Morphological features	Loss of membrane integrity Swelling of cytoplasm, mitochondria and other organelles Complete cell lysis
Biochemical features	Loss of regulation of ion homeostasis Random digestion of DNA
Physiological significance	Affects groups of contiguous cells Phagocytosis by macrophages Significant inflammatory response

1.1.2 Apoptosis in physiological conditions

Only recently has it been recognized that massive numbers of cells are eliminated by apoptosis in physiological conditions, presumably because usually less than 1% of cells are detected as apoptotic in tissue (Wyllie, 1994). Apoptosis is a mechanism of cell clearance in many physiological processes such as embryogenesis, metamorphosis (Vaux and Korsmeyer, 1999). For example, loss of the tadpole's tail involves cell death (Kerr, Harmon *et al.*, 1974). Massive cell death is also observed during the metamorphosis of insects (Schwartz and Truman, 1982). During vertebrate nervous system development, as much as 85% of certain cell populations of developing neurons undergo cell death (Cowan, Fawcett *et al.*, 1984; Hamburger, 1992). Apoptosis plays an important role in the establishment of the immune system: 95% of T-cells are eliminated by apoptosis without leaving the thymus. Adult animals must maintain the correct number of cells within each tissue, and thus cells that have already functioned die as younger cells are generated to replace them. In other words, the coordinate regulation of cell proliferation and cell death provides precise control over tissue size (Hinsull, Bellamy *et al.*, 1977). Cells that pose a danger to the host are eliminated by cell death: cells infected by viruses can be removed before the virus spreads. As shown above, apoptosis is involved in many aspects of life. Thus any disregulation in the apoptotic process can cause serious trouble, as shown below.

1.1.3 Apoptosis in disease

It is now clear that defects in apoptosis occur in several types of disorders in the human body. Inappropriate activation of the apoptotic pathway has been implicated in a number of acute and chronic neuro-degenerative diseases. In Alzheimer's disease, Parkinson's disease, and Huntington's disease, there is now increasing evidence that apoptotic cell death contributes to the loss of specific neuronal populations (Friedlander and Yuan, 1998). Autoimmunity is a consequence of defects occurring in the signaling, execution and clearance pathways involved in apoptosis. For example, defects in the CD95 pathway, which is one of the major apoptotic pathways (see chapter 1.2.1), are found in autoimmune diseases such as in the autoimmune lymphoproliferative syndrome (ALPS) (Fisher, Rosenberg *et al.*, 1995). Inherited non-lethal human caspase 10 abnormalities cause pleiotropic apoptosis defects underlying autoimmunity in the ALPS type II syndrome (Wang, Zheng *et al.*, 1999). The accumulation of neoplastic cells can occur through enhanced proliferation, diminished cell turnover, or a combination of both processes. The demonstration that Bcl-2 can inhibit cell death upon forced overexpression provided the first concrete example of an oncogene that acts by inhibiting cell turnover rather than enhancing proliferation (Tsujimoto, Cossman *et al.*, 1985). Since deregulation of almost any component of the apoptotic machinery can contribute to the transformation process, studies of the mechanism of apoptosis may help in the design of cancer therapies (Kaufmann and Earnshaw, 2000).

1.1.4 Major components involved in apoptosis are conserved

The basic scheme of the apoptosis pathway is evolutionarily conserved from nematodes to humans in general. Genetic studies in *Caenorhabditis elegans*, in which 131 of the 1090 somatic cells generated during development are destined to die, has provided a framework for understanding the components responsible for programmed cell death both in *C. elegans* and higher organisms (Ellis and Horvitz, 1986; Liu and Hengartner, 1999). Figure 1 shows 15 genes of *C. elegans* that function in programmed cell death. The basic scheme of the apoptosis effector mechanism is depicted in figure 2, which compares homologous proteins in nematodes and vertebrates. Caspases, a family of cysteine-dependent aspartate-directed proteases, play critical roles in initiation and execution of the apoptotic pathway. The activation and regulation mechanisms of caspases are discussed in Chapter 1.2. Caspases themselves and their substrates are discussed in Chapter 1.3.

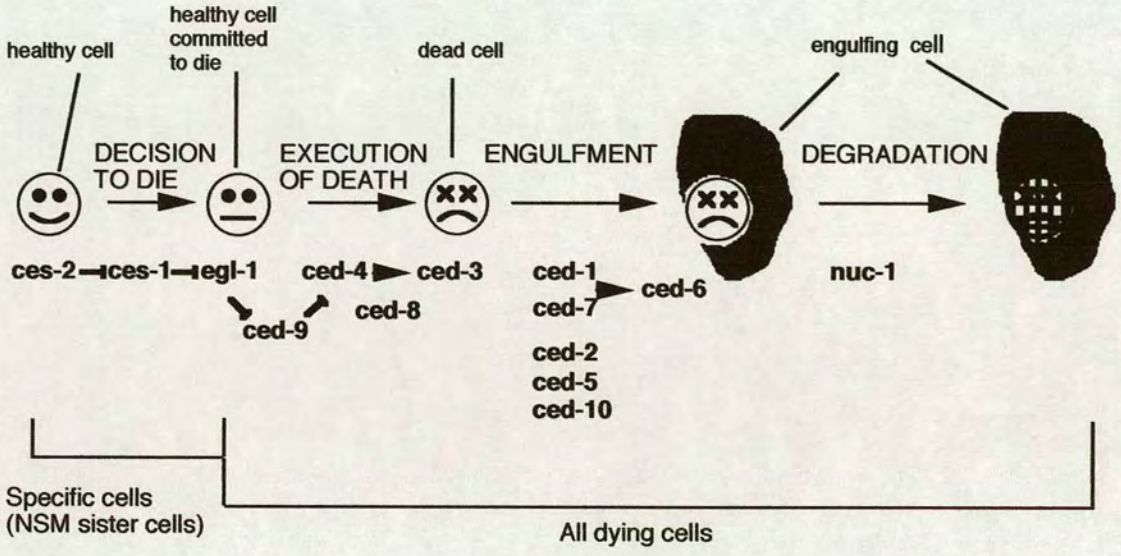

Figure 1. The genetic pathway for programmed cell death in *C. elegans*. In the nematode *C. elegans*, genetic studies led to the discovery of 15 genes involved in programmed cell death. These 15 genes have been divided into four groups based on the order of their activity during the process of programmed cell death: *ces-1* and *ces-2* are involved in the decision making, *ced-3, ced-4, ced-8, ced-9,* and *egl-1* in the process of execution, *ced-1 ced-2, ced-5, ced-6, ced-7* and *ced-10* in the engulfment of dying cells by engulfing cells, and *nuc-1* in the degradation of cell corpses within engulfing cells. Adapted from reference (Liu and Hengartner, 1999).

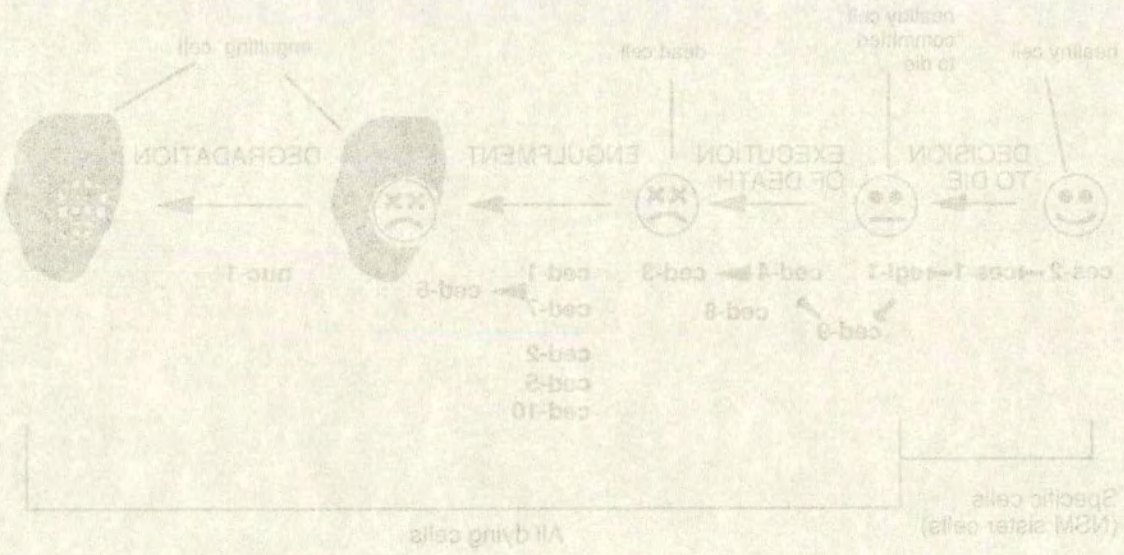

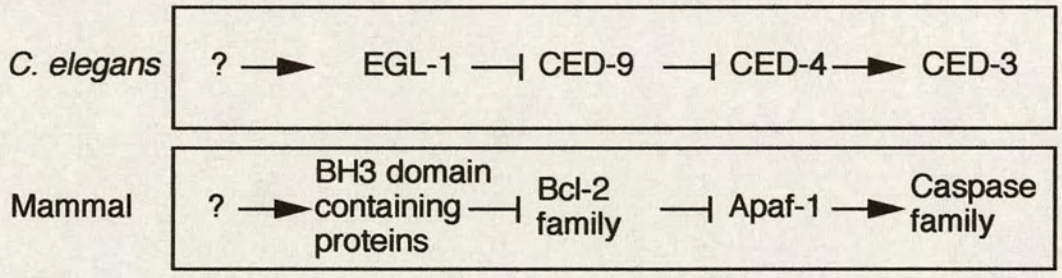

Figure 2. Conservation of the execution step in the genetic pathway for programmed cell death. In *C. elegans*, the execution step in the genetic pathway for programmed cell death comprises four genes, *ced-3, ced-4, ced-9* and *egl-1*. All of these genes have corresponding mammalian homologues: CED-9 is a member of the Bcl-2 family, CED-3 is a caspase family member, CED-4 is homologous to the Apaf-1 protein, and EGL-1 is similar in structure to Bid and other BH3 domain only-containing proteins. Adapted from reference (Liu and Hengartner, 1999).

1.2 Two major apoptotic pathways and their regulation

There are two major cell-intrinsic pathways for inducing apoptosis, one that begins with ligation of cell surface death receptors (receptor-mediated apoptosis) and another that involves mitochondrial release of cytochrome *c* (stress-induced apoptosis). Each pathway activates distinct caspase cascades (Bratton, MacFarlane *et al.*, 2000).

1.2.1 Receptor-mediated apoptosis

Within the plasma membrane of many cells are death receptors, which, when triggered by their corresponding ligand, result in receptor trimerization and initiate rapid activation of caspases. Figure 3 shows a diagram of the receptor-mediated caspase cascade. Death receptors such as CD95/Fas and TNFR1 are members of the tumor necrosis factor (TNF) receptor super family.

In brief, CD95 molecules are pre-oligomerized in living cells through the interaction of the pre-ligand assembly domain (Siegel, Frederiksen *et al.*, 2000). Binding of Fas ligand or agonistic antibodies results in a clustering of the receptors' cytosolic DD (death domain) and recruitment of adapter molecules such as FADD (Fas-associated death domain) via homophilic DD interactions (Ashkenazi and Dixit, 1998). FADD contains also a DED (death effector domain), which can associate with similar DEDs located in the prodomain of caspase-8. This complex of proteins is referred as the DISC (death-inducing signaling complex). Clustering of procaspase-8 within this

complex promotes trans-catalysis to generate active caspase-8 (Medema, Scaffidi *et al.*, 1997; Muzio, Stockwell *et al.*, 1998).

Similarly, trimerized TNFR1 can recruit the adapter protein TRADD (TNFR-associated death domain), which consequently recruits FADD and procaspase-8. In addition, TNFR1 can also activate NF-κB and JNK signaling pathways through other adapter molecules such as RIP (receptor-interacting protein) and TRAF2 (Akiba, Nakano *et al.*, 1998; Gravestein, Amsen *et al.*, 1998). Activation of these signaling pathways protects against apoptosis.

Upon activation, caspase-8 can activate effector caspases -3, -6 and -7 and ensure destruction of the cell. Moreover, caspase-8-mediated cleavage of Bid produces a truncated protein that translocates from the cytosol to the mitochondria where it stimulates release of cytochrome *c* (Li, Zhu *et al.*, 1998; Luo, Budihardjo *et al.*, 1998). This can couple the death-receptor stimulation to the activation of another pathway which is discussed below.

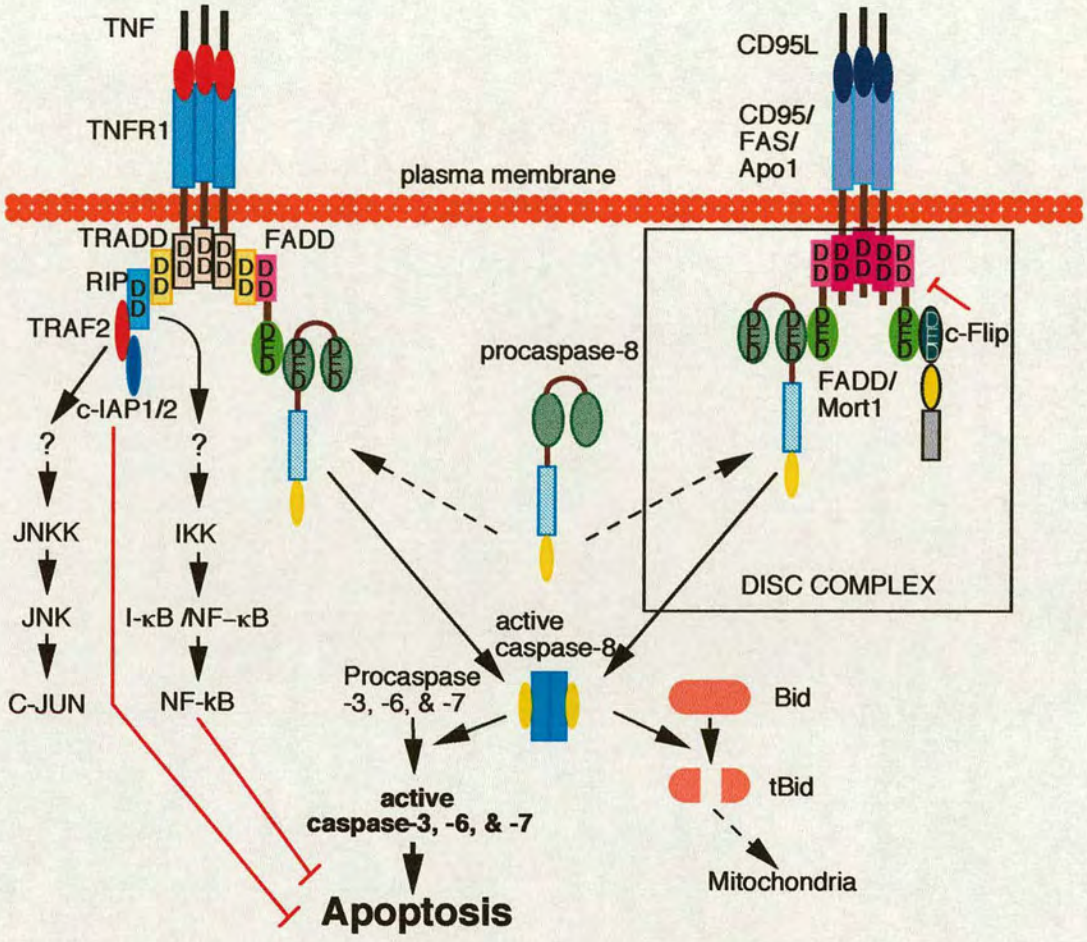

Figure 3. Receptor-mediated caspase cascade. Binding of ligand or agonisitic antobodies to CD95 and TNFR1 receptors initiates recruitment of various adapter proteins through homophilic DD interactions, including FADD, which directly binds and promotes trans-catalytic activation of caspase-8. Stimulation of TNFR1 also activates NF-κB and JNK signaling pathways through RIP and TRAF2, respectively. Adapted from reference (Bratton *et al.*, 2000).

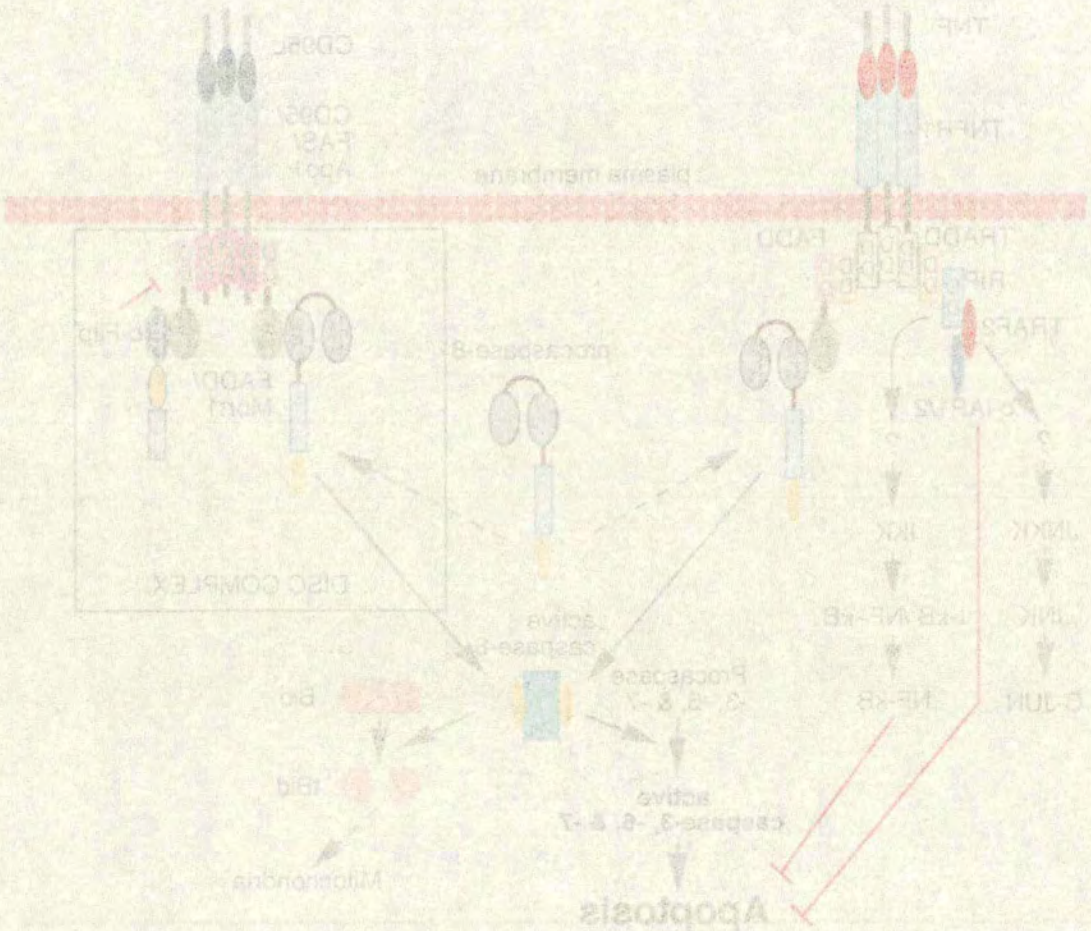
Plasma membrane
DISC COMPLEX
Mitochondria
Apoptosis

1.2.2 Stress-induced apoptosis

The other major apoptotic pathway, the stress-induced apoptosis, is shown in figure 4. In brief, a number of cellular signals induce perturbations in the mitochondria resulting in the release of proapoptotic molecules, including AIF (apoptosis-inducing factor) and cytochrome *c*, from the intermembrane space into the cytoplasm (Green and Reed, 1998; Susin, Lorenzo *et al.*, 1999). Cytochrome *c* release appears to be a common occurrence in apoptosis, but the mechanism controlling its release is not clearly understood. After release, cytochrome *c* interacts with Apaf-1 (CED-4 homologue), dATP/ATP and procaspase-9 to form a complex known as the "apoptosome" (Li, Nijhawan *et al.*, 1997). Caspase-9 in this complex activates caspase-3, -7 and consequently -6 (Li *et al.*, 1997; Zou, Henzel *et al.*, 1997; Srinivasula, Ahmad *et al.*, 1998). Activated caspases-3 -6 and -7 attack cellular proteins and also process other caspases including apical caspases -8 and -9 to amplify the signal. The importance of the Apaf-1 to caspase-9 to caspase-3 pathway was later verified in studies using Apaf-1-/-, caspase-9-/- and caspase-3-/- mice (Yeh, Hakem *et al.*, 1999; Zheng and Flavell, 2000).

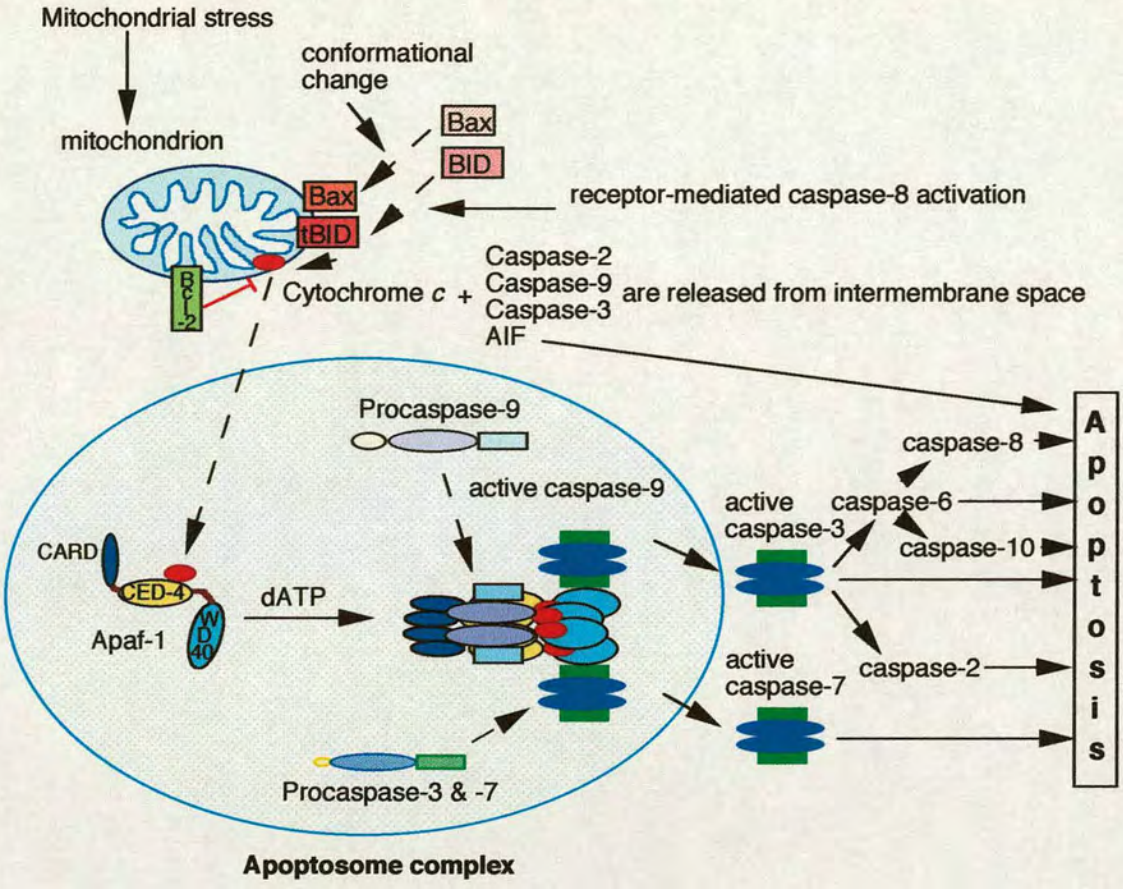

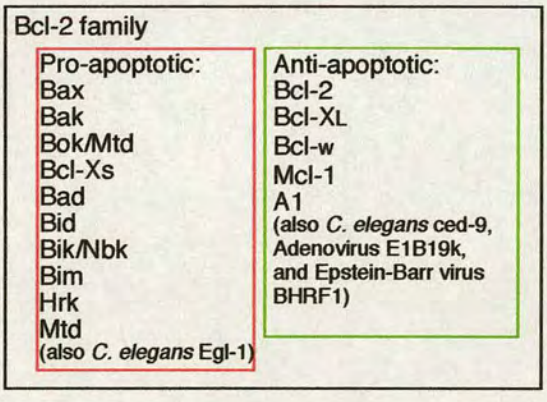

Figure 4. Stress-induced caspase cascade. Mitochondrial stress and/or proapopototic Bcl-2 proteins (e.g. tBid or Bax) induce release of cytochrome *c* into cytoplasm. Caspases -2, -3, and -9 and AIF (apoptosis-inducing factor) are also released from the mitochondrial intermembrane space. Cytochrome *c* and dATP induce a conformational change in Apaf-1 that allows it to oligomerize into an approximately 700-kDa complex (Apoptosome). Caspase-9 in the apoptosome activates caspases-3, -7 and consequently caspase-6. Adapted from reference (Bratton *et al.*, 2000). Pro-apoptotic and anti-apoptotic Bcl-2 family proteins are listed below.

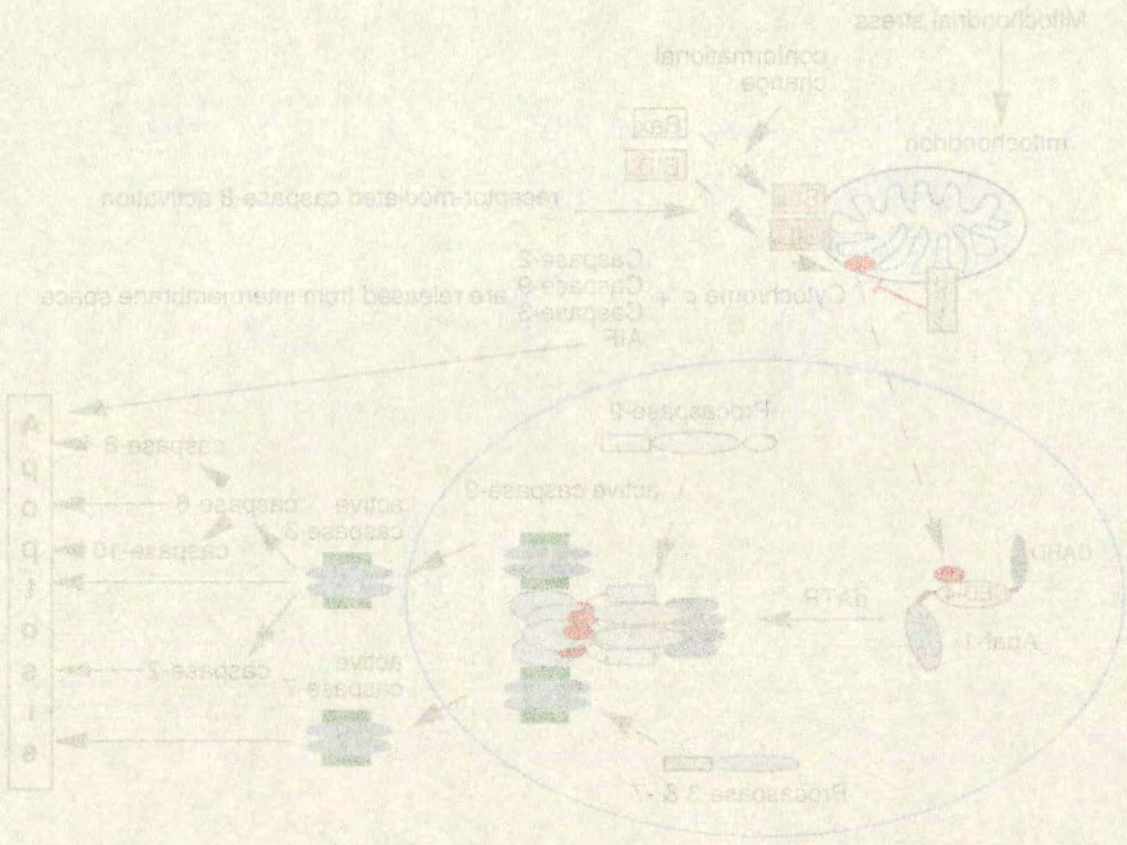

1.2.3 Regulation of apoptotic pathways

A number of proteins exist to regulate the mechanism of caspase activation, presumably because accidental activation of caspases is potentially harmful for cells. For example, the ability of the adaptors, FADD and Apaf-1, to activate the caspases is regulated by proteins that appear to directly interact with the adaptors.

In the receptor-mediated pathway, viral FLICE (caspase-8)-inhibitable proteins (v-FLIPs) and cellular FLIPS (c-FLIPs) inhibit the activation of caspase-8 (Irmler, Thome *et al.*, 1997) (Fig. 3). FLIP contains DEDs, and binds to the prodomains of procaspase 8, thereby interfering with the FADD-caspase-8 interaction (Tschopp, Irmler *et al.*, 1998).

In the stress-induced pathway, Bcl-2 family proteins either inhibit (Bcl-2, Bcl-XL) or promote (Bax, Bak, Bik, Bid) apoptosis through regulation of cytochrome *c* release (Fig. 4). In the case of *C. elegans*, CED-9 can prevent caspase activation by binding to the adaptor CED-4 (Chinnaiyan, Chaudhary *et al.*, 1997; Spector, Desnoyers *et al.*, 1997; Wu, Wallen *et al.*, 1997). Anti-apoptotic Bcl-2 family members can in turn be regulated by other, proapoptotic Bcl-2 family members that interact via the Bcl-2 homology domain BH3 (Muchmore, Sattler *et al.*, 1996; Conradt and Horvitz, 1998). For example, the "BH-3 only" protein BAD can bind to and inhibit Bcl-X, and its ability to do so can be regulated by phosphorylation. This is one way in which signaling molecules such as PKB/AKT can promote cell survival (Zha, Harada *et al.*, 1996).

1.3 Caspases and their role in apoptosis

1.3.1 Structure of caspases and processing of zymogens

The key effector components of apoptosis are caspases, a family of cysteine proteases that cleave their substrates adjacent to aspartate residues. Fourteen mammalian caspases have been identified, including 12 human forms. Caspases are synthesized as zymogens or proenzymes (approximately 30-50 kDa) containing a N-terminal prodomain together with one large (approximately 20 kDa) and one small (approximately 10 kDa) subunit. Crystal structures suggest that the active enzymes are heterodimers, composed of two small and two large subunits, presenting two catalytic sites. Importantly, specific aspartic acid cleavage sites exist between the prodomain of a caspase and each of its subunits, allowing the possibility of a caspase cascade, in which one caspase can process and activate another (Earnshaw, Martins *et al.*, 1999) . With the exception of one other cell death-related protease, granzyme B, the only mammalian enzymes known to activate caspases are the caspases themselves (Darmon, Ley *et al.*, 1996; Martin, Amarante-Mendes *et al.*, 1996).

1.3.2 Initiator and effector caspases

Caspases can be subdivided based on a number of criteria including phylogenetic analysis, substrate specificity, and the length of their prodomains (Fig. 5). "Initiator" caspases, including caspases -8 and- 9, contain long prodomains which allow them to interact with specific adaptor proteins. Such interactions bring initiator caspases in close proximity to one

another and promote the activation of one zymogen by another. Initiator caspases are responsible for directly or indirectly activating various "effector" caspases, including caspases -3, -6, and -7, which contain short prodomains. Effector caspases cleave a number of structural and regulatory proteins and are directly responsible for many of the features of apoptotic execution (Earnshaw *et al.*, 1999).

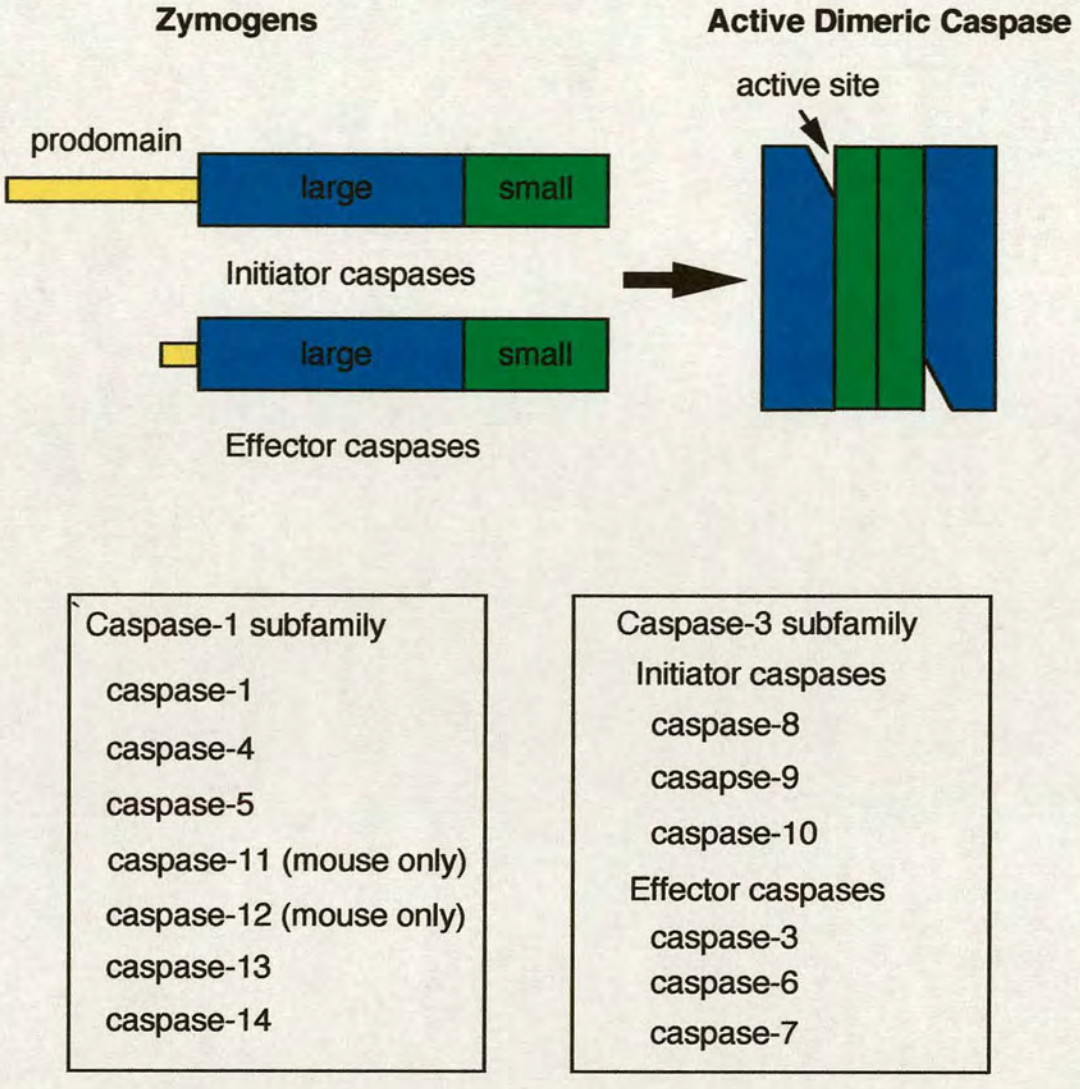

Figure 5. Diagram showing the structure of the caspase zymogens. Initiator and effector caspases and a list of subgroups of caspases. The amino-terminal prodomains are shown in *yellow*, large subunits are in *blue*, and small subunits are shown in *green*. Initiator caspases have a long prodomain which contains either two death effector domains (DED)-caspase 8 and 10 or a caspase recruitment domain (CARD)-caspase 9 (Chinnaiyan, O'Rourke *et al.*, 1995; Hofmann, Bucher *et al.*, 1997). Effector caspases have a short prodomain. The active heterotetrameric enzyme (*right*) results from proteolytic activation. Caspases can be divided into subgroups according to their role. The Caspase-1 subfamily is mainly responsible for inflammatory response. The Caspase-3 subfamily, including initiator caspases and effector caspases, has roles in apoptosis (Earnshaw *et al.*, 1999).

Zymogens
Active Dimeric Caspase
active site
procaspase
initiator caspases
effector caspases
Caspase-8 homodimer
Caspase-9 homodimer
Caspase-2 homodimer
Caspase-1 (mouse only)
Caspase-12 (mouse only)
Caspase-11
Caspase-4
Caspase-8 homodimer
Caspase-9 homodimer
Caspase-10 homodimer
Effector caspases
Caspase-3
Caspase-6
Caspase-7

1.3.3 Regulation of caspases

Caspase activation is tightly regulated at several levels. Caspase zymogen levels are transcriptionally regulated (Droin, Dubrez *et al.*, 1998). Activation of caspase zymogens by death receptor-associated scaffolds can be regulated by FLIP (discussed in chapter 1.2.3). Activation of procaspase-9 by the Apaf-1:cytochrome c scaffold appears to be regulated by anti-apoptotic Bcl-2 family (discussed in chapter 1.2.3). Caspase activation and activity are regulated by interactions with inhibitor-of-apoptosis (IAP) proteins. IAP family proteins were originally identified in viruses but seven mammalian homologues of baculovirus IAP proteins have been identified (Deveraux and Reed, 1999). It was demonstrated that several human IAP proteins inhibit caspases directly(Roy, Deveraux *et al.*, 1997). It was also shown that IAP proteins act upstream of caspases in Drosophila (Wang, Hawkins *et al.*, 1999). Finally, active caspases also appear to be regulated by post-translational modifications. It was demonstrated that caspases are phosphorylated *in vivo* using human leukemia HL60 cell line, and that the phosphorylation can affect their enzymatic activity *in vitro* (Martins, Kottke *et al.*, 1998).

1.3.4 Substrates of caspase and consequence of their cleavage

More than forty caspase substrates have been identified, including a number of structural components of the cytoskeleton and nucleus, as well as numerous proteins involved in signaling pathways (Earnshaw *et al.*, 1999). Figure 6 summarizes these substrates and the consequence of their

cleavages. The cleavages result in turning off the survival pathway and promoting cell death. At least 13 protein kinases are known to be cleaved during apoptosis. Many of these cleavages produce catalytically competent fragments with increased activity that promotes cell death. Furthermore cytoskeleton-associated cell survival pathways are disrupted. To survive, most normal cells in metazoans must be integrated into a tissue via contacts with a specific extracellular matrix and interactions with neighboring cells. Caspases cleave the cytoskeletal proteins on which those signaling pathways depend in addition to disrupting the protein kinase cascade. Transcription factors involved in cell survival pathways are the target of caspases. In addition, cellular damage-monitoring networks are disrupted. Cell cycle arrest and DNA repair mechanisms are impaired by caspase cleavage. Finally cleavages of nuclear structural proteins facilitate the apoptotic morphological changes and caspase cleavage activates/inactivates proteins such as Bid and ICAD, which have direct roles in apoptosis. Particularly, cleavage of ICAD liberates CAD to induce internucleosomal DNA cleavage, which is one of the hallmarks of apoptosis (chapter 1. 4).

To investigate the physiological functions of each caspases, transgenic mice deficient in various caspases have been generated. Although to date, targeted disruption of caspases 1, 2, 3, 8, 9, 11 and 12 in mice have been reported, none of these mutations abolishes all apoptosis during development (Zheng and Flavell, 2000). In each case, defects in apoptosis are both cell type- and stimulus- dependent. Thus, apoptotic pathways must use different caspase repertoires in different tissues and in response to

different stimuli. Since the design of specific small-molecule inhibitors has been a major challenge, this kind of genetic approach will help not only to understand the mechanism of apoptosis but also the contribution of individual caspases in disease processes such as viral infections and neurodegenerative diseases.

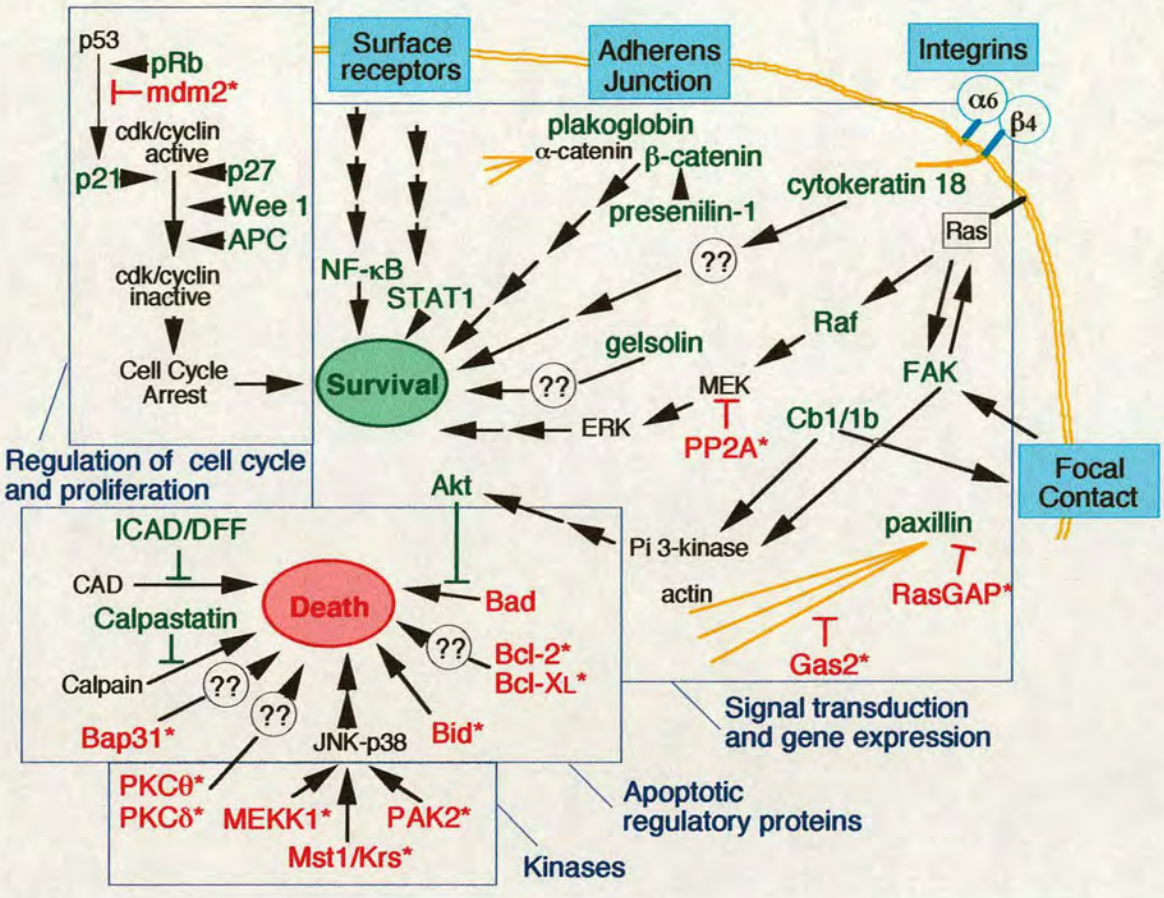

Figure 6. Caspase cleavages promote cell death and turn off survival pathways. Upon caspase cleavage, proteins shown in *red* promote cell death and proteins shown in *green*, which work for cell survival, become impaired. Proteins with * become toxic only after caspase cleavage. From top left, pRb (retinoblastoma), mdm2, p21, p27, Wee1 kinase, and APC (adenomatous polyposis coli) are involved in regulation of cell cycle and proliferation. NF-κB and STAT-1 are involved in gene expression. Plakoglobin, β-catenin, cytokeratin 18, presinilin-1, paxillin, Gas2 and gelsolin are abundant cytoplasmic proteins involved in signal transduction. Raf, FAK (focal adhesion kinase), RasGAP (Ras GTPase-activating protein), PP2A (Protein phosphatase 2A subunit Aα) and Akt (Protein kinase B) are also involved in signal transduction. Bad, Bcl-2, Bcl-XL, Bid, ICAD/DFF, Calpastatin, and Bap31 have direct roles in apoptosis. PAK2, Mst1/Krs, MEKK1, PKCθ, and PKCδ are kinases (Based on a figure by Bill Earnshaw).

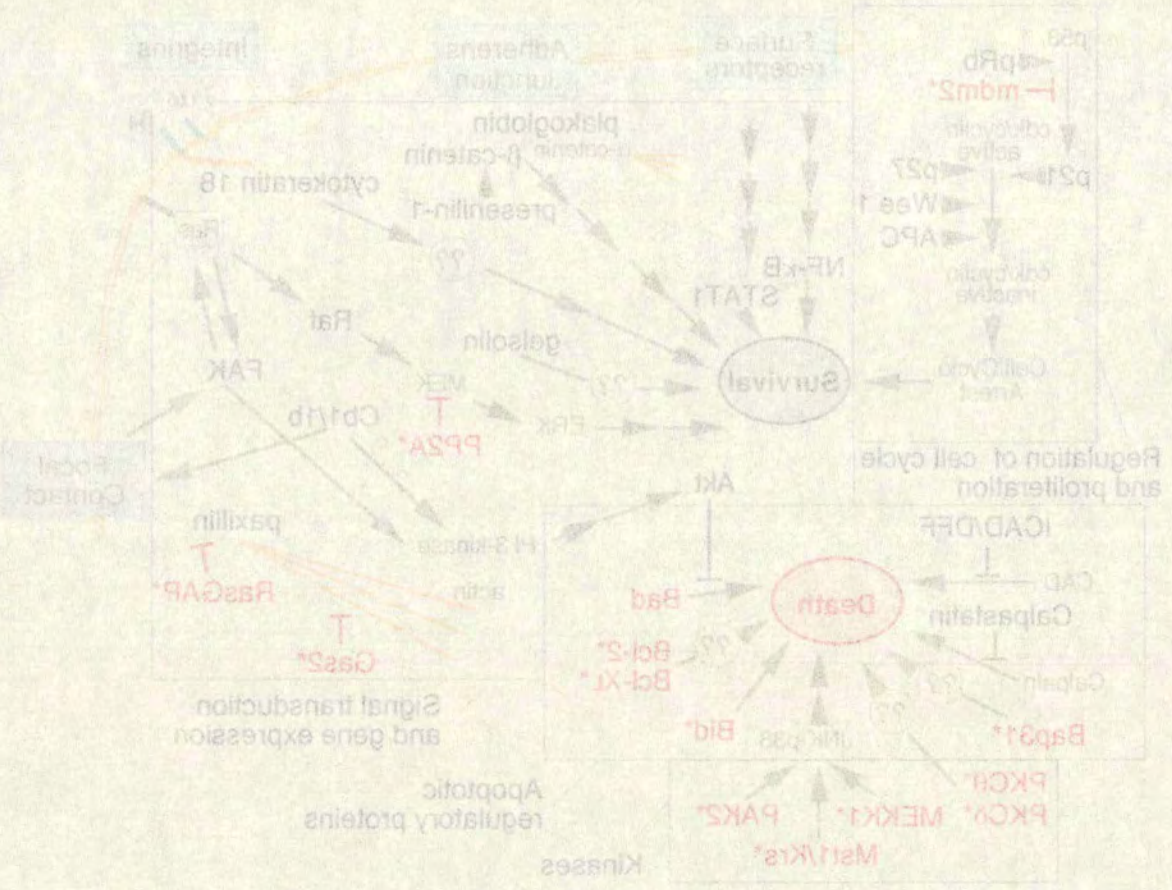
plakoglobin
β-catenin
cytokeratin 18
presenilin-1
NF-κB
STAT1
Survival
Raf
gelsolin
FAK
MEK
ERK
Cbl/cb
PP2A*
Akt
paxillin
PI 3-kinase
actin
RasGAP*
Gas2*
Bad
Death
Bcl-2*
Bcl-Xl*
Bid*
Bap31*
ICAD/DFF
CAD
Calpastatin
Calpain
PKCδ*
PKCδ*
MEKK1*
PAK2*
Mst1/Krs*
pRb
mdm2*
p27
p21
Wee 1
APC
Regulation of cell cycle
and proliferation
Apoptotic
regulatory proteins
Kinases

1.4 CAD and ICAD family proteins and other chromatin condensation factors

CAD (caspase activated deoxyribonuclease) induces internucleosomal DNA cleavage, which is one of the hallmarks of apoptosis (Wyllie, 1980). ICAD is an inhibitor of CAD. CAD, ICAD and CIDE (cell death inducing DFF45 like effector) proteins have homology in their N-terminus (fig. 7). The CIDE-N/CAD domain is responsible for interaction between these proteins.

1.4.1 Identification of apoptotic nuclease

Cleavage of chromatin at internucleosomal sites was first reported in dying cells by the Czech radiobiologist Miroslav Skalka (Skalka, Matyasova *et al.*, 1976). Soon after, a "chromatin ladder" pattern of regular sized DNA fragments was recognized as characteristic of apoptosis (Wyllie, 1980). Despite intensive effort, the identities of the DNase(s) involved in apoptosis were unknown for many years. Cytosolic fractions from apoptotic cells contain a factor(s) that induces DNA degradation in isolated nuclei (Lazebnik, Cole *et al.*, 1993; Newmeyer, Farschon *et al.*, 1994; Enari, Hase *et al.*, 1995), suggesting that a nuclease or its activating molecule(s) is generated in apoptotic cells. Early studies indicated that the DNase worked at a neutral pH and is Ca^{2+}/Mg^{2+}-dependent (Liu, Ribecco *et al.*, 1999). Several candidates for the nuclease including DNase I, cyclophilins, DNase γ and DNase II (despite its acid pH dependence), were reported, but their properties were diverse enough to preclude identity with one another (Barry

and Eastman, 1993; Peitsch, Polzar *et al.*, 1993; Montague, Gaido *et al.*, 1994; Shiokawa and Tanuma, 1998). The enzyme variously called caspase-activated DNase (CAD)/CPAN (caspase-activated nuclease)/DNA fragmentation factor 40 (DFF40) is the first confirmed apoptotic nuclease (Enari, Sakahira *et al.*, 1998; Halenbeck, MacDonald *et al.*, 1998; Liu, Li *et al.*, 1998).

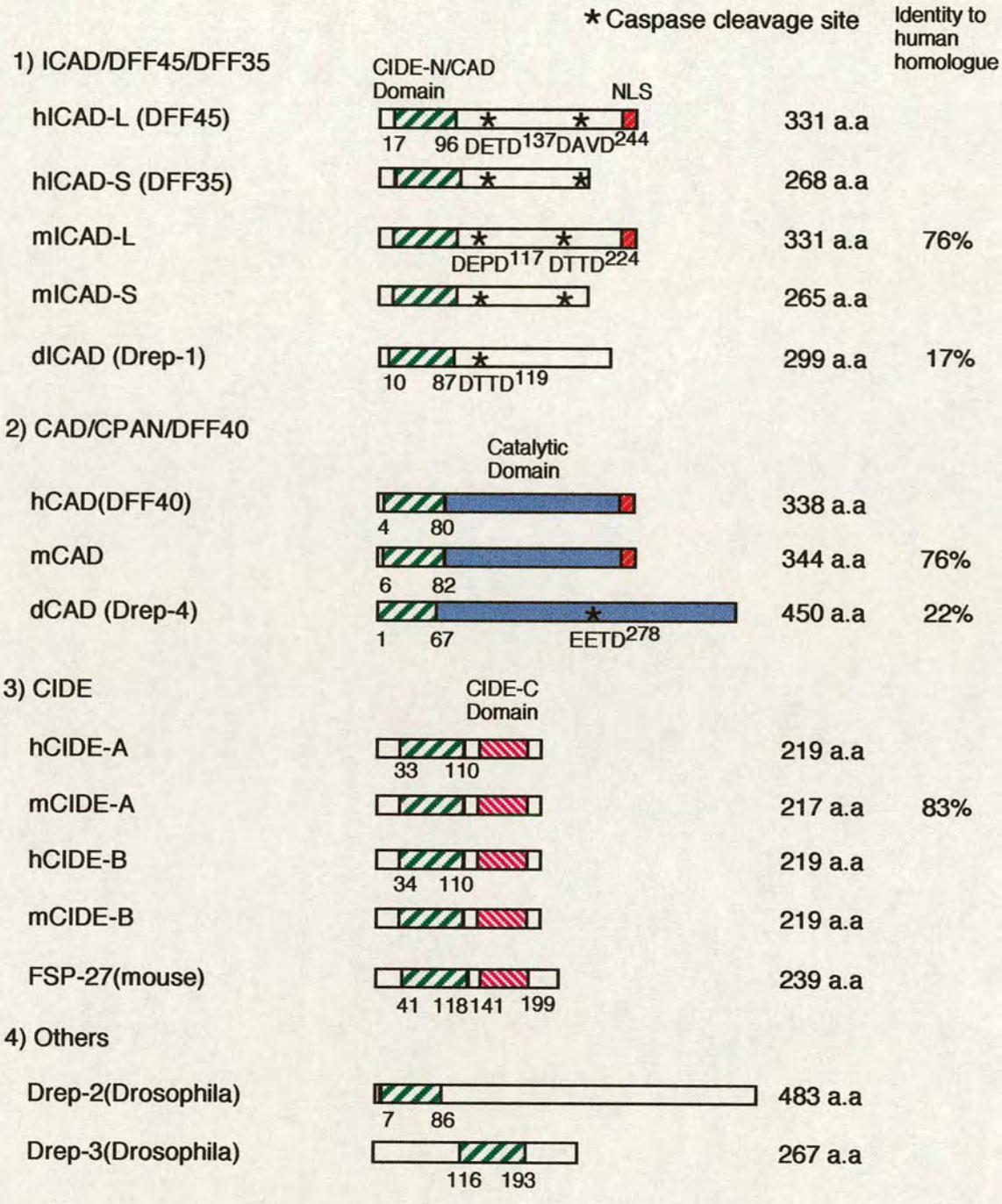

Figure 7. ICAD, CAD family members. Schematic presentation of ICAD and CAD family members from human, mouse and Drosophila. All of them share the CIDE-N/CAD domain, which is important for homophilic interactions between family members. The CAD group has a catalytic domain which is responsible for DNase activity. The CIDE group has a CIDE-C domain, overexpression of which induces apoptosis. The ICAD group and dCAD contain caspase cleavage site(s), cleavage of which is necessary for the activation of CAD. Human and mouse ICAD-L and CAD each have a nuclear localization signal (NLS).

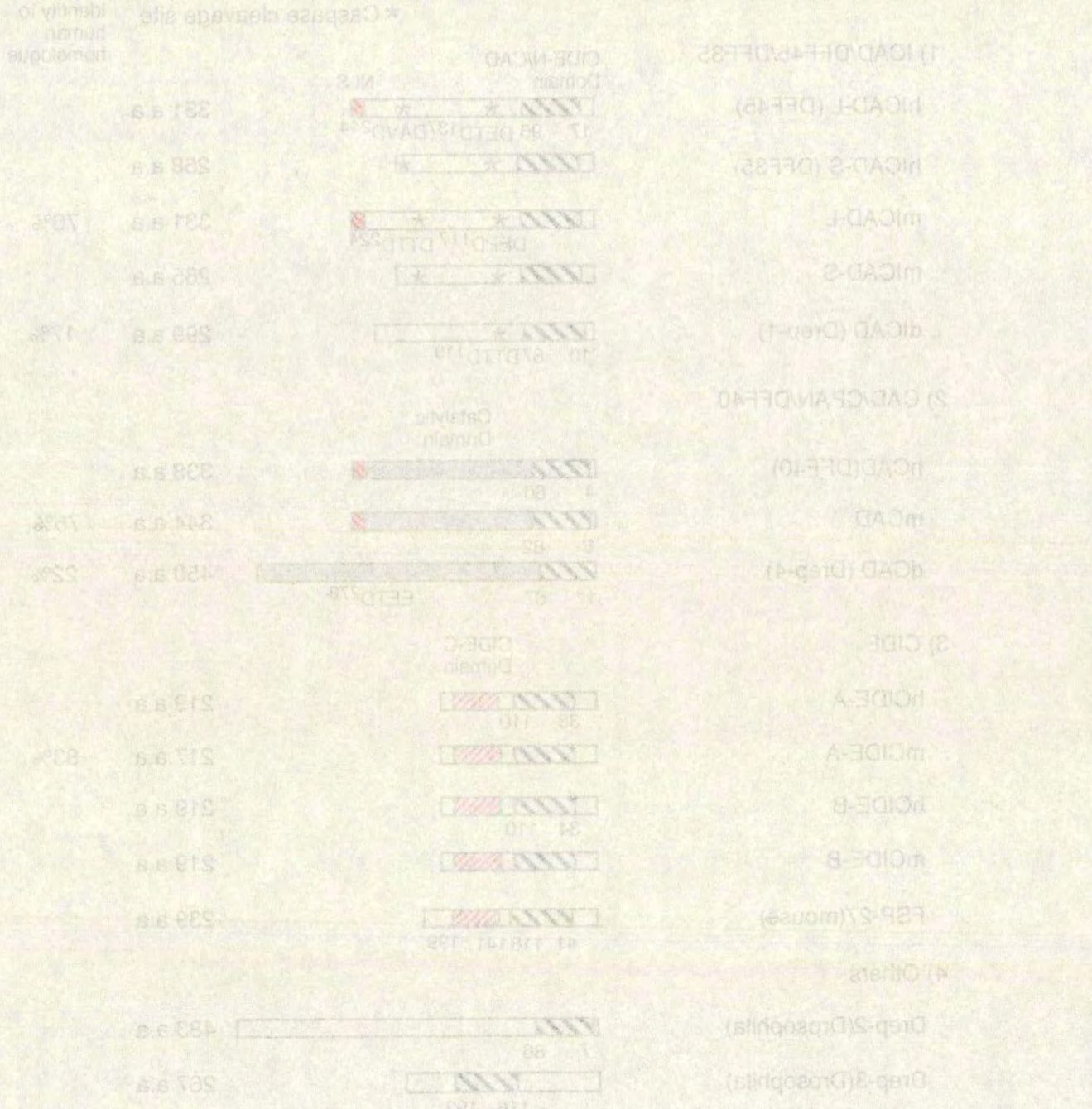

1.4.2 CAD/CPAN/DFF40

Cytosolic extracts from living cells do not cause DNA degradation in nuclei, but treatment of the extracts with caspase-3 converts them to apoptosis-inducing, suggesting that living cells carry a proform of the molecules(s) that induce DNA degradation (Enari, Talanian *et al.*, 1996). The nuclease responsible for DNA degradation was purified from cytosolic extracts of mouse T-cell lymphoma cells and named CAD (caspase-activated nuclease) (Enari *et al.*, 1998). CAD exists as an inactive complex with ICAD-L in healthy cells and cleavage of ICAD by caspase-3 liberates CAD. The released CAD forms a homo-oligomer that is enzymatically active (Liu, Zou *et al.*, 1999). CAD is a basic protein consisting of 343 amino acids with a tell-tale nuclear localization signal at the C-terminus. Subsequently, a human homologue of CAD, CPAN/DFF40, was identified (Halenbeck *et al.*, 1998; Liu *et al.*, 1998).

CAD nuclease works best at pH 7.5, requires $Mg2^{+}$, not $Ca2^{+}$, and is inhibited by $Zn2^{+}$ (Widlak, Li *et al.*, 2000). It generates blunt ends or ends with a base 5'-overhang possessing 5'-phosphate 3'-hydroxyl groups and is specific for double-stranded DNA (Widlak *et al.*, 2000). These properties fulfill the criteria of the apoptotic nuclease that was proposed initially. CAD attacks sites that possess a dyad axis of symmetry with respect to purine and pyrimidine content (Widlak *et al.*, 2000). CAD activity is enhanced by the presence of histone H1, HMG-1 (high mobility group-1), HMG-2, and topoisomerase II, at least against naked DNA (Liu *et al.*, 1998; Toh, Wang *et al.*, 1998; Widlak *et al.*, 2000). One of its most unusual properties is that CAD

is as active against chromatin as it is against naked DNA (Widlak *et al.*, 2000). The enzyme specifically attacks chromatin in the internucleosomal linker, lacks exonuclease activity and does not cause intranucleosomal cleavage (Widlak *et al.*, 2000). Moreover, it has been suggested that CAD is also responsible for initial large-scale chromosomal DNA fragmentation (50-200 kb) (Sakahira, Enari *et al.*, 1999; Zhang, Lee *et al.*, 2000).

1.4.3 ICAD-L/-S (DFF45/DFF35)

Cytosolic extracts from growing cells contain an inhibitory factor that blocks DNA fragmentation. However, treatment of extracts with caspase-3 or with dATP and cytochrome *c* converts them to apoptosis-inducing extracts, suggesting that this inhibitory function can be inactivated by caspase cleavage (Liu, Zou *et al.*, 1997). A heterodimeric protein was purified from HeLa cytosol and was designated DFF (DNA Fragmentation Factor), which consists of two subunits, 40 kDa and 45 kDa. The DFF45 subuit is the inhibitor of the apoptotic nuclease DFF40/CAD; and cleavage of DFF45 by caspases at two sites generates an active nuclease (Liu *et al.*, 1997). Subsequently a protein called inhibitor of CAD (ICAD), which is the mouse homologue of DFF45, was identified (Enari Nature 1998). ICAD has two forms, ICAD-L and ICAD-S (also called DFF45 and DFF35) arising by alternative splicing of a single transcript (Sakahira, Enari *et al.*, 1998) (Gu, Dong *et al.*, 1999). Both isoforms have inhibitory activity against CAD *in vitro;* however, only ICAD-L/DFF45 seems to associate with CAD in living cells. Moreover, only ICAD-L/DFF45 functions as a folding chaperone

during the translation of CAD shown by an *in vitro* translation and baculovirus expression systems (Sakahira, Enari *et al.*, 1999; Sakahira, Iwamatsu *et al.*, 2000). DFF45/ICAD mutant mice showed activity of DFF45 is essential for the folding of active CAD, since the CAD protein level was normal but CAD nuclease activity was entirely defective (Zhang, Liu *et al.*, 1998).

In apoptotic cells, ICAD/DFF45 is cleaved at two sites primarily by caspase-3. Although both caspase-3 and caspase-7 can cleave ICAD at the correct sites *in vitro* (Liu *et al.*, 1997; Sakahira *et al.*, 1998), studies with caspase-3 knockout mouse and MCF-7 cells which lost caspase-3, showed that the endogenous level of caspase-7 fails to activate CAD/DFF40 (Janicke, Ng *et al.*, 1998; Tang and Kidd, 1998; Wolf, Schuler *et al.*, 1999). Cells transformed with a form of DFF45/ICAD-L uncleavable by caspases did not show DNA fragmentation after variety of apoptotic stimuli but were nonetheless killed by a caspase-dependent mechanism (Liu *et al.*, 1998; Sakahira *et al.*, 1998; McIlroy, Sakahira *et al.*, 1999). DFF45/ICAD mutant mice demonstrated that although DFF45/ICAD is critical for the induction of DNA fragmentation and chromatin condensation *in vivo*, it is not required for immune system development (Zhang *et al.*, 1998).

1.4.4 Localization of CAD/ICAD complex

Localization of the inactive CAD/ICAD complex in healthy cells has been controversial. Originally CAD and ICAD were purified from cytosolic extracts and a nuclear localization signal was predicted at the carboxyl

terminus of CAD (Enari *et al.*, 1998). It was initially proposed that the CAD/ICAD complex remains in the cytosol until the activation of CAD by destruction of ICAD, because ICAD shields the CAD NLS from nuclear import receptors. Activated CAD enters the nucleus due to the accessibility of its NLS and digests the chromosomes (Enari *et al.*, 1998). However, we and other groups showed that both CAD and ICAD-L localize in the nuclei in living cells and we identified a functional NLS at the C-terminus of ICAD-L (Liu *et al.*, 1998; Samejima and Earnshaw, 1998; Samejima and Earnshaw, 2000).

The interaction between ICAD and CAD is first mediated by a N-term homology region, CIDE-N/CAD domain, and is then stabilized by interactions between the middle region of ICAD and the C-terminus of CAD (Mukae, Enari *et al.*, 1998; Gu *et al.*, 1999; McCarty, Toh *et al.*, 1999). The solution structure of the CIDE-N/CAD domain was determined by NMR (Lugovskoy, Zhou *et al.*, 1999; Uegaki, Otomo *et al.*, 2000). The CIDE-N/CAD domain, CAD (amino acids 1-87), contains one alpha helix and five beta strands. This is different from other apoptotic domains containing six or more compact alpha helices (Uegaki *et al.*, 2000). The structure was categorized in the ubiquitin superfold family (Uegaki *et al.*, 2000).

1.4.5 CAD and ICAD genes and their expression

In humans, both CAD and ICAD genes are assigned at the short arm of chromosome 1p36 (Mukae *et al.*, 1998). One pseudogene of hCAD was also identified (Mukae *et al.*, 1998). hCAD mRNA expression level is

dependent on the tissue/cell line. The expression level of hCAD seems to be correlated to the extent of DNA fragmentation during apoptosis in differing cell types (Mukae *et al.*, 1998).

In mouse, both the CAD and ICAD genes are assigned to the distal part of murine chromosome 4 which corresponds to human 1p36 (Kawane, Fukuyama *et al.*, 1999). The CAD and ICAD genes comprise about 11 and 16 kb, respectively (Kawane *et al.*, 1999). Both CAD and ICAD mRNAs are expressed at high levels in spleen, thymus, small intestine and lymph nodes (Kawane *et al.*, 1999). The promoter region of the CAD gene is very G and C rich as found in many ubiquitous house-keeping genes (75% G/C). However, the promoter region of ICAD has only 42% G/C and is regulated by different mechanisms (Kawane *et al.*, 1999).

1.4.6 Drosophila CAD and ICAD and other family members

Recently Drosophila ICAD and CAD family members have been identified. These include dICAD/Drep-1, dCAD/Drep-4, Drep-2, Drep-3 (Inohara and Nunez, 1999). They all have a CIDE-N/CAD domain and *in vitro* assays suggest that they interact with each other (Inohara and Nunez, 1999). Similarities of dICAD and dCAD to the human homologues are not very high (identity 17% and 22%, respectively) and dICAD can neither inhibit nor work as a folding chaperone of mCAD (Mukae, Yokoyama *et al.*, 2000). Interestingly, Drosophila seems to have only the ICAD-L form which contains one caspase cleavage site (Mukae *et al.*, 2000). Moreover, dCAD has a caspase cleavage site which has to be cleaved together with the caspase

cleavage site within dICAD (Yokoyama, Mukae *et al.*, 2000). dCAD does not have nuclear localization signal (Yokoyama *et al.*, 2000). All these indicate that the activation and regulation mechanism of ICAD/CAD in Drosophila may differ from those of their mammalian counterparts. The functions of Drep-2 and Drep-3 are not known, but they might be involved in the regulation of dICAD/dCAD.

Mammals express other CAD/ICAD related proteins such as CIDE (cell death inducing DFF45 like effector) -A and -B and FSP-27, whose expression pattern is more limited than those of ICAD/CAD (Inohara, Koseki *et al.*, 1998). These proteins share not only the CIDE-N/CAD domain but also another domain, CIDE-C. Overexpression of CIDE-A in 293T cells induced apoptosis and DNA fragmentation. This activity depends on the CIDE-C domain and is not inhibited by caspase inhibitors (Inohara *et al.*, 1998). DFF45 inhibits the CIDE-C apoptosis-inducing activity but requires the CIDE-N domain for the inhibition (Inohara *et al.*, 1998). Mitochondria localization and dimerization are both required for CIDE-B induced apoptosis (Chen, Guo *et al.*, 2000). Although it is proposed that these proteins have a regulatory role in CAD activation, their physiological functions are not known (Inohara *et al.*, 1998).

1.4.7 Chromatin condensation factors

Several proteins have been identified or claimed as chromatin condensation factors during apoptosis, including CAD (chapter 2), topo IIα (chapter 4), mitochondrial flavoprotein AIF (apoptosis-inducing factor), acinus, L-DNase II, Catheptin, DNase I, and DNase II (Sahara, Aoto *et al.*, 1999; Susin *et al.*, 1999; Zamzami and Kroemer, 1999). For example, once apoptosis is induced, AIF translocates from the mitochondria to the nucleus and causes partial chromatin condensation at the periphery of the nucleus. AIF causes degradation of DNA into fragments greater than around 50 kb in length (Susin *et al.*, 1999). Acinus localizes in the nucleus of healthy cells and cleavage of acinus by caspase-3 and an additional (unknown) protease induces chromatin condensation *in vitro*. Acinus does not induce DNA cleavage (Sahara *et al.*, 1999). It is not known why there are so many chromatin condensation factors. These factors might work in a cell/tissue specific manner or work in a co-operative way. They might be redundant to ensure that chromatin condensation occurs in the case that one of the genes is damaged.

1.5 Cell free systems for the study of apoptosis

1.5.1 Advantages of cell free systems

Biochemical analysis of apoptotic pathways would have been difficult without the use of cell free system. Several cell free systems have been devised that recapitulate the morphological changes of apoptosis using components isolated from cells such as nuclei, cytoplasm, and organelles (Lazebnik *et al.*, 1993; Chow, Weis *et al.*, 1995; Earnshaw, 1995; Enari *et al.*, 1995; Martin, Newmeyer *et al.*, 1995; Liu, Kim *et al.*, 1996; Zamzami, Susin *et al.*, 1996).

One advantage of the cell free system approach is that it can overcome the stochastic nature of the onset of apoptotic events in cell populations. Upon receipt of an apoptotic stimulus, cells enter a condemned phase, a latent period during which the cells are committed to apoptosis but show no overt signs of the cell death process. This condemned phase is followed by an execution phase, during which the cells develop the sequential morphological changes characteristic of apoptosis. The condemned phase is highly variable in length among individual cells. Thus, cells harvested at any moment from a culture undergoing apoptosis will be a mixture of those in the condemned phase and those in different stages of the execution phase. This greatly complicates the biochemical analysis of apoptotic events. Biochemical analysis of apoptosis in tissues is even more difficult, since generally less than one percent of cells can be seen as apoptotic at any given time and apoptotic cells are rapidly removed by phagocytosis.

In a cell free system, added exogenous nuclei reproduce apoptotic changes in a highly synchronous manner. Isolated nuclei from healthy cells exhibit nuclear and chromatin condensation and ultimately result in apoptotic bodies. Internucleosomal DNA cleavage is also observed.

1.5.2 S/M extracts

The first cell free system for apoptosis was developed in our laboratory, using extracts from chicken DU249 hepatoma cells committed to apoptosis as a consequence of a 12 hr cell cycle arrest with aphidicolin (Wood and Earnshaw, 1990). After release from the S-phase block, these DU249 cells proceed normally through the reminder of the cell cycle. 8-10 hr after mitosis, the cells begin to enter the apoptotic execution phase and display an apoptotic morphology. To prepare the extracts, condemned phase cells are harvested in the intervening mitosis, at which time they appear normal by both light and electron microscopy. In practice, 6 hr after release from the S-phase block, cells are blocked again in M-phase with nocodazole. Harvested cells are washed, lysed and centrifuged. The highly concentrated cytoplasmic fraction, obtained as a supernatant, was termed S/M extract due to the double block in S-phase and M-phase. The S/M extracts are capable of inducing all morphological and biochemical changes characteristic of apoptosis in isolated nuclei in the presence of an ATP regeneration system (Lazebnik *et al.*, 1993). The entire apoptotic process is inhibited *in vitro* by caspase inhibitors (Lazebnik, Kaufmann *et al.*, 1994) or millimolar concentration of Zn^{2+} (Lazebnik *et al.*, 1993). Although nuclei

from a wide range of healthy cells are used in these studies, the extracts themselves are derived from the cytoplasm of the DU249 cells (Lazebnik *et al.*, 1993), thus supporting the view that cytoplasmic factors and events have an essential role in the apoptotic pathway (Jacobson, Burne *et al.*, 1994; Schulze-Osthoff, Walczak *et al.*, 1994; Nakajima, Golstein *et al.*, 1995; Martins and Earnshaw, 1996; Kroemer, Zamzami *et al.*, 1997).

1.5.3 Contributions of cell free systems to studies of apoptosis

The first two caspase substrates, PARP and lamins were identified employing S/M extracts (Lazebnik *et al.*, 1994; Lazebnik, Takahashi *et al.*, 1995). Since then many other caspase substrates have been identified using a variety of *in vitro* systems (Earnshaw *et al.*, 1999). Moreover involvement of mitochondria in the apoptotic process was first shown in apoptotic Xenopus egg extracts (Newmeyer *et al.*, 1994). Subsequently it was shown that addition of cytochrome *c* and dATP or ATP can convert non-apoptotic extracts to apoptotic extract (Liu *et al.*, 1996). Apaf-1, DFF and CAD which are also key components of apoptosis process were then isolated from such extracts (Liu *et al.*, 1997; Zou *et al.*, 1997; Enari *et al.*, 1998).

In chapter 2, we describe an extention of this approach by preparing extracts from cells at various stages of the apoptotic pathway in order to further evaluate caspase involvement in nuclear disassembly.

1.6 Purpose of this study

1.6.1 Purpose of this study

The aim of this study was to elucidate the biochemical mechanisms which underlie the morphological changes of the nucleus during apoptotic execution. Although caspases are known to play essential roles during apoptosis, it was not clear whether caspases directly drive the nuclear disassembly or whether downstream factors activated by caspases play such a role. In this study, chromatin condensation and DNA fragmentation were employed as an assay for nuclear apoptosis.

1.6.2 Studies with cell free systems

Cell free systems were employed to clarify the role of caspases in nuclear disassembly. These systems have a number of advantages for the study of apoptotic nuclear morphological changes. First, nuclei incubated in the extracts synchronously enter apoptotic execution phase. Second, biochemical approaches such as fractionation and addition of inhibitors are possible. Third, it is possible to prepare extracts which represent different stages of apoptosis such as the condemned and execution phases. The results obtained with these extracts are shown in Chapters 2 and 4.

1.6.3 Localization of CAD and ICAD

Proteins have to be expressed and/or activated at the right time in the right place to control the progression of apoptosis. Following the identification of chromatin condensation factors, it is important to

investigate their localization before and during apoptosis. It was reported that nuclear transport is necessary for nuclear apoptosis in Fas-mediated apoptosis (Yasuhara, Eguchi *et al.*, 1997). Originally CAD and ICAD were isolated from cytosolic extracts. Thus it was claimed that CAD is the factor which is transported into the nucleus upon the onset of apoptosis. This hypothesis was examined in this study (Chapter 3).

1.6.4 Role of topoisomerase IIα in apoptosis

It was suspected that topoisomerase II, which catalyzes DNA topological transformations in normal cells might also involved in chromatin condensation during apoptosis. Recently it was reported that topo IIα is involved in reversible high molecular weight DNA cleavage after oxidative stress (Li, Chen *et al.*, 1999). Indeed this study provided evidence that topo II does have a role during apoptosis (Chapter 4).

Chapter 2

2. Transition from caspase-dependent to caspase-independent mechanisms at the onset of apoptotic execution

2.1 Introduction

The involvement of caspases in apoptosis was first demonstrated in 1990 (Yuan and Horvitz, 1990; Yuan, 1995). Then the first apoptotic substrate of caspases was identified in 1994 (Lazebnik *et al.*, 1994). Within less than seven years, more than three thousand publications treating of caspases appeared and many of the essential features of caspases were revealed. Nonetheless, the role of caspases in the death pathway remains unclear. Recent studies have suggested that under certain circumstances cells can activate caspases without undergoing apoptosis (Boise and Thompson, 1997; Wang and Lenardo, 2000). Conversely, even though caspase inhibitors usually rescue cells from apoptosis (Villa, Kaufmann *et al.*, 1997), cell death can occur in response to proapoptotic stimuli in the presence of these inhibitors (Xiang, Chao *et al.*, 1996; McCarthy, Whyte *et al.*, 1997; Lavoie, Nguyen *et al.*, 1998).

Careful examination revealed that cells dying in the presence of caspase inhibitors display membrane blebbing and cell surface alternations but no dramatic changes in nuclear morphology (McCarthy *et al.*, 1997). This observation suggests that certain cytoplasmic hallmarks of apoptosis

may be triggered by enzymes other than caspases, but that nuclear events require caspase activity. Consistent with this view, cells from caspase-3-null mice (Woo, Hakem *et al.*, 1998) have been reported to display plasma membrane changes and cleavage of the nuclear protein poly(ADP-ribose) polymerase (PARP) when undergoing apoptosis, but not the chromatin condensation and DNA cleavage that are characteristic of apoptosis (Wyllie, 1980).

The preceding observations suggest that caspases play a role in certain apoptotic events, particularly those occurring in the nucleus. However, it is not known whether caspases have an executive role in initiation of the apoptotic pathway and leave the work of actually disassembling the cell to other downstream factors, or whether they are workhorses whose cleavage of key substrates drives cellular disassembly. Support for an executive role comes from the observation that expression of the caspase cleavage product of the actin-binding protein GAS2 triggers cytoskeletal changes similar to those seen in apoptosis (Brancolini, Benedetti *et al.*, 1995). Likewise, caspase cleavage of ICAD/DFF45 (inhibitor of caspase-activated DNase/DNA fragmentation factor) releases the nuclease CAD/DFF40, allowing it to degrade genomic DNA (Liu *et al.*, 1997; Enari *et al.*, 1998; Sakahira *et al.*, 1998). Thus, certain products of caspase cleavage play important downstream roles in apoptotic events. On the other hand, numerous important structural and nonstructural proteins are also directly cleaved by caspases (Cohen, 1997; Nicholson and Thornberry, 1997; Porter, Ng *et al.*, 1997; Villa *et al.*, 1997), supporting the alternative hypothesis that

caspase do the bulk of work of cutting the cell apart themselves (Martin and Green, 1995).

The aim of the present study was to prepare extracts from cells at various stages of the apoptotic pathway in order to further evaluate caspase involvement in nuclear disassembly. Interestingly, extracts prepared from morphologically normal cells in the latent phase (S/M extracts) and those prepared from overtly apoptotic cells ("execution phase extracts") induced similar apoptotic events in exogenous nuclei but exhibited fundamental biochemical differences. In particular, apoptotic events in S/M extracts were abolished by caspase inhibitors as previously reported (Lazebnik *et al.*, 1994); whereas the same events in execution phase extracts were not affected by the inhibitors. Further examination revealed that execution phase extracts contain at least two caspase-activated factors required for nuclear disassembly, one of which appears to be the nuclease CAD. These experiments not only support the view that caspases act in an executive role in nuclear apoptosis by activating downstream factors that disassemble nuclei, but also suggest that activation of the downstream factors (rather than the caspases) accompanies the transition between the latent and execution phases of apoptosis.

2.2 Materials and Methods

2.2.1 Cell treatment and preparation of extracts

Chicken DU249 cells were presynchronized in S phase with aphidicolin for 12 hr, released from the block for 6 hr, and synchronized in mitosis with nocodazole for 3 hr as described previously (Wood and Earnshaw, 1990; Lazebnik *et al.*, 1993). DU249 cells start to undergo apoptosis asynchronously during and after the aphidicolin treatment, presumably as a result of the cell cycle disruption. E/X ("execution" phase) extracts were prepared from the floating cells (mostly apoptotic) obtained from the flasks just before the addition of nocodazole. S/M extracts were prepared from floating cells (>60% mitotic) obtained from the same flasks by selective detachment after the nocodazole treatment. After harvesting of cells for S/M extract production, cells for the preparation of C/D ("condemned" phase) extracts were obtained from the attached (interphase) cells by rinsing the same flasks with PBS-EDTA and trypsinization. Large scale "roller S/M" extract was prepared as described above for S/M extract except that cells were grown in roller bottles.

In each case, the cells were then washed with KPM buffer (50 mM Pipes-KOH, pH 7.0, 50 mM KCl, 10 mM EGTA, 2 mM $MgCl_2$, 20 µM cytochalasin B (Sigma), 1 mM DTT, 0.1 mM PMSF, 1 µg/ml each chymostatin, leupeptin, antipain, pepstatin A) (Wood and Earnshaw, 1990) and centrifuged in a small glass Dounce homogenizer. The cells were subjected to several cycles of freezing and thawing and further disrupted by grinding during each thawing cycle. The cell lysate was then centrifuged at

139,000 x g for 2 hr, yielding clear cytosolic extracts. The protein concentration of each extract was measured by the Bradford assay (Bradford, 1976). Extract concentrations ranged between 12 and 18 mg/ml.

2.2.2 Time course of caspase activation

DU249 cells were subjected to the synchrony procedure used in preparation of S/M extracts. At the indicated times (0, 5, 10, 15, 20 hr) following the addition of aphidicolin, both floating and attached cells were harvested from two T150 flasks (the former by shake-off, the latter by trypsinization). Cells were washed with MDB buffer (10 mM Pipes-KOH, pH 7.0, 50 mM NaCl, 5 mM EGTA, 2 mM $MgCl_2$, 1 mM DTT) (Wood and Earnshaw, 1990) and the number of cells of each sample was counted using a hemacytometer. The ratio of interphase, mitotic, and apoptotic cells in each sample was determined by examination of the nuclear morphology after cells ($n > 400$ for each time point) were fixed in methanol-acetic acid (3:1) for several min at room temperature and stained with 0.5 µg/ml 4,6-diamidino-2-phenylindole (DAPI; Calbiochem). Cells were lysed by the freeze / thaw / grinding protocol described above. Lysates (the supernatants following centrifugation at 13,000 x g for 15 min at 4°C) were affinity labeled with zEK(bio)D-aomk as described below.

2.2.3 *In vitro* apoptosis reaction

Apoptotic and control extracts were preincubated at 37°C for 15 min with 100 µM caspase inhibitors (YVAD-cmk or DEVD-fmk) or diluent. HeLa

nuclei prepared as previously described (Wood and Earnshaw, 1990; Lazebnik *et al.*, 1993) were then added (up to 1.0 x 10^6 nuclei/10 µl of extract) and incubated at 37°C for up to 2 hr in the presence of an ATP regeneration system (Wood and Earnshaw, 1990; Lazebnik *et al.*, 1993). Nuclei were either stained with DAPI to observe chromatin condensation, solubilized in SDS-sample buffer for analysis of protein cleavage, or lysed for analysis of DNA ladder formation (see chapter 2.2.7).

2.2.4 Caspase labeling

Stock solutions (10 mM in DMSO) of caspase inhibitors (YVAD-cmk or DEVD-fmk from Calbiochem) were diluted immediately before use with MDB buffer. Extracts were preincubated at 37°C for 15 min with 100 µM YVAD-cmk or DEVD-fmk or diluent. After Z-EK(bio)D-aomk (Martins, Kottke *et al.*, 1997)that binds to the catalytic site of caspases was added to a final concentration of 1 µM from a 100X stock solution in DMSO, extracts were incubated at 37°C for 15 min. Labelled proteins were subjected to conventional 16% SDS-PAGE (Laemmli, 1970), transferred to nitrocellulose membrane, probed with peroxidase-coupled streptavidin, and visualized by ECL (Amersham Corp.). Since the catalytic site exist in large subunit, it is possible to recognize different caspases by the size of large subunit (Fig 8, 9).

2.2.5 Fluogenic assays of caspases (Performed by the laboratory of Scott Kaufmanns using extracts prepared by me.)

DEVD-AFC cleavage activity was determined by a slight modification of previously described methods (Martins *et al.*, 1997). Extracts were preincubated with caspase inhibitors or diluent for 15 min at 37°C. Samples containing 20-30 µg of various fractions or 25 µg of cytosolic protein (estimated by the Bradford assay) from etoposide-treated K562 leukemia cells (a positive control) were diluted to 50 µl with buffer A (25 mM HEPES (pH 7.5), 5 mM $MgCl_2$, 5 mM EDTA, 1 mM EGTA supplemented immediately before use with 1 mM PMSF, 1 mM DTT, 10 µg/ml pepstatin A, and 10 µg/ml leupeptin), mixed with 225 µl freshly prepared buffer B (25 mM HEPES (pH 7.5), 0.1% (w/v) CHAPS, 10 mM DTT, 100 U/ml aprotinin, 1 mM PMSF) containing 100 µM DEVD-AFC (Enzyme System Products, Dublin, CA), and incubated for 4 hr at 37°C. Reactions were terminated by addition of 1.225 ml ice cold buffer B. Fluorescence was measured in a Sequoia-Turner spectrofluorometer using an excitation wavelength of 360 nm and emission wavelength of 475 nm. After subtraction of fluorescence in blank samples (lacking protein), amounts of the liberated fluorophore were determined by comparison to a standard curve containing 0-1500 pmoles of 7-amino-4-trifluoromethylcoumarin. Control experiments indicated that product release was linear with respect to incubation time and extract protein under the conditions utilized.

2.2.6 PARP and lamin cleavage

After HeLa nuclei (5×10^5 per loading) were incubated in extract for 2 hr at 37°C, the reaction was stopped by the addition of sample buffer.

Samples were boiled at 95°C for 5 min, sonicated briefly, subjected to 10% conventional SDS-PAGE (Laemmli, 1970; Wood and Earnshaw, 1990; Lazebnik *et al.*, 1993), and transferred to nitrocellulose. PARP and its 89 kDa cleavage product were detected with the C-2-10 monoclonal antibody (Lamarre, Talbot *et al.*, 1988). Lamins A/C and their cleavage product were detected with a rabbit polyclonal antibody recognizing the N-terminus of the protein (gift of Larry Gerace). Bound antibody was detected by ECL.

2.2.7 DNA ladder formation

HeLa nuclei (5x 10^5 per loading) were incubated for 1-2 hr in extract, centrifuged, and lysed in DNA lysis buffer (50 mM Tris:HCl pH 8.0, 10 mM EDTA, 0.5% Sarcosyl, 0.5 mg/ml proteinase K) at 50°C for 1 hr. DNA was treated with RNase at 50°C for 1 hr, phenol/chloroform extracted, ethanol-precipitated overnight at -70°C, resuspended in TE, and loaded onto 1% agarose gels containing 0.5 µg/ml ethidium bromide.

2.2.8 Plasmid DNA digestion assay

Extracts (18 -36 µg protein in 10 µl of KPM buffer) supplemented with an ATP regeneration system (Wood and Earnshaw, 1990) and 100 µM DEVD-fmk (or diluent) were incubated at 37°C for 15 min. Following addition of 160 ng purified GST-ICAD (Sakahira *et al.*, 1998), incubation was continued for an additional 10 min at 37°C. Upon addition of substrate (pBluescript - 1.2 µg), incubation was continued for 30 min. at 37°C. DNA extraction and electrophoresis were then performed as above. Southern

blotting best saw the results of the preincubation assay (Fig. 11). DNA agarose gels were denatured for 30 min with denaturing buffer (1.5 M NaCl, 0.5 M NaOH), neutralized for 30 min with neutralizing buffer (0.5 M Tris:HCl pH 7.5, 1.5 M NaCl, 0.001 M EDTA), and transferred to nylon membrane (Hybond-N -- Amersham corp.) with 20 X SSC buffer. The nylon membrane was UV crosslinked and hybridized (Church and Gilbert, 1984) with a pBluescript probe that was labeled with ^{32}P using the Megaprimer system (Amersham). The film was exposed for 1 hr at -80°C with an intensifying screen.

2.2.9 Electron Microscopy (Steps after fixation were performed by Carol Cooke)

Isolated HeLa cell nuclei incubated in extract or MDB buffer were centrifuged, washed with MDB buffer, placed on adhesion slides (Marienfeld) for 5 min and fixed for 30 min with 2% glutaraldehyde in Dulbecco's PBS pH 7.4. After fixation the nuclei were washed in 0.1 M cacodylate buffer, and postfixed with 4% OsO_4 in 0.1 M sodium cacodylate pH 7.4 for 30 min. Prestaining was done with 3% uranyl acetate in H_2O for 1 hr. The nuclei were dehydrated in ethanol (30%-100%) and embedded in Araldite resin (Agar). Gold sections were cut with a Reichert microtome and placed on copper grids. Images were photographed on a Philips CM100 Biotwin electron microscope.

2.2.10 Expression and purification of double mutant His_6-ICAD

The method used for mutation was the PCR-based megaprimer strategy (Seraphin and Kandels-Lewis, 1996). Caspases absolutely require aspartic acid at the cleavage site, and mutation from D to E produces a caspase-uncleavable mutant. Primer 1 (T7 primer), primer 2 (5'-GCCCTGCTCTCAGGCTCATC-3'), and primer 3 (5'-CAGCTCTGCACATGGGATGTC-3') were used to generate the DEPD^{117}E mutation in the ICAD cDNA in pBluescript. Primer 4 (5'-CTGCTGTCAGAAGAGGACCTC-3'), primer 5 (5'-GCCGACGCCTGTCTCAACTGC-3'), and primer 6 (T3 primer) were used to generate the DAVD^{224}E mutation in ICAD. Pirmers 2 and 5 contain the mutated sequences which are underlined. A second mutation in primer 2 (A) was introduced for selection with a restriction enzyme and did not change the amino acids. Each single mutant was digested with Eco47 III (NEB) and Xba I (NEB) then ligated to generate double mutant ICAD in pBluescript. This double mutant ICAD was digested with Spe I, blunt-ended with T4 DNA polymerase (NEB) plus 100 μM dNTPs, and digested with Kpn I (NEB). The resulting fragment was ligated into pRSET B (Invitrogen) that had been digested with Hind III, blunt-ended with T4 DNA polymerase, and digested with Kpn I. Double mutant ICAD in pRSET B was transformed into *E. coli* BL21 (DE3)Lys S cells. Transformed cells were grown to OD_{600} = 0.5-0.7 and protein expression was induced with IPTG (1 mM) for 3-4 hr. Cells were collected by centrifugation at 5000 x g for 10 min and frozen at -80°C. The cell pellet was thawed on ice for 15 min and resuspended in lysis buffer (50 mM NaH_2PO_4 pH7.5, 300 mM NaCl, 10 mM

imidazole). Lysozyme was added to 1 mg/ml and the suspension was incubated on ice for 30 min, sonicated on ice until 80% of the cells were disrupted, and then centrifuged at 4000 x g for 20 min at 4°C. The supernatant was incubated on a rotating mixer for 1 hr at 4°C with 0.5 ml of Ni-agarose (Qiagen) that had been pre-equilibrated with lysis buffer. The resin was then loaded onto a polyprep chromatography column (Bio-rad) and washed twice with 4 ml of wash buffer (50 mM NaH_2PO_4 pH7.5, 300 mM NaCl, 20 mM imidazole). Protein was eluted four times with 0.5 ml of elution buffer (50 mM NaH_2PO_4 pH7.5, 300 mM NaCl, 250 mM imidazole). All samples were subjected to SDS-PAGE and examined by Coomassie blue staining. The eluted protein was dialyzed for at least 3 hr against two changes of CAD buffer (10 mM Hepes pH 7.4, 50 mM NaCl, 5 mM EGTA, 2 mM $MgCl_2$, 1 mM DTT), aliquoted, and frozen in N_2(l).

2.2.11 Expression and purification of His_6-ICAD/CAD

To express active CAD in *E. coli*, we constructed a bicistronic expression vector in which His_6-ICAD was expressed upstream of CAD. In addition to the N-terminal histidine tag, the ICAD open reading frame was engineered to change the stop codon to TAA, and to insert a Shine-Delgarno sequence (GGAAT) downstream of the stop codon. The wild-type ICAD cDNA in pBluescript was digested with Spe I, blunt-ended with T4 DNA polymerase, and digested with Kpn I. The resulting fragment was ligated into pRSET B that had been digested with Hind III, blunt-ended with T4 DNA polymerase, and digested with Kpn I. The coding region of the CAD

cDNA was extracted from the full length CAD cDNA in pBluescript by PCR using Vent polymerase (NEB) with primer 7 (5'-GGAATTCATGTGCGCGGTGCTCCG-3') and primer 8 (5'-GCGAAGCTTTCACTAGCGCTTCCGAG-3'). The PCR product was digested with Eco RI and Hind III and the resulting fragment was ligated into pBluescript.

To create the C-terminus of ICAD (from the Bsm I site at nucleotide 909) engineering in a TAA stop codon and Shine-Delgarno sequence, primer 9 (5'-GGAAGATCTGCATTCACTCAGGAATC-3') and primer 10 (5'-GGAATTCCTCCTTACGAGGAGTCTCGTTTG-3') were used with Vent polymerase. The PCR product was digested with Bgl II (NEB) and Eco RI and ligated into pRSETB that had been digested with Bgl II and Eco RI. The CAD coding sequence in pBluescript was digested with Eco RI and Hind III and ligated into pRSET B containing the newly modified C-terminus of ICAD with the Shine-Delgarno sequence. This intermediate was then digested with Nhe I and Bsm I, and into it was inserted the His-tagged amino-terminal portion of ICAD, obtained from ICAD in pRSETB that had likewise been digested with Nhe I and Bsm I. This bicistronic vector His_6-ICAD/CAD in pRSET B was transformed into *E. coli* BL21 (DE3)Lys S cells. Protein was expressed and purified by nickel chelate chromatography as described above for double mutant ICAD. The dialyzed ICAD/CAD protein was either frozen directly in $N_2(l)$ or was frozen following addition of glycerol to 40%.

2.2.12 *In vitro* apoptosis with purified CAD

50 µl reactions contained various combinations of the following reagents added sequentially (see legend to Fig. 12): 10 µl ICAD/CAD protein (stored in CAD buffer plus 40% glycerol), 5 µl caspase-3, an ATP regeneration system (final conc. 0.8 mM ATP, 4.5 mM creatine phosphate, 22.5 µg/ml creatine kinase), DEVD-fmk (final conc. 300 µM), double mutant ICAD protein (2 µg), and CAD buffer as needed to make up the final volume. ICAD/CAD complexes were preincubated with caspase-3 at room temperature (approx. 25°C) for 30 min to cleave wild-type ICAD and release active CAD. At the end of this preincubation, diluent, DEVD-fmk or double mutant ICAD were added (defined as t = 0); and the mixture was divided into three aliquots to assay various apoptotic events. To examine ICAD cleavage during the preincubation, a 10 µl aliquot was mixed with sample buffer, boiled, resolved by SDS-PAGE, transferred to nitrocellulose membranes, and probed with ICAD antibody (chapter 3), which was detected by ECL (Amersham). To assay CAD activity against a plasmid DNA substrate, a 6 µl aliquot was supplemented with 0.35 µg pBluescript, BSA (final conc. 1 mg/ml) and 4 µl of CAD buffer. This mixture was further incubated at 37°C for 30 min, extracted with phenol-chloroform, and analyzed on a 1% agarose gel containing ethidium bromide. To examine the ability of the active CAD to induce apoptotic events, HeLa nuclei (1.3×10^6 per sample) in 10 µl CAD buffer were combined with the remaining 34 µl and incubated at 37°C for 2 hr. At the end of this incubation, 1 µl of the reaction mixture was stained with DAPI so that nuclear morphology could

be examined by fluorescence microscopy (> 100 nuclei counted per slide). The remaining HeLa nuclei in 43 µl of reaction mixture were centrifuged and prepared for agarose gel electrophoresis as described above.

2.3 Results

2.3.1 Extracts from three different stages of apoptosis.

The apoptotic pathway can be conceptually divided into at least three stages (Fig. 8A). Upon receipt of a proapoptotic signal, cells enter a "condemned" stage: the death program is initiated, but cells can be rescued by various survival factors. Once cells pass a "point of no return", they are in the "committed" stage and can no longer be rescued. During both of these stages, preapoptotic cells appear morphologically normal. Eventually, committed cells undergo an abrupt transition into apoptotic execution, a period lasting 5 min - 1 hr. during which cellular disassembly and death occur. It is not known where along this pathway caspases are activated and at what point the caspases activate other downstream factors that act during disassembly of the cell.

It was previously noted that active caspases could be detected in extracts from etoposide-treated HL-60 cells several hours before the bulk of the cells in the culture exhibited an overtly apoptotic morphology (Martins *et al.*, 1997). In order to study this phenomenon in greater detail, chicken DU249 cells were collected at various times after subjecting cultures to a synchronization protocol (Fig. 8B) shown previously to induce an apoptotic response in this cell line (Lazebnik *et al.*, 1993). Floating cells obtained 10-15 hr after the addition of aphidicolin were largely (~ 50%) apoptotic and contained high levels of active caspases, as detected by reactivity with the affinity-labeling reagent zEK(biotin)D-aomk (Martins *et al.*, 1997) (Fig. 8 C,D). Floating cells harvested following a change of medium and a two

hour treatment with nocodazole to induce a mitotic block, were predominantly (> 60 %) mitotic, with only 10 - 20 % of apoptotic cells. Despite the normal appearance of these cells, extracts prepared from them also contained high levels of active caspases. Cells that remained attached throughout the protocol were almost entirely in interphase, and extracts prepared from them lacked caspases detectable with zEK(biotin)D-aomk (Fig. 8D, left), although low levels of caspase activity were detectable when more sensitive assays were used (see below).

The results of this experiment suggested that it might be possible to use a similar protocol to prepare extracts sequentially from the same flasks of cells at different stages of apoptosis (see Fig. 9A). C/D ("condemned" phase) extracts were prepared from the morphologically normal attached cells that did not enter mitosis or apoptosis during the synchrony procedure. Previous studies have indicated that these cells ultimately undergo apoptosis if left in culture (Lazebnik *et al.*, 1993). S/M ("committed" phase) extracts (Lazebnik *et al.*, 1993) were prepared from morphologically normal mitotic cells at the conclusion of the synchrony procedure. Because these cells are destined to rapidly undergo apoptosis if left in culture (Lazebnik *et al.*, 1993), we postulate that S/M extracts reproduce events from the committed stage of apoptosis. E/X ("execution" phase) extracts were prepared from cells that were frankly apoptotic after a 12 hr exposure to aphidicolin followed by a 6 hr recovery period in medium. (Note that nonadherant cells were discarded at the end of the aphidicolin treatment, so these cells must have entered apoptosis during the 6 hr recovery period).

To examine the spectrum of active caspases during the three stages of apoptosis, extracts were assayed for their ability to cleave DEVD-AFC, for affinity labeling with z-EK(bio)D-aomk (Martins *et al.*, 1997), and for the ability to cleave known caspase substrates in added nuclei. Collectively, these assays detect all known caspases. DEVD-AFC contains the preferred cleavage site of caspases-3 and 7 (Duan, Orth *et al.*, 1996; Talanian, Quinlan *et al.*, 1997) but is also cleaved by caspases-1, -2, -4, -6, -8 and -10 (Fernandes-Alnemri, Litwack *et al.*, 1995; Fernandes-Alnemri, Takahashi *et al.*, 1995; Boldin, Goncharov *et al.*, 1996; Fernandes-Alnemri, Armstrong *et al.*, 1996; Srinivasula, Fernandes-Alnemri *et al.*, 1996; Talanian *et al.*, 1997). z-EK(bio)D-aomk covalently modifies all caspases tested to date (Martins *et al.*, 1997) and can detect over 30 active caspase species in apoptotic human leukemia cells. PARP is a documented substrate of caspases-3, -7, -8, and -9 (Fernandes-Alnemri *et al.*, 1995; Fernandes-Alnemri *et al.*, 1995; Nicholson, Ali *et al.*, 1995; Tewari, Quan *et al.*, 1995; Duan *et al.*, 1996; Muzio, Chinnaiyan *et al.*, 1996), while lamin A is a substrate of caspase-6 (Takahashi, Alnemri *et al.*, 1996). Application of these assays to C/D ("condemned" phase) extracts revealed low but detectable levels of active caspases (125-fold less than S/M or E/X extracts in the DEVD-AFC assay, Fig. 9B) and some ability to cleave PARP (Fig. 9D, lane C/D), but no evidence of z-EK(biotin)D-aomk labeling or lamin cleavage, suggesting that the latter assays are less sensitive. In contrast, S/M and E/X extracts contained high levels of active caspases that cleaved DEVD-AFC as well as PARP and lamin A (Fig. 9 B, D); and both had a similar pattern of active caspases following

affinity-labeling with z-EK(bio)D-aomk (Fig. 9C). These correspond primarily to active forms of caspases-3 and -6 (Faleiro, Kobayashi *et al.*, 1997; Martins *et al.*, 1997). All caspase activity detectable in these assays was quantitatively inactivated by treatment with YVAD-cmk (Fig. 9 C, D) or DEVD-fmk (Fig. 9 B-D).

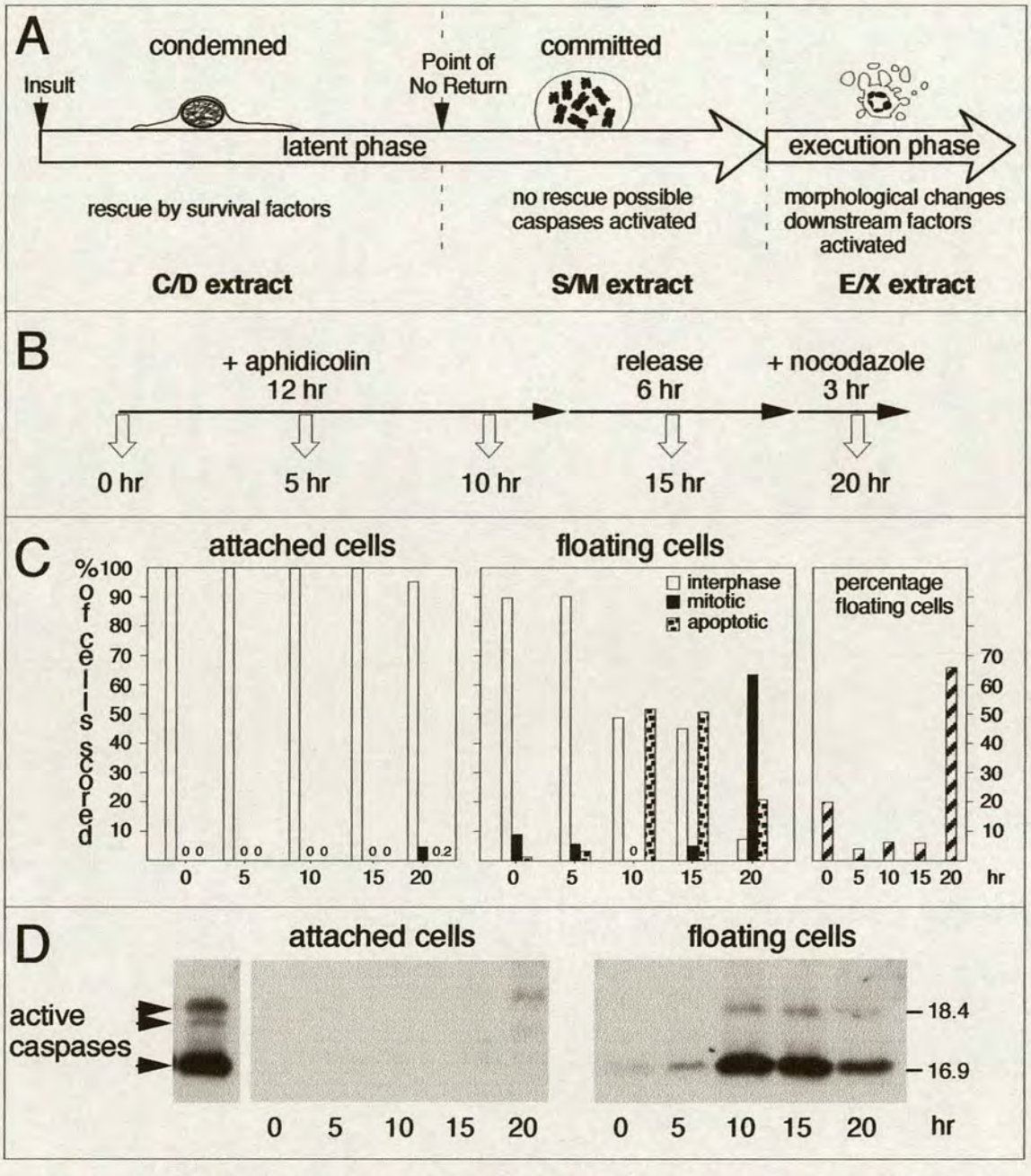

Figure 8. Panel A: Diagram of apoptosis as a three stage process, with the latent phase being subdivided into condemned and committed stages. **Panel B:** The protocol used for harvesting of samples for examination of caspase activation. After addition of the aphidicolin, floating and attached cells were collected separately at every 5 hr. The relation between activation of caspases and nuclear morphology were compared in panel B and C. **Panel C:** The cells harvested as in panel B were scored for their nuclear morphology, based on DAPI staining (n>400/sample). **Panel D:** Affinity labeling of active caspases in whole cell lysates prepared from cells harvested as in panel B. Left panel, attached cells. Right panel, floating cells. The left most lane shows the profile of active caspases in S/M extract.

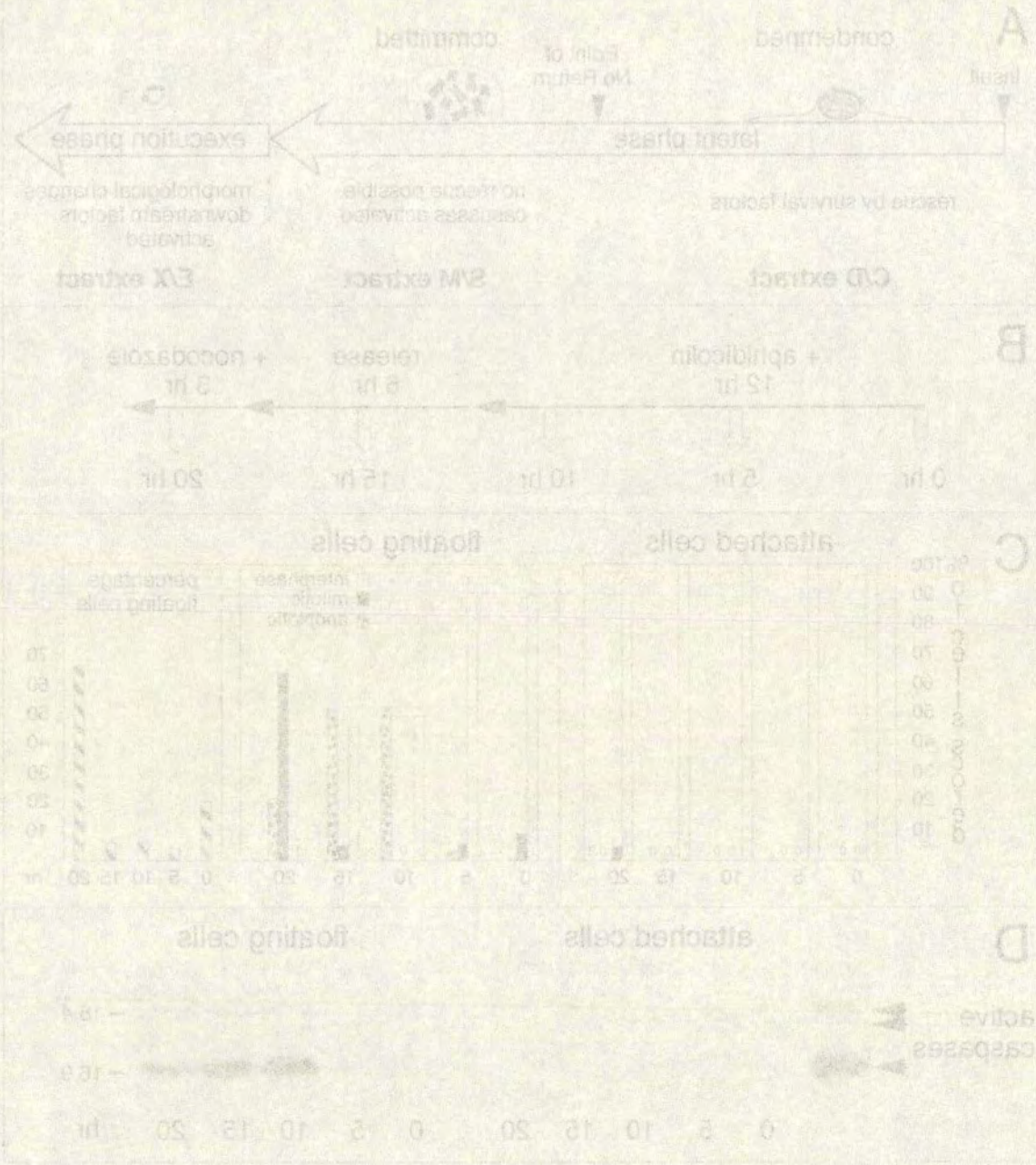

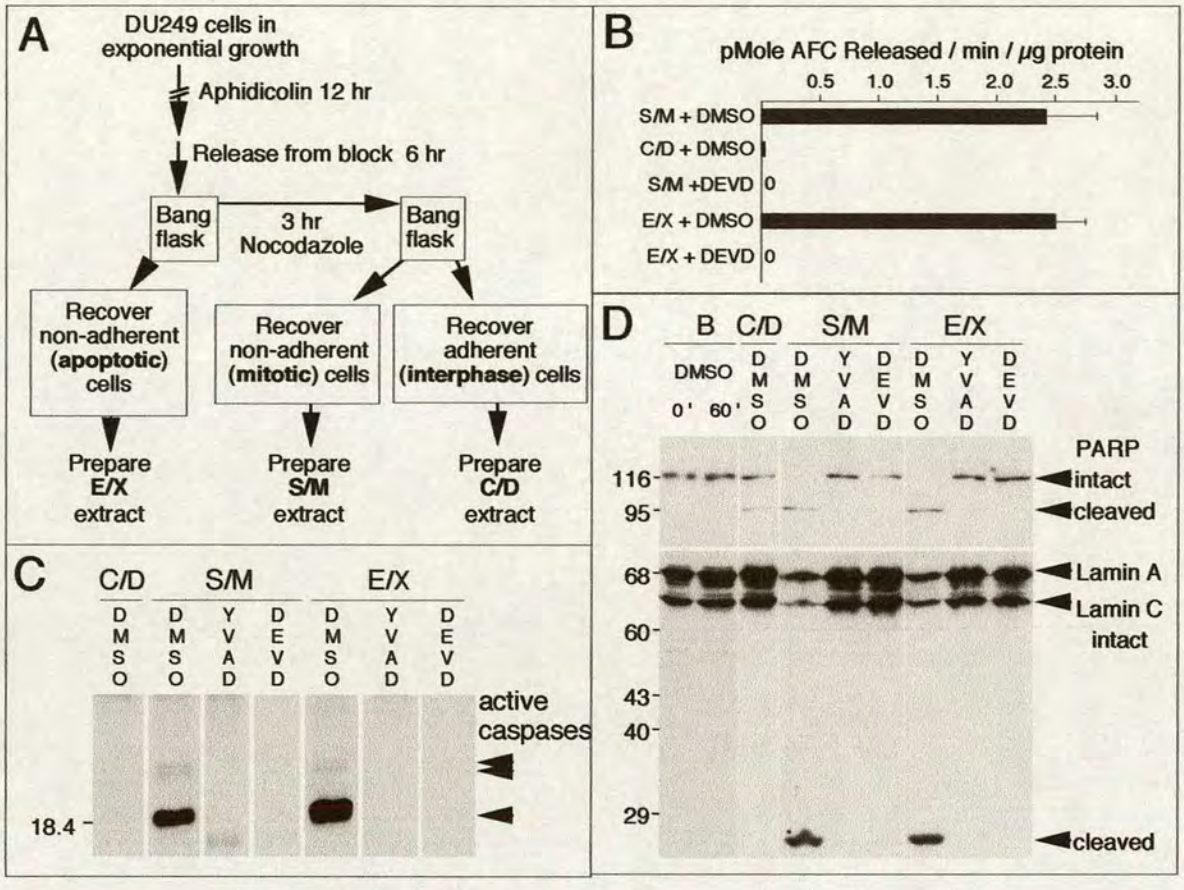

Figure 9. Apoptotic extracts contain active caspases that are functionally inactivated by specific inhibitors. **Panel A:** Protocol used to prepare C/D ("condemned" phase), S/M ("committed phase") and E/X ("execution phase") extracts. **Panel B:** Quantitative analysis of DEVD-AFC cleavage activity in the various extracts. DEVD-fmk treatment of S/M and E/X extracts reduces caspase activity by at least 250- and 150- fold, respectively. Note the low but non-zero level of caspase activity in the C/D extracts. (Experiments in this panel were performed by the laboratory of Scott Kaufmann using extracts prepared by me.) **Panel C:** Several active caspases were labeled with zEK(biotin)D-aomk in S/M and E/X extracts. This labeling was completely blocked by prior incubation of extracts with YVAD-cmk and DEVD-fmk (both at 100 µM). **Panel D:** PARP and Lamin A/C cleavage by caspases in the cell-free extracts is abolished following caspase inactivation with YVAD-cmk and DEVD-fmk. Note that low levels of caspases in the C/D extract cause some PARP cleavage, but fail to cleave lamins.

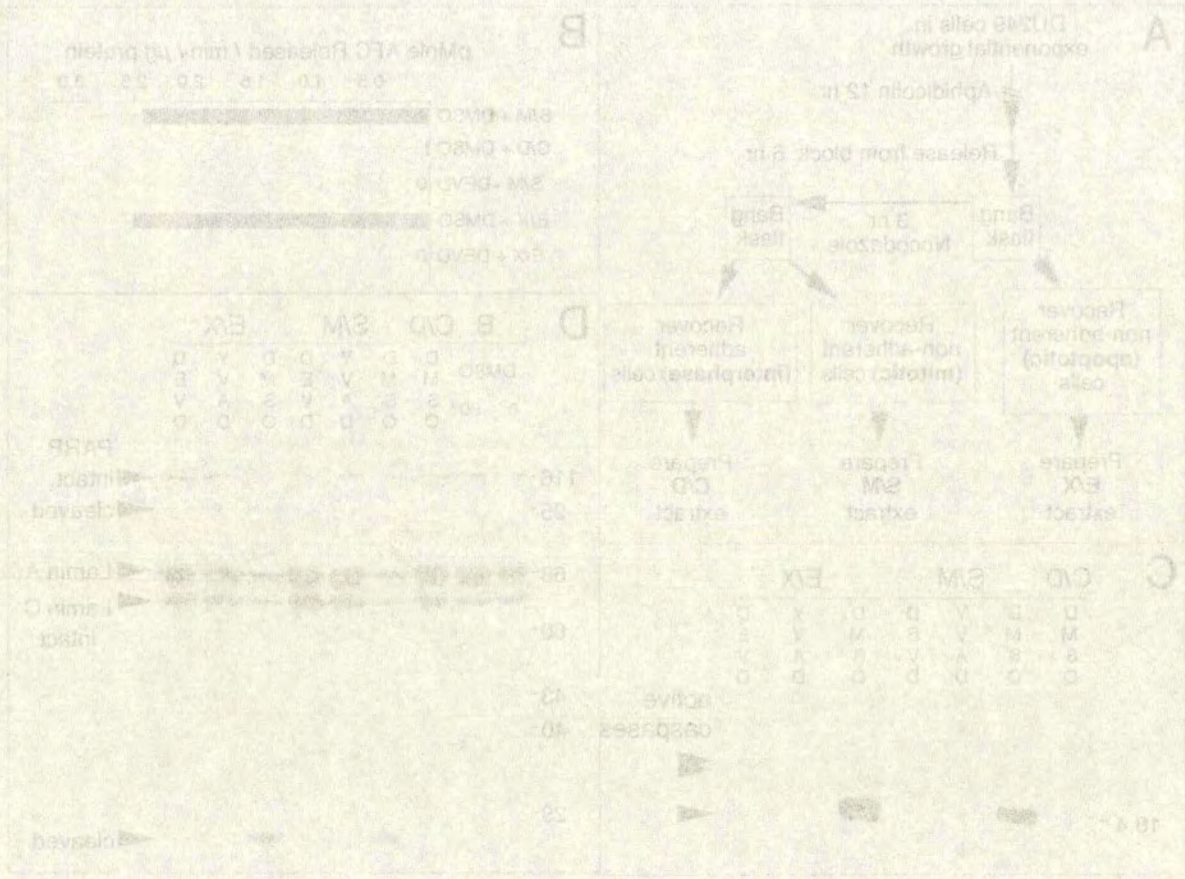

2.3.2 Differences in dependence of S/M and E/X extracts on ongoing caspase activity.

C/D extracts ("condemned" phase) were unable to induce internucleosomal DNA fragmentation and apoptotic morphological changes in exogenous nuclei in spite of the weak caspase activity (Fig. 10 A, B). In contrast, S/M ("committed" phase) and E/X ("execution" phase) extracts showed strong caspase activity and nuclease activity and induced hallmark biochemical and morphological changes of apoptosis such as nuclear and chromatin condensation and DNA ladder formation in added nuclei. Further studies focused on these latter two extracts.

Despite the similarities of the S/M and E/X extracts in terms of caspase activity (Fig. 9) and effects on exogenous nuclei (Fig. 10A,B), the two extracts displayed strikingly different properties following inhibition of the endogenous caspase activity. Pretreatment of S/M extracts with DEVD-fmk or YVAD-cmk prior to addition of nuclei not only inhibited caspase activity (Fig. 9 B-D), but also completely abolished their ability to produce internucleosomal DNA fragmentation (Fig. 10A) and induce morphological apoptotic changes (Fig. 10B). In striking contrast, E/X extracts that had been pretreated with caspase inhibitors continued to strongly induce internucleosomal DNA degradation (Fig. 10A), chromatin condensation and fragmentation of added nuclei (shown both by light and electron microscopy - Fig. 10 B, C) despite a lack of detectable caspase activity (Fig. 9 B-D). My criteria of "non-apoptosis" and "apoptosis" in *in vitro* apoptosis is based on DAPI-stained nuclear morphologies, which are shown in figure 10D.

Figure 10. Caspase inhibitors block apoptosis in S/M but not E/X extracts. **Panel A.** Inhibition of caspases blocks nuclease activity in S/M ("committed phase") extracts but not E/X ("execution phase") extracts. As expected, C/D ("condemned" phase) extracts lack detectable nuclease activity. Experiments shown in Fig. 14 confirm that the nuclease activity is inhibitable by the specific CAD inhibitor ICAD/DFF45 (Enari et al. 1998; Liu, Zou et al. 1997). B- buffer control. **Panel B.** Inhibition of caspases abolishes morphological apoptosis *in vitro* in S/M extracts but not E/X extracts. Nuclei shown in panel B were selected at random. Bar - 5 μm. **Panel C.** Morphological changes characteristic of apoptosis occur in E/X extracts independent of caspase activity: confirmation of apoptotic morphology by electron microscopy. Arrows indicate regions of condensed chromatin. Bar - 1 μm. **Panel D.** Criterian of "non-apoptotic" and "apoptotic" in nuclear morphology stained by DAPI. Apoptosis was defined by chromatin condensation to nuclear periphery or formation of apoptotic bodies.

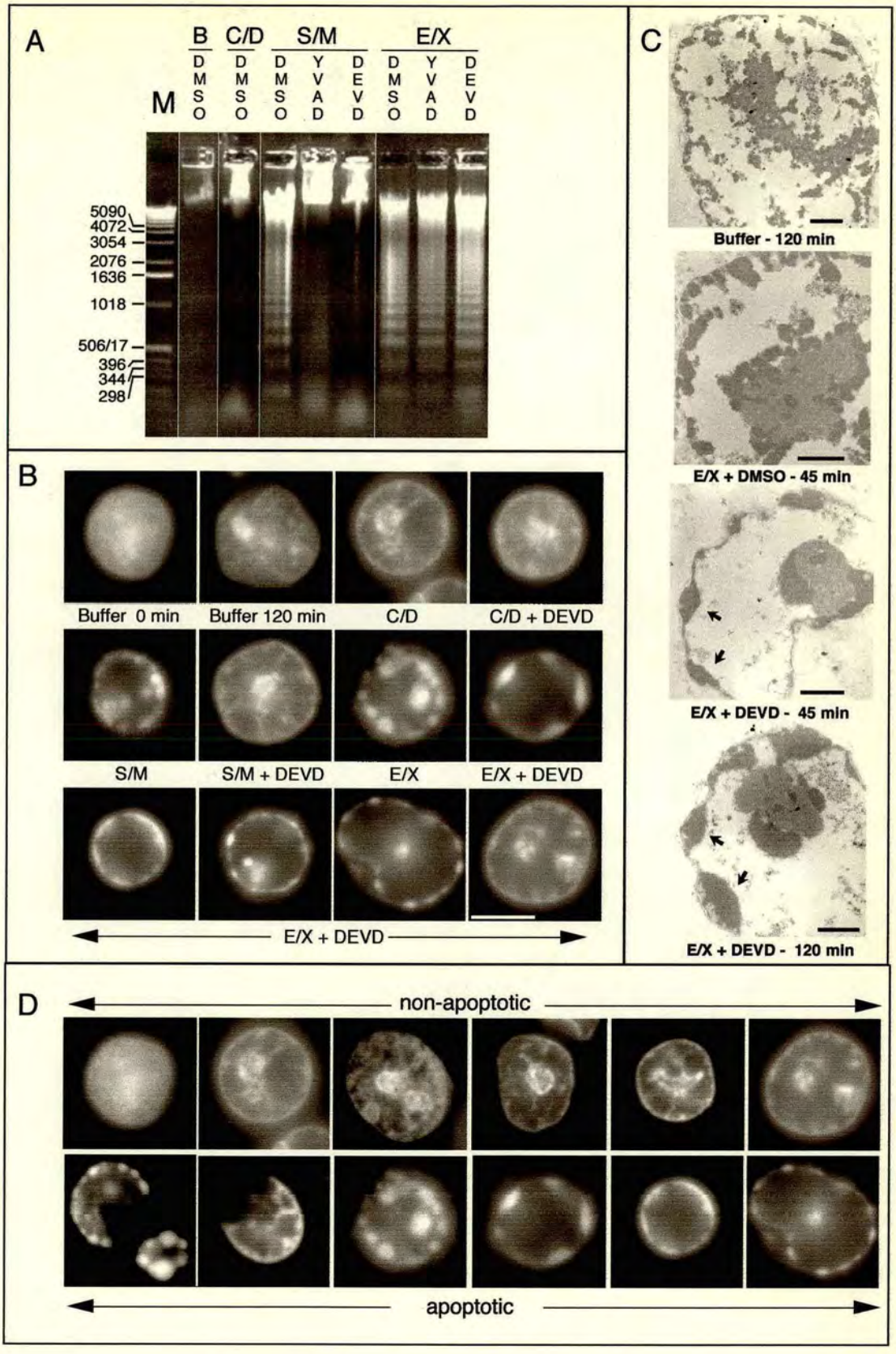
A
B
C/D
S/M
E/X
DMSO
DMSO
DMSO
YVAD
DEVD
DMSO
YVAD
DEVD
M
5090
4072
3054
2076
1636
1018
506/17
396
344
298
B
Buffer 0 min
Buffer 120 min
C/D
C/D + DEVD
S/M
S/M + DEVD
E/X
E/X + DEVD
E/X + DEVD
C
Buffer - 120 min
E/X + DMSO - 45 min
E/X + DEVD - 45 min
E/X + DEVD - 120 min
D
non-apoptotic
apoptotic

2.3.3 Comparison of CAD activation in S/M and E/X extracts.

Because the results presented in Figs. 9 and 10 suggest that the program of nuclear disassembly -- one of the distinguishing features of apoptotic cell death under physiological conditions (Wyllie, 1980; Wyllie, Kerr *et al.*, 1980)-- is initiated by caspase activity but does not require the ongoing participation of caspases for its successful execution, we next turned our attention to caspase-activated downstream activities that might participate in nuclear disassembly. One of these activities is CAD/CPAN, the caspase-activated deoxyribonuclease recently identified in murine and human cells undergoing apoptosis (Enari *et al.*, 1998; Halenbeck *et al.*, 1998). Both S/M and E/X extracts contain an endogenous DNase activity that degrades added plasmid DNA (Fig. 11A lanes 1, 4). Addition of 160 ng of murine ICAD to the extracts abolished this DNase activity (lanes 2, 5), indicating that this activity is functionally homologous to CAD.

Even though CAD-like activity could be inhibited by ICAD in both S/M and E/X extracts, this activity appeared to be regulated differently in the two extracts. DEVD-fmk pretreatment abolished CAD-like activity in S/M ("condemned phase") extracts (Fig. 11A lanes 1, 3), but had no effect on CAD activity in E/X ("execution phase") extracts (Fig. 11A lanes 4, 6). There are at least two potential explanations for this difference. First, active CAD might be unstable in S/M extracts, and might therefore require a constant source of caspase activity in order to continue to generate active enzyme from CAD/ICAD complexes. Second, despite the presence of high levels of endogenous caspases in S/M extracts, the CAD in these extracts might

initially be largely in the form of inactive CAD/ICAD complexes. Active CAD might be released from these complexes by caspase activity during the incubation with DNA substrates.

To distinguish between these possibilities, S/M and E/X extracts were incubated at 30°C for various times in order to allow cleavage of endogenous ICAD by endogenous caspases before adding DNA in the presence or absence of DEVD-fmk (see the experimental protocol in Fig. 11B). This experiment indicated that CAD activity was initially low in S/M extracts but increased gradually with incubation at 30°C (Fig. 11C lanes 1-5). Once activated, CAD was stable in the presence of DEVD-fmk (lanes 1'-5'). In contrast, CAD was fully active at all times in E/X extracts in the presence and absence of DEVD-fmk (Fig. 11D). Collectively, these results indicate that CAD is present but inactive in extracts prepared from "committed" stage cells, and is activated in equivalent extracts prepared from execution phase cells. In addition, this result confirms that the apoptotic activities present in S/M extracts are not due solely to the presence of low levels of contaminating apoptotic cells, since these cells would be expected to have high levels of active CAD.

Figure 11. Differences in the activity of the CAD-like nuclease in S/M and E/X extracts. **Panel A:** CAD-like nuclease in S/M extracts is sensitive to DEVD-fmk, whilst that in E/X extracts is not. Apoptotic extracts cleave a plasmid substrate at 37°C (lanes 1, 4). The nuclease responsible is inhibited by purified murine GST-ICAD (lanes 2, 5), and therefore is functionally related to murine CAD (Enari *et al.*, 1998). In S/M extracts, but not E/X extracts, the nuclease is abolished by addition of DEVD-fmk together with the plasmid DNA (lanes 3, 6). **Panel B:** Diagram of experimental protocol designed to test whether the CAD-like enzyme is active in both S/M and E/X extracts prior to the incubation with DNA. S/M and E/X extracts were preincubated for various length of time at 30°C. Then after addition of plasmid (substrate of CAD-like enzyme), the extracts was further incubated for 30 min at 37°C in the presence or absence of DEVD-fmk. Then Results is shown in panel C. **Panel C:** In S/M extracts, the CAD-like activity increases during pre-incubation of the extract at 30°C prior to addition of the plasmid DNA (lanes 1-5). This activity is now insensitive to the addition of DEVD-fmk at the time of plasmid addition (lanes 1' - 5'). Bracket labeled 'Frags" indicates the products of CAD-like enzyme. **Panel D:** In contrast, preincubation has no effect on the cleavage of plasmid substrate by E/X extracts (lanes 1-5), which is likewise resistant to inhibition with DEVD-fmk (lanes 1'-5'). Lane D - added plasmid DNA alone. Bracket labeled 'Frags" indicates the products of CAD-like enzyme.

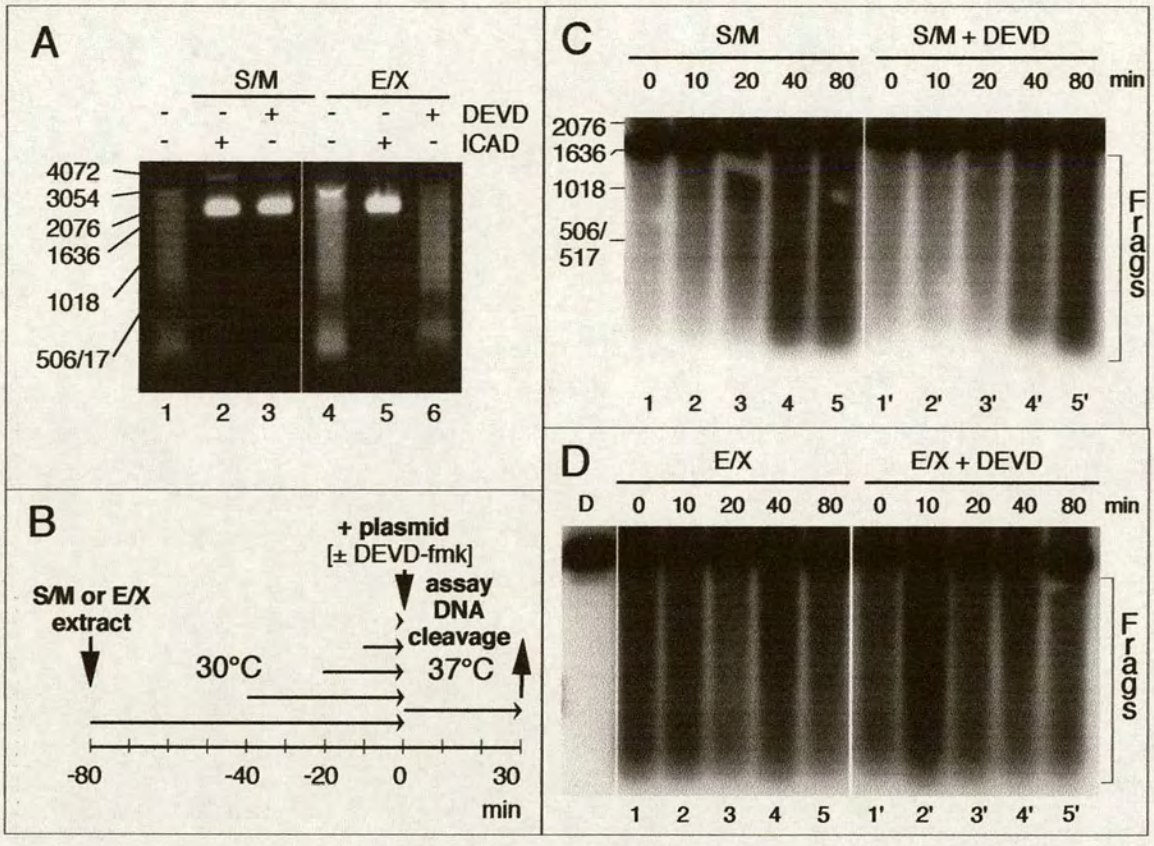
A
S/M
E/X
DEVD
ICAD
4072
3054
2076
1636
1018
506/17
1 2 3 4 5 6
B
+ plasmid
[± DEVD-fmk]
S/M or E/X extract
assay DNA cleavage
30°C
37°C
-80 -40 -20 0 30
min
C
S/M
S/M + DEVD
0 10 20 40 80 0 10 20 40 80 min
2076
1636
1018
506/517
Frags
1 2 3 4 5 1' 2' 3' 4' 5'
D
E/X
E/X + DEVD
D 0 10 20 40 80 0 10 20 40 80 min
Frags
1 2 3 4 5 1' 2' 3' 4' 5'

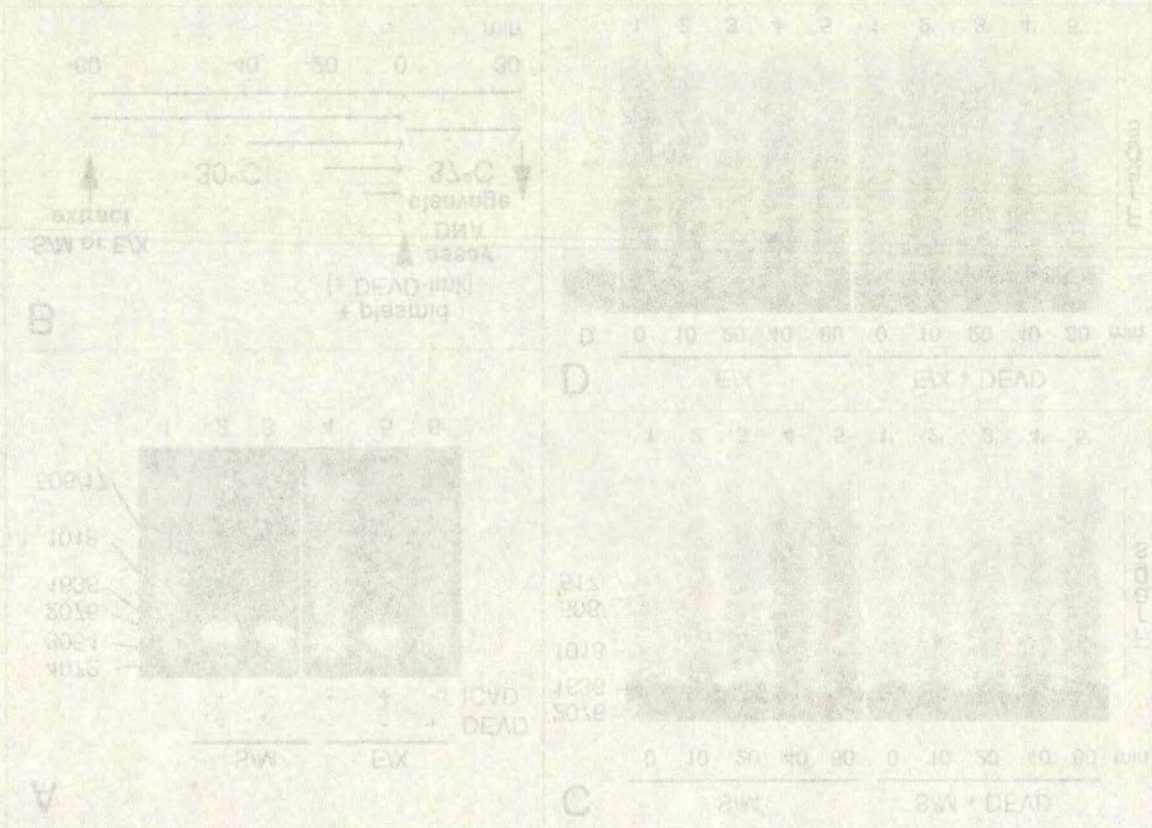

2.3.4 CAD alone is capable of inducing apoptotic morphology in added nuclei.

Collectively, the results presented in Figs. 10 and 11 suggest that CAD might be a major factor that acts downstream of caspases to induce changes in nuclear structure during apoptotic execution. To examine this possibility in greater detail, we exposed isolated nuclei to partly purified cloned murine CAD. Active CAD was expressed in *E. coli* using a bicistronic vector, which ensured that the CAD was translated in the presence of an excess of ICAD (Enari *et al.*, 1998). The resulting CAD/ICAD complex was purified by nickel chelate chromatography and then tested for activity against plasmid and nuclear substrates according to the experimental protocol shown in Fig. 12A. Results obtained with the plasmid substrate are shown in Fig. 12B. The CAD/ICAD complex purified from *E. coli* became activated following a preincubation of 30 min at 25°C either in the absence (Fig. 12B, lane 4) or presence (lane 6) of purified recombinant caspase-3. We assume that activation in the absence of added caspase is due to the presence of contaminating protease activity from the E. coli lysate. Addition of double mutant ICAD (Sakahira *et al.*, 1998) at the start of the preincubation blocked CAD activation in both the absence (lane 5) and presence (lane 7) of caspase-3. Double mutant ICAD also blocked CAD activity if added at the end of the preincubation (lane 8). In contrast, DEVD-fmk blocked CAD activation if added at the start of the preincubation (lane 9) but had no effect if added after cleavage of ICAD (lane 10).

The results obtained with the plasmid substrate were exactly duplicated when we examined the ability of bacterially expressed CAD to induce DNA ladders and morphological changes in HeLa nuclei (Fig. 12 B, C). These morphological changes were confirmed by electron microscopy, where condensed chromatin domains could be seen to be closely to the nuclear envelope (Fig. 13). When CAD was fully active, as detected using either plasmid or nuclear substrates, the enzyme strongly induced condensation of chromatin at the periphery of added nuclei (Fig. 12 lanes/panels 4 and 6). Higher levels of CAD induced the complete disassembly of nuclei into apoptotic bodies (data not shown); however, under these conditions nucleosomal ladders were no longer seen (the DNA was fully degraded). Interestingly, the addition of DEVD-fmk at time T=0 slightly inhibited the morphological apoptosis (Fig. 12 panel 10), although examples of fully apoptotic nuclei could still be seen. It is important to note that caspase-3 alone was unable to induce either DNA cleavage or apoptotic morphology in added nuclei (lanes/panel 3).

Figure 12. Bacterially expressed CAD is capable of inducing apoptotic morphology in added nuclei in the absence of apoptotic extract. **Panel A:** Diagram of the experimental protocol. After CAD was activated during a preincubation with purified caspase-3 at 25°C, substrates were added and incubated for various times with the active enzyme at 37°C. **Panel B:** Effects of various incubations on CAD nuclease activity using either a purified plasmid substrate (pBluescript - upper panels) or added nuclei (lower panels). The morphology of the nuclei in these same incubations is shown in **Panel C**, where the panel numbers refer to lanes in Panel B. Nuclei in buffer at time 0 (panel 0). Buffer and caspase-3 do not possess nuclease activity or induce apoptotic morphology in added nuclei (lanes/panels 2, 3). Preincubation of CAD alone induces nuclease activity and apoptotic morphology (lane/panel 4), presumably due to the presence of a contaminating protease. ICAD is cleaved during this preincubation (data not shown). This spontaneous activation of CAD is not observed if non-cleavable ICAD is present from the start of the preincubation (lane/panel 5). Preincubation of CAD with caspase-3 induces nuclease activity and apoptotic morphology (lane/panel 6). This activity is not observed if non-cleavable ICAD is present either from the start of the preincubation, or if it is added at the end of the preincubation together with the substrate nuclei (lanes/panels 7, 8). Addition of DEVD-fmk to the preincubation blocks CAD activation, but has no effect on nuclease activity or induction of apoptotic morphology if added once the preincubation is complete (lanes/panels 9, 10). The induction of apoptotic morphology by CAD in the presence of DEVD-fmk was slightly, but reproducibly, reduced (panel 10). These results demonstrate that CAD can induce nuclear apoptosis in the absence of caspase-3 activity.

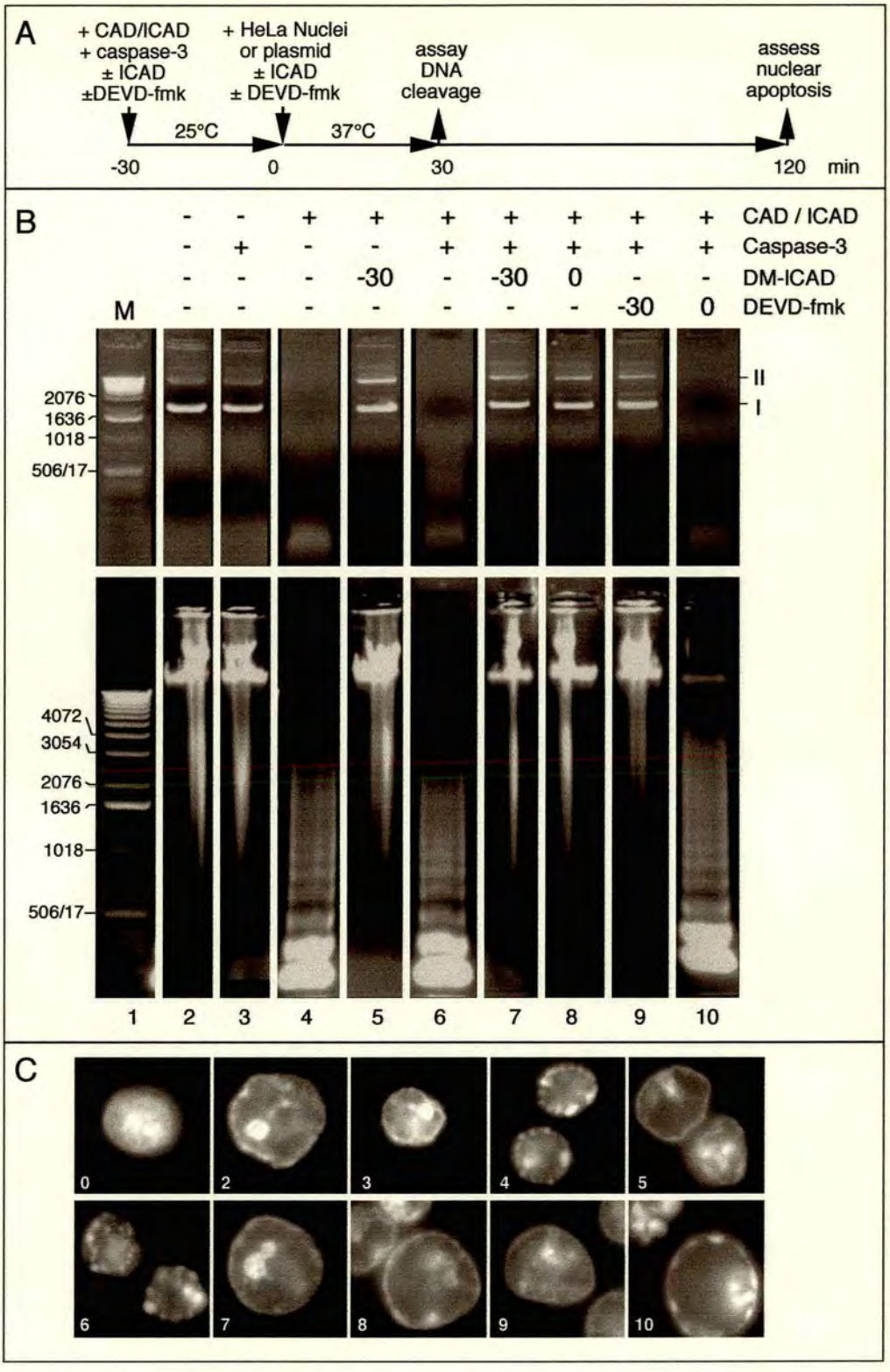

bicistronic vector:His_6-ICAD(stop codon)-RBS-CAD(stop codon)

RBS: ribosome binding site

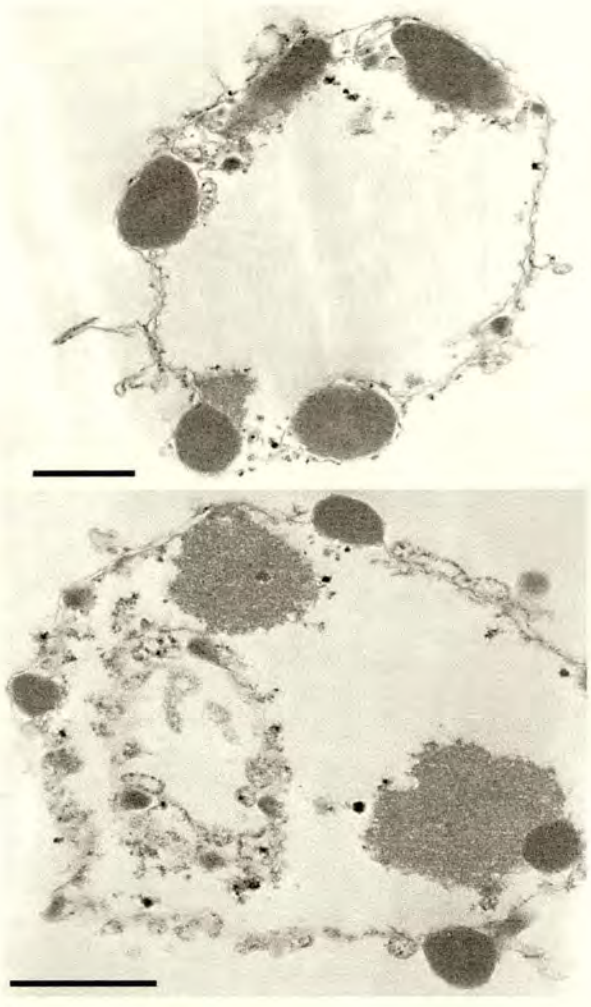

Figure 13. Induction of apoptotic morphology in HeLa nuclei by bacterially expressed CAD: analysis by electron microscopy. Nuclei treated as shown in Figure 12B, lane/panel 6 were embedded in plastic, thin sectioned, and examined in the electron microscope. Regions of condensed chromatin are seen to abut the nuclear envelope, and often protrude as though beginning to bud outwards through the envelope. These images are indistinguishable from previously published images of nuclei treated with complete apoptotic extract (Lazebnik *et al.*, 1993). Bar - 1 μm.

2.3.5 Evidence for a nuclear disassembly factor distinct from CAD.

To determine whether the CAD-like enzyme was the sole activity downstream of caspases that drives nuclear disassembly in these extracts, S/M and E/X extracts were treated with ICAD prior to addition of exogenous nuclei. Although addition of excess ICAD abolished production of a nucleosomal ladder in nuclei added to S/M and E/X extracts (Fig. 14A lanes 3-5 and 9 - 11), ICAD did not block the ability of the extracts to induce chromatin condensation and nuclear fragmentation (Fig. 14B, panels 3, 4, 5, 9, 10, 11). The ability of the extracts to induce morphological changes in the presence of ICAD was even more striking when the number of nuclei in the incubation was reduced ~4-fold (Fig. 14C). These observations indicate that CAD-like activity is not essential for apoptotic morphological changes in nuclei added to either S/M or E/X extracts.

Interestingly, simultaneous inhibition of both ICAD and caspases did block the induction of apoptotic morphology by E/X extracts (Fig. 14B panels 13, 14; Fig. 14C, panel d). Moreover, addition of purified caspase-3 and caspase-6, the major active caspases in cytosol (Faleiro *et al.*, 1997; Martins *et al.*, 1997) and nuclei (Martins *et al.*, 1997; Martins, Mesner *et al.*, 1997), failed to induce apoptotic morphological changes in purified nuclei (identical to Fig. 12, panel 5). These observations appear to rule out the possibility that caspases themselves are capable of inducing chromatin condensation by acting alone on endogenous nuclear substrates. When coupled with these results, the observation in Fig. 14C, panel d, not only suggests that there is a second chromatin condensation factor present in the

extracts, but also raises the possibility that ongoing caspase activity is required for activity of this factor.

Figure 14. Induction of apoptotic morphology in cell extracts is not blocked by inhibition of the CAD-like nuclease. **Panel A:** Induction of nucleosomal ladders in added nuclei by S/M extract is sensitive to ICAD and DEVD-fmk (lanes 3-8). Induction of nucleosomal ladders in added nuclei by E/X extract is sensitive only to ICAD (lanes 9-14). (DEVD-fmk added: none - lanes 1-5, 9-11; 100 μM - lanes 6-8, 12-14. ICAD added: none - lanes 3, 6, 9, 12; 160 ng - lanes 4, 7, 10, 13; 320 ng - lanes 5, 8, 11, 14.) **Panel B:** Both S/M and E/X extracts can induce apoptotic events under conditions where the CAD-like nuclease is inhibited, provided that they retain active caspases (panels 3, 4, 5, 9, 10, 11). E/X extracts, which normally induce apoptosis in the absence of caspase activity (panel 12), are unable to do so if ICAD is added along with DEVD-fmk (panels 13, 14). Panel numbers refer to the gel lanes in panel A. These images come from the same incubations shown in panel A. Time-lapse microscopy analysis reveals that the "C"-shaped nuclei in panels 3, 4, 5, 9, 10 and 11 are apoptotic nuclei in which the nuclear envelope has ruptured following collapse of the chromatin against the nuclear periphery. **Panel C:** E/X extracts can fully induce apoptotic morphology in the absence of CAD-like activity, but this requires ongoing caspase activity. In a different experiment from those shown in panels A and B, the number of nuclei per microliter of extract was reduced. This gives a stronger induction of apoptotic morphology (compare panel with B, panel 9), even when caspases (panel b) or CAD are inhibited (panel c). Extracts produce a range of morphologies in added nuclei. As in the experiment of panels A, B, simultaneous inhibition of both CAD and caspases abolishes morphological apoptosis in the extracts (panel d). These images were selected from images taken at random.

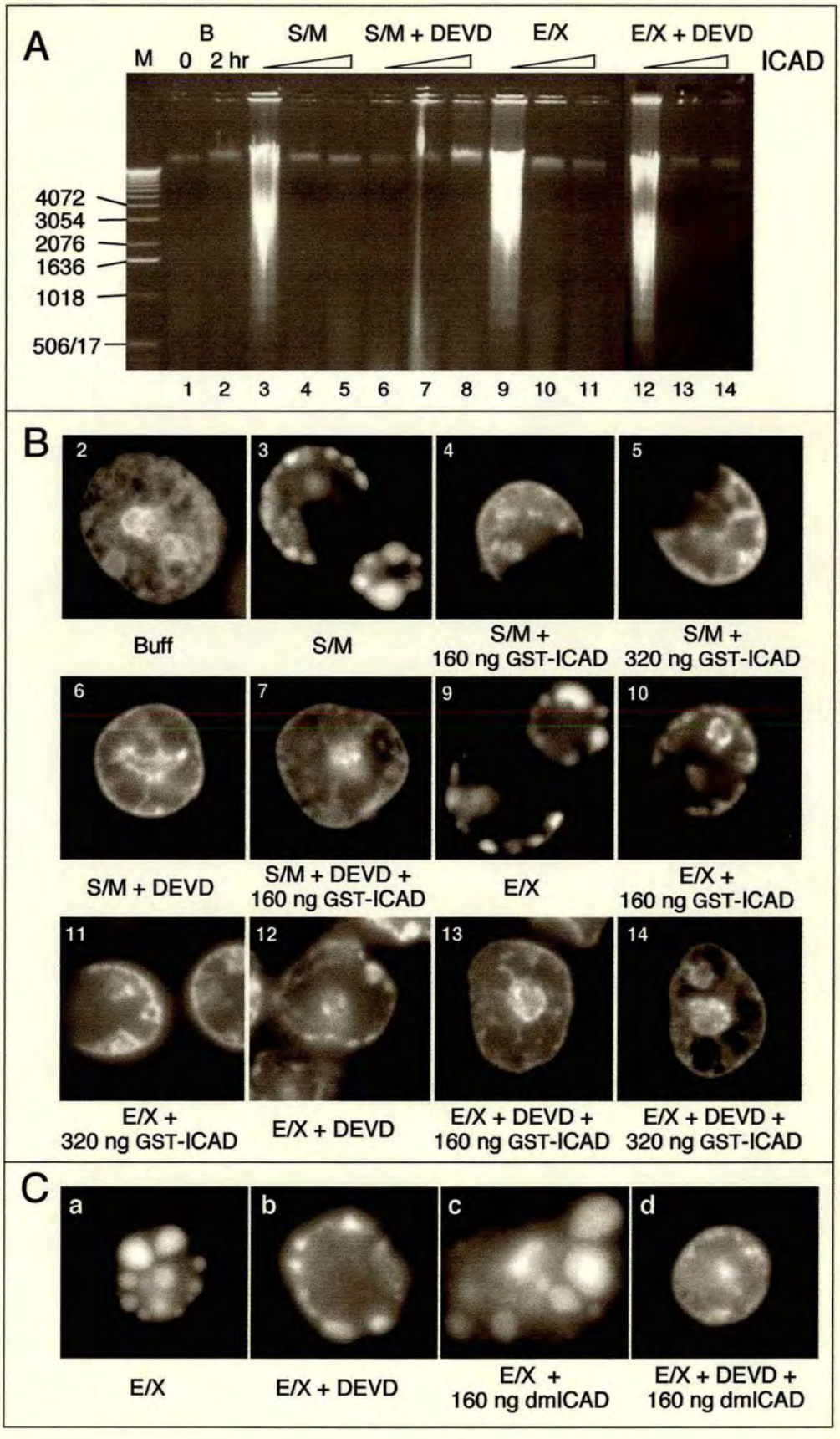
A
B
S/M
S/M + DEVD
E/X
E/X + DEVD
M
0
2 hr
ICAD
4072
3054
2076
1636
1018
506/17
1 2 3 4 5 6 7 8 9 10 11 12 13 14
B
2
3
4
5
Buff
S/M
S/M +
160 ng GST-ICAD
S/M +
320 ng GST-ICAD
6
7
9
10
S/M + DEVD
S/M + DEVD +
160 ng GST-ICAD
E/X
E/X +
160 ng GST-ICAD
11
12
13
14
E/X +
320 ng GST-ICAD
E/X + DEVD
E/X + DEVD +
160 ng GST-ICAD
E/X + DEVD +
320 ng GST-ICAD
C
a
b
c
d
E/X
E/X + DEVD
E/X +
160 ng dmICAD
E/X + DEVD +
160 ng dmICAD

2.4 Discussion

The experiments described above led to a number of novel observations: 1) It is possible to prepare cell-free extracts specific for the latent and execution phases of apoptosis. 2) These extracts, both of which contain active caspases and induce apoptosis in substrate nuclei, exhibit significant biochemical and functional differences that are best explained if the transition from the latent to the execution phase of apoptosis is accompanied by a transition from caspase-dependent to caspase-independent mechanisms of nuclear disassembly. 3) One aspect of this transition appears to involve activation of a CAD-like nuclease, which is initially latent in S/M extracts but is fully active in E/X extracts. 4) Murine CAD can induce an apoptotic morphology in isolated nuclei. 5) In addition to CAD, apoptotic extracts contain a second activity that can also induce apoptotic chromatin condensation in added nuclei in the absence of DNA fragmentation. Each of these points is discussed in greater detail below.

At present there is no accepted biochemical marker to rigorously distinguish between the condemned and committed stages of the latent phase. Here, latent phase cells are defined as those that have received a proapoptotic stimulus but look morphologically normal. Condemned cells are operationally defined as those latent phase cells that yield extracts that lack significant caspase activity and do not induce apoptosis in substrate nuclei. Committed stage cells are defined operationally as those latent phase cells that yield extracts that contain high levels of active caspases together with low levels of active CAD and that strongly induce apoptosis in

substrate nuclei. As expected, these cells contain only low levels of fragmented DNA themselves. Both of these latent phase populations are readily distinguishable from overtly apoptotic cells, which have detached from the substratum and have sustained internucleosomal DNA degradation in response to a proapoptotic stimulus. The various extracts prepared from these three operationally defined cell populations turned out to have remarkably distinct biochemical and functional characteristics.

The most significant difference was the finding that induction of apoptotic events by "committed" stage extracts is dependent on ongoing caspase activity, whereas induction of apoptotic events by "execution" phase extracts is independent of ongoing caspase activity. This observation is best explained by a model in which caspases activate downstream factors that are responsible for condensation of the chromatin during apoptosis. Such a model predicts that if it would be possible to purify the active caspases from apoptotic cells away from the downstream factors, then the caspases on their own should be insufficient to induce apoptotic events in substrate nuclei. It is shown that mixtures of purified caspases-3 and -6 are also unable to induce apoptotic morphology in purified nuclei. Thus, although recent experiments indicate that caspase-3 is essential for nuclear apoptosis (Janicke, Sprengart *et al.*, 1998; Woo *et al.*, 1998), this study indicates that this enzyme is likely to function by activating downstream factors rather than directly disassembling the nucleus itself.

One such downstream factor has recently been identified in murine cell extracts. CAD, the caspase-activated DNase (Enari *et al.*, 1998), interacts

with an inhibitory subunit termed ICAD/DFF45 (Liu *et al.*, 1997; Sakahira *et al.*, 1998) to form an inactive complex that is thought to be sequestered in the cytoplasm. Caspase cleavage of ICAD is proposed to cause the release and subsequent nuclear translocation of CAD, leading to digestion of the chromatin (Sakahira *et al.*, 1998). Here, it is shown that both S/M and E/X extracts from chicken DU249 cells contain a nuclease similar or identical to CAD, as defined by its ability to be quantitatively inhibited by exogenous purified murine ICAD. The fact that ICAD of mouse origin inhibits the apoptotic nuclease in avian (chicken) cell extracts suggests that the CAD nuclease and its interactions with ICAD are widely conserved in phylogeny.

Because the same cohort of caspases is present and active in the S/M and E/X extracts, the transition from the latent to the execution phase of apoptosis may not hinge upon caspase action alone. Instead the transition might involve activation of downstream factors. The CAD-like nuclease appears to be largely inactive in freshly prepared S/M extracts, becoming active only as the extracts are incubated at 30 or 37°C. This activation presumably reflects the cleavage of ICAD/DFF45 by caspases, since CAD activation is blocked by caspase inhibitors. In contrast, the CAD-like nuclease activity appears to be fully active in freshly prepared E/X extracts. Collectively, these observations suggest that caspase activation occurs during the latent phase of apoptosis, whereas CAD activation accompanies the transition from the latent to execution phase of apoptosis. One implication of this conclusion is that cells might simultaneously contain active caspases and inactive complexes of ICAD/DFF bound to CAD and

possibly other downstream factors. This would be possible if caspases were segregated from their downstream targets such as ICAD/DFF - possibly by being sequestered in a different cellular compartment. The onset of apoptotic execution might then be triggered not by activation of the caspases, but by a change in the localization of either caspases or targets. An alternative explanation of our data, that caspases are inactive in the cells from which S/M extracts are made and become activated during preparation of the extract (Zapata, Takahashi *et al.*, 1998), is unlikely for two reasons. First, it was previously demonstrated that caspase activity in similar extracts prepared from latent phase HL-60 cells was paralleled by cleavage of PARP and procaspase-3 *in vivo* (Martins *et al.*, 1997). Second, the caspase-3 activation observed during extract preparation in the Zapata study was explained by the detergent-induced release of granzyme B from cytoplasmic vesicles (Zapata *et al.*, 1998). In this study, detergents were avoided during extract preparation; and cells lacking granzyme B were utilized.

In support of the notion that caspases and their targets might be segregated during the latent phase, it was noted that procaspases have largely been observed in the cytoplasm (Duan, Chinnaiyan *et al.*, 1996; Krajewska, Wang *et al.*, 1997; Mancini, Nicholson *et al.*, 1998), microsomes (Ng, Nguyen *et al.*, 1997; Zhivotovsky, Samali *et al.*, 1999; Nakagawa, Zhu *et al.*, 2000), or mitochondria (Mancini *et al.*, 1998; Susin, Lorenzo *et al.*, 1999), whereas subcellular fractionation studies have revealed significant levels of active caspases within the nucleus (Martins *et al.*, 1997; Martins *et al.*, 1997).

An additional study has indicated that interference with nuclear transport renders cells resistant to Fas-mediated apoptosis (Yasuhara *et al.*, 1997). Moreover, functional nuclear transport is necessary for acinus to induce chromatin condensation, whilst acinus itself is a nuclear protein in nonapoptotic cells and requires caspase-3 and an unknown protease to be activated (Sahara *et al.*, 1999).

In this study a novel vector has been developed to coordinately express CAD and ICAD in E. coli, and partially purified CAD was prepared to demonstrate that CAD can induce an apoptotic morphology in isolated nuclei, as confirmed by both light and electron microscopy. This reaction does not require ongoing caspase activity. This result is consistent with earlier observations indicating that addition of micrococcal nuclease to isolated nuclei can cause clumping of chromatin (Arends, Morris *et al.*, 1990), although the pattern of condensation seen with CAD more closely resembles that seen in apoptotic cells. However, CAD does not appear to be the only factor downstream of caspases that is capable of inducing apoptotic nuclear changes. Addition of purified ICAD to either S/M or E/X extracts abolished all detectable DNase activity against both chromosomal and plasmid DNA substrates, but did not abolish the ability of those extracts to induce an apoptotic morphology in substrate nuclei. This observation is consistent with previous reports that morphologically normal apoptosis can occur in the absence of internucleosomal DNA fragmentation *in vivo* (Ucker, Obermiller *et al.*, 1992; Oberhammer, Wilson *et al.*, 1993; Oberhammer, Hochegger *et al.*, 1994; Sakahira *et al.*, 1998). At present, the nature of the

second downstream factor(s) that promotes apoptotic chromatin condensation is unknown. Although two recent studies suggest that serine (Shimizu and Pommier, 1997) or cysteine proteases (Vaux, Wilhelm *et al.*, 1997) may be involved, the fact that apoptotic morphological changes can be detected in the presence of DEVD-fmk as well as a battery of serine, cysteine, and acid protease inhibitors (see METHODS) suggest that the chromatin condensing activity might not be a protease. On the other hand, simultaneous addition of both DEVD-fmk and ICAD to E/X extracts abolished the induction of apoptotic morphology in substrate nuclei. This result suggests that the morphogenic factor might either bind to ICAD or be regulated by other molecules that interact with ICAD.

In summary, the experiments reported here demonstrate that it is possible to use cell-free extracts for a biochemical and functional dissection of the sequential phases of the apoptotic pathway. This study reveals that the transition from the latent to the execution phase of apoptosis appears to be accompanied by a change from caspase-dependent to caspase-independent mechanisms. Since the discovery that caspases are capable of cleaving abundant nuclear proteins like PARP (Lazebnik *et al.*, 1994) and the lamins (Lazebnik *et al.*, 1995; Orth, Chinnaiyan *et al.*, 1996; Rao, Perez *et al.*, 1996; Takahashi *et al.*, 1996) and the absence of nuclear apoptosis in caspase-3-null cells (Janicke *et al.*, 1998; Woo *et al.*, 1998), we and others had widely assumed that caspases are directly responsible for nuclear disassembly. The inability of purified caspases to produce apoptotic morphological changes in isolated nuclei, coupled with the inability of caspase inhibitors to abolish the

induction of these morphological changes by E/X extracts, argues that caspases are unlikely to be workhorses that are solely responsible for nuclear disassembly. Instead, the present results provide support for a view in which caspases play an executive role in nuclear disassembly by activating factors that in turn disassemble the nucleus. At least one of the downstream activities is a CAD-like nuclease; but another downstream activity required for the induction of apoptotic morphology appears to be distinct from CAD.

Chapter 3

3. CAD and ICAD localization: The CAD/ICAD complex is nuclear in nonapoptotic cells

3.1 Introduction

One aspect of the regulation of apoptotic execution that has recently attracted considerable study is the movement of apoptotic factors from one intracellular compartment to another. The best studied example of this involves movement of factors, including cytochrome *c*, AIF and caspases from the mitochondrial intermembrane space into the cytosol at the onset of apoptotic execution (Liu *et al.*, 1996; Susin, Zamzami *et al.*, 1996; Susin *et al.*, 1999). Less well understood is the requirement for nuclear transport of proteins, which is essential for the onset of apoptotic execution following the induction of apoptosis by Fas/CD95 (Yasuhara *et al.*, 1997). The recently discovered protein acinus, which is activated by caspase-3 and an unknown protease, requires nuclear transport to induce chromatin condensation (Sahara *et al.*, 1999). Originally it was claimed that the apoptotic nuclease CAD/CPAN/ DFF40 which is also activated by caspase-3 indirectly is the essential factor to be transported into nucleus (Enari *et al.*, 1998; Halenbeck *et al.*, 1998; Liu *et al.*, 1998; Mukae *et al.*, 1998). However, the identity of essential factors that must enter the nucleus is not yet firmly established.

In healthy cells, CAD/CPAN/DFF40 exists in a complex with its inhibitory chaperone ICAD-L/DFF-45. ICAD-L, after functioning as a folding chaperone for CAD during translation (Enari *et al.*, 1998), then remains bound to the nuclease, keeping it in inactive form. The absolute requirement for ICAD-L as a folding chaperone is revealed by the phenotype of DFF-45 knockout mice, whose cells undergo apoptosis in the absence of detectable DNA cleavage despite the continued presence of CAD (Zhang *et al.*, 1998). At the onset of apoptosis, caspases with specificities characteristic of caspases -3 and -7 cleave ICAD-L at two sites (Liu *et al.*, 1997; Sakahira *et al.*, 1998). This relieves the inhibition of CAD and initiates the fragmentation of the chromosomal DNA during apoptosis (Sakahira *et al.*, 1998). CAD activation is observed after diverse apoptotic stimuli in a variety of cultured cells (McIlroy *et al.*, 1999) as well as in animals, where CAD may play a role after traumatic brain injury (Zhang, Raghupathi *et al.*, 1999).

The location of CAD/CPAN/DFF40 in healthy cells remains controversial. In the original descriptions, CAD was predicted to have a nuclear localization signal (NLS) on its C-terminus but no obvious NLS was noted within DFF45/ICAD-L (Enari *et al.*, 1998). It was therefore suggested that ICAD might complex with nascent CAD on the ribosome, first helping it to fold, and then restraining it in the cytoplasm by occluding the CAD NLS. This latter activity was proposed to function similarly to the retention of NF-κB in the cytoplasm by IκB (Enari *et al.*, 1998). As is the case for IκB:NFκB, it was proposed that cleavage of ICAD releases CAD, thereby

enabling it enter the nucleus and attack the cellular DNA (Sakahira *et al.*, 1998).

In the present study, this hypothesis for the role of ICAD in regulation of CAD has been examined. Two different approaches have been used to localize ICAD-L in cultured cells. First, it was demonstrated that a GFP:ICAD-L fusion protein is nuclear in transfected human, pig and chicken cells. Second, an antibody to murine ICAD was prepared. Subcellular fractionation and immunoblotting experiments with this antibody showed that the endogenous protein is likewise concentrated in cell nuclei. Next the mechanism of ICAD-L entry into the nucleus was examined, in particular whether ICAD-L enters the nucleus as a consequence of the function of an NLS that was not recognized in previous studies, or whether the protein must enter the nucleus in a complex with another NLS-bearing protein or proteins. The data presented here clearly indicate that the C-terminus of ICAD-L functions as an autonomous NLS that is able to direct the entry of a GFP fusion protein into the nucleus.

3.2 Materials and Methods

3.2.1 Materials

Reagents were obtained from the following suppliers: antipain, chymostatin, pepstain A, PMSF, isopropyl β-D thiogalactopyranoside (IPTG), etoposide, and 4,4-diamidino-2-phenylindole (DAPI) were from Sigma; staurosporine and leupeptin were from Calbiochem; Hybond-C membrane, horseradish perixidase conjugated anti-mouse, anti-human, and anti-rabbit antibodies, and enhanced chemiluminescence (ECL) reagents were from Amersham Corp.; Super Signal Ultra chemiluminescence reagents were from Pierce; Ni-NTA agarose from Qiagen. All restriction enzymes were from New England Biolabs. Monoclonal antibody to GFP was a gift of I. Davis (ICMB Edinburgh). Monoclonal antibody to tubulin was a gift of L. Binder (Northwestern University, Chicago. IL). Human autoantibody to DNA topoisomerase I has been described previously (Shero, Bordwell *et al.*, 1986).

3.2.2 Expression and purification of His_6-ICAD and antigen preparation

The ICAD cDNA in pBluescript (Stratagene) was digested with Spe I, blunt-ended with T4 DNA polymerase (NEB) plus 100 μM dNTPs, and digested with Kpn I (NEB). The resulting fragment was ligated into pRSET B (Invitrogen) that had been digested with Hind III, blunt-ended with T4 DNA polymerase, and digested with Kpn I. ICAD in pRSET B was transformed into *E. coli* BL21(DE3)Lys S cells. Transformed cells were grown to OD_{600} = 0.5 - 0.7 and protein expression was induced with IPTG (1

mM) for 3-4 hr. Cells were collected by centrifugation at 5000 x g for 10 min and frozen at -80°C. The cell pellet was thawed on ice for 15 min and resuspended in sonication buffer (50 mM NaH_2PO_4 pH 7.5; 300 mM NaCl; 10 mM imidazole). Lysozyme was added to 1 mg/ml and the suspension was incubated on ice for 30 min; sonicated on ice until 80% of the cells were disrupted and then centrifuged at 4000 x g for 20 min at 4°C. The supernatant fraction was incubated on a rotating mixer for 1 hr at 4°C with 0.5 ml of Ni-agarose that had been pre-equilibrated with sonication buffer then loaded onto a polyprep chromatography column (Bio-rad). The column was washed with 4 ml of wash buffer (50 mM NaH_2PO_4 pH7.5; 300 mM NaCl; 20 mM imidazole) twice. Protein was eluted with 0.5 ml of elution buffer (50 mM NaH_2PO_4 pH7.5; 300 mM NaCl; 250 mM imidazole) four times. All samples were subjected to SDS-PAGE and examined by Coomassie Blue staining. For antigen preparation, purified ICAD was subjected to SDS-PAGE, then the gel was washed in distilled water three times for 10 min each, stained with aqueous Coomassie Blue (0.1%) for 1 hr and rinsed with water until the induced protein band became obvious. The band was excised, frozen at -80°C, and then ground to a fine powder under $N_2(l)$ with a mortar and pestle. This powder was resuspended in PBS buffer and used to immunise two rabbits at the Scottish Antibody Production Unit (Now Diagnostics Scotland) (Carluke, Lanarkshire).

3.2.3 Construction of clones

3.2.3.1 Construction of GFP:ICAD-L$^{1-331}$

The ICAD cDNA in pBluescript (Stratagene) was digested with Hind III, blunt-ended with T4 DNA polymerase (New England Biolabs) plus 100 μM dNTPs, and digested with Xba I (New England Biolabs). The resulting fragment was ligated into a vector containing enhanced GFP-with a flexible linker (gift of Larry M. Karnitz, Mayo Research Foundation, Rochester, MN) in pCDNA3 (Invitrogen) that had been digested with Not I (New England Biolabs), blunt-ended with T4 DNA polymerase and digested with Xba I.

3.2.3.2 Construction of GFP:ICAD-L$^{1-311}$

The C-terminus of ICAD-L lacking 20 amino acids was obtained by PCR using primer (5'-CTGCTGTCAGAAGAGGACCTC-3') and primer (5'-GCCCAAGCTTCTAGAATTCTTATGCTGATAG-3'), then digested with Hinc II and Hind III. The resulting fragment was ligated into vector pRSET A (Invitrogen) containing full length ICAD-L$^{1-331}$ that had been digested with Hinc II and Hind III. Next, pRSET A ICAD-L$^{1-311}$ was digested with Xho I and Xba I and the resulting fragment was ligated into vector pCDNA GFP:ICAD-L (4.2.3.1) that had been digested with Xho I and Xba I.

3.2.3.3 Construction of GFP:ICAD-S$^{1-265}$

The C-terminus of ICAD-S was obtained by PCR using primer (5'-CTGCTGTCAGAAGAGGACCTC-3') and primer (5'-TAGGGCCCTTAGTTCTTGCCCACCTCCAAATCCTG-3'), then digested

with Xcm I and Apa I. The resulting fragment was ligated into a vector pCDNA GFP:ICAD-L that had been digested with Xcm I and Apa I.

3.2.3.4 Construction of GFP:ICAD-S^{1-261}

The C-terminus of ICAD-S^{1-261} lacking 4 amino acids was obtained by PCR using primer (5'-CTGCTGTCAGAAGAGGACCTC-3') and primer (5'-GCCCAAGCTTCTAGAATTCTTACTCCAAATC-3'), then digested with Hinc II and Hind III. The resulting fragment was ligated into vector pRSET A ICAD-L (Invitrogen) that had been digested with Hinc II and Hind III. Next, this pRSET A ICAD-S^{1-261} was digested with Xho I and Xba I. The resulting fragment was ligated into a vector pCDNA GFP:ICAD-L that had been digested with Xho I and Xba I.

3.2.3.5 Construction of Zeo GFP:ICAD-L, Zeo GFP:ICAD-L^{1-311}, Zeo GFP:ICAD-S, and Zeo GFP:ICAD-S^{1-261}

GFP:ICAD-L, GFP:ICAD-L^{1-311}, GFP:ICAD-S, and GFP:ICAD-S^{1-261} in pCDNA3 (Invitrogen) were digested with Hind III and Apa I. The resulting fragments were ligated into vector pZeo $SV2^{+}$ (Invitrogen) that had been digested with Hind III and Apa I.

3.2.3.6 Construction of Zeo GFP:CAD

CAD in pBluescript KS (Stratagene) was digested with Not I and Xho I. The resulting fragment was ligated into vector pCDNA3 GFP linearised

by digestion of the multiple cloning sites (MCS) with Not I and Xho I. This GFP:CAD was digested with Hind III and ligated into vector pZeo SV2+ that had been digested with Hind III.

3.2.3.7 Construction of pCDNA3 GFP with MCS

pBluescript KS was digested with Not I and Apa I. The resulting fragment, a part of multiple cloning site (MCS), was ligated into pCDNA3 (Invitrogen) containing enhanced GFP with a flexible linker (gift of Larry M. Karnitz, Mayo Research Foundation, Rochester, MN) that had been digested with Not I and Apa I.

3.2.3.8 Construction of pCDNA3 GFP:ICAD-L$^{312-331}$ from ICAD-L

The C-terminal 20 amino acids of ICAD-L was obtained by PCR using primer (5'-CATAGCGGCCGCAGGAGGAGCCCAC-3') and primer (5'-GCACCTTCCAGGGTCAAG-3'), then digested with Not I and Apa I. The resulting fragment was ligated into pCDNA3 GFP linearised by digestion of the MCS with Not I and Apa I.

3.2.4 Subcellular fractionation

HeLa cells were maintained in RPMI 1640 medium containing 5% (v/v) calf serum. Cells were collected by trypsinization and centrifuged at 1400 x g for 5 min at room temperature. Cell pellets were washed once in PBS, once in nuclei solution that is very hypotonic (10 mM Pipes pH 7.0, 10 mM KCl, 1.5 mM $MgCl_2$, 1 mM DTT, 100μM PMSF, 10 μM cytochalasin B,

plus 1 μM each of antipain, chymostatin, pepstatin A, and leupeptin) and resuspended into 200 μl of nuclei solution. This suspension was incubated on ice with occasional agitation, and then lysed by passage through a 21G needle. The lysate was fractionated into crude nuclei and cytosol by centrifugation at 2400 x g for 10 min at 4°C. The supernatant and pellet were immediately resuspended into SDS sample buffer and boiled for 5 min and subjected to SDS-PAGE (Laemmli, 1970).

3.2.5 Induction of apoptosis

Apoptosis was induced in cells 20-24 hr after they were electroporated either with a construct expressing GFP-ICAD or in the absence of added DNA (mock transfection). Cells were either treated with 68 μM etoposide for 1 hr and kept in drug-free media for a subsequent 6-7 hr or treated with 1 μM staurosporine for 16-24 hr. To examine GFP-ICAD cleavage, both floating cells and attached cells were collected, resuspended into sample buffer and subjected to SDS-PAGE.

3.2.6 Microscopy

Chicken DU249 cells and LLCPK cells were cultured in RPMI 1640 medium containing 10% (v/v) fetal bovine serum. HeLa cells were cultured in RPMI 1640 medium containing 5% (v/v) calf serum. After electroporation with various constructs (Mackay, Eckley *et al.*, 1993), cells were grown on coverslips overnight. These coverslips were rinsed with PBS, fixed in a 4% formaldehyde solution for 5 min, stained with DAPI (2

μg/ml) for 5 min, rinsed with PBS, and mounted with Vectashield (Vector). Images were acquired on a Zeiss Axioplan II epifluorescence microscope equipped with a Princeton Instruments Micromax cooled CCD camera, driven by IP Lab Spectrum software.

3.3 Results

3.3.1 ICAD-L/DFF45 is nuclear in growing cells

The initial evidence that ICAD-L/DFF45 is a nuclear protein in a variety of cell types was obtained when we constructed a fusion protein in which the *A. victoria* green fluorescent protein (GFP) attached to the N-terminus of murine ICAD-L. Although GFP-ICAD-L expressed in *E. coli* was relatively insoluble, this protein was able to inhibit the CAD-mediated cleavage of plasmid DNA, indicating that this molecule remains competent to interact with CAD. Following transient transfection, this GFP-ICAD-L fusion protein was detected solely in the nucleus of healthy human, pig and chicken cells (Fig. 15). The GFP-ICAD-L fusion protein was excluded from nucleoli. Otherwise this protein showed a relatively homogeneous distribution throughout the nucleus. GFP on its own does not target to the nucleus (Fig. 20).

Although the nuclear localization of GFP-ICAD-L fusion protein was extremely reproducible, being nuclear in all transfected cells, it was nevertheless important to demonstrate that these results reflect the distribution of the endogenous ICAD/DFF, particularly since both ICAD and DFF were originally isolated from cytoplasmic lysates (Liu *et al.*, 1997; Enari *et al.*, 1998). We therefore subcloned murine ICAD-L into a vector that expressed the protein in *E. coli* as a fusion with a hexa-histidine tag (His_6). This protein was expressed in *E. coli*, purified to homogeneity by nickel chelate chromatography, and used to immunise two rabbits. The resultant sera recognized both murine and human ICAD in immunoblots (Fig. 16).

The specificity of one of these ICAD antisera is shown in figure 16A. The serum recognized a single polypeptide of approximately 45 kDa in nuclei isolated from HeLa cells (lane n). As expected (Sakahira *et al.*, 1998), this endogenous polypeptide was cleaved when untransfected cells were induced to undergo apoptosis in the presence of 1 μM staurosporine (data not shown). When nuclei were isolated from HeLa cells transfected with GFP-ICAD-L, the antibody recognized both the endogenous human ICAD/DFF, as well as the 75 kDa GFP-ICAD-L fusion protein (lane n'). The antiserum did not recognise any polypeptides in a clarified cytosolic fraction prepared by sedimentation of a post-nuclear supernatant at 85,000 x g for 1 hr. (lane c). Unfortunately this antiserum did not give a distinct signal above background by indirect immunofluorescence.

The localization of endogenous ICAD-L in nuclei was confirmed in subsequent experiments in which HeLa cells were lysed and subjected to a single centrifugation at 2,400 x g for 10 min (Fig. 16B). This process is sufficient to fractionate cells into a crude nuclear pellet and cytosolic supernatant. The efficacy of this fractionation was confirmed by immunoblotting with antibodies to the nuclear protein DNA topoisomerase I and the cytoplasmic β-tubulin. As expected, topoisomerase I was found predominantly in nuclei (lane n), with a small proportion of the protein being found in the crude cytosol (lane c). This cytosolic material may arise from low levels of nuclear breakage during cell lysis. When cells were fractionated by this method, β-tubulin was found solely in the cytosol.

The distribution of ICAD-L in two independent fractionation experiments is also shown in figure 16B. In both experiments, the endogenous ICAD-L was found to be predominantly nuclear, with a trace amount of the antigen being detected in the crude cytosol. Given the presence of low levels of topoisomerase I in the cytoplasm in these experiments, it is likely that some or all of the cytoplasmic ICAD-L is derived from nuclear breakage. This would be consistent with the absence of detectable ICAD-L in clarified cytosol (Fig. 16A). However, the presence of a small pool of cytoplasmic ICAD-L cannot be excluded by these experiments. Presumably ICAD/DFF was isolated from cytosol in previous experiments because the protein leaked from nuclei during extract preparation (Liu *et al.*, 1997; Sakahira *et al.*, 1998).

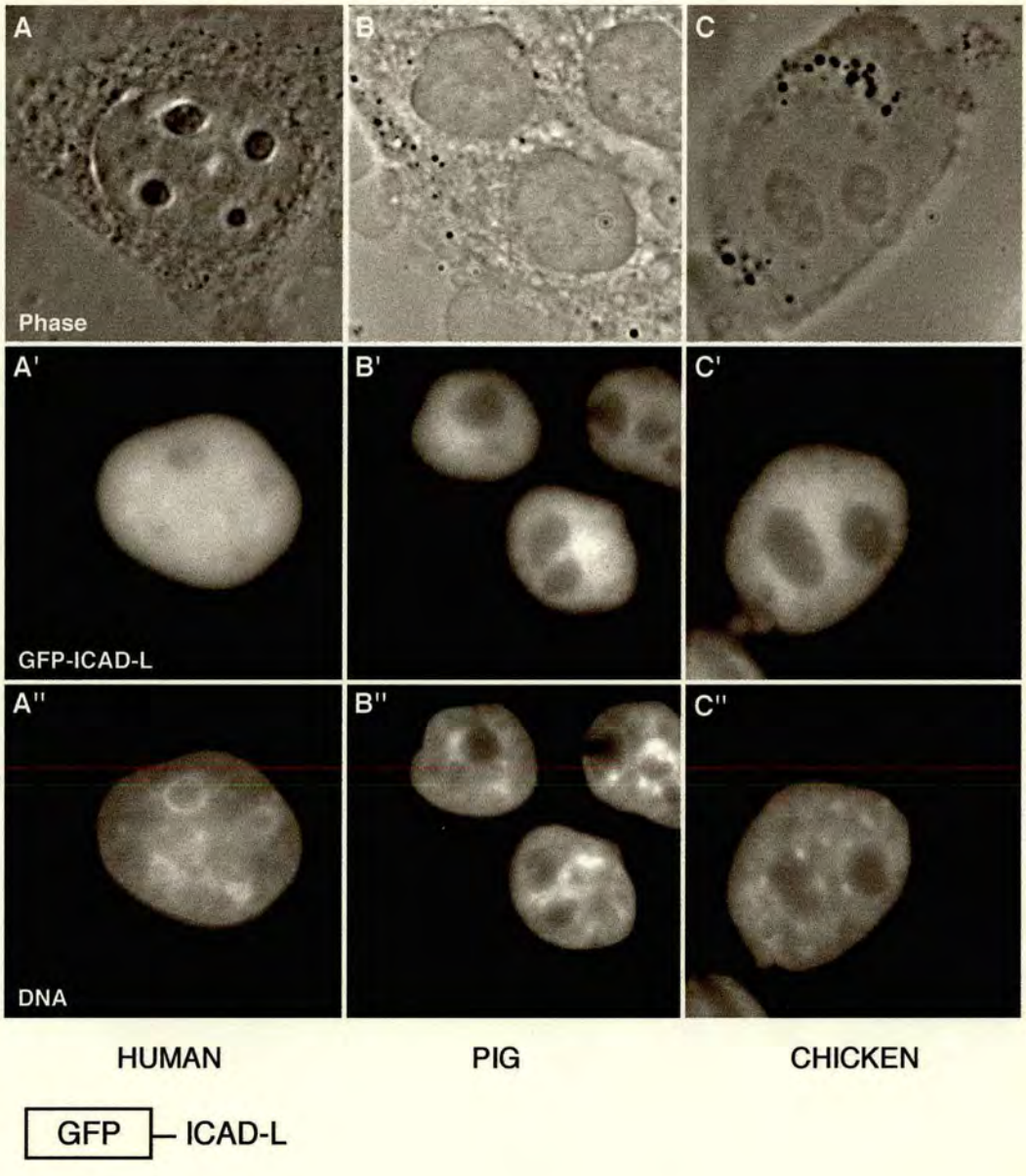

Figure 15. GFP-ICAD-L is a nuclear protein. Aequoria victoria green fluorescent protein (GFP) was fused in frame to N-terminus of murine ICAD and expressed by transient transfection in **(A)** human (HeLa), **(B)** pig (LLCPK) and **(C)** chicken (DU249) cells. The expressed protein was observed solely in cell nuclei. Panels A-C - phase contrast. Panels A' - C' - GFP fluorescence. Panels A'' - C'' - DNA stained with DAPI.

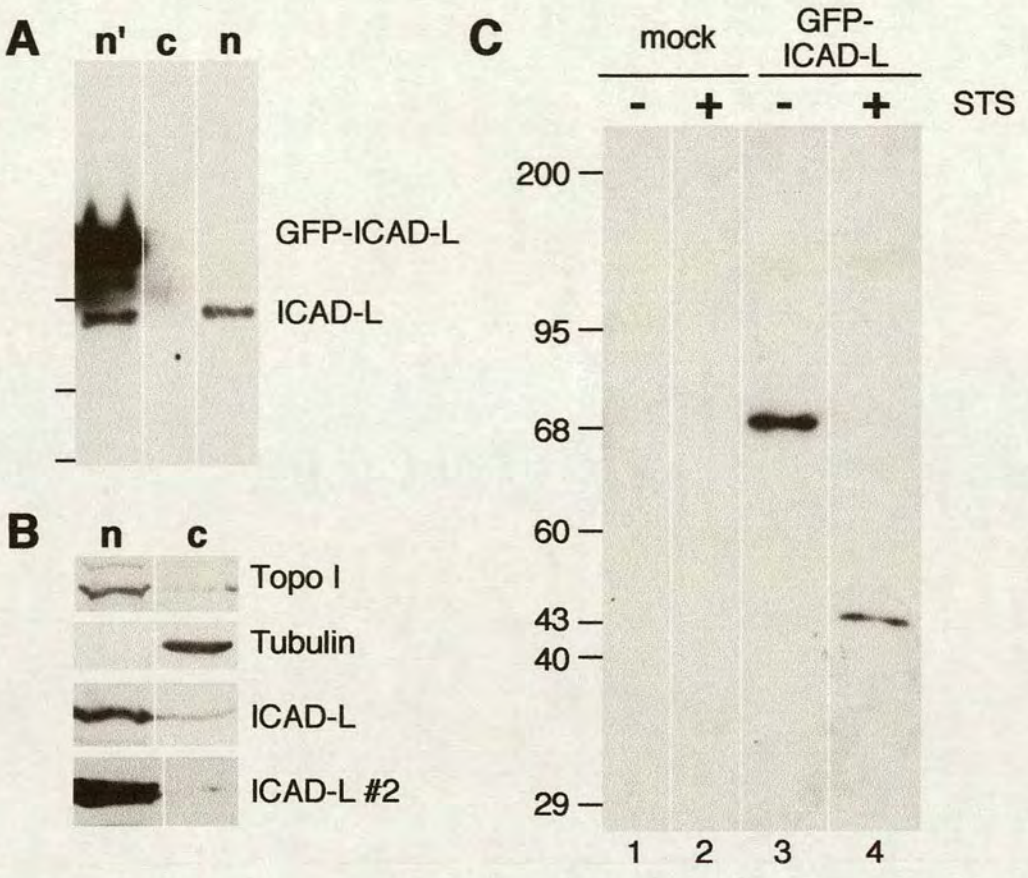

Figure 16. Subcellular fractionation confirms that ICAD-L is a nuclear protein. **(A)** Confirmation of the specificity of the ICAD antibody. Anti-ICAD recognizes endogenous human ICAD in a crude nuclear fraction prepared by centrifugation of HeLa whole cell extract at 2,400 x g for 10 min **(lane n)**. ICAD is not detected in clarified cytosol (85,000 x g, 1 hr - **lane c**). Anti-ICAD recognizes GFP-ICAD-L in a similar fractionation of transfected cells **(lane n')**. **(B)** Subcellular fractionation confirms that ICAD is highly enriched in nuclei of HeLa cells and detected at only trace amounts in crude cytosol (lysates were centrifuged 2,400 x g for 10 min yielding nuclei, **lane n**, and cytosol, **lane c**). **(C)** GFP-ICAD-L is cleaved in transfected cells following induction of apoptosis by exposure of cells to staurosporine. Mock transfected cells (lanes 1, 2) or cells transfected with a construct expressing GFP-ICAD-L (lanes 3, 4) were cultured as normal (lanes 1, 3) or exposed to 1 μM staurosporine for 24 hr (lanes 2, 4), then lysed and subjected to SDS-PAGE and immunoblotting. Detection was with a monoclonal antibody to GFP (gift of Ilan Davis).

3.3.2 GFP-ICAD-L can remain associated with DNA in apoptotic cells.

Current models of ICAD/DFF function assume that the protein is cytoplasmic, and experiments reveal that the protein is destroyed at the onset of apoptotic execution (Liu *et al.*, 1997; Sakahira *et al.*, 1998). Since it is shown that endogenous and GFP-fusion ICAD-L/DFF 45 is predominantly nuclear, it has to be confirmed that the fusion protein is in fact processed normally during apoptosis. In addition the fate of the GFP moiety during apoptosis was examined. If GFP remains intact during apoptosis, then the GFP derived from GFP-ICAD-L might serve as a marker of nuclear integrity during apoptotic execution.

In order to follow the fate of GFP-ICAD-L during apoptosis, HeLa cultures transfected with constructs expressing the chimeric protein were induced to enter apoptosis by exposure to either etoposide or staurosporine. Six hrs after a one hr exposure to 68 μM etoposide ~ 10% of transfected HeLa cells had an apoptotic morphology. Following exposure to 1 μM staurosporine for 24 hr, all cells had an abnormal morphology, with the majority of these cells looking clearly apoptotic. Following induction of apoptosis, cells were harvested, lysed by passage through a needle, and a crude nuclear fraction prepared by centrifugation at 2,400 x g for 10 min. The integrity of the GFP-ICAD-L in this fraction was followed by immunoblotting with a monoclonal antibody to GFP (gift of Ilan Davis). These experiments revealed that GFP-ICAD-L is cleaved as expected in apoptotic HeLa cells (Fig. 16C). GFP is not degraded, at least during the early stages of apoptotic execution. This experiment shows that although

the chimeric protein is predominantly located in the cell nucleus, it remains accessible to the caspases that target ICAD during apoptosis.

The fate of the GFP moiety derived from GFP-ICAD-L following induction of apoptosis in HeLa cells was followed by fluorescence microscopy. In many apoptotic cells (class 1), GFP remained in close association with the chromatin, both in condensed and non-condensed regions (Fig. 17A). In other apoptotic cells (class 2), much of the GFP signal appeared to be no longer associated with the DNA (Fig. 17C). Both classes of cells could be seen to have at least two types of cytoplasmic blebs, some which contained both DNA and GFP, and others that were negative for both. The difference in the localization of GFP may be due to the cleavage of GFP-ICAD-L protein by caspases.

Because GFP expressed on its own is distributed evenly throughout the cytoplasm of transfected cells (Rizzuto, Brini *et al.*, 1995), the fluorescence signal would be expected to diffuse relatively freely following caspase cleavage of the ICAD-L. Therefore, since GFP-ICAD-L is completely cleaved in these apoptotic cells (Fig. 16), this suggests that the nuclear envelope is likely to remain intact in those cells where the GFP stayed in close association with the condensed chromatin. This is consistent with the observation of apparently intact nuclear envelopes in apoptotic cells examined by electron microscopy (Wyllie *et al.*, 1980). Cells with a more widespread distribution of GFP are likely to represent those in which apoptotic execution was accompanied by a loss of nuclear envelope integrity. Blebs in these cells that lack detectable GFP (arrows, Fig. 17C) may

have formed and been sealed off prior to the loss of nuclear envelope integrity. In other studies, we directly observed lysis of the nuclear envelope in time-lapse movies of late stage apoptotic HeLa cells expressing a GFP-lamin A chimera.

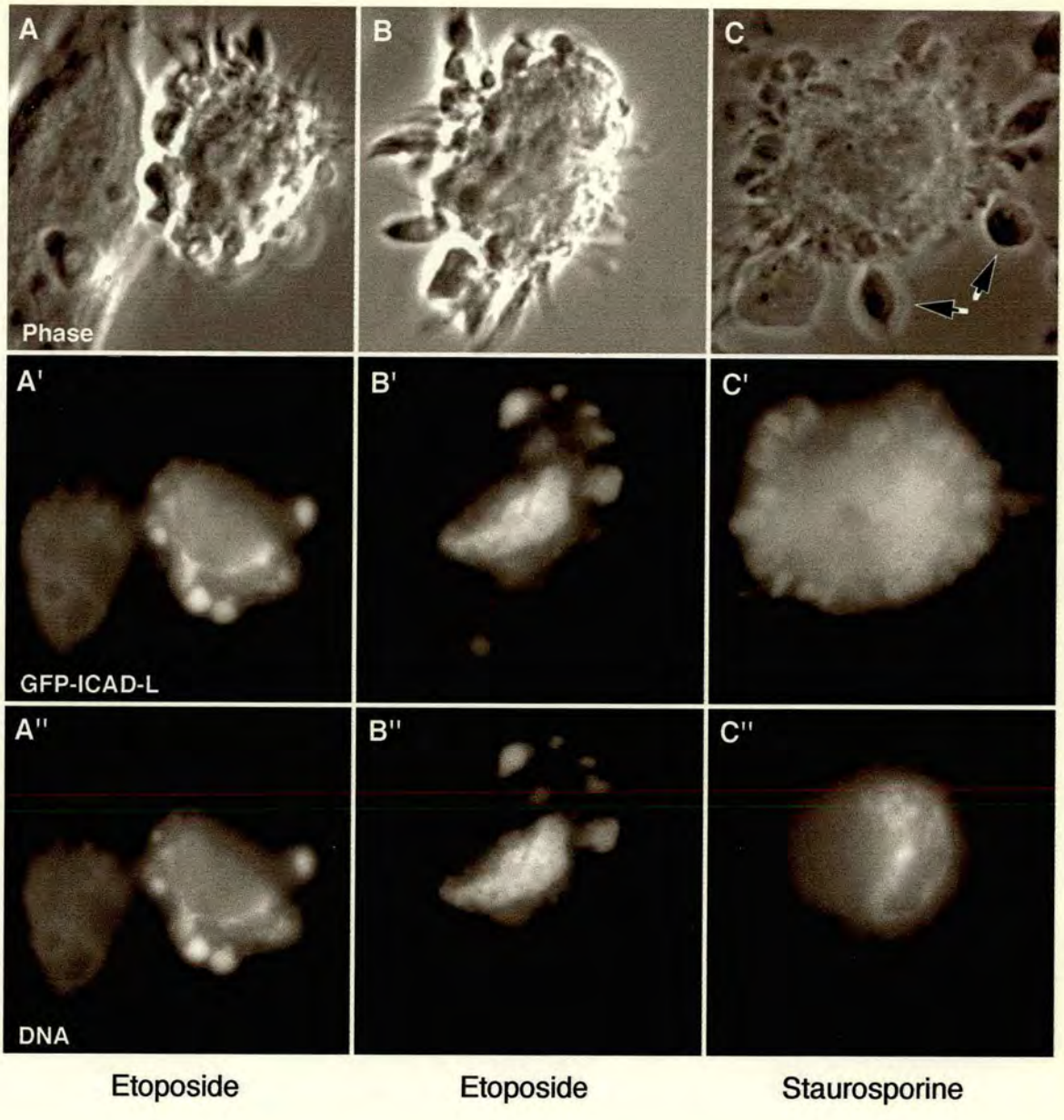

Figure 17. Distribution of the GFP-L moiety of GFP-ICAD-L fusion protein in apoptotic HeLa cells. Cells transiently transfected with a construct expressing GFP-ICAD-L were exposed to **(A, B)** etoposide or **(C)** staurosporine to induce apoptosis. The expressed protein was observed either in association with the DNA, or in certain cases throughout the entire cytoplasm. In the case where the GFP was cytoplasmic, not all prominent surface blebs were observed to contain the GFP fragment (arrows in Panel C). Panels A-C - phase contrast. Panels A' - C' - GFP fluorescence. Panels A" - C" - DNA stained with DAPI.

3.3.3 The C-terminus determines the nuclear localization of ICAD-L/DFF45

In order to investigate the mechanisms underlying the subcellular localization of ICAD-L and ICAD-S, we constructed fusion proteins between murine ICAD and the *Aequoria victoria* green fluorescent protein (GFP). Following transient transfection, GFP:ICAD-L fusion protein was detected solely in the nucleus of healthy human epithelial and chicken hepatoma cells (Fig. 18, panels A). In contrast, a GFP:ICAD-S fusion protein was located diffusely throughout the cell (Fig. 18, panels B).

The transcripts encoding ICAD-L/DFF45 and ICAD-S/DFF35 arise by alternative splicing of a single precursor transcript (Sakahira *et al.*, 1998). The two proteins are identical except for their C-terminal regions, in which the seventy C-terminal residues of ICAD-L are replaced by four different residues in ICAD-S. It therefore appeared likely that the different localization of ICAD-L and ICAD-S might be due to the differing C-termini of these proteins. Two hypotheses can explain the differential localization of the two proteins. First, a nuclear localization signal might be present in the seventy residues of ICAD-L that are missing from ICAD-S. Second, the four different amino acids at the C-terminus of ICAD-S might function as part of a cytoplasmic retention or nuclear export signal.

To test the latter hypothesis, we constructed a GFP:ICAD-S fusion that lacks the four novel C-terminal amino acids (GFP:ICAD-S$^{1-261}$). When expressed by transient transfection, GFP:ICAD-S$^{1-261}$ was distributed diffusely throughout the cell, appearing indistinguishable from the

GFP:ICAD-S protein (Fig. 18, panels C). This indicated that the C-terminus of ICAD-S does not specify the cytoplasmic localization of this protein. It therefore seemed much more likely that the C-terminal region of ICAD-L contains a nuclear localization signal (NLS).

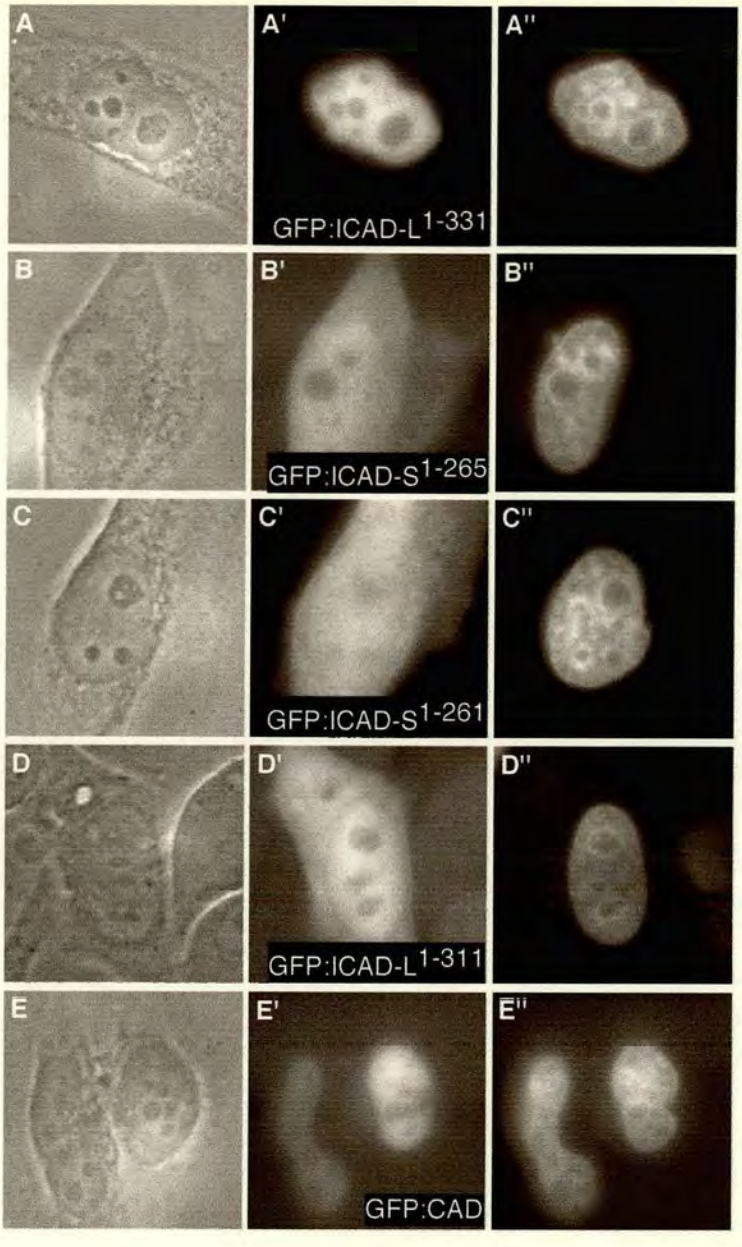

Figure 18. The C-terminal 20 aa of ICAD-L is required for localization of the protein in cell nuclei. *Aequoria victoria* green fluorescent protein (GFP) was fused in frame to N-terminus of murine ICAD-L, ICAD-S and CAD and expressed by transient transfection in human (HeLa) cells. (**panels A**) The expressed GFP:ICAD-L^{1-331} (full length ICAD-L) was solely observed in nuclei. In contrast, GFP:ICAD-S^{1-265} (full length ICAD-S) (**panels B**), GFP:ICAD-S^{1-261} (**panels C**), and GFP:ICAD-L^{1-311} (**panels D**) were all found to be distributed throughout the cell in both nucleus and cytoplasm. (**panels E**) GFP:CAD was highly concentrated in nuclei. Panels A-E - phase contrast; Panels A′-E′ - detection of GFP fluorescence; Panels A″ - E″ - DAPI fluorescence of cellular DNA. Bar 10 μm

3.3.4 Identification of a nuclear localization signal at the C-terminus of ICAD-L

The nuclear localization of ICAD-L/DFF45 could be explained by the protein having its own nuclear localization signal or by an interaction with other proteins such as CAD/CPAN/DFF40. We suspected that the nuclear localization of ICAD-L was unlikely to be due to the protein being transported into the nucleus in a complex with a carrier protein such as CAD, since the GFP:ICAD-L protein was detected almost solely in the nucleus, even in cells where the transfected protein was highly overexpressed.

Previous descriptions of the sequence of ICAD-L/DFF45 have yet to describe a putative nuclear localization signal within the molecule. Nonetheless, upon examination of the ICAD-L deduced amino acid sequence we noticed a cluster of basic residues in the C-terminal twenty amino acids that might function as a bipartite nuclear localization signal (Fig. 19) (Robbins, Dilworth *et al.*, 1991). To test the possibility that this region functions as a nuclear localization sequence, we constructed a fusion protein between GFP and ICAD-L from which this twenty amino acids had been removed (GFP:ICAD-L^{1-311}). Following transient transfection, GFP:ICAD-L^{1-311} was localized diffusely throughout the cell, thus confirming that this region of ICAD-L is essential for the nuclear localization of the protein (Fig. 18, Panels D). It is worth noting that these twenty amino acids do not include the region which has been proposed to be necessary for

interaction between ICAD and CAD (Gu *et al.*, 1999; Inohara, Koseki *et al.*, 1999).

To confirm that the C-terminal twenty amino acids of ICAD-L possesses autonomous NLS function, we constructed a vector encoding a fusion between GFP and this twenty amino acid peptide (GFP:ICAD-$L^{312-331}$). In control experiments, GFP on its own did not target to the nucleus (Fig. 20 panels B). However, following transient transfection, GFP:ICAD-$L^{312-331}$ was predominantly nuclear (Fig. 20 panels A). This result strongly supports the hypothesis that ICAD-L localizes in the nucleus due to the action of a C-terminal nuclear localization signal.

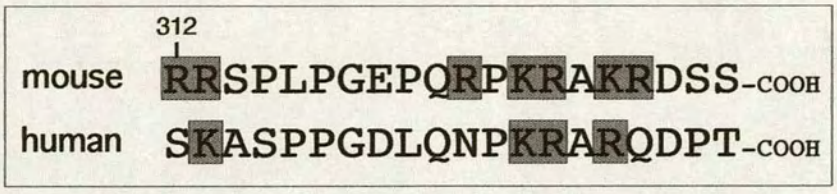

Figure 19. A possible bipartite NLS in the C-terminal 20 amino acid residues of ICAD-L is conserved between mouse and human. Basic residues are shadowed.

Ольга Сергеевна Кузнецова
Ольга Сергеевна Кузнецова
Ольга Сергеевна Кузнецова

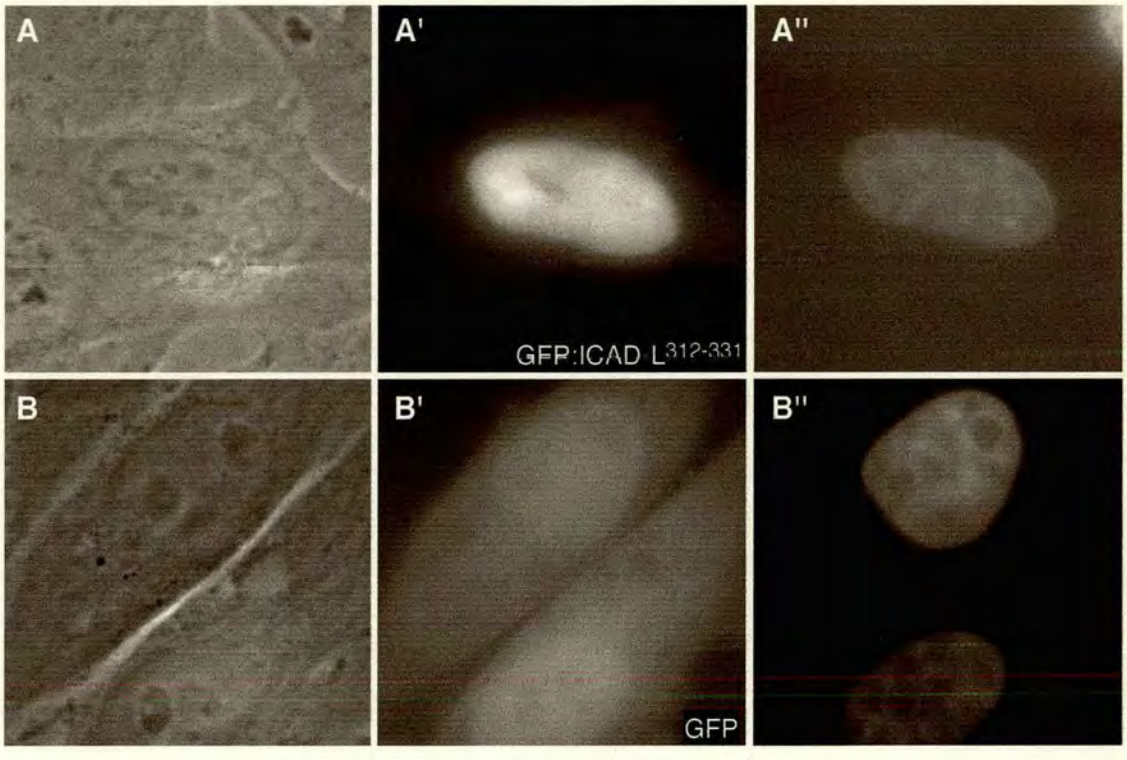

Figure 20. The C-terminal 20 aa of ICAD-L functions as an autonomous nuclear localization sequence capable of targeting GFP to the cell nucleus. *Aequoria victoria* green fluorescent protein (GFP) was fused in frame to a peptide comprising the C-terminal 20 amino acids from murine ICAD-L and expressed by transient transfection in HeLa cells. (**panels A**) The expressed GFP:ICAD-L$^{312-331}$ was highly concentrated in nuclei. (**panels B**) GFP expressed on its own is distributed throughout the cell in both nucleus and cytoplasm. Panels A, B - phase contrast; Panels A′, B′ - detection of GFP fluorescence; Panels A″, B″ - DAPI fluorescence of cellular DNA. Bar 10 μm

3.3.5 CAD is also a nuclear protein

It has been proposed that CAD/CPAN/DFF40 exists as a one to one complex with ICAD-L/DFF45 in healthy cells (Liu *et al.*, 1997; Enari *et al.*, 1998), although it has not proven possible to detect significant complexes between CAD and ICAD-S/DFF35 in cells (Sakahira *et al.*, 1999). Furthermore, it has been claimed that CAD contains a nuclear localization signal near its C-terminus (CAD: amino acid residues 331-345) (Enari *et al.*, 1998). To confirm the localization of CAD within cells, a plasmid encoding a GFP: CAD fusion protein was constructed. Following transient transfection, this fusion protein was detected almost solely in the nucleus of human epithelial and chicken hepatoma cells (Fig. 18, panels E). To exclude the possibility that the nuclear localization of GFP:CAD was due to its overexpression and failure to form a complex with ICAD, plasmids expressing GFP:CAD plus HA-tagged ICAD-L were co-transfected into HeLa cells. Both proteins were highly concentrated in the nucleus of human epithelial cells (data not shown). In addition, endogenous CAD was detected in the nuclear fraction following subcellular fractionation and immunoblotting (chapter 4 Fig. 24).

3.4 Discussion

The CAD:ICAD-L complex is stored within nuclei

The locations of ICAD-L/DFF45 and CAD/CPAN/DFF40 in cells have been remained controversial, with the original claims that these proteins are located in the cytoplasm (Enari *et al.*, 1998). However, this and other people's studies have shown that expressed exogenous ICAD and CAD are in the nucleus (Liu *et al.*, 1998; Samejima and Earnshaw, 1998; Samejima and Earnshaw, 2000). In general, studies that have examined the location of expressed ICAD-L/DFF45 and CAD/CPAN/DFF40 in transfected cells have found the protein in the nucleus (Liu *et al.*, 1998; Samejima and Earnshaw, 1998), whilst subcellular fractionation studies have found and ICAD-L/DFF45 to be cytoplasmic to a greater or lesser extent (Sabol, Li *et al.*, 1998; Zhang *et al.*, 1999; Zhivotovsky *et al.*, 1999). However, subcellular fractionation in the present study using HeLa cells found the endogenous ICAD-L/DFF45 protein to be predominantly nuclear when steps were taken to minimize leakage from nuclei (Samejima and Earnshaw, 1998). Apart from methodological differences, it is, of course, possible that the localization of these proteins could vary between differing cell types. To clarify this issue, we examined the sequence of ICAD-L and found a putative nuclear localization signal on its C-terminus that had not been predicted previously. The data presented here confirmed that both CAD and its inhibitory chaperone ICAD-L possess autonomous nuclear localization sequences. We also showed that ICAD-L/DFF45 was primarily located in apoptotic HeLa nuclei.

Cells contain two forms of ICAD:ICAD-L and ICAD-S, which differ at their C-termini. Because the region of ICAD-L that is missing from ICAD-S contains a bipartite NLS, these two splice forms occupy very different cellular locations. ICAD-S is found in both the nucleus and cytoplasm, whereas ICAD-L is almost exclusively nuclear. Interestingly, these two forms of ICAD are functionally distinct (Gu *et al.*, 1999; Sakahira *et al.*, 1999). Whether ICAD-S has a distinct function in the cytoplasm is not currently known, nor is it known whether the cytoplasmic pool of ICAD-S is associated with CAD. All in all, current results are consistent with models in which the primary location of CAD in proliferating cells is nuclear, making it unlikely that regulation of CAD entry into the nucleus is a critical factor in the control of the onset of apoptotic execution.

Studies using a model for the induction of apoptosis by Fas/CD95 showed previously that nuclear transport of proteins is essential for cells to enter apoptotic execution (Yasuhara *et al.*, 1997). The results presented here suggest that activated CAD is unlikely to be the key factor that must translocate into the nucleus since CAD localizes already in the nucleus as an inactive complex. Interestingly the recently identified Drosophila CAD homologue, dCAD/Drep-4 does not have its own NLS. When incubated with nuclei, recombinant dCAD/Drep-4 does not cause DNA cleavage in nuclei despite its DNase activity against naked DNA (Yokoyama *et al.*, 2000). It will be very interesting to determine the activation and translocation mechanism of dCAD/Drep-4 *in vivo*.

The nature of the critical translocating factor in the Fas/CD95 experiment is unknown (Yasuhara *et al.*, 1997). Likely candidates include apoptosis inducing factor AIF (Susin *et al.*, 1999), acinus (Sahara *et al.*, 1999), and in view of the results described here, activated caspase-3 and possibly caspase-7, since these enzymes appear to be responsible for the activation of CAD in cells (Janicke *et al.*, 1998; Mitamura, Ikawa *et al.*, 1998; Tang and Kidd, 1998; Zheng, Schlosser *et al.*, 1998; Liu *et al.*, 1999; Wolf *et al.*, 1999). The intracellular localization and translocation of caspases during apoptosis is still under investigation, however, we previously reported the detection of an activity comigrating with activated caspase-3 in the nucleus by activity labeling and two-dimensional gel analysis (Martins *et al.*, 1997). It has recently been reported that following cleavage of procaspase-3, which exists primarily in the cytoplasm and mitochondria (Mancini *et al.*, 1998; Samali, Zhivotovsky *et al.*, 1998), active caspase-3 is found in the nuclear, mitochondrial, and cytosolic fractions (Chandler, Cohen *et al.*, 1998; Zhivotovsky *et al.*, 1999). In contrast, caspase-7 shifts quantitatively from the cytosol to the microsomal fraction following activation (Zhivotovsky *et al.*, 1999).

What is the role of ICAD-S?

The levels of expression of ICAD-L/DFF-45 and ICAD-S/DFF35 are similar at least in mouse WR19L and human Jurkat T lymphoma cells (Sakahira *et al.*, 1999). It has been suggested that ICAD-S might function as a safety device to prevent the mistaken activation of CAD in healthy cells (Gu

et al., 1999). Promoter analysis of the murine ICAD and CAD genes suggests that expression of these genes is regulated by different mechanisms (Kawane *et al.*, 1999). Alternative splicing of the ICAD pre-mRNA could serve as a mechanism to regulate the level of ICAD-L in response to the expression level of functional CAD. Changes in the efficiency of alternative splicing of the ICAD pre-mRNA would alter the ratio of ICAD-L to ICAD-S without necessitating changes in the transcription of the gene.

Although ICAD-S/DFF35 cannot act as a folding chaperone to enable the synthesis of functional CAD/CPAN/DFF40, it can bind to active CAD/DFF40 and inhibit its nuclease activity *in vitro* (Gu *et al.*, 1999; Sakahira *et al.*, 1999). This is because amino acid residues 101-180 of DFF35/45 mediate the binding to DFF40 while residues 23-100 are implicated in the inhibition of the nuclease *in vitro* (Gu *et al.*, 1999). Despite the fact that ICAD-S can inhibit CAD in cells (Sakahira *et al.*, 1998; Gu *et al.*, 1999), ICAD-S exists primarily in free form *in vivo* (Sakahira *et al.*, 1999). The data from this study suggest that this may be because much of ICAD-S is cytoplasmic whilst CAD is nuclear. Whether ICAD-S has a distinct cytoplasmic function in addition to interaction with CAD is not currently known. Recently a Drosophila ICAD-L/DFF45 homologue, Drep-1/dICAD was identified (Inohara and Nunez, 1999; Mukae *et al.*, 2000). Drosophila has apparently only the long-form of ICAD, suggesting the possibility that ICAD-S may not have an essential role. However, a preliminary yeast two hybrid study suggested an association of ICAD with cytoskeletal components, possibly indicative of unknown functions for ICAD in the

cytoplasm either during apoptosis or in healthy cells.

Chapter 4

4. DNA topoisomerase IIα interacts with CAD nuclease and is involved in chromatin condensation during apoptotic execution

4.1 Introduction

DNA topoisomerase II (topo II) is an enzyme which catalyzes DNA topological transformations by transiently cleaving double strand DNA. One of the major cellular functions of topo II, is to prevent excessive supercoiling of intracellular DNA, which can occur during replication, transcription, recombination, chromosome condensation or sister chromatid segregation. Moreover, it has been known for over ten years that topo II is one of the major components of the metaphase chromosome scaffold (Earnshaw, Halligan *et al.*, 1985; Mirkovitch, Gasser *et al.*, 1987). Thus topo II is essential for remodelling of the chromatin structure during the normal cell cycle. In eukaryotes, topo IIα is a homodimer of a 170 kDa subunit. Vertebrates also express a second type of topo II, topo IIβ, a 180 kDa protein. Although they exhibit some differences in cell cycle regulated expression level and localization (Zini, Martelli *et al.*, 1992; Adachi, Miyaike *et al.*, 1997; Warburton and Earnshaw, 1997; McPherson and Goldenberg, 1998), the functional difference between α and β is largely unknown.

It has been shown that apoptotic degradation of genomic DNA in mammalian cells starts by excision of large DNA fragments ranging in size

from 50 kilobases to more than 300 kilobases (Oberhammer *et al.*, 1993). It was suggested that the above fragments could represent chromosomal DNA loops. A role of topo II for the generation of these fragments during apoptotic execution has been controversial (Lagarkova, Iarovaia *et al.*, 1995; Beere, Chresta *et al.*, 1996; McPherson and Goldenberg, 1998; Li *et al.*, 1999).

Previous studies in our lab had raised the possibility that topo IIα might have a role in chromatin condensation during apoptotic execution. We found that the topo IIα level in chick erythroblasts drops drastically during development. The extent of chromatin condensation of chicken erythrocyte nuclei incubated in S/M extracts correlates with the level of endogenous topo II present in the added nuclei (Wood and Earnshaw, 1990).

In chapter 2, it is demonstrated that our E/X extracts contain another factor(s) apart from CAD which is responsible for chromatin condensation. It was suspected that topo II might be one such factor. In this study, the function of topo II during apoptotic execution was investigated using both biochemical approaches and highly specific topo II inhibitors (Gorbsky, 1994) which interfere with the catalytic activity of the topoisomerase, but do not trap the cleavable complex.

4.2 Materials and Methods

4.2.1 Preparation of apoptotic extracts and *in vitro* apoptosis reaction

Apoptotic (E/X) extracts were prepared from chicken DU249 cells as described (chapters 1.5 and 2.2.1). The *in vitro* apoptosis reaction was performed as described (chapter 2.2.3) with the following exceptions. For certain experiments, the HeLa nuclei were preincubated for 30 min at 37°C with either a topo II inhibitor ICRF-187 (50 mg/ml, gift of Dr. A. Imondi, Pharmacia) or diluent. For CAD inhibition, E/X extracts were preincubated with ICAD-L or CAD buffer (10 mM HEPES, pH 7.4, 50 mM NaCl, 5 mM EGTA, 2 mM $MgCl_2$, 1 mM DTT) for 15 min at 37°C. For caspase inhibition, E/X extracts were preincubated with DEVD-fmk (100 µM, Calbiochem) or diluent for 15 min at 37°C. In certain experiments 1.5 µg of purified human topo IIα (corresponding to a ~4x higher-than-physiological level of 1.7×10^6 molecules per nucleus) was added to the incubation (human topo II was prepared from baculovirus infected insect cells.). Nuclei were subsequently stained with DAPI to observe chromatin condensation.

4.2.2 Construction of clones and bacterial expression of cloned proteins

4.2.2.1 Construction of clones

For construction of ***intein-ICAD***, mouse full length ICAD-L (Enari *et al.*, 1998) (gift of S. Nagata, Osaka) was cloned into the Nco I/Sma I cloning sites of pTYB4 (New England Biolabs Inc.). ***GST-CAD*** was prepared by cloning full length murine CAD into the pGEX 4T-1 (Pharmacia Biotech) Eco RI and Xho I cloning site. To make the plasmid encoding the GST-CAD

His_6-ICAD combination, ***GST-CAD/His$_6$-ICAD***, His_6-ICAD in pRSET B (chapter 3.2.2) was obtained by PCR with primer (5'-TGAGACGTCTAATACGACTCAC-3') and primer (5'-GTCGACGTCAGCAAAAAACCCC-3') and cloned into the Aat II site of pGEX 4T-1 containing GST-CAD. To make the ***Zeo:His:HA vector***, first a His_6 tag was constructed by ligation of oligos (5'-CTAGCATGCATCATCATCATCATCACCGCGGA-3') and (5'-AGCTTCCGCGGTGATGATGATGATGATGCATG-3'). The resulting fragment was ligated into vector pZeo $SV2^+$ (Invitrogen) that had been digested with Nhe I and Hind III. The HA tag in pBluescript KS (Stratagene) was digested with Sac II and blunt-ended with T4 DNA polymerase plus 100 µM dNTPs, and digested with Eco RI. The resulting fragment was ligated into vector pZeo His that had been digested with Kpn I and blunt-ended with T4 DNA polymerase plus 100 µM dNTPs, and digested with Eco RI. To make ***Zeo:His:HA:CAD*** and ***Zeo:His:HA:GFP***, the CAD ORF was obtained by PCR from a plasmid containing the full-length CAD cDNA (gift of S. Nagata), cloned into pBluescript KS (Stratagene) and digested with Eco RI and Xho I. GFP was obtained by PCR using primer T7 and primer (5'-CCGCTCGAGTTACTTGTACAGC-3') from an enhanced GFP: lamin A in pCDNA 3 (gift of Larry M. Karnitz, Mayo Research Foundation, Rochester, MN), then digested with Eco RI and Xho I. The resulting fragments were ligated into vector Zeo:His:HA that had been digested with Eco RI and Xho I.

4.2.2.2 Expression and Purification of GST-ICAD, GST-CAD, GST-CAD/His_6-ICAD, and GST

Plasmids encoding ***GST-ICAD, GST-CAD, GST-CAD/His_6-ICAD, GST-BubR1, GST-hAIRK2*** **and** ***GST*** **alone** transformed into *E. coli* BL21(DE3)Lys S cells were grown to OD_{600} = 0.5-0.7, and protein expression was induced with IPTG (0.3-0.5 mM) for 3-5 hr. Cells were collected by centrifugation at 5,000 g for 10 min and frozen at -80°C.

GST-CAD/His_6-ICAD was first purified with 0.5 ml of Ni-agarose (Qiagen, Catswirth, CA) as described previously for the purification of His_6-ICAD protein (chapter 3.2.2). Protein eluted from Ni-agarose column was diluted 20-fold into GST wash buffer (PBS, 5 mM EDTA, 5 mM DTT, 1% Triton), and then purified a second time over glutathione sepharose as described below.

Pellets of *E. coli* expressing GST-ICAD, GST-CAD, or GST were thawed on ice and resuspended in lysis buffer (PBS, 5 mM EDTA, 5 mM DTT) with lysozyme (final conc. 1mg/ml) and incubated on ice for 30 min. After sonication, Triton X-100 was added to 1% and the lysate was centrifuged at 4,000 x g for 20 min. The supernatant was mixed with Glutathione Sepharose 4B (Pharmacia Biotech) which had been equilibrated with PBS and incubated on a rotating mixer for 1 hr at 4°C. The sepharose beads were washed in batch 3 times with wash buffer. GST-ICAD and GST were eluted with elution buffer 1 (10 mM glutathione, 50 mM Tris:HCl (pH 8.0)). GST-CAD, and GST-CAD/His-ICAD were eluted with elution buffer 2 (20 mM glutathione, 100 mM Tris:HCl (pH 8.0), 120 mM NaCl). The eluted

proteins were dialyzed for at least 3 hr against two changes of CAD buffer (10 mM HEPES, pH 7.4, 50 mM NaCl, 5 mM EGTA, 2 mM $MgCl_2$, 1 mM DTT), aliquoted, and frozen in N2(l).

Intein-ICAD encoded by pTYB4/ICAD-L was expressed in *E. coli* strain ER2566 and purified using the IMPACT^{TM} T7 system (New England Biolabs Inc.) following the manufacturer's instructions. Intein-ICAD bound to chitin beads was left at 4°C overnight in Cleavage Buffer (20 mM Tris:HCl, pH 8.0, 50 mM NaCl, 0.1 mM EDTA, 30 mM DTT). The protein was eluted with Cleavage Buffer without DTT. The eluted protein was dialyzed for at least 3 hr against two changes of CAD buffer, aliquoted and frozen in N2(l).

4.2.3 Binding of topo IIα to GST- fusion proteins *in vitro*

125 ng of purified topo IIα and 53.3 ng of purified PARP (in PBS + 5 mM DTT, 10 mM EDTA and 1% Triton X-100) were incubated with glutathione sepharose beads either alone, or with bound GST, GST-ICAD-L, GST-CAD, GST-cBubR1 or GST-hAIRK2. The bound fraction was resolved by SDS-PAGE (10% gel), and topo IIα was detected by immunoblotting with monoclonal antibody Ki-S1. PARP was detected by immunoblotting with monoclonal antibody C2-10.

4.2.4 Immunoprecipitation of HA-tagged CAD and GFP from stable cell lines (Steps after establishment of stable cell lines were performed by Stefanie Kandels-Lewis)

Stable lines of MSB-1 chicken lymphoblastoid cells expressing His:HA:CAD and His:HA:GFP were obtained by electroporation with Zeo:His:HA:CAD and Zeo:His:HA:GFP (310 V 975 μF (BioRad Gene-Pulser with 0.4 mm cuvettes)), selected with 400 μg/ml Zeosin (Invitrogen) and confirmed by immunoblotting with anti HA tag antibody. For immunoprecipitation, cells were harvested, washed twice with PBS/EDTA and lysed by sonication for 5 seconds at setting 4 (max) with microtip in IPP 150 (10 mM Tris:HCl pH 8.0, 150 mM NaCl, 0.1% NP-40), and insoluble material removed by centrifugation for 5 min at 8161 x G at 4°C. HA-conjugated proteins were immunoadsorbed using mAb 12CA5 preloaded onto Affi-Prep Protein A Support beads (BioRad). After incubation for 1 hr at 4°C the beads were washed 3 times for 5 min with 25 bed volumes of either IPP150, IPP200 (200 mM NaCl) or IPP300 (300 mM NaCl). Bound proteins were subjected to SDS-PAGE in 10 % Prosieve 50 Acrylamide gels (FMC, Rockland, Maine USA), transferred to Hybond C nitrocellulose (Amersham), and detected by ECL. Detection of topo IIα was with Rabbit G (Hoffmann, Heck *et al.*, 1989) at a 1:1000 dilution. Detection of HA-CAD was with mouse mAB 12CA5 diluted 1:1000.

4.2.5 Kinetoplast minicircle decatenation assay (GST-fusion proteins were prepared by Kumiko Samejima. The assay was performed in the laboratory of Prof. Neil Osheroff.)

0.3 μg of kinetoplast DNA was incubated with 10 nM purified human topo IIα plus 10 nM of GST:CAD, GST:ICAD, GST:CAD + GST:ICAD, or GST alone for 10 min at 37 °C. The reaction was stopped by addition of DNA loading buffer, heated at 65°C for 10 min, loaded onto a 1% agarose gel containing 0.5 mg/ml ethidium bromide and run at 90V for 2 hr (Fig 23B), and the minicircles released by decatenation were quantified. No detectable intact minicircles were released in incubations with GST-CAD or GST-CAD + His-ICAD-L in the absence of topo IIα. Under these conditions, the GST-CAD is catalytically inactive and does not interfere with the assay.

4.3 Results

4.3.1 Topo IIα has a role in chromatin condensation during apoptosis

HeLa nuclei incubated in E/X extracts underwent chromatin condensation in two stages: condensation against the nuclear rim was followed by the formation of discrete apoptotic bodies (Fig. 21B). The rim-condensation also occurred when caspase activity was inhibited with the peptide fluoromethylketone inhibitor DEVD-fmk (Fig. 21C -see also chapter 2 Fig. 10). Strikingly, simultaneous inhibition of caspase and topo II activity completely abolished apoptotic chromatin condensation (Fig. 21E). This inhibition of apoptotic chromatin condensation was unlikely to arise from global changes in the accessibility of chromatin to condensation factors, since simultaneous inhibition of caspases and topo II had no effect on the ability of CAD nuclease to cleave the nuclear DNA to an oligonucleosomal ladder (performed by Francoise Durriu and data not shown).

The abolition of apoptotic chromatin condensation following simultaneous inhibition of topo II and caspases was seen with the highly specific topo II inhibitor, ICRF-187, suggesting that the effect is due to action of the drug on topo II(Gorbsky, 1994). In a further control, apoptotic chromatin condensation was restored when highly purified human topo IIα was added to nuclei in E/X extract in the presence of the topo II and caspase inhibitors (Fig. 21F). Topo IIα alone had no effect on the morphology of nuclei in buffer after 2 hr (Fig. 21J).

Simultaneous inhibition of caspases and CAD (by addition of the ICAD-L) also blocked chromatin condensation in E/X extracts (Fig. 21H). This confirmed our previous results suggesting that CAD and caspases act in parallel pathways of apoptotic chromatin condensation (chapter 2.3.5). Surprisingly, this inhibition of chromatin condensation could be partially reversed upon addition of purified human topo IIα (Fig 21I).

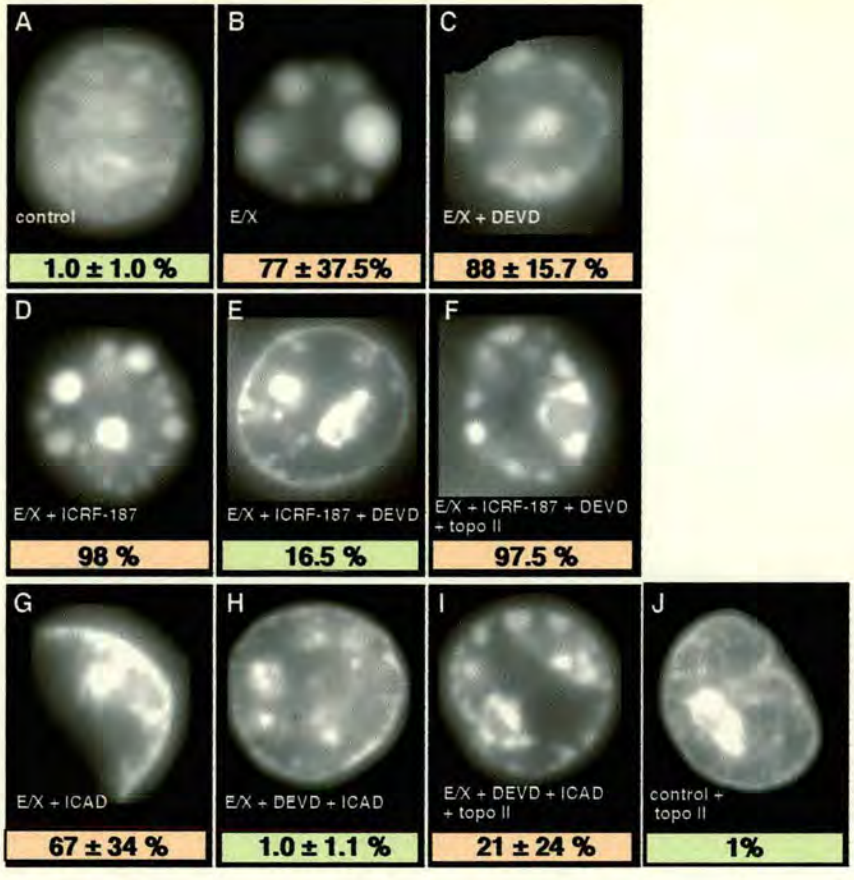

Figure 21. Topo IIα is required for apoptotic chromatin condensation in the absence of caspase activity. Isolated HeLa cell nuclei were preincubated either with diluent alone (**A-C**) or 50 μg/ml ICRF-187 (**D-F**). The nuclei were then added to buffer (**A**) or apoptotic E/X extract (chapter 2) (**B-I**) and further incubated for 2 hr at 37°C. (**D**) -Inhibition of topo IIα did not inhibit apoptotic chromatin condensation. (**E**) - Inhibition of topo IIα plus caspases (with 100 μM DEVD-fmk) abolished chromatin condensation. (**F**) - This block was reversed if 1.5 μg (4.5 pM) purified human topo IIα was added at the start of the 37°C incubation. (**G**) Inhibition of CAD with 160 ng of DM-ICAD-L does not block apoptotic chromatin condensation (**H**) Simultaneous inhibition of CAD plus caspases blocks morphological apoptosis; (**I**) Simultaneous inhibition of CAD plus caspases - rescue of apoptotic morphology with 1.5 μg added topo IIα. (**J**) Purified human topo IIα (1.5 μg = 4.5 pM) did not induce chromatin condensation in nuclei in buffer. The panels below each micrograph indicate the percentage of apoptotic cells scored in the microscope. Green panels were interpreted as a normal morphology. Red panels were interpreted as showing an apoptotic morphology. These images were selected from images taken at random.

4.3.2 Interaction between topo IIα and CAD

Physical interactions between topo IIα and CAD were readily detected both *in vitro* and *in vivo*. Purified topo IIα bound quantitatively to GST-CAD on glutathione sepharose, but not to GST alone, GST:ICAD-L, GST:BubR1, GST:AIRK2, GST:β tubulin (not shown), or the sepharose alone (Fig. 22A). As a control, purified PARP added to the mix did not bind to any protein (Fig. 22A). Similar topo IIα binding was also observed with Intein-CAD (not shown).

To confirm that topo IIα can bind CAD in cell extracts, we made stable sublines of chicken MSB-1 cells expressing His-HA-GFP or very low levels of His-HA-CAD. Lysates were prepared, and the expressed CAD was immunoprecipitated using anti-HA antibody. These immunoprecipitates reproducibly contained topo IIα, which was not seen in control immunoprecipitates of the much more highly expressed control protein, His-HA-GFP (Fig. 22B). This demonstrates that CAD can interact with topo IIα in cell extracts. It is not surprising that only a fraction of topo IIα was bound to CAD, as topo IIα is very abundant in MSB-1 cells, and thus is presumably present in a vast excess over CAD.

Importantly, the interaction between topo IIα and CAD appears to be functionally significant. In a quantitative assay for DNA decatenation, purified GST-CAD either on its own or as a complex with His-tagged ICAD-L, stimulated the decatenation activity of topo IIα two to three fold, whilst

buffer, GST or GST-ICAD-L had no effect (Fig. 23A). It is important to note that under these conditions the CAD is enzymatically inactive, and does not interfere with the topo II assay (which measures the release of intact minicircles from kinetoplast networks (Fig. 23B). In other experiments, we could not detect an effect of topo II inhibition or addition on nuclease activity of CAD against nuclear chromatin (data not shown).

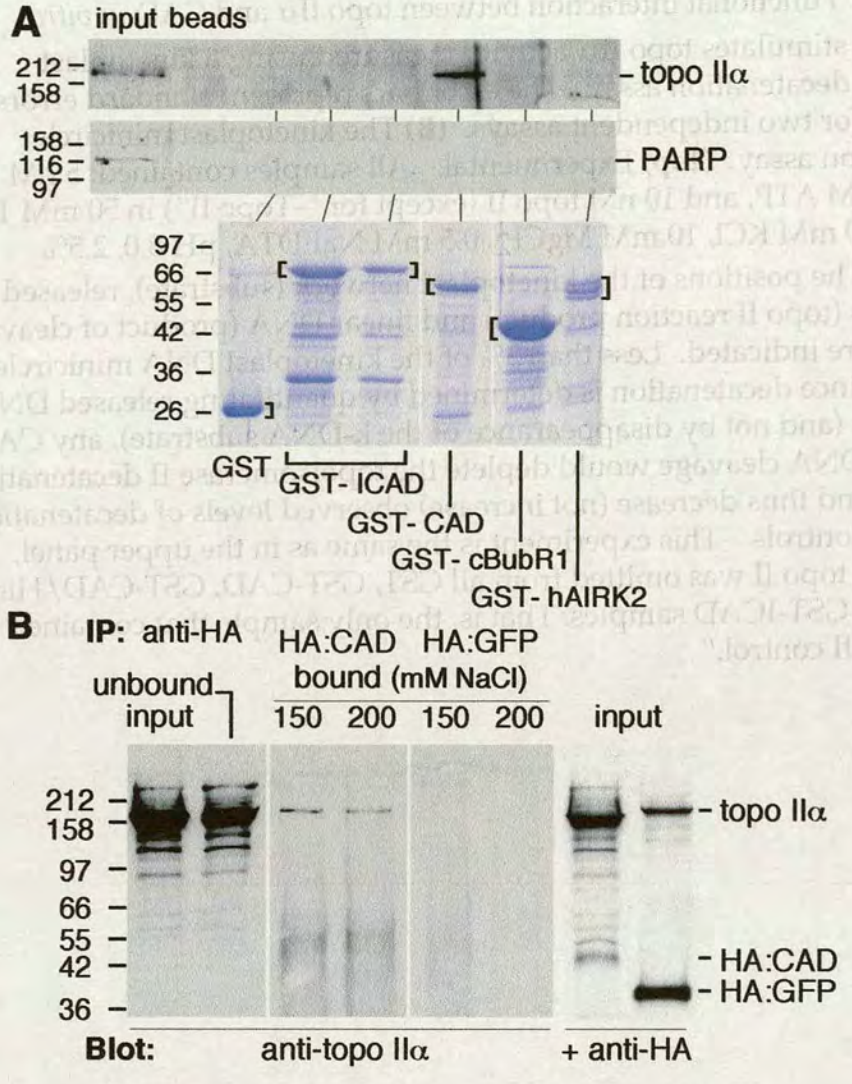

Figure 22. Physical interaction between topo IIα and CAD *in vitro* and *in vivo*. **(A)** Human topo IIα 125ng/100µl binds *in vitro* to GST-CAD, but not to GST, GST-ICAD-L, GST-cBubR1 or GST-hAIRK2: PARP 53.3ng/100µl tested as a control does not bind any of these proteins. The Coomassie Blue-stained gel shows the relative amount of each protein on the beads. **(B)** A subfraction of endogenous topo IIα associates with tagged CAD *in vivo*. HA-tagged proteins were immunoprecipitated from stable transfectants expressing His-HA-CAD or His-HA-GFP and subjected to SDS-PAGE. Left - blot with anti-topo IIα showing the input and unbound fractions (equivalent to 8 x 10^5 cells), and the fractions bound to the beads (5x10^6 cells for His-HA-CAD and 1 x10^6 cells for His-HA-GFP). Right - blot with anti-HA showing the input and unbound fractions (equivalent to 8 x 10^5 cells for His-HA-CAD and 1.6 x10^5 cells for His-HA-GFP). We estimate that His-HA-GFP is expressed roughly 25-100- fold more abundantly than His-HA-CAD in these cells.

Figure 23. Functional interaction between topo IIα and CAD *in vitro.* **(A)** GST-CAD stimulates topo IIα activity measured using a kinetoplast minicircle decatenation assay. The error bars represent standard errors of the mean for two independent assays. **(B)** The kinetoplast minicircle decatenation assay. (**top**) Experimental. All samples contained: 5 nM k-DNA, 1 mM ATP, and 10 nM topo II (except for "-Topo II") in 50 mM Tris, pH 7.9, 100 mM KCl, 10 mM $MgCl_2$, 0.5 mM NaEDTA, pH 8.0, 2.5% glycerol. The positions of the kinetoplast network (substrate), released minicircles (topo II reaction product) and linear DNA (product of cleavage by CAD) are indicated. Less than 3% of the kinetoplast DNA minicircles are cleaved. Since decatenation is determined by quantitating released DNA minicircles (and not by disappearance of the k-DNA substrate), any CAD-mediated DNA cleavage would deplete the topoisomerase II decatenation substrate and thus decrease (not increase) observed levels of decatenation. (**bottom**) Controls. This experiment is the same as in the upper panel, except that topo II was omitted from all GST, GST-CAD, GST-CAD/His-ICAD, and GST-ICAD samples. That is, the only sample that contained topo II is "Topo II control."

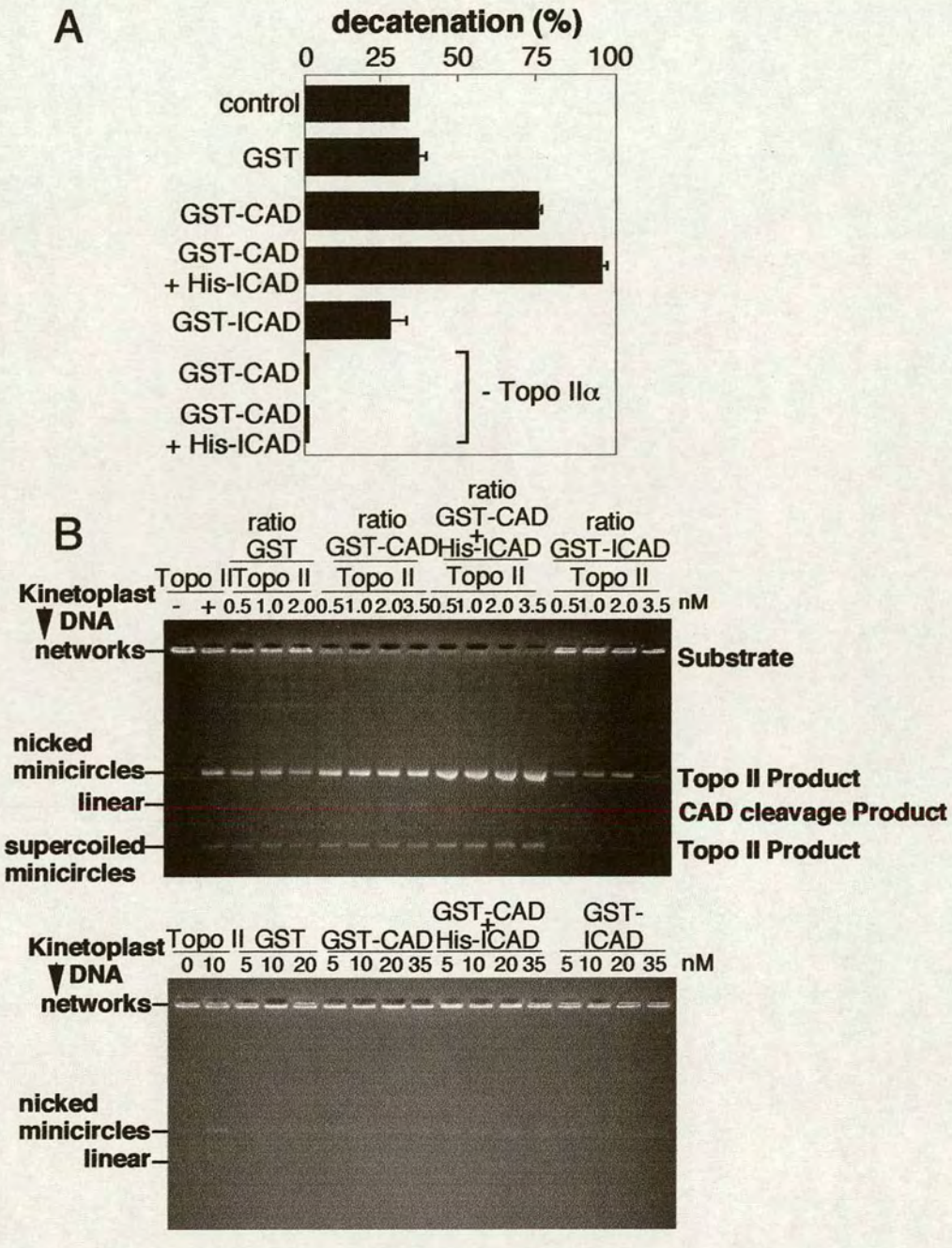
A
decatenation (%)
0
25
50
75
100
control
GST
GST-CAD
GST-CAD
+ His-ICAD
GST-ICAD
GST-CAD
GST-CAD
+ His-ICAD
- Topo IIα
B
ratio
GST
Topo II
Topo II
-
+
0.5
1.0
2.0
ratio
GST-CAD
Topo II
0.5
1.0
2.0
3.5
ratio
GST-CAD
+
His-ICAD
Topo II
0.5
1.0
2.0
3.5
ratio
GST-ICAD
Topo II
0.5
1.0
2.0
3.5
nM
Kinetoplast
DNA
networks
nicked
minicircles
linear
supercoiled
minicircles
Substrate
Topo II Product
CAD cleavage Product
Topo II Product
GST-CAD
+
His-ICAD
GST-
ICAD
Topo II
GST
GST-CAD
0
10
5
10
20
5
10
20
35
5
10
20
35
5
10
20
35
nM
Kinetoplast
DNA
networks
nicked
minicircles
linear

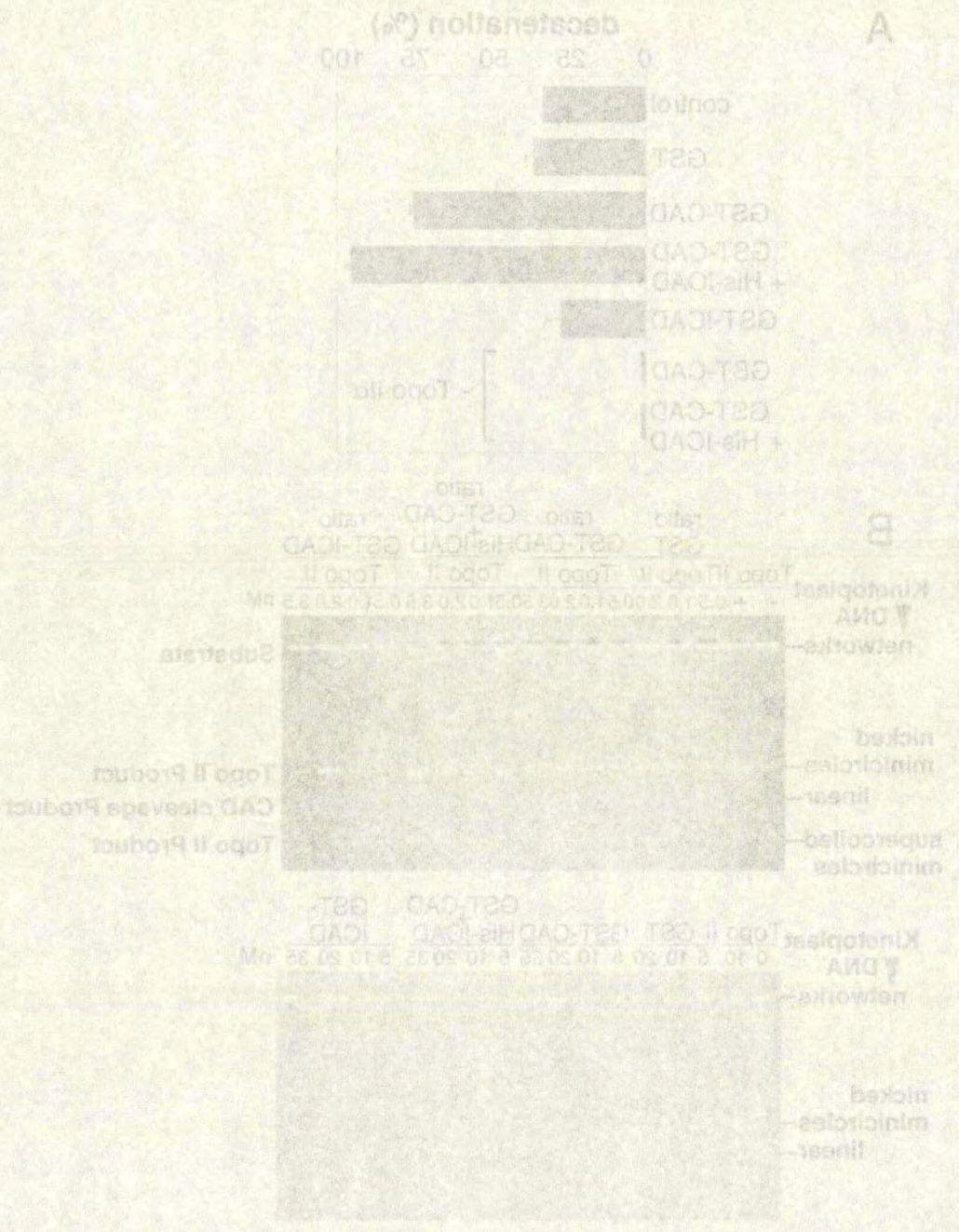

4.3.3 Topo IIα and GFP-CAD colocalize in healthy cell nuclei.

It is widely accepted that topo IIα is nuclear (Adachi *et al.*, 1997), and that CAD must be nuclear during apoptotic execution (Enari *et al.*, 1998). However the location of CAD in non-apoptotic cells has been much more controversial. Initial biochemical fractionation results that identified first DFF (Liu *et al.*, 1997), and then CAD/ICAD (Enari *et al.*, 1998) were obtained using cytoplasmic extracts. However, these experiments did not take special steps to minimize leakage of soluble proteins from nuclei during extract preparation. The first evidence suggesting that the CAD/ICAD complex might be nuclear came with the observation that exogenous ICAD is nuclear when expressed in a variety of cell types (chapter 3) (Liu *et al.*, 1998). In addition, our subcellular fractionation experiments confirmed that endogenous ICAD is predominantly nuclear (chapter 3). Consistent with this localization, we have recently identified an autonomous NLS at the C-terminus of ICAD-L (chapter 3). In the present study we have addressed the localization of the CAD nuclease itself.

GFP-CAD is exclusively nuclear when expressed at low-to-moderate levels in cultured cells (Fig. 24A, panel 2 - see also chapter 3 Fig. 18E). The expressed protein is distributed throughout the nucleus in a micropunctate pattern that largely follows the distribution of the DNA. Endogenous topo IIα has a similar distribution in interphase cell nuclei (Fig. 24A, panel 3), and in a merged image (Fig. 24A, panel 4), the CAD and topo IIα signals superimpose as a yellow signal distributed throughout the nucleus. In order

to confirm the nuclear localization of endogenous CAD, we prepared a rabbit antiserum to cloned murine CAD and used this in subcellular fractionation experiments (Fig. 24B). These results reveal that a substantial portion of the CAD is found in the nuclear fraction. Although we cannot exclude the possibility that a portion of CAD is normally resident in the cytoplasm, our results reveal that much of this protein is nuclear, and would therefore be available to interact with topo IIα in cells.

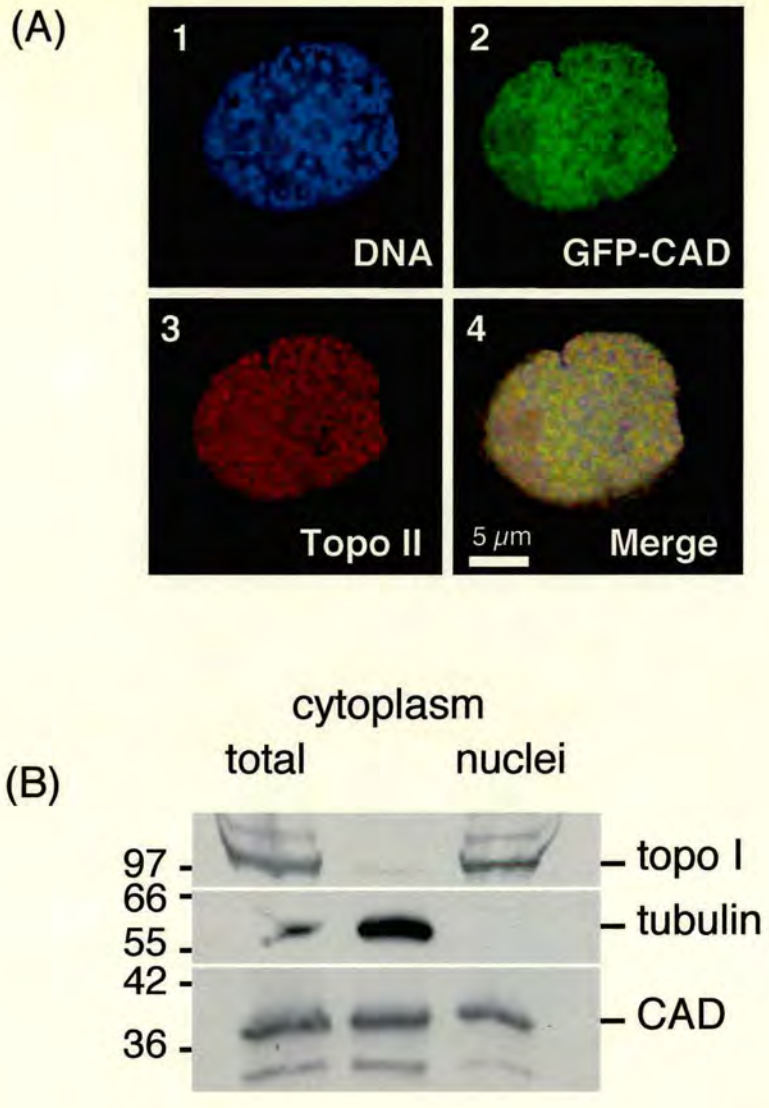

Figure 24. **(A)** Topo IIα and GFP-CAD colocalize in healthy cell nuclei. Chicken DU249 cells were transfected with constructs expressing GFP-CAD and then stained for endogenous topo IIα. The two proteins were distributed throughout the nuclei in an overlapping micropunctate pattern. The image shown is a single deconvolved optical section obtained with a DeltaVision microscope. (microscopy by Bill Earnshaw) **(B)** A significant portion of endogenous CAD is nuclear. HeLa S3 cells were fractionated into nucleus and cytoplasm (chapter 3.2.4) and immunoblotted with rabbit antibody raised against murine CAD, mouse anti-tubulin, and human autoantibody against topo I.

4.4 Discussion

The experiments described above provide the first evidence that topo IIα has a role in chromatin condensation during apoptosis. They show that simultaneous inhibition of either caspase plus topo II or caspases plus CAD blocked chromatin condensation in E/X extracts. This inhibition was reversed by the addition of purified topo IIα. The rescue by purified topo IIα in the presence of the ICRF-187 inhibitor raises the possibility that topo IIα could be functioning in a non-enzymatic role, either as a structural or targeting factor, as has been proposed for its role in mitotic chromosome condensation (Adachi, Luke *et al.*, 1991). The suprising result that addition of purified topo IIα can reverse the effect of the simultaneous inhibition of caspases plus CAD suggests that topo IIα acts downstream of CAD or promotes condensation in a pathway parallel to the CAD pathway. However, it was also possible that the added topo IIα might interfere with the interaction between CAD and the exogenous ICAD added to these reactions as a CAD inhibitor.

These results might be explained if CAD and topo II functionally interact in cells. The present study showed that topo IIα and CAD physically interact *in vitro* and *in vivo*. Functional interaction between CAD and topo II was shown by an *in vitro* assay. Co-localization of topo II and CAD in the nucleus was shown by the experiment with GFP:CAD and a cell fractionation assay. All these results strongly suggest that CAD and topo II

functionally interact in normal cells, and presumably, in apoptotic cells to induce chromatin condensation.

The results presented in this chapter reveal that the control of apoptotic chromatin condensation is likely to be complex. The results are consistent with models in which CAD and topo IIα act in independent pathways in E/X extracts, but both have their activities modulated by caspases. Recent results have identified several other molecules that appear to be able to induce apoptotic chromatin condensation in nuclei. These include the mitochondrial flavoprotein AIF (apoptosis-inducing factor) (Susin *et al.*, 1999), L-DNase II (Torriglia, Perani *et al.*, 1998) and acinus (Sahara *et al.*, 1999). The experiments reported here suggest that in the absence of caspases, none of these activities is sufficient to induce apoptotic chromatin condensation unless either CAD or topo IIα is also present and functional. It is possible that AIF and Acinus might function in the same pathways as CAD or topo IIα during apoptotic chromatin condensation.

Although a role for topo IIα in apoptotic execution has been controversial (Lagarkova *et al.*, 1995; Beere *et al.*, 1996), a recent study clearly demonstrated an involvement of the enzyme in the generation of reversible high molecular weight DNA fragments following oxidative stress (Li *et al.*, 1999). In addition, a more recent study has shown that topo IIα can stimulate the activity of CAD against a naked DNA substrate approximately 8-fold, although the cleavage of chromatin substrates was essentially unaffected (Widlak *et al.*, 2000). A direct interaction such as demonstrated

here between topo IIα and CAD might result in targeting of CAD to sites occupied by topo IIα at the base of chromosomal loop domains. At those sites, CAD might initially stimulate the activity of topo IIα, and then subsequently, upon cleavage of ICAD-L by caspases, CAD might commence the wholesale digestion of the DNA that is characteristic of apoptotic execution, possibly being further stimulated by interactions with topo IIα. The present results predict that CAD cleavage might initiate at or near topo IIα binding sites.

CONCLUSION

Purpose of this study

One of the hallmarks of apoptosis is the dramatic changes of nuclear morphology that occur during apoptotic execution. However, the mechanisms underlying these changes are not understood. In this study, chromatin condensation and DNA fragmentation were used to assay nuclear disassembly. The goal of this study was to elucidate the biochemical mechanism of the changes in nuclear morphology. The initial aim was to clarify whether caspases drive nuclear disassembly directly or whether caspases play an executive role, activating downstream factors which induce nuclear disassembly.

Further characterization of the cell free system

A revision of the protocol for preparing S/M extracts revealed that it is possible to prepare a variety of extracts which represent different stages of apoptosis (C/D, S/M and E/X extracts) from cells in the same culture. Both S/M and E/X extracts, which represent the committed and execution phases, respectively, were found to induce apoptosis in isolated nuclei. However, they showed strikingly different effects when a caspase-inhibitor was added to the extracts: S/M extracts required caspase activity to induce apoptosis; while E/X extracts induced apoptosis in a caspase-independent manner.

These data demonstrated that caspase-activated downstream factors are responsible for chromatin condensation during apoptotic execution rather than caspases themselves (chapter 2). It was also found that PARP and lamin cleavage by caspases are dispensable for chromatin condensation, at least in an *in vitro* system.

In addition, it was shown that internucleosomal DNA cleavage and chromatin condensation are independent during apoptosis as addition of ICAD protein to E/X extracts inhibited DNA fragmentation but not chromatin condensation. Interestingly, simultaneous inhibition of topo II and caspases abolished chromatin condensation activity of E/X extract, however, DNA fragmentation was not suppressed.

CAD is a nuclear protein

Since inappropriate activation of CAD is potentially harmful for cells, the protein must be carefully regulated. One mechanism regulating apoptotic pathways could involve translocation of key factors such as cytochrome *c*, AIF, Bid, and caspases between subcellular compartments. Moreover, it was reported that translocation of unknown factors is necessary for nuclear disassembly in Fas-mediated apoptosis (Yasuhara *et al.*, 1997). Here I tested the hypothesis that CAD/ICAD is sequestered within the cytoplasm of living cells and then, after liberation of CAD by caspase mediated cleavage of ICAD, CAD translocates into the nucleus where it induces apoptosis. The data presented in chapter 3 demonstrated that the

CAD/ICAD complex is nuclear in healthy cells. Thus CAD cannot be the factor which is transported into the nucleus at the onset of apoptosis.

Caspase-3 is known to cleave nuclear proteins such as ICAD and PARP during apoptosis (Lazebnik *et al.*, 1994; Liu *et al.*, 1997). Interestingly, in this study nuclei incubated with caspases did not exhibit chromatin condensation although PARP and lamins were cleaved. This suggests either that extensive DNA fragmentation is needed to induce chromatin condensation when nuclei are incubated with recombinant CAD; or that the physiological level of CAD in nucleus may be insufficient to induce chromatin condensation (the caspases would have been expected to activate nuclear CAD); or, interestingly, that an additional co-factor(s) may be required.

CAD and topo II are chromatin condensation factors

I demonstrated that E/X extracts contain at least two factors capable of inducing chromatin condensation. One such factor is CAD (chapter 2). CAD induces both chromatin condensation and internucleosomal DNA cleavage. The other is topo II, which interacts with CAD (chapter 4). The activities of both CAD and topo II are modulated by caspases. CAD and topo II appear to work in parallel during apoptotic chromatin condensation (chapter 4) and preliminary evidence suggests that AIF and topo II might work on the same pathway (data not shown).

Other proteins, including AIF, acinus, and L-DNase II were previously reported as chromatin condensation factors (chapter 1.4).

However, it is shown here that none of these factors is sufficient to induce chromatin condensation under conditions in which caspases plus CAD or caspases plus topo II are inhibited (chapter 4).

Final remark

The results presented in this thesis contributed to the identification of two components, CAD and topo II, involved in the mechanics of apoptotic execution. I believe that basic apoptosis research such as this will further our understanding of biological functions which will ultimately contribute to therapeutic discoveries and aid in curing a wide range of diseases.

FUTURE DIRECTIONS

This study showed that caspase-activated downstream factors are responsible for chromatin condensation during apoptotic execution. E/X extracts appear to contain at least two such factors: CAD and topo II. Initial characterization of these two factors revealed that both CAD and topo II locate in the nucleus and interact with each other in non-apoptotic cells but work in parallel during apoptotic chromatin condensation, suggesting that more than one pathway exists. In addition, using an *in vitro* system it was shown that PARP and lamin cleavage by caspases were dispensable for chromatin condensation. Furthermore, internucleosomal DNA cleavage is unnecessary for nuclear apoptosis and chromatin condensation.

Although these results and the identification of several chromatin condensation factors, including CAD and topo II, greatly contributed to the understanding of the mechanism of chromatin condensation in apoptosis, many questions still remain. It is not known whether any of these proteins work in the same pathway. The regulation of these factors is largely unknown. Furthermore, nothing is known about how these factors change the state of chromatin. It is not clear whether any component that is involved in mitotic chromatin condensation also functions in apoptotic chromatin condensation, other than topo II.

In my future studies, I would like to focus on the following points. The first aim is to identify the relationships between the known chromatin condensation factors. Preliminary results have suggested AIF and topo II

might work in the same pathway. The second aim is to investigate the mechanism of the chromatin condensation activity of CAD. This might be independent from its nuclease activity. The third aim is to identify factors which are involved in either CAD regulation or chromatin condensation directly. The final aim is to clarify the state of histone phosphorylation and chromatin condensation. Each project is discussed in more detail below.

A combination of genetic and biochemical approaches will be suitable for these projects. As a genetic approach, cell lines will be prepared in which a gene of interest such as CAD or topo II, is knocked out. To knock-out genes, the chicken DT40 B cell lymphoma line has a number of advantages: efficient gene targeting, stable genotype, double/triple and conditional knock-outs are possible, and the small genome size of the chicken allows greater ease for obtaining a true gene, rather than a pseudo gene. In addition, cytosolic extracts and nuclei can be prepared for *in vitro* experiments from these cells and cytological analysis is possible.

Cell lines deficient in a chromatin condensation factor will be useful to identify other factors which operate in the same pathway. The CAD knock-out will be prepared in DT40 cells. A human conditional topo II knock-out has been prepared in HT1080 cells (gift of Andy Porter) and these cells will be used to look at topo II function. In addition, microinjection of recombinant AIF into nuclei of topo II null cells will give us clear answer if topo II works upstream or downstream of AIF. In the latter case, chromatin condensation against the nuclear periphery would be suppressed in the topo II null cells. Since addition of inhibitors to living cells is difficult to control

in terms of specificity and dose dependency, knock-out cells may produce more reliable data.

Secondly, CAD knock-out cells will be useful to confirm *in vivo* whether CAD has separate functions in chromatin condensation and DNA cleavage. It may be possible to identify the catalytic site of CAD nuclease either from the crystal structure or computer modeling, comparing the sequence with those of other known nucleases. Mutation of crucial amino acids located in the catalytic site might create an inactive nuclease but one still capable of inducing chromatin condensation. In addition, replacing the endogenous gene with a GFP-fusion CAD gene under its endogenous promoter may avoid problems accompanied with overexpression and make it possible to follow the localization of functional CAD in living and apoptotic cells under the microscope.

Third, taking advantage of chicken lymphoblast stable MSB-1 cell lines which constitutively over-expresses 6xHis and HA tagged mouse ICAD and/or CAD, biochemical analysis will be performed to identify proteins that are bound to CAD and ICAD *in vivo*. Such proteins might be involved in the regulation of CAD/ICAD or in the chromatin condensation working downstream of CAD. CIDE proteins which share CIDE-N/CAD domain and interact with CAD/ICAD *in vitro* are expected to be isolated from this approach. It is reported that overexpression of CIDE-A protein in cells induces apoptosis (Inohara *et al.*, 1998) and mitochondrial localization and dimerization are required for CIDE-B to induce apoptosis (Chen, Guo *et al.*, 2000), however, the molecular mechanisms are not known. The CAD

null cell line will be useful to investigate whether the apoptosis-inducing activity of CIDE protein depends on CAD.

Lastly it may be worthwhile investigating the relationship between the state of histone phosphorylation and apoptotic chromatin condensation. Histone H3 phosphorylation is known to be involved in chromatin remodeling in mitotic cells. Furthermore, it was recently reported that histone H2B and/or H2AX are phosphorylated in apoptotic cells (Ajiro, 2000; Rogakou, Nieves-Neira *et al.*, 2000). Phosphorylation of histone H2B and/or H2AX might be involved in apoptotic chromatin condensation. Genetic approaches and specific antibodies which recognize only the phosphorylated form of histones will be useful for this project. Histone genes are clustered - usually 6 genes exist for each histone in case of chicken. One Japanese group has created a DT40 cell line in which about half of histone gene clusters are removed. Amazingly, the cell line is still alive. If the remaining histone H2B or H2AX gene can be replaced with the non-phosphorylatable form of the histone and apoptotic chromatin condensation is suppressed, this would mean that specific phosphorylation is a key factor of apoptotic chromatin condensation. Even if this is not the case, the specific histone phosphorylation of H2B and/or H2AX might be useful as an assay for initial DNA cleavage during apoptosis.

I believe that these approaches will reveal the mechanisms of nuclear disassembly during apoptosis in the near future. Furthermore, it will be interesting and important to determine whether a failure of chromatin condensation and fragmentation underlies apoptosis-related human

disorders, taking into account that chromosome condensation and nuclear fragmentation are supposed to facilitate the engulfment and digestion by neighbouring cells or macrophages. In addition, since the initial DNA cleavage during apoptosis is supposed to release chromatin loops, these studies of apoptosis may also help us to understand the chromatin structure in living cells.

REFERENCES

Adachi, N., M. Miyaike, S. Kato, R. Kanamaru, H. Koyama and A. Kikuchi (1997). "Cellular distribution of mammalian DNA topoisomerase II is determined by its catalytically dispensable C-terminal domain." Nucleic Acids Res 25(15): 3135-42.

Adachi, Y., M. Luke and U. K. Laemmli (1991). "Chromosome assembly in vitro: topoisomerase II is required for condensation." CELL 64(1): 137-148.

Ajiro, K. (2000). "Histone H2B phosphorylation in mammalian apoptotic cells. An association with DNA fragmentation." J Biol Chem 275(1): 439-43.

Akiba, H., H. Nakano, S. Nishinaka, M. Shindo, T. Kobata, M. Atsuta, C. Morimoto, C. F. Ware, N. L. Malinin, D. Wallach, H. Yagita and K. Okumura (1998). "CD27, a member of the tumor necrosis factor receptor superfamily, activates NF-kappaB and stress-activated protein kinase/c-Jun N- terminal kinase via TRAF2, TRAF5, and NF-kappaB-inducing kinase." J Biol Chem 273(21): 13353-8.

Arends, M. J., R. G. Morris and A. H. Wyllie (1990). "Apoptosis: the role of the endonuclease." Am. J. Pathol. 136: 593-608.

Ashkenazi, A. and V. M. Dixit (1998). "Death receptors: signaling and modulation." Science 281(5381): 1305-8.

Barry, M. A. and A. Eastman (1993). "Identification of deoxyribonuclease II as an endonuclease involved in apoptosis." Arch. Biochem. Biophys. 300: 440-450.

Beere, H. M., C. M. Chresta and J. A. Hickman (1996). "Selective inhibition of topoisomerase II by ICRF-193 does not support a role for topoisomerase II activity in the fragmentation of chromatin during apoptosis of human leukemia cells." Mol. Pharmacol. 49: 842-851.

Boise, L. H. and C. B. Thompson (1997). "Bcl-x(L) can inhibit apoptosis in cells that have undergone Fas-induced protease activation." Proc. Natl. Acad. Sci. (USA) 94: 3759-3764.

Boldin, M. P., T. M. Goncharov, Y. V. Goltsev and D. Wallach (1996). "Involvement of MACH, a novel MORT1/FADD-interacting protease in Fas/APO-1- and TNF receptor-induced cell death." Cell 85: 803-815.

Bradford, M. M. (1976). "A rapid and sensitive method for the quantitation of microgram quantities of protein utilizing the principle of protein-dye binding." Anal Biochem 72: 248-54.

Brancolini, C., M. Benedetti and C. Schneider (1995). "Microfilament reorganization during apoptosis: the role of Gas2, a possible substrate for ICE-like proteases." EMBO J. 14(21): 5179-5190.

Bratton, S. B., M. MacFarlane, K. Cain and G. M. Cohen (2000). "Protein complexes activate distinct caspase cascades in death receptor and stress-induced apoptosis." Exp Cell Res 256(1): 27-33.

Chandler, J. M., G. M. Cohen and M. MacFarlane (1998). "Different subcellular distribution of caspase-3 and caspase-7 following Fas-induced apoptosis in mouse liver." J. Biol. Chem. 273: 10815-10818.

Chen, Z., K. Guo, S. Y. Toh, Z. Zhou and P. Li (2000). "Mitochondria Localization and Dimerization Are Required for CIDE-B to Induce Apoptosis." J Biol Chem 275(30): 22619-22622.

Chen, Z., K. Guo, S. Y. Toh, Z. Zhou and P. Li (2000). "Mitochondria localization and dimerization are required for CIDE-B to induce apoptosis [In Process Citation]." J Biol Chem 275(30): 22619-22.

Chinnaiyan, A. M., D. Chaudhary, K. O'Rourke, E. V. Koonin and V. M. Dixit (1997). "Role of CED-4 in the activation of CED-3." Nature 388(6644): 728-9.

Chinnaiyan, A. M., K. O'Rourke, M. Tewari and V. M. Dixit (1995). "FADD, a novel death domain-containing protein, interacts with the death domain of Fas and initiates apoptosis." Cell 81: 505-512.

Chow, S. C., M. Weis, G. Kass, T. H. Holmstrom, J. E. Eriksson and S. Orrenius (1995). "Involvement of multiple proteases during Fas-mediated apoptosis in T lymphocytes." FEBS Lett. 364(2): 134-138.

Church, G. M. and W. Gilbert (1984). "Genomic sequencing." Proc Natl Acad Sci U S A 81(7): 1991-5.

Cohen, G. M. (1997). "Caspases: the executioners of apoptosis." Biochem. J. 326: 1-16.

Conradt, B. and H. R. Horvitz (1998). "The C. elegans protein EGL-1 is required for programmed cell death and interacts with the Bcl-2-like protein CED-9." Cell 93(4): 519-29.

Cowan, W. M., J. W. Fawcett, D. D. O'Leary and B. B. Stanfield (1984). "Regressive events in neurogenesis." Science 225(4668): 1258-65.

Darmon, A. J., T. J. Ley, D. W. Nicholson and R. C. Bleackley (1996). "Cleavage of CPP32 by granzyme B represents a critical role for granzyme B in the induction of target cell DNA fragmentation." J Biol Chem 271(36): 21709-12.

Deveraux, Q. L. and J. C. Reed (1999). "IAP family proteins--suppressors of apoptosis." Genes Dev 13(3): 239-52.

Droin, N., L. Dubrez, B. Eymin, C. Renvoize, J. Breard, M. T. Dimanche-Boitrel and E. Solary (1998). "Upregulation of CASP genes in human tumor cells undergoing etoposide- induced apoptosis." Oncogene 16(22): 2885-94.

Duan, H., A. M. Chinnaiyan, P. L. Hudson, J. P. Wing, W.-W. He and V. M. Dixit (1996). "ICE-LAP3, a novel mammalian homologue of the Caenorhabditis elegans cell death protein Ced-3 is activated during Fas- and tumor necrosis factor-induced apoptosis." J. Biol. Chem. 271(3): 1621-1625.

Duan, H., K. Orth, A. M. Chinnaiyan, G. G. Poirier, C. J. Froelich, W.-W. He and V. M. Dixit (1996). "ICE-LAP6, a novel member of the ICE/Ced-3 genefamily, Is activated by the cytotoxic T cell protease granzyme B." J. Biol. Chem. 271: 16720-16724.

Earnshaw, W. C. (1995). "Apoptosis: Lessons from in vitro systems." Trends Cell Biol. 5: 217-220.

Earnshaw, W. C., B. Halligan, C. A. Cooke, M. M. Heck and L. F. Liu (1985). "Topoisomerase II is a structural component of mitotic chromosome scaffolds." J Cell Biol 100(5): 1706-15.

Earnshaw, W. C., L. M. Martins and S. H. Kaufmann (1999). "Mammalian caspases: Structure, activation, substrates and functions during apoptosis." Ann. Rev. Biochem. 68: 383-424.

Ellis, H. M. and H. R. Horvitz (1986). "Genetic control of programmed cell death in the nematode C. elegans." Cell 44(6): 817-29.

Enari, M., A. Hase and S. Nagata (1995). "Apoptosis by a cytosolic extract from Fas-activated cells." EMBO J. 14(21): 5201-5208.

Enari, M., H. Sakahira, H. Yokoyama, K. Okawa, A. Iwamatsu and S. Nagata (1998). "A caspase-activated DNase that degrades DNA during apoptosis, and its inhibitor ICAD." Nature 391(6662): 43-50.

Enari, M., R. V. Talanian, W. W. Wong and S. Nagata (1996). "Sequential activation of ICE-like and CPP32-like proteases during Fas-mediated apoptosis." Nature 380: 723-726.

Faleiro, L., R. Kobayashi, H. Fearnhead and Y. Lazebnik (1997). "Multiple species of CPP32 and Mch2 are the major active caspases present in apoptotic cells." EMBO J. 16: 2271 - 2281.

Fernandes-Alnemri, T., R. C. Armstrong, J. Krebs, S. M. Srinivasula, L. Wang, F. Bullrich, L. C. Fritz, J. A. Trapani, K. J. Tomaselli, L. G. and E. S. Alnemri (1996). "In vitro activation of CPP32 and Mch3 by Mch4, a novel human apoptotic cysteine kprotease containing two FADD-like domains." Proceedings of the National Academy of Sciences U.S.A. 93: 14486-14491.

Fernandes-Alnemri, T., G. Litwack and E. Alnemri (1995). "Mch2, a New Member of the Apoptotic Ced-3/Ice Cysteine Protease Gene Family." Cancer Research 55: 2737-2742.

Fernandes-Alnemri, T., A. Takahashi, R. Armstrong, J. Krebs, L. Fritz, K. Tomaselli, L. Wang, Z. Yu, C. M. Croce, G. Salvesen, W. C. Earnshaw, G. Litwack and E. S. Alnemri (1995). "Mch3, a novel human apoptotic cysteine protease highly related to CPP32." Cancer Res. 55: 6045-6052.

Fisher, G. H., F. J. Rosenberg, S. E. Straus, J. K. Dale, L. A. Middelton, A. Y. Lin, W. Strober, M. J. Lenardo and J. M. Puck (1995). "Dominant interfering fas gene mutations impair apoptosis in a human autoimmune lymphoproliferative syndrome." Cell 81(6): 935-946.

Friedlander, R. M. and J. Yuan (1998). "ICE, neuronal apoptosis and neurodegeneration." Cell Death Differ 5(10): 823-31.

Gorbsky, G. J. (1994). "Cell cycle progression and chromosome segregation in mammalian cells cultured in the presence of the topoisomerase II inhibitors ICRF-187 [(+)-1,2-bis(3,5-dioxopiperazinyl-1-yl)propane; ADR-529] and ICRF-159 (Razoxane)." Cancer Res 54(4): 1042-8.

Gravestein, L. A., D. Amsen, M. Boes, C. R. Calvo, A. M. Kruisbeek and J. Borst (1998). "The TNF receptor family member CD27 signals to Jun N-terminal kinase via Traf-2." Eur J Immunol 28(7): 2208-16.

Green, D. R. and J. C. Reed (1998). "Mitochondria and apoptosis." Science 281(5381): 1309-12.

Gu, J., R. P. Dong, C. Zhang, D. F. McLaughlin, M. X. Wu and S. F. Schlossman (1999). "Functional interaction of DFF35 and DFF45 with caspase-activated DNA fragmentation nuclease DFF40." J. Biol. Chem. 274: 20759-20762.

Halenbeck, R., H. MacDonald, A. Roulston, T. T. Chen, L. Conroy and L. T. Williams (1998). "CPAN, a human nuclease regulated by the caspase-sensitive inhibitor DFF-45." Curr. Biol. 8: 537-540.

Hamburger, V. (1992). "History of the discovery of neuronal death in embryos." J Neurobiol 23(9): 1116-23.

Hinsull, S. M., D. Bellamy and A. Franklin (1977). "A quantitative histological assessment of cellular death, in relation to mitosis, in rat thymus during growth and age involution." Age Ageing 6(2): 77-84.

Hoffmann, A., M. M. Heck, B. J. Bordwell, N. F. Rothfield and W. C. Earnshaw (1989). "Human autoantibody to topoisomerase II." Exp Cell Res 180(2): 409-18.

Hofmann, K., P. Bucher and J. Tschopp (1997). "The CARD domain: a new apoptotic signaling motif." Trends Biochem. Sci. 22: 155-156.

Inohara, N., T. Koseki, S. Chen, M. A. Benedict and G. Nunez (1999). "Identification of regulatory and catalytic domains in the apoptosis nuclease DFF40/CAD." J. Biol. Chem. 274: 270-274.

Inohara, N., T. Koseki, S. Chen, X. Wu and G. Núnez (1998). "CIDE, a novel family of cell death activators with homology fo the 45 kDa subunit of the DNA fragmentation factor." EMBO J. 17: 2526-2533.

Inohara, N. and G. Nunez (1999). "Genes with homology to DFF/CIDEs found in Drosophila melanogaster." Cell Death Differ 6(9): 823-4.

Irmler, M., M. Thome, M. Hahne, P. Schneider, K. Hofmann, V. Steiner, J. L. Bodmer, M. Schroter, K. Burns, C. Mattmann, D. Rimoldi, L. E. French and J. Tschopp (1997). "Inhibition of death receptor signals by cellular FLIP." Nature 388(6638): 190-5.

Jacobson, M. D., J. F. Burne and M. C. Raff (1994). "Programmed cell death and Bcl-2 protection in the absence of a nucleus." Embo J 13(8): 1899-910.

Janicke, R. U., P. Ng, M. L. Sprengart and A. G. Porter (1998). "Caspase-3 is required for alpha-fodrin cleavage but dispensable for cleavage of other death substrates in apoptosis." J Biol Chem 273(25): 15540-5.

Janicke, R. U., M. L. Sprengart, M. R. Wati and A. G. Porter (1998). "Caspase-3 is required for DNA fragmentation and morphological changes associated with apoptosis." J Biol Chem 273(16): 9357-60.

Kaufmann, S. H. and W. C. Earnshaw (2000). "Induction of apoptosis by cancer chemotherapy." Exp Cell Res 256(1): 42-9.

Kawane, K., H. Fukuyama, M. Adachi, S. H., N. G. Copeland, D. J. Gilbert, N. A. Jenkin and S. Nagata (1999). "Structure and promoter analysis of murine CAD and ICAD genes." Cell Death Differ. 6: 745-752.

Kerr, J. F. R. (1971). "Shrinkage necrosis: a distinct mode of cellular death." J. Pathol. 105: 13-20.

Kerr, J. F. R., B. Harmon and J. Searle (1974). "An electron microscope study of cell deletion in the anuran tadpole tail during spontaneous metamorphosis with special reference to apoptosis of striated muscle fibres." J. Cell Sci. 14: 571-585.

Krajewska, M., H. G. Wang, S. Krajewski, J. M. Zapata, A. Shabaik, R. Gascoyne and J. C. Reed (1997). "Immunohistochemical analysis of in vivo patterns of expression of CPP32 (Caspase-3), a cell death protease." Cancer Res. 57: 1605-1613.

Kroemer, G., N. Zamzami and S. A. Susin (1997). "Mitochondrial control of apoptosis." Immunol Today 18: 44-51.

Laemmli, U. K. (1970). "Cleavage of structural proteins during the assembly of the head of bacteriophage T4." Nature 227(259): 680-5.

Lagarkova, M. A., O. V. Iarovaia and S. V. Razin (1995). "Large-scale fragmentation of mammalian DNA in the course of apoptosis proceeds via excision of chromosomal DNA loops and their oligomers." J Biol Chem 270(35): 20239-41.

Lamarre, D., B. Talbot, G. de Murcia, C. Laplante, Y. Leduc, A. Mazen and G. G. Poirier (1988). "Structural and functional analysis of poly(ADP-ribose) polymerase: an immunological study." Biochem. Biophys. Acta 950: 147-160.

Lavoie, J. N., M. Nguyen, R. C. Marcellus, P. E. Branton and G. C. Shore (1998). "E4orf4, a novel adenovirus death factor that induces p53-independent apoptosis by a pathway that is not inhibited by zVAD-fmk." J Cell Biol 140: 637-645.

Lazebnik, Y. A., S. Cole, C. A. Cooke, W. G. Nelson and W. C. Earnshaw (1993). "Nuclear events of apoptosis in vitro in cell-free mitotic extracts: a model system for analysis of the active phase of apoptosis." J. Cell Biol. 123: 7-22.

Lazebnik, Y. A., S. H. Kaufmann, S. Desnoyers, G. G. Poirier and W. C. Earnshaw (1994). "Cleavage of poly(ADP-ribose) polymerase by a protease with properties like ICE." Nature 371: 346-347.

Lazebnik, Y. A., A. Takahashi, R. D. Moir, R. D. Goldman, G. G. Poirier, S. H. Kaufmann and W. C. Earnshaw (1995). "Studies of the lamin proteinase reveal multiple parallel biochemical pathways during apoptotic execution." Proc Natl Acad Sci U S A 92(20): 9042-6.

Li, H., H. Zhu, C. J. Xu and J. Yuan (1998). "Cleavage of BID by caspase 8 mediates the mitochondrial damage in the Fas pathway of apoptosis." Cell 94: 491-501.

Li, P., D. Nijhawan, I. Budihardjo, S. M. Srinivasula, M. Ahmad, E. S. Alnemri and X. Wang (1997). "Cytochrome c and dATP-dependent formation of Apaf-1/caspase-9 complex initiates an apoptotic protease cascade." Cell 91: 479-489.

Li, T. K., A. Y. Chen, C. Yu, Y. Mao, H. Wang and L. F. Liu (1999). "Activation of topoisomerase II-mediated excision of chromosomal DNA loops during oxidative stress." Genes Dev. 13: 1553-1560.

Liu, Q. A. and M. O. Hengartner (1999). "The molecular mechanism of programmed cell death in C. elegans." Ann N Y Acad Sci 887: 92-104.

Liu, Q. Y., M. Ribecco, S. Pandey, P. R. Walker and M. Sikorska (1999). "Apoptosis-related functional features of the DNaseI-like family of nucleases." Ann N Y Acad Sci 887: 60-76.

Liu, X., C. N. Kim, J. Yang, R. Jemmerson and X. Wang (1996). "Induction of apoptotic program in cell-free extracts: requirement for dATP and cytochrome C." Cell 86(July 12): 147-157.

Liu, X., P. Li, P. Widlak, H. Zou, X. Luo, W. T. Garrard and X. Wang (1998). "The 40-kDa subunit of DNA fragmentation factor induces DNA fragmentation and chromatin condensation during apoptosis." Proc Natl Acad Sci U S A 95(15): 8461-6.

Liu, X., H. Zou, C. Slaughter and X. Wang (1997). "DFF, a heterodimeric protein that functions downstream of caspase-3 to trigger DNA fragmentation during apoptosis." Cell 89(July 12): 175-184.

Liu, X., H. Zou, P. Widlak, W. Garrard and X. Wang (1999). "Activation of the apoptotic endonuclease DFF40 (caspase-activated DNase or nuclease). Oligomerization and direct interaction with histone H1." J. Biol. Chem. 274: 13836-13840.

Lugovskoy, A. A., P. Zhou, J. J. Chou, J. S. McCarty, P. Li and G. Wagner (1999). "Solution structure of the CIDE-N domain of CIDE-B and a model for CIDE- N/CIDE-N interactions in the DNA fragmentation pathway of apoptosis." Cell 99(7): 747-55.

Luo, X., I. Budihardjo, H. Zou and C. W. Slaughter, X. (1998). "Bid, a Bcl2 interacting protein, mediates cytochrome c release from mitochondria in response to activation of cell surface death receptors." Cell 94: 481-490.

Mackay, A. M., D. M. Eckley, C. Chue and W. C. Earnshaw (1993). "Molecular analysis of the INCENPs (inner centromere proteins): separate domains are required for association with microtubules during interphase and with the central spindle during anaphase." J Cell Biol 123(2): 373-85.

Mancini, M., D. W. Nicholson, S. Roy, N. A. Thornberry, E. P. Peterson, L. A. Casciola-Rosen and A. Rosen (1998). "The caspase-3 precursor has a cytosolic and mitochondrial distribution: implications for apoptotic signaling." J. Cell Biol. 140: 1485-1495.

Martin, S. J., G. P. Amarante-Mendes, L. Shi, T. H. Chuang, C. A. Casiano, G. A. 'Brien, P. Fitzgerald, E. M. Tan4, G. M. Bokoch, A. H. Greenberg and D. R. Green (1996). "The cytotoxic cell protease granzyme B initiates apoptosis in a cell-free system by proteolytic processing and activation of the ICE/CED-3 family protease, CPP32, via a novel two-step mechanism." EMBO J. 15: 2407-2416.

Martin, S. J. and D. R. Green (1995). "Protease activation during apoptosis: Death by a thousand cuts?" Cell 82: 349-352.

Martin, S. J., D. D. Newmeyer, S. Mathias, D. M. Farschon, H.-G. Wang, J. C. Reed, R. N. Kolesnick and D. R. Green (1995). "Cell-free reconstitution of Fas-, UV radiation- and ceramide-induced apoptosis." EMBO J. 14(21): 5191-5200.

Martins, L. M. and W. C. Earnshaw (1996). "Apoptosis: alive and kicking in 1997." Trends Cell Biol. 7: 111-114.

Martins, L. M., T. Kottke, P. W. Mesner, G. S. Basi, S. Sinha, N. Frigon, Jr., E. Tatar, J. S. Tung, K. Bryant, A. Takahashi, P. A. Svingen, B. J. Madden, D. J. McCormick, W. C. Earnshaw and S. H. Kaufmann (1997). "Activation of multiple interleukin-1beta converting enzyme homologues in cytosol and nuclei of HL-60 cells during etoposide-induced apoptosis." J Biol Chem 272(11): 7421-30.

Martins, L. M., T. J. Kottke, S. H. Kaufmann and W. C. Earnshaw (1998). "Phosphorylated forms of activated caspases are present in cytosol from HL-60 cells during etoposide-induced apoptosis." Blood 92: 3042-3049.

Martins, L. M., P. W. Mesner, T. J. Kottke, G. S. Basi, S. Sinha, J. S. Tung, P. A. Svingen, B. J. Madden, A. Takahashi, D. J. McCormick, W. C. Earnshaw and S. H. Kaufmann (1997). "Comparison of caspase activation and subcellular localization in HL-60 and K562 cells undergoing etoposide-induced apoptosis." Blood 90: 4283-4296.

McCarthy, N. J., M. K. Whyte, C. S. Gilbert and G. I. Evan (1997). "Inhibition of Ced-3/ICE-related proteases does not prevent cell death induced by oncogenes, DNA damage, or the Bcl-2 homologue Bak." J. Cell Biol. 136: 215-227.

McCarty, J. S., S. Y. Toh and P. Li (1999). "Multiple domains of DFF45 bind synergistically to DFF40: roles of caspasecleavage and sequestration of activator domain of DFF40." Biochem. Biophys. Res. Commun. 264: 181-185.

McIlroy, D., H. Sakahira, R. V. Talanian and S. Nagata (1999). "Involvement of caspase 3-activated DNase in internucleosomal DNA cleavage induced by diverse apoptotic stimuli." Oncogene 18: 4401-4408.

McPherson, J. P. and G. J. Goldenberg (1998). "Induction of apoptosis by deregulated expression of DNA topoisomerase IIalpha." Cancer Res 58(20): 4519-24.

Medema, J. P., C. Scaffidi, F. C. Kischkel, A. Shevchenko, M. Mann, P. H. Krammer and M. E. Peter (1997). "FLICE is activated by association with the CD95 death-inducing signaling complex (DISC)." EMBO J. 16: 2794 - 2804.

Mirkovitch, J., S. M. Gasser and U. K. Laemmli (1987). "Relation of chromosome structure and gene expression." Philos Trans R Soc Lond B Biol Sci 317(1187): 563-74.

Mitamura, S., H. Ikawa, N. Mizuno, Y. Kaziro and H. Itoh (1998). "Cytosolic nuclease activated by caspase-3 and inhibited by DFF-45." Biochem. Biophys. Res. Commun. 243: 480-484.

Montague, J. W., M. L. Gaido, C. Frye and J. A. Cidlowski (1994). "A calcium-dependent nuclease from apoptotic rat thymocytes is homologous with cyclophilin." J. Biol. Chem. 269: 18877-18880.

Muchmore, S. W., M. Sattler, H. Liang, R. P. Meadows, J. E. Harlan, H. S. Yoon, D. Nettesheim, B. S. Chang, C. B. Thompson, S. L. Wong, S. L. Ng and S. W. Fesik (1996). "X-ray and NMR structure of human Bcl-xL, an inhibitor of programmed cell death." Nature 381(6580): 335-41.

Mukae, N., M. Enari, H. Sakahira, Y. Fukuda, J. Inazawa, H. Toh and S. Nagata (1998). "Molecular cloning and characterization of human caspase-activated DNase." Proc. Natl. Acad. Sci. U.S.A. 95: 9123-9128.

Mukae, N., H. Yokoyama, T. Yokokura, Y. Sakoyama, H. Sakahira and S. Nagata (2000). "Identification and developmental expression of inhibitor of caspase- activated DNase (ICAD) in drosophila melanogaster." J Biol Chem 275(28): 21402-8.

Muzio, M., A. M. Chinnaiyan, F. C. Kischkel, K. O'Rourke, A. Shevchenko, J. Ni, R. Gentz, M. Mann, P. H. Krammer, M. E. Peter and V. M. Dixit (1996). "FLICE, a novel FADD-homologous ICE/CED-3-like protease, is recruited to the CD95 (Fas/APO-1) death-inducing signaling complex." Cell 85: 817-827.

Muzio, M., B. R. Stockwell, H. R. Stennicke, G. S. Salvesen and V. M. Dixit (1998). "An induced proximity model for caspase-8 activation." J Biol Chem 273(5): 2926-30.

Nagata, S. (1997). "Apoptosis by death factor." Cell 88: 355-365.

Nakagawa, T., H. Zhu, N. Morishima, E. Li, J. Xu, B. A. Yankner and J. Yuan (2000). "Caspase-12 mediates endoplasmic-reticulum-specific apoptosis and cytotoxicity by amyloid-beta." Nature 403(6765): 98-103.

Nakajima, H., P. Golstein and P. A. Henkart (1995). "The target cell nucleus is not required for cell-mediated granzyme- or Fas-based cytotoxicity." J Exp Med 181(5): 1905-9.

Newmeyer, D. D., D. M. Farschon and J. C. Reed (1994). "Cell-free apoptosis in Xenopus egg extracts - inhibition by Bcl-2 and requirement for an organelle fraction enriched in mitochondria." Cell 79(2): 353-364.

Ng, F. W., M. Nguyen, T. Kwan, P. E. Branton, D. W. Nicholson, J. A. Cromlish and G. C. Shore (1997). "p28 Bap31, a Bcl-2/Bcl-XL- and procaspase-8-associated protein in the endoplasmic reticulum." J Cell Biol 139(2): 327-38.

Nicholson, D. W., A. Ali, N. A. Thornberry, J. P. Vaillancourt, C. K. Ding, M. Gallant, Y. Gareau, P. R. Griffin, M. Labelle, Y. A. Lazebnik, N. A. Munday, S. M. Raju, M. E. Smulson, T.-T. Yamin, V. L. Yu and D. K. Miller (1995). "Identification and inhibition of the ICE/CED-3 protease necessary for mammalian apoptosis." Nature 376: 37-43.

Nicholson, D. W. and N. A. Thornberry (1997). "Caspases: killer proteases." Trends Biochem Sci 22(8): 299-306.

Oberhammer, F., J. W. Wilson, D. C., I. D. Morris, J. A. Hickman, A. E. Wakeling, P. R. Walker and M. Sikorska (1993). "Apoptotic death in epithelial cells: cleavage of DNA to 300 and/or 50 kb fragments prior to or in the absence of internucleosomal fragmentation." EMBO J. 12: 3679-3684.

Oberhammer, F. A., K. Hochegger, G. Fröschl, R. Tiefenbacher and M. Pavelka (1994). "Chromatin condensation during apoptosis is accompanied by degradation of lamin A + B, without enhanced activation of cdc2 kinase." J. Cell Biol. 126: 827-837.

Orth, K., A. M. Chinnaiyan, M. Garg, C. J. Froelich and V. M. Dixit (1996). "The CED-3/ICE-like protease Mch2 is activated during apoptosis and cleaves the death substrate lamin A." J. Biol. Chem. 271: 16443-16446.

Peitsch, M. C., B. Polzar, H. Stephan, T. Crompton, M. H. R., H. G. Mannherz and J. Tschopp (1993). "Characterization of the endogenous deoxyribonuclease involved in nuclear DNA degradation during apoptosis (programmed cell death)." EMBO J. 12: 371-377.

Porter, A. G., P. Ng and R. U. Janicke (1997). "Death substrates come alive." Bioessays 19(6): 501-7.

Raff, M. C. (1992). "Social control on cell survival and cell death." Nature 356: 397-400.

Rao, L., D. Perez and E. White (1996). "Lamin proteolysis facilitates nuclear events during apoptosis." J. Cell Biol. 135: 1441-1455.

Rizzuto, R., M. Brini, P. Pizzo, M. Murgia and T. Pozzan (1995). "Chimeric green fluorescent protein as a tool for visualizing subcellular organelles in living cells." Curr Biol 5(6): 635-42.

Robbins, J., S. M. Dilworth, R. A. Laskey and C. Dingwall (1991). "Two interdependent basic domains in nucleoplasmin nuclear targeting sequence: identification of a class of bipartite nuclear targeting sequence." Cell 64(3): 615-23.

Rogakou, E. P., W. Nieves-Neira, C. Boon, Y. Pommier and W. M. Bonner (2000). "Initiation of DNA fragmentation during apoptosis induces phosphorylation of H2AX histone at serine 139." J Biol Chem 275(13): 9390-5.

Roy, N., Q. L. Deveraux, R. Takahashi, G. S. Salvesen and J. C. Reed (1997). "The c-IAP-1 and c-IAP-2 proteins are direct inhibitors of specific caspases." EMBO J. 16: 6914-6925.

Sabol, S. L., R. Li, T. Y. Lee and R. Abdul-Khalek (1998). "Inhibition of apoptosis-associated DNA fragmentation activity in nonapoptotic cells: the role of DNA fragmentation factor-45 (DFF45/ICAD)." Biochem. Biophys. Res. Commun. 253: 151-158.

Sahara, S., M. Aoto, Y. Eguchi, N. Imamoto, Y. Yoneda and Y. Tsujimoto (1999). "Acinus is a caspase-3-activated protein required for apoptotic chromatin condensation." Nature 401: 168-173.

Sakahira, H., M. Enari and S. Nagata (1998). "Cleavage of CAD inhibitor in CAD activation and DNA degradation during apoptosis." Nature 391: 96-99.

Sakahira, H., M. Enari and S. Nagata (1999). "Functional differences of two forms of the inhibitor of caspase- activated DNase, ICAD-L, and ICAD-S." J Biol Chem 274(22): 15740-4.
Sakahira, H., M. Enari, Y. Ohsawa, Y. Uchiyama and S. Nagata (1999). "Apoptotic nuclear morphological change without DNA fragmentation." Curr. Biol. 9: 543-546.
Sakahira, H., A. Iwamatsu and S. Nagata (2000). "Specific chaperone-like activity of inhibitor of caspase-activated DNase for caspase-activated DNase." J Biol Chem 275(11): 8091-6.
Samali, A., B. Zhivotovsky, D. P. Jones and S. Orrenius (1998). "Detection of pro-caspase-3 in cytosol and mitochondria of various tissues." FEBS Lett. 431: 167-169.
Samejima, K. and W. C. Earnshaw (1998). "ICAD/DFF regulator of apoptotic nuclease is nuclear." Exp. Cell Res. 243: 453-459.
Samejima, K. and W. C. Earnshaw (2000). "Differential localization of ICAD-L and ICAD-S in cells due to removal of a C-terminal NLS from ICAD-L by alternative splicing." Exp Cell Res 255(2): 314-20.
Schulze-Osthoff, K., H. Walczak, W. Dröge and P. H. Krammer (1994). "Cell nucleus and DNA fragmentation are not required for apoptosis." J. Cell Biol. 127: 15-20.
Schwartz, L. M. and J. W. Truman (1982). "Peptide and steroid regulation of muscle degeneration in an insect." Science 215(4538): 1420-1.
Seraphin, B. and S. Kandels-Lewis (1996). "An efficient PCR mutagenesis strategy without gel purification [correction of purificiation] step that is amenable to automation." Nucleic Acids Res 24(16): 3276-7.
Shero, J. H., B. Bordwell, N. F. Rothfield and W. C. Earnshaw (1986). "High titers of autoantibodies to topoisomerase I (Scl-70) in sera from scleroderma patients." Science 231(4739): 737-40.
Shimizu, T. and Y. Pommier (1997). "Camptothecin-induced apoptosis in p53-null human leukemia HL60 cells and their isolated nuclei: effects of the protease inhibitors Z-VAD-fmk and dichloroisocoumarin suggest an involvement of both caspases and serine proteases." Leukemia 11: 1238-1244.
Shiokawa, D. and S.-i. Tanuma (1998). "Molecular cloning and expression of a cDNA encoding an apoptotic endonuclease DNase gamma." Biochem. J. 332: 713-720.
Siegel, R. M., J. K. Frederiksen, D. A. Zacharias, F. K. Chan, M. Johnson, D. Lynch, R. Y. Tsien and M. J. Lenardo (2000). "Fas preassociation required for apoptosis signaling and dominant inhibition by pathogenic mutations [see comments]." Science 288(5475): 2354-7.
Skalka, M., J. Matyasova and M. Cejkova (1976). "DNA in chomatin of irradiated lymphoid tissues degrades in vovo into regular fragments." FEBS LETTERS 72(2): 271-74.
Spector, M. S., S. Desnoyers, D. J. Hoeppner and M. O. Hengartner (1997). "Interaction between the C. elegans cell-death regulators CED-9 and CED-4." Nature 385: 653-656.

Srinivasula, S. M., M. Ahmad, T. Fernandes-Alnemri and E. S. Alnemri (1998). "Autoactivation of procaspase-9 by Apaf-1-mediated oligomerization." Mol. Cell 1: 949-957.

Srinivasula, S. M., T. Fernandes-Alnemri, J. Zangrill, N. Robertson, R. C. Armstrong, L. Wang, J. A. Trapani, K. Tomaselli, G. Litwack and E. S. Alnemri (1996). "The Ced3/interleukin 1b converting enzyme-like homolog Mch6 and the lamin-cleaving enzyme Mch2a are substrates for the apoptotic mediator CPP32." J. Biol. Chem 271: 27099-27106.

Susin, S. A., H. K. Lorenzo, N. Zamzami, I. Marzo, C. Brenner, N. Larochette, M. C. Prevost, P. M. Alzari and G. Kroemer (1999). "Mitochondrial release of caspase-2 and -9 during the apoptotic process." J Exp Med 189(2): 381-94.

Susin, S. A., H. K. Lorenzo, N. Zamzami, I. Marzo, B. E. Snow, G. M. Brothers, J. Mangion, E. Jacotot, P. Constantini, M. Loeffler, N. Larochette, D. R. Goodlett, R. Aebersold, D. P. Siderovski, J. M. Penninger and G. Kroemer (1999). "Molecular characterisation of mitochondrial apoptosis-inducing factor (AIF)." Nature 397: 441-446.

Susin, S. A., N. Zamzami, M. Castedo, T. Hirsch, P. Marchetti, A. Macho, E. Daugas, M. Geuskens and G. Kroemer (1996). "Bcl-2 inhibits the mitochondrial release of an apoptogenic protease." J. Exp. Med. 184: 1331-1342.

Takahashi, A., E. Alnemri, Y. A. Lazebnik, T. Fernandes-Alnemri, G. Litwack, R. D. Moir, R. D. Goldman, G. G. Poirier, S. H. Kaufmann and W. C. Earnshaw (1996). "Cleavage of lamin A by Mch2a but not CPP32: Multiple ICE-related proteases with distinct substrate recognition properties are active in apoptosis." Proc. Nat. Acad. Sci. (USA) 93: 8395-8400.

Talanian, R. V., C. Quinlan, S. Trautz, M. C. Hackett, J. A. Mankovich, D. Banach, T. Ghayur, K. D. Brady and W. W. Wong (1997). "Substrate specificities of caspase family proteases." J. Biol. Chem. 272: 9677-9682.

Tang, D. and V. J. Kidd (1998). "Cleavage of DFF-45/ICAD by multiple caspases is essential for its function during apoptosis." J. Biol. Chem. 273: 28549-28552.

Tewari, M., L. T. Quan, K. O'Rourke, S. Desnoyers, Z. Zeng, D. R. Beidler, G. G. Poirier, G. S. Salvesen and V. M. Dixit (1995). "Yama/CPP32b, a mammalian homolog of CED-3, is a CrmA-inhibitable protease that cleaves the death substrate poly(ADP-ribose) polymerase." Cell 81: 801-809.

Thompson, C. B. (1995). "Apoptosis in the pathogenesis and treatment of disease." Science 267(5203): 1456-1462.

Toh, S. Y., X. Wang and P. Li (1998). "Identification of the nuclear factor HMG2 as an activator for DFF nuclease activity." Biochem Biophys Res Commun 250(3): 598-601.

Torriglia, A., P. Perani, J. Y. Brossas, E. Chaudun, J. Treton, Y. Courtois and M. F. Counis (1998). "L-DNase II, a molecule that links proteases and endonucleases in apoptosis, derives from the ubiquitous serpin leukocyte elastase inhibitor." Mol. Cell. Biol. 18: 3612-3619.

Tschopp, J., M. Irmler and M. Thome (1998). "Inhibition of fas death signals by FLIPs." Curr Opin Immunol 10(5): 552-8.

Tsujimoto, Y., J. Cossman, E. Jaffe and C. M. Croce (1985). "Involvement of the bcl-2 gene in human follicular lymphoma." Science 228(4706): 1440-3.

Ucker, D. S., P. S. Obermiller, W. Eckhart, J. R. Apgar, N. A. Berger and J. Meyers (1992). "Genome digestion is a dispensible consequence of physiological cell death mediated by cytotoxic T lymphocytes." Mol. Cell. Biol. 12: 3060-3069.

Uegaki, K., T. Otomo, H. Sakahira, M. Shimizu, N. Yumoto, Y. Kyogoku, S. Nagata and T. Yamazaki (2000). "Structure of the CAD domain of caspase-activated DNase and interaction with the CAD domain of its inhibitor." J Mol Biol 297(5): 1121-8.

Vaux, D. L. and S. J. Korsmeyer (1999). "Cell death in development." Cell 96(2): 245-54.

Vaux, D. L., S. Wilhelm and G. Hacker (1997). "Requirements for proteolysis during apoptosis." Mol Cell Biol 17: 6502-6507.

Villa, P., S. H. Kaufmann and W. C. Earnshaw (1997). "Caspases and caspase inhibitors." Trends Biochem Sci 22(10): 388-93.

Wang, J. and M. J. Lenardo (2000). "Roles of caspases in apoptosis, development, and cytokine maturation revealed by homozygous gene deficiencies." J Cell Sci 113(Pt 5): 753-7.

Wang, J., L. Zheng, A. Lobito, F. K. Chan, J. Dale, M. Sneller, X. Yao, J. M. Puck, S. E. Straus and M. J. Lenardo (1999). "Inherited human Caspase 10 mutations underlie defective lymphocyte and dendritic cell apoptosis in autoimmune lymphoproliferative syndrome type II." Cell 98(1): 47-58.

Wang, S. L., C. J. Hawkins, S. J. Yoo, H. A. Muller and B. A. Hay (1999). "The Drosophila caspase inhibitor DIAP1 is essential for cell survival and is negatively regulated by HID." Cell 98(4): 453-63.

Warburton, P. E. and W. C. Earnshaw (1997). "Untangling the role of DNA topoisomerase II in mitotic chromosome structure and function." Bioessays 19(2): 97-9.

Widlak, P., P. Li, X. Wang and W. T. Garrard (2000). "Cleavage preferences of the apoptotic endonuclease DFF40 (caspase- activated DNase or nuclease) on naked DNA and chromatin substrates." J Biol Chem 275(11): 8226-32.

Wolf, B. B., M. Schuler, F. Echeverri and D. R. Green (1999). "Caspase-3 is the primary activator of apoptotic DNA fragmentation via DNA fragmentation factor-45/Inhibitor of caspase-activated DNase inactivation." J. Biol. Chem. 274: 30651-30656.

Woo, M., R. Hakem, M. S. Soengas, G. S. Duncan, A. Shahinian, D. Kägi, A. Hakem, M. McCurrach, W. Khoo, S. A. Kaufman, G. Senaldi, T. Howard, S. W. Lowe and T. W. Mak (1998). "Essential contribution of caspase 3/CPP32 to apoptosis and its associated nuclear changes." Genes Dev. 12: 806-819.

Wood, E. R. and W. C. Earnshaw (1990). "Mitotic chromatin condensation in vitro using somatic cell extracts and nuclei with variable levels of endogenous topoisomerase II." J. Cell Biol. 111: 2839-2850.

Wu, D., H. D. Wallen and G. Nunez (1997). "Interaction and regulation of subcellular localization of CED-4 by CED-9." Science 275: 1126-1129.

Wyllie, A. H. (1980). "Glucocorticoid-induced thymocyte apoptosis is associated with endogenous endonuclease activation." Nature 284: 555-556.

Wyllie, A. H. (1994). "Death from inside out: an overview." Philos Trans R Soc Lond B Biol Sci 345(1313): 237-41.

Wyllie, A. H., J. F. R. Kerr and A. R. Currie (1980). "Cell death: The significance of apoptosis." Int. Rev. Cytol. 68: 251-305.

Xiang, J., D. T. Chao and S. J. Korsmeyer (1996). "BAX-induced cell death may not require interleukin 1 beta-converting enzyme-like proteases." Proc. Natl. Acad. Sci. (USA) 93: 14559-14563.

Yasuhara, N., Y. Eguchi, T. Tachibana, N. Imamoto, Y. Yoneda and Y. Tsujimoto (1997). "Essential role of active nuclear transport in apoptosis." Genes Cells 2(1): 55-64.

Yeh, W. C., R. Hakem, M. Woo and T. W. Mak (1999). "Gene targeting in the analysis of mammalian apoptosis and TNF receptor superfamily signaling." Immunol Rev 169: 283-302.

Yokoyama, H., N. Mukae, H. Sakahira, K. Okawa, A. Iwamatsu and S. Nagata (2000). "A novel activation mechanism of caspase-activated DNase from Drosophila melanogaster." J Biol Chem 275(17): 12978-86.

Yuan, J. Y. (1995). "Molecular control of life and death." Curr Opin Cell Biol 7(2): 211-214.

Yuan, J. Y. and H. R. Horvitz (1990). "The Caenorhabditis elegans genes ced-3 and ced-4 act cell autonomously to cause programmed cell death." Dev. Biol. 138: 33-41.

Zamzami, N. and G. Kroemer (1999). "Condensed matter in cell death." Nature 401: 127-128.

Zamzami, N., S. A. Susin, P. Marchetti, T. Hirsch, I. Gomez-Monterrey, M. Castedo and G. Kroemer (1996). "Mitochondrial control of nuclear apoptosis." J. Exp. Med. 183(April 96): 1533-1544.

Zapata, J. M., R. Takahashi, G. S. Salvesen and J. C. Reed (1998). "Granzyme release and caspase activation in activated human T-lymphocytes." J. Biol. Chem. 273: 6916-6920.

Zha, J., H. Harada, E. Yang, J. Jockel and S. J. Korsmeyer (1996). "Serine phosphorylation of death agonist BAD in response to survival factor results in binding to 14-3-3, not Bcl-XL." Cell 87: 619-628.

Zhang, C., R. Raghupathi, K. E. Saatman, M. C. LaPlaca and T. K. McIntosh (1999). "Regional and temporal alterations in DNA fragmentation factor (DFF)-like proteins following experimental brain trauma in the rat." J. Neurochem. 73: 1650-1659.

Zhang, J., H. Lee, D. W. Lou, G. P. Bovin and M. Xu (2000). "Lack of obvious 50 kilobase pair DNA fragments in DNA fragmentation factor 45-deficient thymocytes upon activation of apoptosis [In Process Citation]." Biochem Biophys Res Commun 274(1): 225-9.

Zhang, J., X. Liu, D. C. Scherer, L. van Kaer, X. Wang and M. Xu (1998). "Resistance to DNA fragmentation and chromatin condensation in mice lacking the DNA fragmentation factor 45." Proc Natl Acad Sci U S A 95(21): 12480-5.

Zheng, T. S. and R. A. Flavell (2000). "Divinations and surprises: genetic analysis of caspase function in mice." Exp Cell Res 256(1): 67-73.

Zheng, T. S., S. F. Schlosser, T. Dao, R. Hingorani, I. N. Crispe, J. L. Boyer and R. A. Flavell (1998). "Caspase-3 controls both cytoplasmic and nuclear events associated with Fas-mediated apoptosis in vivo." Proc. Natl. Acad. Sci. (USA) 95: 13618-13623.

Zhivotovsky, B., A. Samali, A. Gahm and S. Orrenius (1999). "Caspases: their intracellular localization and translocation during apoptosis." Cell Death Differ. 6: 644-651.

Zini, N., A. M. Martelli, P. Sabatelli, S. Santi, C. Negri, G. C. Astaldi Ricotti and N. M. Maraldi (1992). "The 180-kDa isoform of topoisomerase II is localized in the nucleolus and belongs to the structural elements of the nucleolar remnant." Exp Cell Res 200(2): 460-6.

Zou, H., W. J. Henzel, X. Liu, A. Lutschg and X. Wang (1997). "Apaf-1, a human protein homologous to C. elegans CED-4, participates in cytochrome c-dependent activation of caspase-3." Cell 90: 405-413.

PUBLICATIONS

Transition from Caspase-dependent to Caspase-independent Mechanisms at the Onset of Apoptotic Execution

Kumiko Samejima,* Shigenobu Toné,* Timothy J. Kottke,‡ Masato Enari,§ Hideki Sakahira,§ Carol A. Cooke,* Françoise Durrieu,* Luis M. Martins,* Shigekazu Nagata,§ Scott H. Kaufmann,‡ and William C. Earnshaw*

*Institute of Cell and Molecular Biology, University of Edinburgh, Kings' Buildings, Edinburgh, EH9 3JR, Scotland, United Kingdom; ‡Division of Oncology Research, Mayo Clinic, Rochester, Minnesota 55905; and §Department of Genetics, Osaka University Medical School, Suita, Osaka 565, Japan

Abstract. We have compared cytoplasmic extracts from chicken DU249 cells at various stages along the apoptotic pathway. Extracts from morphologically normal "committed stage" cells induce apoptotic morphology and DNA cleavage in substrate nuclei but require ongoing caspase activity to do so. In contrast, extracts from frankly apoptotic cells induce apoptotic events in added nuclei in a caspase-independent manner. Biochemical fractionation of these extracts reveals that a column fraction enriched in endogenous active caspases is unable to induce DNA fragmentation or chromatin condensation in substrate nuclei, whereas a caspase-depleted fraction induces both changes. Further characterization of the "execution phase" extracts revealed the presence of an ICAD/DFF45 (inhibitor of caspase-activated DNase/DNA fragmentation factor)-inhibitable nuclease resembling CAD, plus another activity that was required for the apoptotic chromatin condensation. Despite the presence of active caspases, committed stage extracts lacked these downstream activities, suggesting that the caspases and downstream factors are segregated from one another in vivo during the latent phase. These observations not only indicate that caspases act in an executive fashion, serving to activate downstream factors that disassemble the nucleus rather than disassembling it themselves, but they also suggest that activation of the downstream factors (rather than the caspases) is the critical event that occurs at the transition from the latent to active phase of apoptosis.

Key words: apoptosis • caspases • CAD • ICAD • DFF

Apoptosis is a cellular disassembly pathway that is activated by members of a distinct family of cysteine proteases called caspases (Cohen, 1997; Nicholson and Thornberry, 1997; Villa et al., 1997; Cryns and Yuan, 1998). Genetic analyses show clearly that caspases such as CED-3 and caspase-3 are essential for apoptotic death (Yuan and Horvitz, 1990; Kuida et al., 1996; Woo et al., 1998). Nonetheless, the role of these enzymes in the death pathway remains unclear. One recent study has suggested that cells can activate caspases without undergoing apoptosis (Boise and Thompson, 1997). Conversely, even though caspase inhibitors usually rescue cells from apoptosis (for review see Villa et al., 1997), cell death can occur in response to proapoptotic stimuli in the presence of these inhibitors (Xiang et al., 1996; McCarthy et al., 1997; Lavoie et al., 1998).

Careful examination has revealed that cells dying in the presence of caspase inhibitors display membrane blebbing and cell surface alterations but no changes in nuclear morphology (McCarthy et al., 1997). This observation suggests that certain cytoplasmic hallmarks of apoptosis may be triggered by enzymes other than caspases, but that nuclear events require caspase activity. Consistent with this view, cells from caspase-3–null mice (Woo et al., 1998) have been reported to display plasma membrane changes and cleavage of the nuclear protein poly(ADP-ribose) polymerase (PARP)[1] when undergoing apoptosis, but not the chromatin condensation and DNA cleavage that are characteristic of apoptosis (Wyllie et al., 1980).

Although the preceding observations suggest that cas-

K. Samejima and S. Toné contributed equally to this work.

Correspondence should be addressed to W.C. Earnshaw, Institute of Cell and Molecular Biology, University of Edinburgh, Kings' Buildings, Mayfield Road, Edinburgh, EH9 3JR, Scotland, UK. Tel.: 44-(0)131-650-7101. Fax: 44-(0)131-650-7100. E-mail: bill.earnshaw@ed.ac.uk

1. *Abbreviations used in this paper*: CAD, caspase-activated DNase; C/D extract, nonapoptotic extract from cells in the condemned phase; DAPI, 4,6-diamidino-2-phenylindole; DFF, DNA fragmentation factor; E/X extract, apoptotic extract from execution phase cells; Fr-2 and Fr-3, fractions 2 and 3 from heparin–agarose chromatography of S/M extract; ICAD, inhibitor of CAD; S/M extract, proapoptotic extract from committed phase cells; PARP, poly(ADP-ribose) polymerase.

pases play a role in certain apoptotic events, particularly those occurring in the nucleus, it is not known whether caspases function in an executive role to initiate the apoptotic pathway and leave the work of actually disassembling the cell to other downstream factors, or whether they are workhorses whose cleavage of key substrates drives cellular disassembly. Support for an executive role comes from the observation that expression of the caspase cleavage product of the actin-binding protein GAS2 triggers cytoskeletal changes similar to those seen in apoptosis (Brancolini et al., 1995). Likewise, caspase cleavage of ICAD/DFF (inhibitor of caspase-activated DNase/DNA fragmentation factor) releases the nuclease CAD, presumably allowing it to enter the nucleus and degrade genomic DNA (Liu et al., 1997; Enari et al., 1998; Sakahira et al., 1998). Thus, certain products of caspase cleavage play important downstream roles in apoptotic events. On the other hand, numerous important structural and nonstructural proteins are also directly cleaved by caspases (Cohen, 1997; Nicholson and Thornberry, 1997; Porter et al., 1997; Villa et al., 1997), supporting the alternative hypothesis that caspases do the bulk of the work of cutting the cell apart themselves (Martin and Green, 1995).

Current understanding of caspase function has been facilitated by the development of cell-free systems for the study of apoptosis (Lazebnik et al., 1993; Solary et al., 1993; Newmeyer et al., 1994; Enari et al., 1995*a*; Martin et al., 1995; Schlegel et al., 1995; Liu et al., 1996). One such system uses extracts from DU249 chicken hepatoma cells that become committed to apoptosis after perturbation of the cell cycle (Lazebnik et al., 1993). Highly concentrated cytosolic extracts prepared from these morphologically normal cells (S/M extracts) reproduce all of the biochemical features of apoptosis in substrate nuclei (Lazebnik et al., 1993), including genome digestion (Wyllie et al., 1980; Lazebnik et al., 1993); cleavage of a subset of nuclear proteins, including PARP and lamins (Kaufmann, 1989; Ucker et al., 1992*a*; Lazebnik et al., 1994, 1995); chromatin condensation; and nuclear fragmentation into apoptotic bodies (Lazebnik et al., 1993). This entire program of apoptotic events is inhibited in vitro by caspase inhibitors (Lazebnik et al., 1994) or millimolar concentrations of Zn^{2+} (Lazebnik et al., 1993) just as in intact cells. Although nuclei are used as the substrate in these studies, the extracts themselves are derived from the cytoplasm of the DU249 cells (Lazebnik et al., 1993), thus supporting the view that cytoplasmic factors and events have an essential role in the apoptotic pathway (Jacobson et al., 1994; Schulze-Osthoff et al., 1994; Nakajima et al., 1995; Martin et al., 1996; Kroemer, 1997).

The aim of the present study was to extend this approach by preparing extracts from cells at various stages of the apoptotic pathway to further evaluate caspase involvement in nuclear disassembly. Interestingly, extracts prepared from morphologically normal cells in the latent phase (S/M extracts) and those prepared from frankly apoptotic cells (execution phase extracts) induced similar apoptotic events in exogenous nuclei but exhibited fundamental biochemical differences. In particular, apoptotic events in the S/M extracts were abolished by caspase inhibitors as previously reported (Lazebnik et al., 1994), whereas the same events in execution phase extracts were not. Further examination revealed that execution phase extracts contain at least two caspase-activated factors required for nuclear disassembly, one of which appears to be the nuclease CAD. These experiments not only support the view that caspases act in an executive role in nuclear apoptosis by activating downstream factors that disassemble nuclei but also suggest that activation of the downstream factors (rather than the caspases) accompanies the transition between the latent and execution phases of apoptosis.

Materials and Methods

Cell Treatment and Preparation of Extracts

Chicken DU249 cells were presynchronized in S phase with aphidicolin for 12 h, released from the block for 6 h, and synchronized in mitosis with nocodazole for 3 h as described previously (Wood and Earnshaw, 1990; Lazebnik et al., 1993). DU249 cells start to undergo apoptosis asynchronously during and after the aphidicolin treatment, presumably as a result of the cell cycle disruption. Execution phase (E/X) extracts were prepared from the floating cells (mostly apoptotic) obtained from the flasks just before the addition of nocodazole. S/M extracts were prepared from floating cells (>60% mitotic) obtained from the same flasks by selective detachment after the nocodazole treatment. After harvesting of cells for S/M extract production, cells for the preparation of condemned phase (C/D) extracts were obtained from the attached (interphase) cells by rinsing the same flasks with PBS-EDTA and trypsinization. Large scale "roller S/M" extract was prepared as described above for S/M extract except that cells were grown in roller bottles.

In each case, the cells were then washed with KPM buffer (50 mM Pipes-KOH, pH 7.0, 50 mM KCl, 10 mM EGTA, 2 mM $MgCl_2$, 20 μM cytochalasin B [Sigma Chemical Co., St. Louis, MO], 1 mM DTT, 0.1 mM PMSF, 1 μg/ml each chymostatin, leupeptin, antipain, pepstatin A) (Wood and Earnshaw, 1990) and centrifuged in a small glass Dounce homogenizer. The cells were subjected to several cycles of freezing and thawing and further disrupted by grinding during each thawing cycle. The cell lysate was then centrifuged at 139,000 *g* for 2 h, yielding clear cytosolic extracts. Protein concentration of each extract was measured by the Bradford assay (Bradford, 1976). Extract concentrations ranged between 12 and 18 mg/ml.

Time Course of Caspase Activation

DU249 cells were subjected to the synchrony procedure used in preparation of S/M extracts. At the indicated times (0, 5, 10, 15, and 20 h) after the addition of aphidicolin, both floating and attached cells were harvested from two T150 flasks (the former by shake-off, the latter by trypsinization). Cells were washed with MDB buffer, and the number of cells in each sample was counted using a hemacytometer. The ratio of interphase, mitotic, and apoptotic cells in each sample was determined by examination of the nuclear morphology after cells ($n > 400$ for each time point) were fixed in methanol/acetic acid (3:1) and stained with 0.5 μg/ml 4,6-diamidino-2-phenylindole (DAPI; Calbiochem, La Jolla, CA). Cells were lysed by the freeze/thaw/grinding protocol described above. Lysates (the supernatants after centrifugation at 13,000 *g* for 15 min at 4°C) were affinity labeled with z-EK(biotin)D-aomk as described below.

Fractionation of S/M Extracts with Heparin–Agarose Resin

Roller S/M extract (typically 7 mg of protein) prepared in KPM buffer containing 60 mM KCl was mixed with 360 μl of heparin–agarose resin (HiTrapHeparin; Pharmacia Biotech, Piscataway, NJ), which was preequilibrated with KPM buffer. This mixture was rotated at 4°C for 1 h and centrifuged in a microcentrifuge at 5,000 rpm for 5 min, and the supernatant was recovered (fraction 1; data not shown). Three cycles of absorption with heparin–agarose were needed to completely absorb all DNase activities from S/M extracts. After extensive washing of the resin with KPM buffer containing 60 mM KCl, bound proteins were eluted first with 450 μl of KPM containing 0.2 M KCl (fraction 2), and subsequently with 450 μl

of KPM containing 0.6 M KCl (fraction 3). The eluted fractions were desalted and concentrated to 4–8 mg/ml protein by centrifugation using Ultrafree-0.5 filters (5K cut; Millipore, Bedford, MA).

In Vitro Apoptosis Reaction

Apoptotic and control extracts were preincubated at 37°C for 15 min with 100 μM caspase inhibitors (YVAD-cmk or DEVD-fmk) or diluent. HeLa nuclei prepared as previously described (Wood and Earnshaw, 1990; Lazebnik et al., 1993) were then added (up to 1.0×10^6 nuclei/10 μl of extract) and incubated at 37°C for up to 2 h in the presence of an ATP regeneration system (Wood and Earnshaw, 1990; Lazebnik et al., 1993). Nuclei were either stained with DAPI to observe chromatin condensation, solubilized in SDS–sample buffer for analysis of protein cleavage, or lysed for analysis of DNA ladder formation.

Caspase Labeling and Fluorogenic Assays

Labeling. Stock solutions (10 mM in DMSO) of caspase inhibitors (YVAD-cmk or DEVD-fmk from Calbiochem) were diluted immediately before use with MDB buffer (Wood and Earnshaw, 1990). Extracts were preincubated at 37°C for 15 min with 100 μM YVAD-cmk or DEVD-fmk or diluent. After Z-EK(bio)D-aomk (Martins et al., 1997*a*) was added to a final concentration of 1 μM from a 100× stock solution in DMSO, extracts were incubated at 37°C for 15 min. Labeled proteins were subjected to conventional 16% SDS-PAGE (Laemmli, 1970), transferred to nitrocellulose membrane, probed with peroxidase-coupled streptavidin, and visualized by ECL (Amersham Corp., Arlington Heights, IL).

Fluorogenic Assays. DEVD-AFC cleavage activity was determined by a slight modification of previously described methods (Martins et al., 1997*a*). Extracts were preincubated with caspase inhibitors or diluent for 15 min at 37°C. Samples containing 20–30 μg of various fractions or 25 μg of cytosolic protein (estimated by the Bradford assay) from etoposide-treated K562 leukemia cells (a positive control) were diluted to 50 μl with buffer A (25 mM Hepes, pH 7.5, 5 mM $MgCl_2$, 5 mM EDTA, 1 mM EGTA supplemented immediately before use with 1 mM PMSF, 1 mM DTT, 10 μg/ml pepstatin A, and 10 μg/ml leupeptin), mixed with 225 μl freshly prepared buffer B (25 mM Hepes, pH 7.5, 0.1% [wt/vol] CHAPS, 10 mM DTT, 100 U/ml aprotinin, 1 mM PMSF) containing 100 μM DEVD-AFC (Enzyme System Products, Dublin, CA), and incubated for 4 h at 37°C. Reactions were terminated by addition of 1.225 ml ice-cold buffer B. Fluorescence was measured in a Sequoia-Turner spectrofluorometer using an excitation wavelength of 360 nm and emission wavelength of 475 nm. After subtraction of fluorescence in blank samples (lacking protein), amounts of the liberated fluorophore were determined by comparison to a standard curve containing 0–1,500 pmol of 7-amino-4-trifluoromethylcoumarin. Control experiments indicated that product release was linear with respect to incubation time and extract protein under the conditions used.

Protein and DNA Gel Electrophoresis

PARP and Lamin Cleavage. After HeLa nuclei (5×10^5 per loading) were incubated in extract for 2 h at 37°C, the reaction was stopped by the addition of sample buffer. Samples were boiled at 95°C for 5 min, sonicated briefly, subjected to 10% conventional SDS-PAGE (Laemmli, 1970; Wood and Earnshaw, 1990; Lazebnik et al., 1993), and transferred to nitrocellulose. PARP and its 89-kD cleavage product were detected with the C-2-10 monoclonal antibody (Lamarre et al., 1988). Lamins A/C and their cleavage product were detected with a rabbit polyclonal antibody recognizing the NH_2 terminus of the protein (gift of Larry Gerace). Bound antibody was detected by ECL.

DNA Ladder Formation. HeLa nuclei (5×10^5 per loading) were incubated for 1–2 h in extract, centrifuged, and lysed in DNA lysis buffer (50 mM Tris-HCl, pH 8.0, 10 mM EDTA, 0.5% Sarcosyl, 0.5 mg/ml proteinase K) at 50°C for 1 h. DNA was treated with RNase at 50°C for 1 h, phenol/chloroform extracted, ethanol-precipitated overnight at −70°C, resuspended in TE, and loaded onto 1% agarose gels containing 0.5 μg/ml ethidium bromide.

Plasmid DNA Digestion Assay. Extracts (18–36 μg protein in 10 μl of KPM buffer) supplemented with an ATP regeneration system (Wood and Earnshaw, 1990) and 100 μM DEVD-fmk (or diluent) were incubated at 37°C for 15 min. After addition of 160 ng purified glutathione-S-transferase–ICAD (GST-ICAD) (Sakahira et al., 1998), incubation was continued for an additional 10 min at 37°C. Upon addition of substrate (pBluescript, 1.2 μg), incubation was continued for 30 min at 37°C. DNA extraction and electrophoresis were then performed as above. The results of the preincubation assay (Fig. 5) were best seen by Southern blotting. DNA agarose gels were denatured for 30 min with denaturing buffer (1.5 M NaCl, 0.5 M NaOH), neutralized for 30 min with neutralizing buffer (0.5 M Tris-HCl, pH 7.5, 1.5 M NaCl, 1 mM EDTA), and transferred to nylon membrane (Hybond-N; Amersham Corp.) with 20× SSC buffer. The nylon membrane was UV cross-linked and hybridized (Church and Gilbert, 1984) with a pBluescript probe that was labeled with ^{32}P using the megaprimer system (Amersham Corp.). The film was exposed for 1 h at −80°C with an intensifying screen.

Pulsed-Field Gel Electrophoresis. HeLa nuclei (5×10^5) were incubated with each fraction (10 μl) for the specified time and embedded in 1.5% low melting agarose (Sea Plaque GTG agarose, FMK). Gel blocks were soaked in nuclei lysis buffer (10 mM Tris-HCl, pH 9.5, 500 mM EDTA, 1 mg/ml proteinase K, 1% sarkosyl) for 20 h at 50°C and then stored in TE buffer at 4°C. Blocks were transferred into the wells of an agarose gel and sealed in place by the addition of a small volume of agarose. Contour-clamped homogeneous (CHEF) electrophoresis was performed using a CHEF system purchased from Bio-Rad Laboratories Ltd. (Watford, England) with a model 200/2.0 power supply and a Pulsewave 760 switcher. Horizontal gels (1% agarose; Sigma Chemical Co.) were run at 14°C at 200 V for 20 h with a pulse ramp of 4–40 s and stained with ethidium bromide.

Electron Microscopy. Isolated HeLa cell nuclei incubated in extract or MDB buffer were centrifuged, washed with MDB buffer, placed on adhesion slides (Marienfeld) for 5 min, and fixed for 30 min with 2% glutaraldehyde in Dulbecco's PBS, pH 7.4. After fixation the nuclei were washed in 0.1 M cacodylate buffer, and postfixed with 4% OsO_4 in 0.1 M sodium cacodylate, pH 7.4, for 30 min. Prestaining was done with 3% uranyl acetate in H_2O for 1 h. The nuclei were dehydrated in ethanol (30–100%) and embedded in Araldite resin (Agar). Gold sections were cut with a Reichert (Vienna, Austria) microtome and placed on copper grids. Images were photographed on an electron microscope (model CM100 Biotwin; Philips Electron Optics, Mahwah, NJ).

Expression and Purification of Double Mutant His_6-ICAD

The method used for mutation was the PCR-based megaprimer strategy (Seraphin and Kandels-Lewis, 1996). Primer 1 (T7 primer), primer 2 (5′-GCCCTGCTCTCAGGCTCATC-3′), and primer 3 (5′-CAGCTCTG-CACATGGGATGTC-3′) were used to generate the $DEPD^{117}E$ mutation in the ICAD cDNA in pBluescript. Primer 4 (5′-CTGCTGTCAGAA-GAGGACCTC-3′), primer 5 (5′-GCCGACGCCTGTCTCAACTGC-3′), and primer 6 (T3 primer) were used to generate the $DAVD^{224}E$ mutation in ICAD. Each single mutant was digested with Eco47III (New England Biolabs, Hitchin, UK) and XbaI (New England Biolabs) and then ligated to generate double mutant ICAD in pBluescript. This double mutant ICAD was digested with SpeI, blunt-ended with T4 DNA polymerase (New England Biolabs) plus 100 μM dNTPs, and digested with KpnI (New England Biolabs). The resulting fragment was ligated into pRSET B (Invitrogen, Carlsbad, CA) that had been digested with HindIII, blunt-ended with T4 DNA polymerase, and digested with KpnI. Double mutant ICAD in pRSETB was transformed into *Escherichia coli* BL21 (DE3)Lys S cells. Transformed cells were grown to $OD_{600} = 0.5–0.7$, and protein expression was induced with IPTG (1 mM) for 3–4 h. Cells were collected by centrifugation at 5,000 *g* for 10 min and frozen at −80°C. The cell pellet was thawed on ice for 15 min and resuspended in lysis buffer (50 mM NaH_2PO_4 pH 7.5, 300 mM NaCl, 10 mM imidazole). Lysozyme was added to 1 mg/ml, and the suspension was incubated on ice for 30 min, sonicated on ice until 80% of the cells were disrupted, and then centrifuged at 4,000 *g* for 20 min at 4°C. The supernatant was incubated on a rotating mixer for 1 h at 4°C with 0.5 ml of Ni-agarose (Qiagen, Chatsworth, CA) that had been preequilibrated with lysis buffer. The resin was then loaded onto a polyprep chromatography column (Bio-Rad Laboratories) and washed twice with 4 ml of wash buffer (50 mM NaH_2PO_4 pH 7.5, 300 mM NaCl, 20 mM imidazole). Protein was eluted with 2 ml of elution buffer (50 mM NaH_2PO_4 pH 7.5, 300 mM NaCl, 250 mM imidazole). All samples were subjected to SDS-PAGE and examined by Coomassie blue staining. The eluted protein was dialyzed for at least 3 h against two changes of CAD buffer (10 mM Hepes, pH 7.4, 50 mM NaCl, 5 mM EGTA, 2 mM $MgCl_2$, 1 mM DTT), aliquoted, and frozen in $N_2(l)$.

Expression and Purification of His_6-ICAD/CAD

To express active CAD in *E. coli*, we constructed a bicistronic expression vector in which His_6-ICAD was expressed upstream of CAD. In addition

to the NH_2-terminal histidine tag, the ICAD open reading frame was engineered to change the stop codon to TAA and to insert a Shine-Delgarno sequence (GGAAT) downstream of the stop codon. The wild-type ICAD cDNA in pBluescript was digested with SpeI, blunt-ended with T4 DNA polymerase, and digested with KpnI. The resulting fragment was ligated into pRSET B that had been digested with HindIII, blunt-ended with T4 DNA polymerase, and digested with KpnI. The coding region of the CAD cDNA was extracted from the full-length CAD cDNA in pBluescript by PCR using Vent polymerase (New England Biolabs) with primer 7 (5′-GGAATTCATGTGCGCGGTGCTCCG-3′) and primer 8 (5′-GCGAAGCTTTCACTAGCGCTTCCGAG-3′). The PCR product was digested with EcoRI and HindIII, and the resulting fragment was ligated into pBluescript.

To create the COOH terminus of ICAD (from the BsmI site at nucleotide 909) engineering in a TAA stop codon and Shine-Delgarno sequence, primer 9 (5′-GGAAGATCTGCATTCACTCAGGAATC-3′) and primer 10 (5′-GGAATTCCTCCTTACGAGGAGTCTCGTTTG-3′) were used with Vent polymerase. The PCR product was digested with BglII (New England Biolabs) and EcoRI and ligated into pRSETB that had been digested with BglII and EcoRI. The CAD coding sequence in pBluescript was digested with EcoRI and HindIII and ligated into pRSET B containing the newly modified COOH terminus of ICAD with the Shine-Delgarno sequence. This intermediate was then digested with NheI and BsmI, and into it was inserted the His-tagged NH_2-terminal portion of ICAD, obtained from ICAD in pRSETB that had likewise been digested with NheI and BsmI. This bicistronic vector His_6-ICAD/CAD in pRSET B was transformed into *E. coli* BL21 (DE3)Lys S cells. Protein was expressed and purified by nickel chelate chromatography as described above for double mutant ICAD. The dialyzed ICAD/CAD protein was frozen in N_2(l) either directly or following addition of glycerol to 40%.

In Vitro Apoptosis with Purified CAD

50-μl reactions contained various combinations of the following reagents added sequentially (see legend to Fig. 6): 10 μl ICAD/CAD protein (stored in CAD buffer plus 40% glycerol), 5 μl caspase-3, an ATP regeneration system (final concentration 0.8 mM ATP, 4.5 mM creatine phosphate, 22.5 μg/ml creatine kinase), DEVD-fmk (final concentration 300 μM), double mutant ICAD protein (2 μg), and CAD buffer as needed to make up the final volume. ICAD/CAD complexes were preincubated with caspase-3 at room temperature (~25°C) for 30 min to cleave wild-type ICAD and release active CAD. At the end of this preincubation, diluent, DEVD-fmk, or double mutant ICAD were added (defined as $t = 0$), and the mixture was divided into three aliquots to assay various apoptotic events. To examine ICAD cleavage during the preincubation, a 10-μl aliquot was mixed with sample buffer, boiled, resolved by SDS-PAGE, transferred to nitrocellulose membranes, and probed with ICAD antibody (Samejima and Earnshaw, 1998), which was detected by ECL (Amersham Corp.). To assay CAD activity against a plasmid DNA substrate, a 6-μl aliquot was supplemented with 0.35 μg pBluescript, BSA (final concentration 1 mg/ml), and 4 μl of CAD buffer. This mixture was further incubated at 37°C for 30 min, extracted with phenol-chloroform, and analyzed on a 1% agarose gel containing ethidium bromide. To examine the ability of the active CAD to induce apoptotic events, HeLa nuclei (1.3×10^6 per sample) in 10 μl CAD buffer were combined with the remaining 34 μl and incubated at 37°C for 2 h. At the end of this incubation, 1 μl of the reaction mixture was stained with DAPI so that nuclear morphology could be examined by fluorescence microscopy (>100 nuclei counted per slide). The remaining HeLa nuclei in 43 μl of reaction mixture were centrifuged and prepared for agarose gel electrophoresis as described above.

Results

Extracts from Three Different Stages of Apoptosis

The apoptotic pathway can be conceptually divided into at least three stages (Fig. 1 *A*). Upon receipt of a proapop-

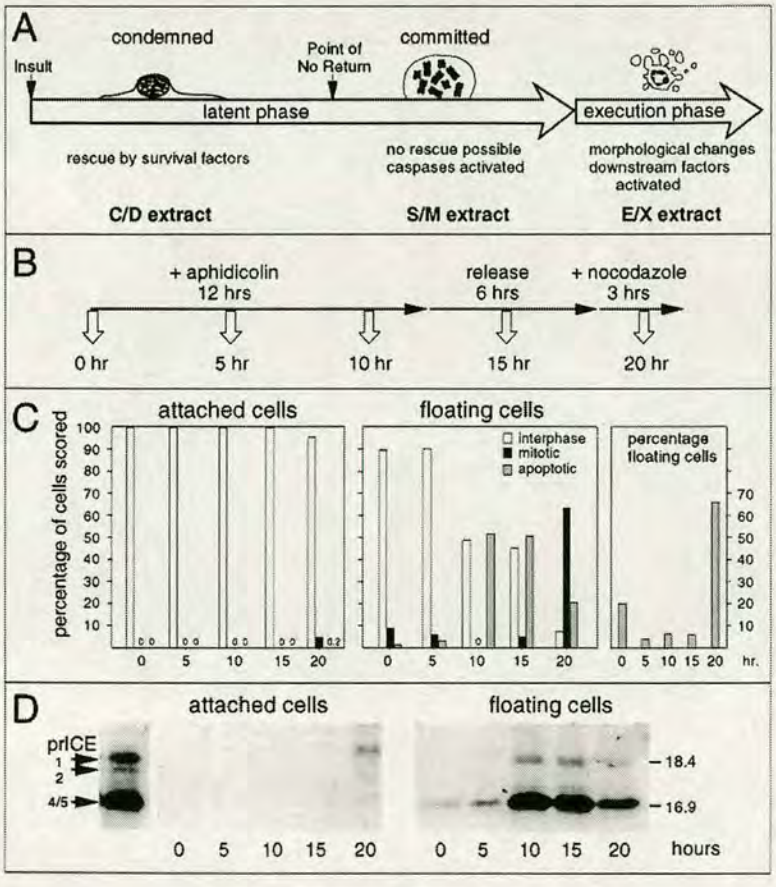

Figure 1. (*A*) Diagram of apoptosis as a three stage process, with the latent phase being subdivided into condemned and committed stages. (*B*) The protocol used for harvesting of samples for examination of caspase activation. (*C*) The cells harvested at each time point were scored for their nuclear morphology, based on DAPI staining. (*D*) Caspase activity in whole cell lysates prepared from cells harvested at various times points after the addition of aphidicolin to the culture (time in hours shown at bottom). *Left*, attached cells; *right*, floating cells. The left-most lane shows the profile of active caspases in S/M extract.

totic signal, cells enter a "condemned" stage: the death program is initiated, but cells can be rescued by various survival factors. Once cells pass a point of no return, they are in the "committed" stage and can no longer be rescued. During both of these stages, preapoptotic cells appear morphologically normal. Eventually, committed cells undergo an abrupt transition into apoptotic execution, a period lasting from 5 min to 1 h, during which cellular disassembly and death occur. It is not known where along this pathway caspases are activated and at what point the caspases activate other downstream factors that act during disassembly of the cell.

We previously noted that active caspases could be detected in extracts from etoposide-treated HL-60 cells several hours before the bulk of the cells in the culture exhibited an overtly apoptotic morphology (Martins et al., 1997*a*). To study this phenomenon in greater detail, we harvested chicken DU249 cells at various times after subjecting cultures to a synchronization protocol (Fig. 1 *B*) shown previously to induce an apoptotic response in this cell line (Lazebnik et al., 1993). Floating cells obtained 10–15 h after the addition of aphidicolin were largely (~ 50%) apoptotic and contained high levels of active caspases, as detected by reactivity with the affinity-labeling reagent z-EK(biotin)D-aomk (Martins et al., 1997*a*) (Fig. 1, *C* and *D*). Floating cells harvested after a change of medium and a 2-h treatment with nocodazole to induce a mitotic block were predominantly (>60%) mitotic, with only 10–20% of apoptotic cells. Despite the normal appearance of the vast majority of these cells, extracts prepared from them also contained high levels of active caspases. Cells that remained attached throughout the protocol were almost entirely in interphase, and extracts prepared from them lacked caspases detectable with z-EK(biotin)D-aomk (Fig. 1 *D*, *left*), although low levels of caspase activity were detectable when more sensitive assays were used (see below).

The results of this experiment suggested that it might be possible to use a similar protocol to prepare extracts sequentially from the same flasks of cells at different stages of apoptosis (Fig. 2 *A*). C/D (condemned phase) extracts were prepared from the morphologically normal attached cells that did not enter mitosis or apoptosis during the synchrony procedure. Previous studies have indicated that these cells ultimately undergo apoptosis if left in culture (Lazebnik et al., 1993). S/M (committed phase) extracts

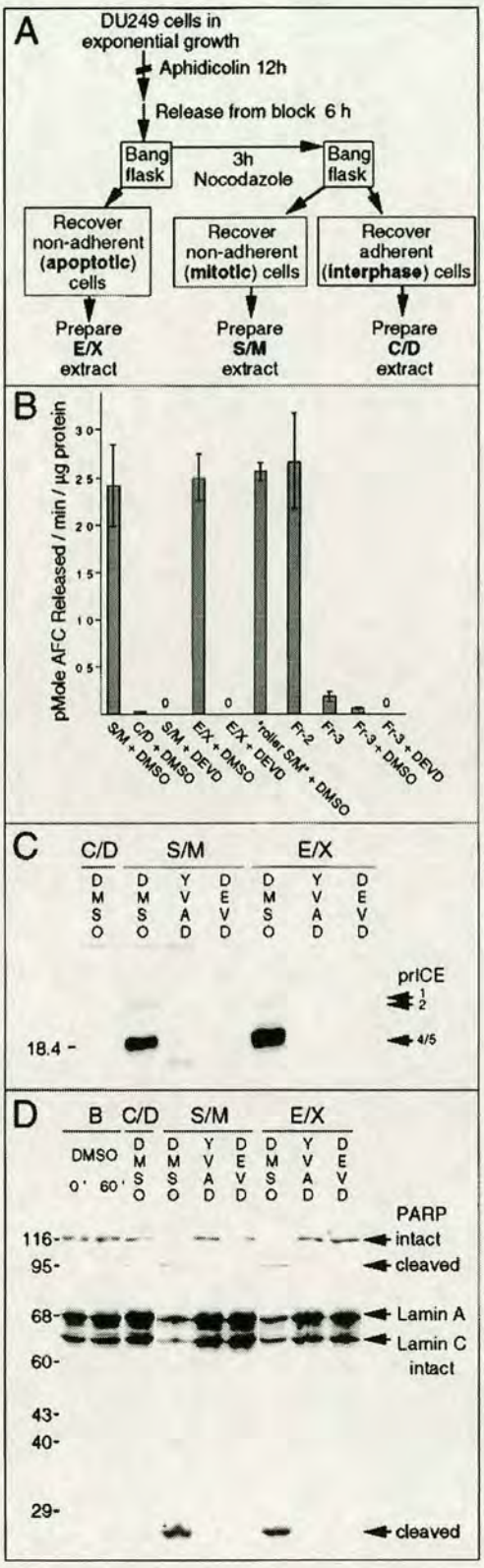

Figure 2. Apoptotic extracts contain active caspases that are functionally inactivated by specific inhibitors. (*A*) Protocol used to prepare C/D, S/M, and E/X extracts. (*B*) Quantitative analysis of DEVD-AFC cleavage activity in the various extracts. DEVD-fmk treatment of S/M and E/X extracts reduces caspase activity by at least 250- and 150-fold, respectively. Note the low but nonzero level of caspase activity in the C/D extracts. Fr-3 (see Fig. 4) has ~8% the caspase activity seen in S/M extract. Treatment of Fr-3 with DEVD-fmk further reduces this activity by ≥130-fold relative to the S/M extract. (*C*) Active caspases were labeled with zEK(biotin)D-aomk in S/M and E/X extracts. This labeling was completely blocked by prior incubation of extracts with YVAD-cmk and DEVD-fmk (both at 100 µM). (*D*) PARP and lamin A/C cleavage by caspases in the cell-free extracts is abolished after caspase inactivation with YVAD-cmk and DEVD-fmk. Note that low levels of caspases in the C/D extract cause some PARP cleavage but fail to cleave lamins.

(Lazebnik et al., 1993) were prepared from morphologically normal mitotic cells at the conclusion of the synchrony procedure. Because these cells are destined to rapidly undergo apoptosis if left in culture (Lazebnik et al., 1993), we postulate that S/M extracts reproduce events from the committed stage of apoptosis. E/X (execution phase) extracts were prepared from cells that were frankly apoptotic after a 12-h exposure to aphidicolin followed by a 6-h recovery period in medium. (Note that nonadherent cells were discarded at the end of the aphidicolin treatment, so these cells must have entered apoptosis during the 6-h recovery period).

To examine the spectrum of active caspases during the three stages of apoptosis, extracts were assayed for their ability to cleave DEVD-AFC, for affinity labeling with z-EK(bio)D-aomk (Martins et al., 1997*a*), and for the ability to cleave known caspase substrates in added nuclei. Collectively, these assays detect all known caspases. DEVD-AFC contains the preferred cleavage site of caspases-3 and -7 (Talanian et al., 1997; Duan et al., 1996*b*) but is also cleaved by caspases-1, -2, -4, -6, -8, and -10 (Fernandes-Alnemri et al., 1995*a*, 1996; Boldin et al., 1996; Srinivasula et al., 1996; Talanian et al., 1997). z-EK(bio)D-aomk covalently modifies all caspases tested to date (Martins et al., 1997*a*) and can detect over 30 active caspase species in apoptotic human leukemia cells (Martins, L.M., and W.C. Earnshaw, unpublished observations). PARP is a documented substrate of caspases-3, -7, -8, and -9 (Nicholson et al., 1995; Tewari et al., 1995; Fernandes-Alnemri et al., 1995*a*,*b*; Duan et al., 1996*b*; Muzio et al., 1996), while lamin A is a substrate of caspase-6 (Takahashi et al., 1996). Application of these assays to C/D extracts revealed low but detectable levels of active caspases (125-fold less than S/M or E/X extracts in the DEVD-AFC assay; Fig. 2 *B*) and some ability to cleave PARP (Fig. 2 *D*, lane *C/D*), but no evidence of z-EK(biotin)D-aomk labeling or lamin cleavage, suggesting that the latter assays are less sensitive. In contrast, S/M and E/X extracts contained high levels of active caspases that cleaved DEVD-AFC as well as PARP and lamin A (Fig. 2, *B* and *D*), and both had a similar pattern of active caspases after affinity-labeling with z-EK(bio)D-aomk (Fig. 2 *C*). These correspond primarily to active forms of caspases-3 and -6 (Martins et al., 1997*a*; Faleiro et al., 1997). All caspase activity detectable in these assays was quantitatively inactivated by treatment with YVAD-cmk (Fig. 2, *C* and *D*) or DEVD-fmk (Fig. 2, *B–D*).

Differences in Dependence of S/M and E/X Extracts on Ongoing Caspase Activity

C/D extracts were unable to induce internucleosomal DNA fragmentation and apoptotic morphological changes in exogenous nuclei (Fig. 3, *A* and *B*). In contrast, S/M and

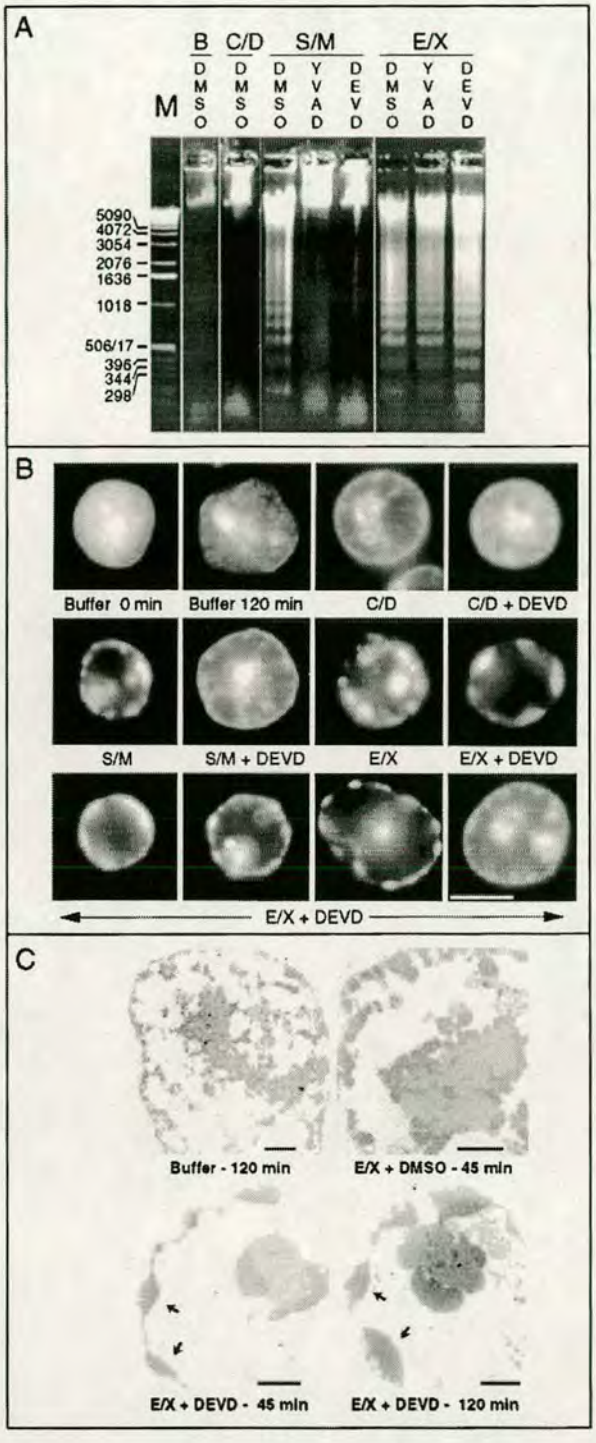

Figure 3. Caspase inhibitors block apoptosis in S/M but not E/X extracts. (*A*) Inhibition of caspases blocks nuclease activity in S/M extracts but not E/X extracts. As expected, C/D extracts lack detectable nuclease activity. Experiments shown in Fig. 8 confirm that the nuclease activity is inhibitable by the specific CAD inhibitor ICAD/DFF45 (Enari et al., 1995*b*; Liu et al., 1997). Lane *B*, buffer control. (*B*) Inhibition of caspases abolishes morphological apoptosis in vitro in S/M extracts but not execution phase extracts. Nuclei shown in *B* were selected at random. (*C*) Morphological changes characteristic of apoptosis occur in E/X extracts independently of caspase activity: confirmation of apoptotic morphology by electron microscopy. Arrows indicate regions of condensed chromatin. Bars: (*B*) 5 μm; (*C*) 1 μm.

E/X extracts induced hallmark biochemical and morphological changes of apoptosis in added nuclei. Further studies focused on these latter two extracts.

Despite the similarities of the S/M and E/X extracts in terms of caspase activity (Fig. 2) and effects on exogenous nuclei (Fig. 3, *A* and *B*), the two extracts displayed strikingly different properties after inhibition of the endogenous caspase activity. Pretreatment of S/M extracts with DEVD-fmk or YVAD-cmk before addition of nuclei not only inhibited caspase activity (Fig. 2, *B–D*) but also completely abolished their ability to produce internucleosomal DNA fragmentation (Fig. 3 *A*) and induce morphological apoptotic changes (Fig. 3 *B*). In striking contrast, E/X extracts that had been pretreated with caspase inhibitors continued to strongly induce internucleosomal DNA degradation (Fig. 3 *A*), chromatin condensation, and fragmentation of added nuclei (shown both by light and electron microscopy; Fig. 3, *B* and *C*) despite a lack of detectable caspase activity (Fig. 2, *B–D*).

Fractionation of Active Extracts

Further evidence for the ability of extracts to induce nuclear apoptotic events in the absence of caspase activity

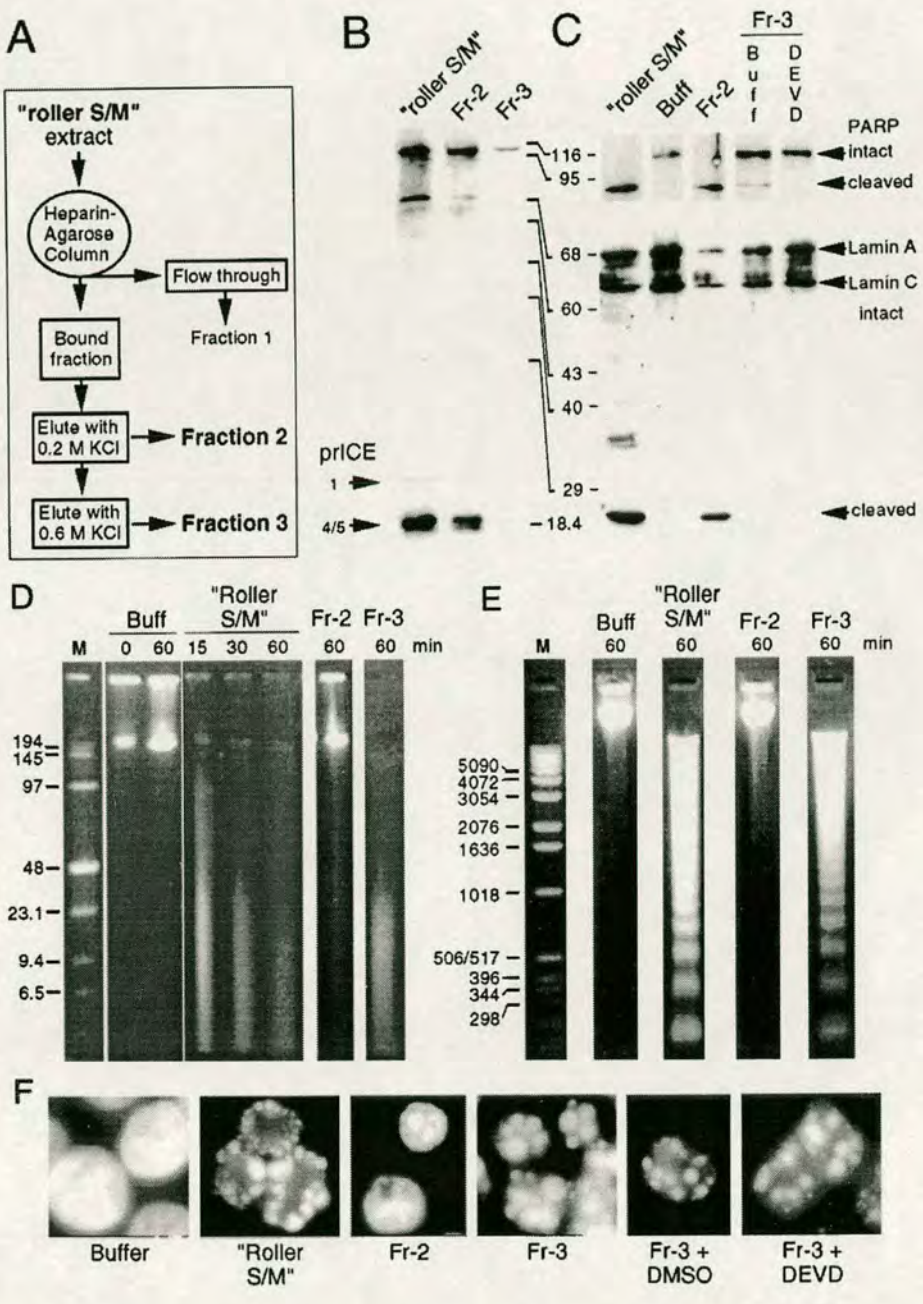

Figure 4. A fraction rich in endogenous caspases fails to induce apoptotic events in added nuclei. (*A*) Protocol used to prepare fractions 1–3 by heparin–agarose chromatography of roller S/M extract. (*B*) Active caspases were labeled with zEK(biotin)D-aomk in roller S/M extract and fraction 2, but could not be detected in Fr-3. The bands in the upper portion of the gel are cellular proteins that bind to the streptavidin probe. (*C*) PARP and lamin A are efficiently cleaved by roller S/M extract and by Fr-2. Fr-3 has low levels of PARP cleavage activity that are abolished by pretreatment with DEVD-fmk. (*D*) Pulsed field gel electrophoresis. High molecular weight DNA fragments were produced in HeLa nuclei incubated in roller S/M extracts and Fr-3 (caspase-deficient), but not in nuclei incubated in buffer or Fr-2, which contains high levels of active caspases. Lane *M*, DNA markers (sizes shown in kilobase pairs). (*E*) Conventional agarose gel electrophoresis. An oligonucleosomal DNA ladder is formed in nuclei incubated in roller S/M extracts and Fr-3, but not in nuclei incubated in buffer or Fr-2. Lane *M*, DNA markers (sizes shown in base pairs). (*F*) Fr-3 induces very strong morphological apoptosis even when all detectable caspase activity is abolished by pretreatment with DEVD-fmk. In contrast, Fr-2, which has a distribution and concentration of caspases essentially identical to S/M extract, does not induce morphological apoptosis in HeLa nuclei.

was obtained through biochemical fractionation of large-scale roller S/M extracts prepared using cells growing in roller bottles. These extracts appeared to functionally resemble a mixture of S/M and E/X extracts (i.e., were only partly inhibited by DEVD-fmk or YVAD-cmk). We believe that this is because a much higher percentage of apoptotic cells was present among the committed phase cells at the time of harvest. When roller S/M extracts were fractionated on heparin agarose (Fig. 4 *A*), proteins eluted from the column at 0.2 M KCl (fraction 2 [Fr-2]) included many of the active endogenous caspases, as shown by their ability to cleave the peptide substrate DEVD-AFC (Fig. 2 *B*), by activity labeling with z-EK(biotin)D-aomk (Fig. 4 *B*), and by cleavage of PARP and lamin A (Fig. 4 *C*). Factors eluted from the column at 0.6 M KCl (fraction 3 [Fr-3]) were substantially depleted of caspases, and this fraction resembled C/D extracts in several regards. DEVD-AFC cleavage activity in Fr-3 was reduced 13-fold relative to roller S/M extract (Fig. 2 *B*), and only trace levels of PARP cleavage activity were detected (compare Fig. 4 *C*, lanes *Fr-3*, with Fig. 2 *D*, lane *C/D*). Both zEK(biotin)D-aomk binding activity and lamin A cleaving activity were undetectable in Fr-3 (Fig. 4, *B* and *C*).

Although fraction 2 contained high levels of endogenous caspase activity, it was unable to trigger either internucleosomal DNA fragmentation or morphological apoptosis in added nuclei. In contrast, fraction 3 was a more potent inducer of apoptosis than the starting roller S/M extract, inducing both high molecular weight and oligonucleosomal DNA fragmentation (Fig. 4, *D* and *E*) as well as morphological apoptosis in substrate nuclei (Fig. 4 *F*). This activity was not due to the low levels of residual caspases present in fraction 3. Pretreatment with DEVD-fmk, which abolished all detectable caspase activity (Fig. 2 *B*), had no effect on the ability of fraction 3 to induce DNA fragmentation (not shown) or apoptotic morphology in added nuclei (Fig. 4 *F*). Thus, a column fraction rich in endogenous apoptotic caspases (Fr-2) was unable to induce morphological apoptosis in isolated nuclei, while a second fraction prepared on the same column from the same extract (Fr-3) strongly induced apoptotic events despite being severely depleted or devoid (after inhibitor treatment) of detectable caspase activity.

Comparison of CAD Activation in S/M and E/X Extracts

Because the results presented in Figs. 2–4 suggest that the program of nuclear disassembly—one of the distinguishing features of apoptotic cell death under physiological conditions (Wyllie et al., 1980)—is initiated by caspase activity

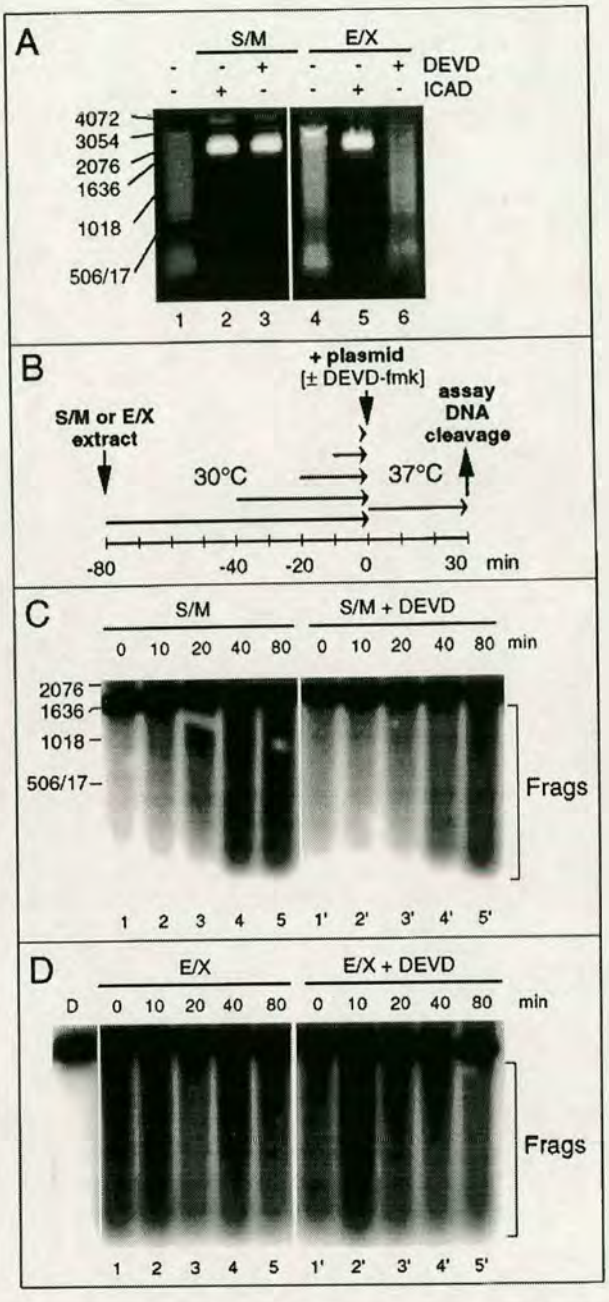

Figure 5. Differences in the activity of the CAD-like nuclease in S/M and E/X extracts. (*A*) CAD-like nuclease in S/M extracts is sensitive to DEVD-fmk, whereas that in E/X extracts is not. Apoptotic extracts cleave a plasmid substrate at 37°C (lanes *1* and *4*). The nuclease responsible is inhibited by purified murine GST-ICAD (lanes *2* and *5*) and therefore is functionally related to murine CAD (Enari et al., 1998). In S/M extracts, but not E/X extracts, the nuclease is abolished by addition of DEVD-fmk together with the plasmid DNA (lanes *3* and *6*). (*B*) Diagram of experimental protocol designed to test whether the CAD-like enzyme is active in both S/M and E/X extracts before the incubation with DNA. (*C*) In S/M extracts, the CAD-like activity increases during preincubation of the extract at 30°C before addition of the plasmid DNA (lanes *1–5*). This activity is now insensitive to the addition of DEVD-fmk at the time of plasmid addition (lanes *1′–5′*). Bracket labeled "Frags" indicates the products of caspase cleavage. The DNA cleavage activity in lane *1′* may arise from some limited activation of CAD before all caspases were inhibited since DNA and DEVD-fmk were added at the same time. (*D*) In contrast, preincubation has no effect on the cleavage of plasmid substrate by E/X extracts (lanes *1–5*), which is likewise resistant to inhibition with DEVD-fmk (lanes *1′–5′*). Lane *D*, added plasmid DNA alone. Bracket labeled "Frags" indicates the products of caspase cleavage.

but does not require the ongoing participation of caspases for its successful execution, we next turned our attention to caspase-activated downstream activities that might participate in nuclear disassembly. One of these activities is CAD/CPAN, the recently identified caspase-activated deoxyribonuclease identified in murine and human cells undergoing apoptosis (Enari et al., 1998; Halenbeck et al., 1998). Both S/M and E/X extracts contain an endogenous DNase activity that degrades added plasmid DNA (Fig. 5 *A*, lanes *1* and *4*). Addition of 160 ng of murine ICAD to the extracts abolished this DNase activity (lanes *2* and *5*), indicating that this activity is functionally homologous to CAD.

Even though CAD-like activity could be inhibited by ICAD in both S/M and E/X extracts, this activity appeared to be regulated differently in the two extracts. DEVD-fmk pretreatment abolished CAD-like activity in S/M extracts (Fig. 5 *A*, lanes *1* and *3*) but had no effect on CAD activity in E/X extracts (Fig. 5 *A*, lanes *4* and *6*). There are at least two potential explanations for this difference. First, active CAD might be unstable in S/M extracts and might therefore require a constant source of caspase activity to continue to generate active enzyme from CAD/ICAD complexes. Second, despite the presence of high levels of endogenous caspases in S/M extracts, the CAD in these extracts might initially be largely in the form of inactive CAD/ICAD complexes. Active CAD might be released from these complexes by caspase activity during the incu-

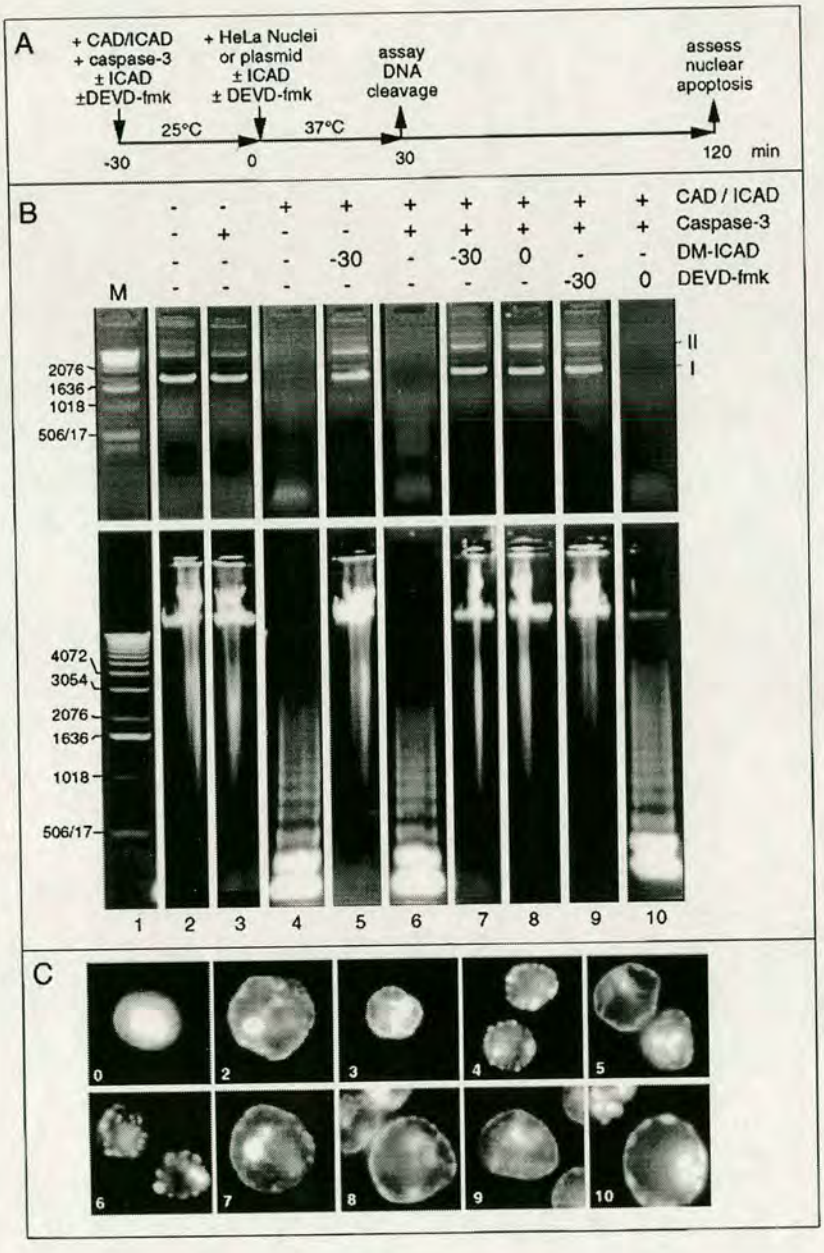

Figure 6. Bacterially expressed CAD is capable of inducing apoptotic morphology in added nuclei in the absence of apoptotic extract. (*A*) Diagram of the experimental protocol. After CAD was activated during a preincubation with purified caspase-3 at 25°C, substrates were added and incubated for various times with the active enzyme at 37°C. (*B*) Effects of various incubations on CAD nuclease activity using either a purified plasmid substrate (pBluescript, *upper panels*) or added nuclei (*lower panels*). The morphology of the nuclei in these same incubations is shown in *C*, where the panel numbers refer to lanes in *B*. Buffer and caspase-3 do not possess nuclease activity or induce apoptotic morphology in added nuclei (lanes and panels *2* and *3*). Preincubation of CAD alone induces nuclease activity and apoptotic morphology (lane and panel *4*), presumably because of the presence of a contaminating protease. ICAD is cleaved during this preincubation (data not shown). This spontaneous activation of CAD is not observed if noncleavable ICAD is present from the start of the preincubation (lane and panel *5*). Preincubation of CAD with caspase-3 induces nuclease activity and apoptotic morphology (lane and panel *6*). This activity is not observed if noncleavable ICAD is present either from the start of the preincubation, or if it is added at the end of the preincubation together with the substrate nuclei (lanes and panels *7* and *8*). Addition of DEVD-fmk to the preincubation blocks CAD activation but has no effect on nuclease activity or induction of apoptotic morphology if added once the preincubation is complete (lanes and panels *9* and *10*). The induction of apoptotic morphology by CAD in the presence of DEVD-fmk was slightly, but reproducibly, reduced (panel *10*). These results demonstrate that CAD can induce nuclear apoptosis in the absence of caspase-3 activity. I and II at the right of *B* indicate the migration of form I (supercoiled) and form II (nicked circular) plasmid DNA.

bation with DNA substrates.

To distinguish between these possibilities, we preincubated S/M and E/X extracts at 30°C for various times to allow cleavage of endogenous ICAD by endogenous caspases before adding DNA in the presence or absence of DEVD-fmk (see the experimental protocol in Fig. 5 *B*). This experiment indicated that CAD activity was initially low in S/M extracts but increased gradually with incubation at 30°C (Fig. 5 *C*, lanes *1–5*). Once activated, CAD was stable in the presence of DEVD-fmk (lanes *1′–5′*). In contrast, CAD was fully active at all times in E/X extracts in the presence and absence of DEVD-fmk (Fig. 5 *D*). Collectively, these results indicate that CAD is present but inactive in extracts prepared from committed stage cells and is activated in equivalent extracts prepared from execution phase cells. In addition, this result confirms that the apoptotic activities present in S/M extracts are not due solely to the presence of low levels of contaminating apoptotic cells since these cells would be expected to have high levels of active CAD.

CAD Alone Is Also Capable of Inducing Apoptotic Morphology in Added Nuclei

Collectively, the results presented in Figs. 3 and 5 suggest that CAD might be a major factor that acts downstream of caspases to induce changes in nuclear structure during apoptotic execution. To examine this possibility in greater detail, we exposed isolated nuclei to partly purified cloned murine CAD. Active CAD was expressed in *E. coli* using a bicistronic vector, which ensured that the CAD was translated in the presence of an excess of ICAD (Enari et al., 1998). The resulting CAD/ICAD complex was purified by nickel chelate chromatography and then tested for activity against plasmid and nuclear substrates according to the experimental protocol shown in Fig. 6 *A*. Results obtained with the plasmid substrate are shown in Fig. 6 *B*. The CAD/ICAD complex purified from *E. coli* became activated after a preincubation of 30 min at 25°C either in the absence (Fig. 6 *B*, lane *4*) or presence (lane *6*) of purified recombinant caspase-3. We assume that activation in the absence of added caspase is due to the presence of contaminating protease activity from the *E. coli* lysate. Addition of double mutant ICAD (Sakahira et al., 1998) at the start of the preincubation blocked CAD activation in both the absence (lane *5*) and presence (lane *7*) of caspase-3. Double mutant ICAD also blocked CAD activity if added at the end of the preincubation (lane *8*). In contrast, DEVD-fmk blocked CAD activation if added at the start of the preincubation (lane *9*) but had no effect if added after cleavage of ICAD (lane *10*).

The results obtained with the plasmid substrate were exactly duplicated when we examined the ability of bacterially expressed CAD to induce DNA ladders and morphological changes in HeLa nuclei (Fig. 6, *B* and *C*). These morphological changes were confirmed by electron microscopy, where condensed chromatin domains could be seen to be closely apposed to the nuclear envelope (Fig. 7). When CAD was fully active, as detected using either plasmid or nuclear substrates, the enzyme strongly induced condensation of chromatin at the periphery of added nuclei (Fig. 6, *B* and *C*, lanes and panels *4* and *6*).

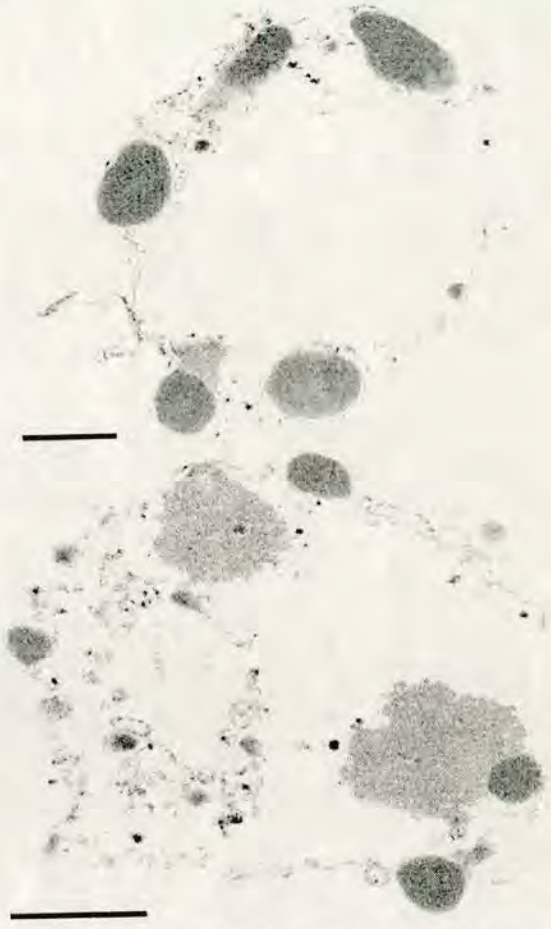

Figure 7. Induction of apoptotic morphology in HeLa nuclei by bacterially expressed CAD: analysis by electron microscopy. Nuclei treated with CAD—as shown in Fig. 6 *B*, lane and panel *6*—were embedded in plastic, thin sectioned, and examined in the electron microscope. Regions of condensed chromatin are seen to abut the nuclear envelope, and often protrude as though beginning to bud outwards through the envelope. These images are indistinguishable from previously published images of nuclei treated with complete apoptotic extract (Lazebnik et al., 1993). Bar, 1 μm.

Higher levels of CAD induced the complete disassembly of nuclei into apoptotic bodies (data not shown); however, under these conditions nucleosomal ladders were no longer seen (the DNA was fully degraded). Interestingly, the addition of DEVD-fmk at time $t = 0$ slightly inhibited the morphological apoptosis (Fig. 6 *C*, panel *10*), although examples of fully apoptotic nuclei could still be seen. It is important to note that caspase-3 alone was unable to induce either DNA cleavage or apoptotic morphology in added nuclei (lane and panel *3*), consistent with the results obtained with fraction 2 described above (Fig. 4 *F*).

Evidence for a Nuclear Disassembly Factor Distinct from CAD

To determine whether the CAD-like enzyme was the sole

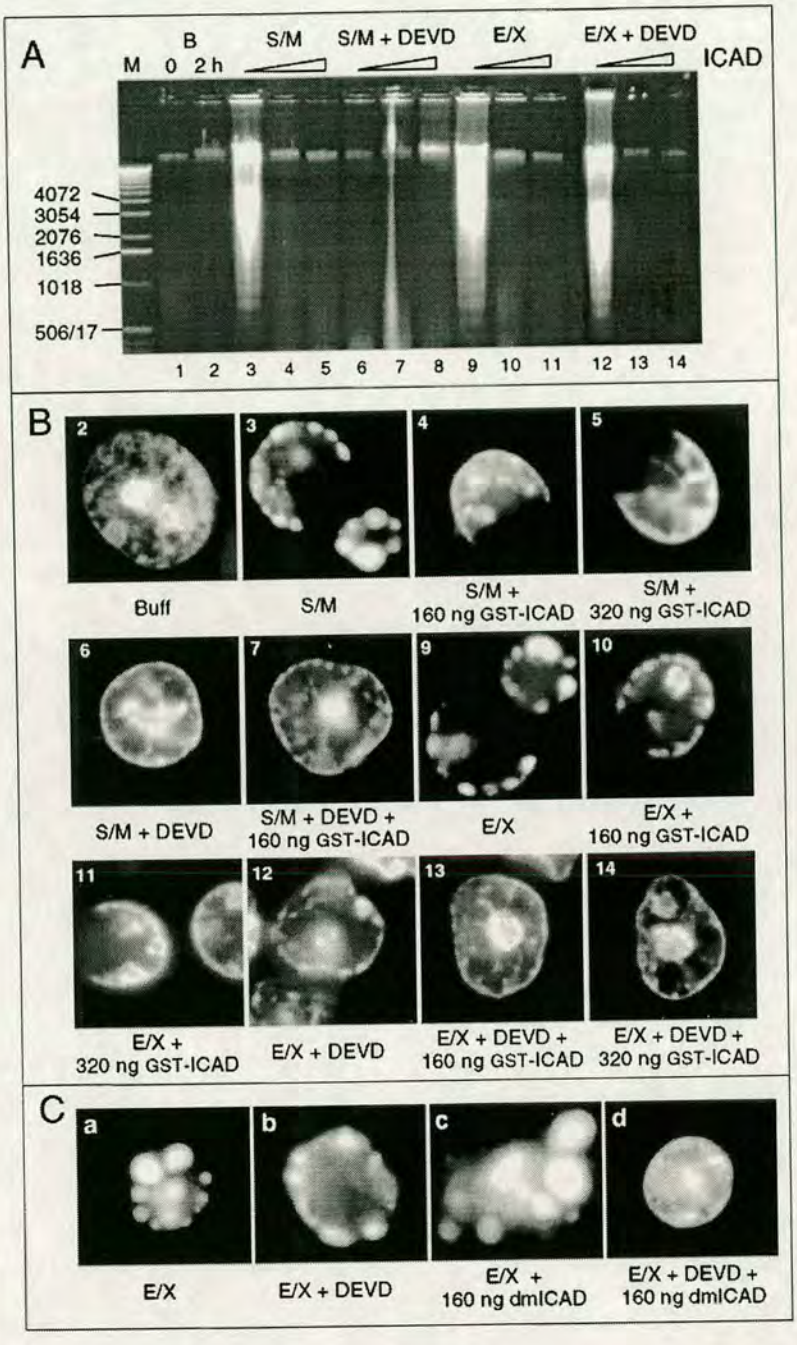

Figure 8. Induction of apoptotic morphology in cell extracts is not blocked by inhibition of the CAD-like nuclease. (*A*) Induction of nucleosomal ladders in added nuclei by S/M extract is sensitive to ICAD and DEVD-fmk (lanes *3–8*). Induction of nucleosomal ladders in added nuclei by E/X extract is sensitive only to ICAD (lanes *9–14*). (DEVD-fmk added: none, lanes *1–5* and *9–11*; 100 μM, lanes *6–8* and *12–14*. ICAD added: none, lanes *3*, *6*, *9*, and *12*; 160 ng, lanes *4*, *7*, *10*, and *13*; 320 ng, lanes *5*, *8*, *11*, and *14*.) (*B*) Both S/M and E/X extracts can induce apoptotic events under conditions where the CAD-like nuclease is inhibited, provided that they retain active caspases (panels *3–5* and *9–11*). E/X extracts, which normally induce apoptosis in the absence of caspase activity (panel *12*), are unable to do so if ICAD is added along with DEVD-fmk (panels *13* and *14*). Panel numbers refer to the gel lanes in *A*. These images come from the same incubations shown in *A*. Time-lapse microscopy analysis reveals that the C-shaped nuclei in panels *3–5* and *9–11* are apoptotic nuclei in which the nuclear envelope has ruptured after collapse of the chromatin against the nuclear periphery. (*C*) E/X extracts can fully induce apoptotic morphology in the absence of CAD-like activity, but this requires ongoing caspase activity. In a different experiment from that shown in *A* and *B*, the number of nuclei per microliter of extract was reduced. This gives a stronger induction of apoptotic morphology (compare *a* with *B*, panel *9*), even when caspases (*b*) or CAD are inhibited (*c*). Extracts produce a range of morphologies in added nuclei. As in the experiment of *A* and *B*, simultaneous inhibition of both CAD and caspases abolishes morphological apoptosis in the extracts (*d*). These images were selected from images taken at random.

activity downstream of caspases that drives nuclear disassembly in these extracts, S/M and E/X extracts were treated with ICAD before addition of exogenous nuclei. Although addition of excess ICAD abolished production of a nucleosomal ladder in nuclei added to S/M and E/X extracts (Fig. 8 *A*, lanes *3–5* and *9–11*), ICAD did not block the ability of the extracts to induce chromatin condensation and nuclear fragmentation (Fig. 8 *B*, panels *3–5* and *9–11*). The ability of the extracts to induce morphological changes in the presence of ICAD was even more striking when the number of nuclei in the incubation was reduced approximately fourfold (Fig. 8 *C*). These observations indicate that CAD-like activity is not essential for apoptotic morphological changes in nuclei added to either S/M or E/X extracts.

Interestingly, simultaneous inhibition of both CAD and caspases did block the induction of apoptotic morphology by E/X extracts (Fig. 8 *B*, panels *13* and *14*; Fig. 8 *C*, *d*). As indicated above, the caspase-rich column fraction Fr-2 lacked the ability to induce apoptotic morphological changes in exogenous nuclei (Fig. 4 *F*). Moreover, addition of purified caspases-3 and -6, the major active caspases in

cytosol (Faleiro et al., 1997; Martins et al., 1997*a*) and nuclei (Martins et al., 1997*a*,*b*), failed to induce apoptotic morphological changes in purified nuclei (data not shown; identical to Fig. 6 *C*, panel *5*). These observations appear to rule out the possibility that caspases themselves are capable of inducing chromatin condensation by acting alone on endogenous nuclear substrates. When coupled with these results, the observation in Fig. 8 *C*, *d*, not only suggests that there is a second chromatin condensation factor present in the extracts but also raises the possibility that ongoing caspase activity is required for activity of this factor.

Discussion

The experiments described above have led to a number of novel observations: (*a*) It is possible to prepare cell-free extracts specific for the latent and execution phases of apoptosis. (*b*) These extracts, both of which contain active caspases and induce apoptosis in substrate nuclei, exhibit significant biochemical and functional differences that are best explained if the transition from the latent to the execution phase of apoptosis is accompanied by a transition from caspase-dependent to caspase-independent mechanisms. (*c*) One aspect of this transition appears to involve activation of a CAD-like nuclease, which is initially latent in S/M extracts but is fully active in E/X extracts. (*d*) Murine CAD can induce an apoptotic morphology in isolated nuclei. (*e*) In addition to CAD, apoptotic extracts contain a second activity that can also induce apoptotic chromatin condensation in added nuclei in the absence of DNA fragmentation. Each of these points is discussed in greater detail below.

At present, there is no accepted biochemical marker to rigorously distinguish between the condemned and committed stages of the latent phase. Here, we define latent phase cells as those that have received a proapoptotic stimulus but look morphologically normal. We then operationally define condemned cells as those that yield extracts that lack significant caspase activity and do not induce apoptosis in substrate nuclei. We operationally define committed stage cells as those that yield extracts that contain high levels of active caspases together with low levels of active CAD and that strongly induce apoptosis in substrate nuclei. As expected, these cells contain only low levels of fragmented DNA themselves. Both of these latent phase populations are readily distinguishable from overtly apoptotic cells, which have detached from the substratum and have sustained internucleosomal DNA degradation in response to a proapoptotic stimulus. The various extracts prepared from these three operationally defined cell populations turned out to have remarkably distinct biochemical and functional characteristics.

The most significant difference was the finding that induction of apoptotic events by committed stage extracts is dependent on ongoing caspase activity, whereas induction of apoptotic events by execution phase extracts is independent of ongoing caspase activity. This observation is best explained by a model in which caspases activate downstream factors that are responsible for condensation of the chromatin during apoptosis. Such a model predicts that if we were able to purify the active caspases from apoptotic cells away from the downstream factors, then the caspases on their own should be insufficient to induce apoptotic events in substrate nuclei. To test this hypothesis, so-called roller S/M extracts (large scale extracts functionally intermediate between S/M and E/X extracts) were fractionated on heparin–agarose. The fraction eluting with 0.2 M KCl (Fr-2) appeared to not only encompass the entire range of endogenous caspases activated during apoptosis in these cells but was also highly active in the cleavage of caspase target proteins. Nonetheless, this fraction was completely unable to induce either DNA fragmentation or apoptotic morphology in substrate nuclei. We have independently shown that mixtures of purified caspases-3 and -6 are also unable to induce apoptotic morphology in purified nuclei (unpublished results). Thus, although recent experiments indicate that caspase-3 is essential for nuclear apoptosis (Jänicke et al., 1998; Woo et al., 1998), our experiments indicate that this enzyme is likely to function by activating downstream factors rather than directly disassembling the nucleus itself.

A subsequent 0.6 M KCl wash of the same heparin–agarose column yielded a fraction (Fr-3) that is rich in downstream apoptosis-promoting activities. Fr-3 strongly induces DNA fragmentation and apoptotic morphology despite the fact that it contains only very low levels of caspases, similar to those seen in C/D extracts (which do not induce apoptotic events in substrate nuclei). Furthermore, treatment of Fr-3 with caspase inhibitors (as well as other protease inhibitors; see Materials and Methods) had no effect on its apoptosis-promoting activity. Thus, this fraction is a potential source of downstream factors activated during the apoptotic pathway.

One such downstream factor has recently been identified in murine cell extracts. CAD, the caspase-activated DNase (Enari et al., 1998), interacts with an inhibitory subunit termed ICAD/DFF45 (Sakahira et al., 1998; Liu et al., 1997) to form an inactive complex that is thought to be sequestered in the cytoplasm. Caspase cleavage of ICAD is proposed to cause the release and subsequent nuclear translocation of CAD, leading to digestion of the chromatin (Sakahira et al., 1998). Here, we have shown that both S/M and E/X extracts from chicken DU249 cells contain a nuclease similar or identical to CAD, as defined by its ability to be quantitatively inhibited by exogenous purified mouse ICAD. The fact that ICAD of mouse origin inhibits the apoptotic nuclease in avian (chicken) cell extracts suggests that the CAD nuclease and its interactions with ICAD are widely conserved in phylogeny.

Because the same cohort of caspases is present and active in the S/M and E/X extracts, the transition from the latent to the execution phase of apoptosis may not hinge upon caspase action alone. Instead, the transition might involve activation of downstream factors. The CAD-like nuclease appears to be largely inactive in freshly prepared S/M extracts, becoming active only as the extracts are incubated at 30 or 37°C. This activation presumably reflects the cleavage of ICAD/DFF45 by caspases since CAD activation is blocked by caspase inhibitors. In contrast, the CAD-like nuclease activity appears to be fully active in freshly prepared E/X extracts. Collectively, these observations suggest that caspase activation occurs during the latent phase of apoptosis, whereas CAD activation accompanies the transition from the latent to execution phase of

apoptosis. One implication of this conclusion is that cells might simultaneously contain active caspases and inactive complexes of ICAD/DFF bound to CAD and possibly other downstream factors. This would be possible if caspases were segregated from their downstream targets such as ICAD/DFF, possibly by being sequestered in a different cellular compartment. The onset of apoptotic execution might then be triggered not by activation of the caspases but by a change in the localization of either caspases or targets. An alternative explanation of our data, that caspases are inactive in the cells from which S/M extracts are made and become activated during preparation of the extract (Zapata et al., 1998), is unlikely for two reasons. First, we previously demonstrated that caspase activity in similar extracts prepared from latent phase HL-60 cells was paralleled by cleavage of PARP and procaspase-3 in vivo (Martins et al., 1997*a*). Second, the caspase-3 activation observed during extract preparation in the previous study was explained by the detergent-induced release of granzyme B from cytoplasmic vesicles (Zapata et al., 1998). In our study, detergents were avoided during extract preparation, and cells lacking granzyme B were used.

In support of the notion that caspases and their targets might be segregated during the latent phase, we note that procaspases have largely been observed in the cytoplasm (Duan et al., 1996*a*; Krajewska et al., 1997; Mancini et al., 1998) (Mesner, P.W., and S.H. Kaufmann, unpublished observations) or mitochondria (Mancini et al., 1998), whereas our subcellular fractionation studies have revealed significant levels of active caspases within the nucleus (Martins et al., 1997*a*,*b*). An additional study has indicated that interference with nuclear transport renders cells resistant to Fas-mediated apoptosis (Yasuhara et al., 1997).

We have developed a novel vector to coordinately express CAD and ICAD in *E. coli* and have used this partially purified CAD to demonstrate that CAD can induce an apoptotic morphology in isolated nuclei, as confirmed by both light and electron microscopy. This reaction does not require ongoing caspase activity. This result is consistent with earlier observations, indicating that addition of micrococcal nuclease to isolated nuclei can cause clumping of chromatin (Arends et al., 1990), although the pattern of condensation seen with CAD more closely resembles that seen in apoptotic cells. However, CAD does not appear to be the only factor downstream of caspases that is capable of inducing apoptotic nuclear changes. Addition of purified ICAD to either S/M or E/X extracts abolished all detectable DNase activity against both chromosomal and plasmid DNA substrates but did not abolish the ability of those extracts to induce an apoptotic morphology in substrate nuclei. This observation is consistent with previous reports that morphologically normal apoptosis can occur in the absence of internucleosomal DNA fragmentation in vivo (Ucker et al., 1992*b*; Oberhammer et al., 1993; Sakahira et al., 1998). At present, the nature of the second downstream factor(s) that promotes apoptotic chromatin condensation is unknown. Although two recent studies suggest that serine (Shimizu and Pommier, 1997) or cysteine proteases (Vaux et al., 1997) may be involved, the fact that we can detect apoptotic morphological changes in the presence of DEVD-fmk as well as a battery of serine, cysteine, and acid protease inhibitors (see Materials and Methods) suggest that the chromatin-condensing activity might not be a protease. On the other hand, simultaneous addition of both DEVD-fmk and ICAD to E/X extracts abolished the induction of apoptotic morphology in substrate nuclei. This result suggests that the morphogenic factor either binds to ICAD or is regulated by other molecules that interact with ICAD.

In summary, the experiments reported here demonstrate that it is possible to use cell-free extracts for a biochemical and functional dissection of the sequential phases of the apoptotic pathway. Our studies reveal that the transition from the latent to the execution phase of apoptosis appears to be accompanied by a change from caspase-dependent to caspase-independent mechanisms. The discovery that caspases are capable of cleaving abundant nuclear proteins like PARP (Lazebnik et al., 1994) and the lamins (Lazebnik et al., 1995; Takahashi et al., 1996; Orth et al., 1996; Rao et al., 1996), along with the observation that apoptotic nuclear fragmentation is absent in caspase-3–null cells (Woo et al., 1998; Janicke et al., 1998), led us and others to previously assume that caspases are directly responsible for nuclear disassembly. However, the inability of purified caspases to produce apoptotic morphological changes in isolated nuclei, coupled with the inability of caspase inhibitors to abolish the induction of these morphological changes by E/X extracts, argues that caspases are unlikely to be workhorses that are solely responsible for nuclear disassembly. Instead, the present results provide support for a view in which caspases play an executive role in nuclear disassembly by activating factors that in turn disassemble the nucleus. At least one of the downstream activities is a CAD-like nuclease; but another downstream activity capable of inducing nuclear morphological changes appears to be distinct from CAD.

We would like to thank David Dryden and Peter Warburton for advice on using heparin agarose; Dr. Richard Hayward for advice on the design of the bicistronic vector; our colleagues Drs. David Boyle, Joe Lewis, David Leach, Chris French, and Brian Kilby for helpful discussions; Larry Gerace (The Scripps Research Institute, La Jolla, CA) for anti–lamin A antibody; and Drs. A. Ainsztein, J. Craig, and S. Wheatley for their comments on the manuscript.

This work was supported by grants from the Wellcome Trust (W.C. Earnshaw) and The National Institutes of Health (S.H. Kaufmann and W.C. Earnshaw). S.H. Kaufmann was a Scholar of the Leukemia Society of America. W.C. Earnshaw is a Principal Research Fellow of the Wellcome Trust.

Received for publication 20 July 1998.

References

Arends, M.J., R.G. Morris, and A.H. Wyllie. 1990. Apoptosis: the role of the endonuclease. *Am. J. Pathol.* 136:593–608.

Boise, L.H., and C.B. Thompson. 1997. Bcl-x(L) can inhibit apoptosis in cells that have undergone Fas-induced protease activation. *Proc. Natl. Acad. Sci. USA*. 94:3759–3764.

Boldin, M.P., T.M. Goncharov, Y.V. Goltsev, and D. Wallach. 1996. Involvement of MACH, a novel MORT1/FADD-interacting protease in Fas/APO-1- and TNF receptor-induced cell death. *Cell*. 85:803–815.

Bradford, M.M. 1976. A rapid and sensitive method for the quantitation of microgram quantities of protein utilizing the principle of protein-dye binding. *Anal. Biochem.* 72:248–254.

Brancolini, C., M. Benedetti, and C. Schneider. 1995. Microfilament reorganization during apoptosis: the role of Gas2, a possible substrate for ICE-like proteases. *EMBO (Eur. Mol. Biol. Organ.) J.* 14:5179–5190.

Church, G.M., and W. Gilbert. 1984. Genomic sequencing. *Proc. Natl. Acad. Sci. USA.* 81:1991–1995.

Cohen, G.M. 1997. Caspases: the executioners of apoptosis. *Biochem. J.* 326:1–16.

Cryns, V., and J. Yuan. 1998. Proteases to die for. *Genes Dev.* 12:1551–1570.

Duan, H., A.M. Chinnaiyan, P.L. Hudson, J.P. Wing, W.-W. He, and V.M. Dixit. 1996*a*. ICE-LAP3, a novel mammalian homologue of the *Caenorhabditis elegans* cell death protein Ced-3 is activated during Fas- and tumor necrosis factor-induced apoptosis. *J. Biol. Chem.* 271:1621–1625.

Duan, H., K. Orth, A.M. Chinnaiyan, G.G. Poirier, C.J. Froelich, W.-W. He, and V.M. Dixit. 1996*b*. ICE-LAP6, a novel member of the ICE/Ced-3 gene family, is activated by the cytotoxic T cell protease granzyme B. *J. Biol. Chem.* 271:16720–16724.

Enari, M., A. Hase, and S. Nagata. 1995*a*. Apoptosis by a cytosolic extract from Fas-activated cells. *EMBO (Eur. Mol. Biol. Organ.) J.* 14:5201–5208.

Enari, M., H. Hug, and S. Nagata. 1995*b*. Involvement of an ICE-like protease in Fas-mediated apoptosis. *Nature.* 375:78–81.

Enari, M., H. Sakahira, H. Yokoyama, K. Okawa, A. Iwamatsu, and S. Nagata. 1998. A caspase-activated DNase that degrades DNA during apoptosis, and its inhibitor ICAD. *Nature.* 391:43–50.

Faleiro, L., R. Kobayashi, H. Fearnhead, and Y. Lazebnik. 1997. Multiple species of CPP32 and Mch2 are the major active caspases present in apoptotic cells. *EMBO (Eur. Mol. Biol. Organ.) J.* 16:2271–2281.

Fernandes-Alnemri, T., G. Litwack, and E. Alnemri. 1995*a*. Mch2, a new member of the apoptotic Ced-3/ICE cysteine protease gene family. *Cancer Res.* 55:2737–2742.

Fernandes-Alnemri, T., A. Takahashi, R. Armstrong, J. Krebs, L. Fritz, K. Tomaselli, L. Wang, Z. Yu, C.M. Croce, G. Salvesen, et al. 1995*b*. *Mch3*, a novel human apoptotic cysteine protease highly related to CPP32. *Cancer Res.* 55:6045–6052.

Fernandes-Alnemri, T., R.C. Armstrong, J. Krebs, S.M. Srinivasula, L. Wang, F. Bullrich, L.C. Fritz, J.A. Trapani, K.J. Tomaselli, G. Litwack, and E.S. Alnemri. 1996. In vitro activation of CPP32 and Mch3 by Mch4, a novel human apoptotic cysteine protease containing two FADD-like domains. *Proc. Natl. Acad. Sci. USA.* 93:14486–14491.

Halenbeck, R., H. MacDonald, A. Roulston, T.T. Chen, L. Conroy, and L.T. Williams. 1998. CPAN, a human nuclease regulated by the caspase-sensitive inhibitor DFF-45. *Curr. Biol.* 8:537–540.

Jacobson, M.D., J.F. Burne, and M.C. Raff. 1994. Programmed cell death and Bcl-2 protection in the absence of a nucleus. *EMBO (Eur. Mol. Biol. Organ.) J.* 13:1899–1910.

Jänicke, R.U., M.L. Sprengart, M.R. Wati, and A.G. Porter. 1998. Caspase-3 is required for DNA fragmentation and morphological changes associated with apoptosis. *J. Biol. Chem.* 273:9357–9360.

Kaufmann, S.H. 1989. Induction of endonucleolytic DNA cleavage in human acute myelogenous leukemia cells by etoposide, camptothecin, and other cytotoxic anticancer drugs: a cautionary note. *Cancer Res.* 49:5870–5878.

Krajewska, M., H.G. Wang, S. Krajewski, J.M. Zapata, A. Shabaik, R. Gascoyne, and J.C. Reed. 1997. Immunohistochemical analysis of in vivo patterns of expression of CPP32 (Caspase-3), a cell death protease. *Cancer Res.* 57:1605–1613.

Kroemer, G. 1997. The proto-oncogene Bcl-2 and its role in regulating apoptosis. *Nat. Med.* 3:614–620.

Kuida, K., T.S. Zheng, S. Na, C. Kuan, D. Yang, H. Karasuyama, P. Rakic, and R.A. Flavell. 1996. Decreased apoptosis in the brain and premature lethality in CPP32-deficient mice. *Nature.* 384:368–372.

Laemmli, U.K. 1970. Cleavage of structural proteins during the assembly of the head of the head of bacteriophage T4. *Nature.* 227:680–685.

Lamarre, D., B. Talbot, G. de Murcia, C. Laplante, Y. Leduc, A. Mazen, and G.G. Poirier. 1988. Structural and functional analysis of poly(ADP-ribose) polymerase: an immunological study. *Biochim. Biophys. Acta.* 950:147–160.

Lavoie, J.N., M. Nguyen, R.C. Marcellus, P.E. Branton, and G.C. Shore. 1998. E4orf4, a novel adenovirus death factor that induces p53-independent apoptosis by a pathway that is not inhibited by zVAD-fmk. *J. Cell Biol.* 140:637–645.

Lazebnik, Y.A., S. Cole, C.A. Cooke, W.G. Nelson, and W.C. Earnshaw. 1993. Nuclear events of apoptosis in vitro in cell-free mitotic extracts: a model system for analysis of the active phase of apoptosis. *J. Cell Biol.* 123:7–22.

Lazebnik, Y.A., S.H. Kaufmann, S. Desnoyers, G.G. Poirier, and W.C. Earnshaw. 1994. Cleavage of poly(ADP-ribose) polymerase by a protease with properties like ICE. *Nature.* 371:346–347.

Lazebnik, Y.A., A. Takahashi, R. Moir, R. Goldman, G.G. Poirier, S.H. Kaufmann, and W.C. Earnshaw. 1995. Studies of the lamin proteinase reveal multiple parallel biochemical pathways during apoptotic execution. *Proc. Nat. Acad. Sci. USA.* 92:9042–9046.

Liu, X., C.N. Kim, J. Yang, R. Jemmerson, and X. Wang. 1996. Induction of apoptotic program in cell-free extracts: requirement for dATP and cytochrome C. *Cell.* 86:147–157.

Liu, X., H. Zou, C. Slaughter, and X. Wang. 1997. DFF, a heterodimeric protein that functions downstream of caspase-3 to trigger DNA fragmentation during apoptosis. *Cell.* 89:175–184.

Mancini, M., D.W. Nicholson, S. Roy, N.A. Thornberry, E.P. Peterson, L.A. Casciola-Rosen, and A. Rosen. 1998. The caspase-3 precursor has a cytosolic and mitochondrial distribution: implications for apoptotic signaling. *J. Cell Biol.* 140:1485–1495.

Martin, S.J., and D.R. Green. 1995. Protease activation during apoptosis: death by a thousand cuts? *Cell.* 82:349–352.

Martin, S.J., D.D. Newmeyer, S. Mathias, D.M. Farschon, H.-G. Wang, J.C. Reed, R.N. Kolesnick, and D.R. Green. 1995. Cell-free reconstitution of Fas-, UV radiation-, and ceramide-induced apoptosis. *EMBO (Eur. Mol. Biol. Organ.) J.* 14:5191–5200.

Martin, S.J., D.M. Finucane, G.P. Amarante-Mendes, G.A. O'Brien, and D.R. Green. 1996. Phosphatidylserine externalization during CD95-induced apoptosis of cells and cytoplasts requires ICE/CED-3 protease activity. *J. Biol. Chem.* 271:28753–28756.

Martins, L.M., T. Kottke, P.W. Mesner, G.S. Basi, S. Sinha, N.J. Frigon, E. Tatar, J.S. Tung, K. Bryant, A. Takahashi, et al. 1997*a*. Activation of multiple Interleukin-1β converting enzyme homologues in cytosol and nuclei of HL-60 human leukemia cells during etoposide-induced apoptosis. *J. Biol. Chem.* 272:7421–7430.

Martins, L.M., P.W. Mesner, T.J. Kottke, G.S. Basi, S. Sinha, J.S. Tung, P.A. Svingen, B.J. Madden, A. Takahashi, D.J. McCormick, et al. 1997*b*. Comparison of caspase activation and subcellular localization in HL-60 and K562 cells undergoing etoposide-induced apoptosis. *Blood.* 90:4283–4296.

McCarthy, N.J., M.K. Whyte, C.S. Gilbert, and G.I. Evan. 1997. Inhibition of Ced-3/ICE-related proteases does not prevent cell death induced by oncogenes, DNA damage, or the Bcl-2 homologue Bak. *J. Cell Biol.* 136:215–227.

Muzio, M., A.M. Chinnaiyan, F.C. Kischkel, K. O'Rourke, A. Shevchenko, J. Ni, R. Gentz, M. Mann, P.H. Krammer, M.E. Peter, and V.M. Dixit. 1996. FLICE, a novel FADD-homologous ICE/CED-3-like protease, is recruited to the CD95 (Fas/APO-1) death-inducing signaling complex. *Cell.* 85:817–827.

Nakajima, H., P. Golstein, and P.A. Henkart. 1995. The target cell nucleus is not required for cell-mediated granzyme- or Fas-based cytotoxicity. *J. Exp. Med.* 181:1905–1909.

Newmeyer, D.D., D.M. Farschon, and J.C. Reed. 1994. Cell-free apoptosis in *Xenopus* egg extracts—inhibition by Bcl-2 and requirement for an organelle fraction enriched in mitochondria. *Cell.* 79:353–364.

Nicholson, D.W., and N.A. Thornberry. 1997. Caspases: killer proteases. *Trends Biochem. Sci.* 22:299–306.

Nicholson, D.W., A. Ali, N.A. Thornberry, J.P. Vaillancourt, C.K. Ding, M. Gallant, Y. Gareau, P.R. Griffin, M. Labelle, Y.A. Lazebnik, et al. 1995. Identification and inhibition of the ICE/CED-3 protease necessary for mammalian apoptosis. *Nature.* 376:37–43.

Oberhammer, F., J.W. Wilson, C. Dive, I.D. Morris, J.A. Hickman, A.E. Wakeling, P.R. Walker, and M. Sikorska. 1993. Apoptotic death in epithelial cells: cleavage of DNA to 300 and/or 50 kb fragments prior to or in the absence of internucleosomal fragmentation. *EMBO (Eur. Mol. Biol. Organ.) J.* 12: 3679–3684.

Orth, K., A.M. Chinnaiyan, M. Garg, C.J. Froelich, and V.M. Dixit. 1996. The CED-3/ICE-like protease Mch2 is activated during apoptosis and cleaves the death substrate lamin A. *J. Biol. Chem.* 271:16443–16446.

Porter, A.G., P. Ng, and R.U. Jänicke. 1997. Death substrates come alive. *Bioessays.* 19:501–507.

Rao, L., D. Perez, and E. White. 1996. Lamin proteolysis facilitates nuclear events during apoptosis. *J. Cell Biol.* 135:1441–1455.

Sakahira, H., M. Enari, and S. Nagata. 1998. Cleavage of CAD inhibitor in CAD activation and DNA degradation during apoptosis. *Nature.* 391:96–99.

Samejima, K., and W.C. Earnshaw. 1998. ICAD/DFF regulator of apoptotic nuclease is nuclear. *Exp. Cell Res.* 243:453–459.

Schlegel, J., I. Peters, and S. Orrenius. 1995. Isolation and partial characterization of a protease involved in Fas-induced apoptosis. *FEBS Lett.* 364:139–142.

Schulze-Osthoff, K., H. Walczak, W. Dröge, and P.H. Krammer. 1994. Cell nucleus and DNA fragmentation are not required for apoptosis. *J. Cell Biol.* 127:15–20.

Seraphin, B., and S. Kandels-Lewis. 1996. An efficient PCR mutagenesis strategy without gel purification step that is amenable to automation. *Nucleic Acids Res.* 24:3276–3277.

Shimizu, T., and Y. Pommier. 1997. Camptothecin-induced apoptosis in p53-null human leukemia HL60 cells and their isolated nuclei: effects of the protease inhibitors Z-VAD-fmk and dichloroisocoumarin suggest an involvement of both caspases and serine proteases. *Leukemia.* 11:1238–1244.

Solary, E., R. Bertrand, K.W. Kohn, and Y. Pommier. 1993. Differential induction of apoptosis in undifferentiated and differentiated HL-60 cells by DNA topoisomerase I and II inhibitors. *Blood.* 81:1359–1368.

Srinivasula, S.M., T. Fernandes-Alnemri, J. Zangrill, N. Robertson, R.C. Armstrong, L. Wang, J.A. Trapani, K. Tomaselli, G. Litwack, and E.S. Alnemri. 1996. The Ced3/interleukin 1β converting enzyme-like homolog Mch6 and the lamin-cleaving enzyme Mch2α are substrates for the apoptotic mediator CPP32. *J. Biol. Chem.* 271:27099–27106.

Takahashi, A., E. Alnemri, Y.A. Lazebnik, T. Fernandes-Alnemri, G. Litwack, R.D. Moir, R.D. Goldman, G.G. Poirier, S.H. Kaufmann, and W.C. Earnshaw. 1996. Cleavage of lamin A by Mch2a but not CPP32: multiple ICE-related proteases with distinct substrate recognition properties are active in apoptosis. *Proc. Natl. Acad. Sci. USA.* 93:8395–8400.

Talanian, R.V., C. Quinlan, S. Trautz, M.C. Hackett, J.A. Mankovich, D. Banach, T. Ghayur, K.D. Brady, and W.W. Wong. 1997. Substrate specificities of caspase family proteases. *J. Biol. Chem.* 272:9677–9682.

Tewari, M., L.T. Quan, K. O'Rourke, S. Desnoyers, Z. Zeng, D.R. Beidler,

G.G. Poirier, G.S. Salvesen, and V.M. Dixit. 1995. Yama/CPP32β, a mammalian homolog of CED-3, is a CrmA-inhibitable protease that cleaves the death substrate poly(ADP-ribose) polymerase. *Cell.* 81:801–809.

Ucker, D.S., J. Meyers, and P.S. Obermiller. 1992*a*. Activation driven T cell death. II. Quantitative differences alone distinguish stimuli triggering nontransformed T cell proliferation or death. *J. Immunol.* 149:1583–1592.

Ucker, D.S., P.S. Obermiller, W. Eckhart, J.R. Apgar, N.A. Berger, and J. Meyers. 1992*b*. Genome digestion is a dispensable consequence of physiological cell death mediated by cytotoxic T lymphocytes. *Mol. Cell. Biol.* 12:3060–3069.

Vaux, D.L., S. Wilhelm, and G. Hacker. 1997. Requirements for proteolysis during apoptosis. *Mol. Cell. Biol.* 17:6502–6507.

Villa, P., S.H. Kaufmann, and W.C. Earnshaw. 1997. Caspases and caspase inhibitors. *Trends Biochem. Sci.* 22:388–393.

Woo, M., R. Haken, M.S. Soengas, G.S. Duncan, A. Shahinian, D. Kägi, A. Hakem, M. McCurrach, W. Khoo, S.A. Kaufman, et al. 1998. Essential contribution of caspase 3/CPP32 to apoptosis and its associated nuclear changes. *Genes Dev.* 12:806–819.

Wood, E.R., and W.C. Earnshaw. 1990. Mitotic chromatin condensation in vitro using somatic cell extracts and nuclei with variable levels of endogenous topoisomerase II. *J. Cell Biol.* 111:2839–2850.

Wyllie, A.H., J.F.R. Kerr, and A.R. Currie. 1980. Cell death: the significance of apoptosis. *Int. Rev. Cytol.* 68:251–305.

Xiang, J., D.T. Chao, and S.J. Korsmeyer. 1996. BAX-induced cell death may not require interleukin 1 β-converting enzyme-like proteases. *Proc. Natl. Acad. Sci. USA.* 93:14559–14563.

Yasuhara, N., Y. Eguchi, T. Tachibana, N. Imamoto, Y. Yoneda, and Y. Tsujimoto. 1997. Essential role of active nuclear transport in apoptosis. *Genes Cells.* 2:55–64.

Yuan, J.Y., and H.R. Horvitz. 1990. The *Caenorhabditis elegans* genes ced-3 and ced-4 act cell autonomously to cause programmed cell death. *Dev. Biol.* 138:33–41.

Zapata, J.M., R. Takahashi, G.S. Salvesen, and J.C. Reed. 1998. Granzyme release and caspase activation in activated human T-lymphocytes. *J. Biol. Chem.* 273:6916–6920.

XPERIMENTAL CELL RESEARCH **243,** 453–459 (1998)
RTICLE NO. EX984212

RAPID COMMUNICATION

ICAD/DFF Regulator of Apoptotic Nuclease Is Nuclear

Kumiko Samejima and William C. Earnshaw[1]

Institute of Cell and Molecular Biology, University of Edinburgh, Michael Swann Building, King's Buildings, Mayfield Road, Edinburgh EH9 3JR Scotland, United Kingdom

In nonapoptotic cells, the caspase-activated DNase CAD/CPAN is associated with a regulatory subunit, CAD/DFF, that binds to it and blocks its enzymatic ctivity. It has been proposed that a major function of CAD is to restrain CAD in the cytoplasm in healthy ells. The experiments presented here demonstrate hat rather than being cytoplasmic, a GFP–ICAD fu- ion protein is nuclear in healthy human, pig, and hicken cells. Furthermore, immunoblots using anti- odies to murine ICAD confirm the presence of endo- enous ICAD and the marker protein DNA topoisomer- se I in human nuclei, while tubulin was found solely n the cytosolic fraction. Since ICAD is located in cell uclei, it is unlikely that the protein functions primar- ly in the cytoplasm either as an anchor for CAD/CPAN r as a factor that enters the nucleus following caspase leavage in order to activate resident endonucleases.

INTRODUCTION

Apoptotic execution is a cellular disassembly path- vay in which nuclear and cytoplasmic structures are reatly altered, both to terminate the life of the cell and o favor its engulfment by other healthy cells. The iochemical mechanisms of apoptotic execution are till under intensive study, with particular attention ocusing on the role of proteases and nucleases. A great eal is now known about the identity and targets of the aspase proteases that appear to be the driving force ehind the apoptotic pathway [1–3]. Paradoxically, de- pite the fact that DNases were the first biochemical ctivities to be identified in apoptotic cells [4], until ery recently much less has been known about the dentities of the DNases involved in processing of the enome during apoptotic execution.

In recent years it has been suggested that apoptotic cells harness one or more of the well-known digestive enzymes, such as DNase I or DNase II, for use in apoptosis [5, 6]. These conclusions have been based upon a variety of analyses ranging from examination of the DNA ends produced during apoptosis [7–9] to inhibitor, antibody, and PCR studies looking at the expression and cellular distribution of these enzymes [5, 6]. Other studies have suggested that the apoptotic nuclease might be a novel enzyme, DNase γ [8], or a well-known protein, cyclophilin, which was not previously suspected to have nuclease activity [10]. Given the existence of these conflicting studies proposing that each of these different enzymes is *the* apoptotic nuclease, it must be considered that in fact there is no single enzyme that fulfills this role in all cell types. Furthermore, it is important to bear in mind that DNA fragmentation does not appear to be a universal requirement in apoptosis [11–14].

The study of DNA metabolism during apoptosis has recently been greatly stimulated by the discovery, purification, and cloning of a *c*aspase-*a*ctivated *D*Nase, CAD, in murine cells [15]. A human homologue of this enzyme, termed caspase-activated nuclease (CPAN), has also been identified [16]. These enzymes have attracted considerable interest, largely because of the demonstration that their activity is regulated in an apoptosis-specific manner. CAD/CPAN is expressed in healthy cells, where it is held in an inactive state, apparently through association with a regulatory subunit, which the discoverers of CAD termed ICAD [14, 15]. ICAD had previously been identified as a cytoplasmic factor, DFF (*D*NA *f*ragmentation *f*actor), whose cleavage by caspase-3 was proposed to be responsible for activation of the apoptotic nuclease [17].

Published studies have suggested three possible mechanisms of ICAD/DFF function. First, it was proposed that upon cleavage by caspases, DFF enters the cell nucleus and activates a resident nuclease [17]. This model is now considered somewhat less likely, given the observation that DFF is normally complexed with the nuclease CPAN. CPAN apparently corre-

[1] To whom correspondence and reprint requests should be addressed. Fax: 0131-650-7100. E-mail: bill.earnshaw@ed.ac.uk.

0014-4827/98 $25.00

ponds to the 40-kDa subunit originally identified as a omponent of the DFF protein [17]. It has now been hown that ICAD/DFF can act as a direct inhibitor of ne apoptotic nuclease. Binding of ICAD/DFF to CAD/ PAN inactivates its enzymatic function [15]. Impor- antly, this inactivation is specific for CAD/CPAN. CAD does not inactivate either DNase I or DNase II *in itro* [15]. A second unexpected activity of ICAD/DFF is s a chaperone that promotes the stable folding of ctive CAD/CPAN. This was shown most clearly for *in itro* transcription/translation experiments in which ctive CAD was produced only in the presence of ICAD 15]. However, evidence consistent with this model was lso obtained in baculovirus expression studies, in vhich it was found that active CAD could be obtained nly when Sf9 cells were co-infected with viruses ex- ressing both CAD and ICAD [16]. Finally, analysis of he predicted polypeptide sequences of CAD and ICAD uggested a possible further role for ICAD. CAD, but ot ICAD, has a predicted nuclear localization signal 15]. It was therefore suggested that ICAD might com- lex with nascent CAD on the ribosome, first helping it o fold and then restraining it in the cytoplasm. This atter activity was proposed to function similarly to the etention of NFκB in the cytoplasm by IκB [15], and it vas proposed that cleavage of ICAD releases CAD, hereby enabling it to enter the nucleus and attack the ellular DNA [14].

In the present study, we have performed an initial est of this hypothesis for the role of ICAD in regula- ion of CAD. We have used two different approaches to ocalize ICAD in cultured cells. First, we have shown hat a GFP–ICAD fusion protein is nuclear in trans- ected human, pig, and chicken cells. Second, we have repared an antibody to murine ICAD and used this in mmunoblotting experiments to show that the endoge- ous protein is likewise concentrated in cell nuclei. These observations make it unlikely that ICAD fulfills ts major cellular functions in the cytoplasm.

MATERIALS AND METHODS

Materials. Reagents were obtained from the following suppliers: ntipain, chymostatin, pepstatin A, PMSF, isopropyl β-D-thiogalac- opyranoside (IPTG), etoposide, and 4,4-diamidino-2-phenylin- ole(DAPI) were from Sigma; staurosporine and leupeptin were from albiochem; Hybond-C membranes, horseradish peroxidase- onjugated anti-mouse, anti-human, and anti-rabbit antibodies, and nhanced chemiluminescence (ECL) reagents were from Amersham orp.; Super Signal Ultra chemiluminescence reagents were from ierce; Ni-NTA agarose was from Qiagen. Monoclonal antibody to FP was a gift of I. Davis (ICMB, Edinburgh). Monoclonal antibody o tubulin was a gift of L. Binder (Northwestern University, Chicago. L). Human autoantibody to DNA topoisomerase I has been de- cribed previously [18].

Expression and purification of His_6-ICAD. The ICAD cDNA in Bluescript (Stratagene) was digested with *Spe*I, blunt-ended with 4 DNA polymerase (NEB) plus 100 μM dNTPs, and digested with *Kpn*I (NEB). The resulting fragment was ligated into pRSET B (Invitrogen) that had been digested with *Hin*dIII, blunt-ended with T4 DNA polymerase, and digested with *Kpn*I. ICAD in pRSETB was transformed into *Escherichia coli* BL21(DE3)Lys S cells. Transformed cells were grown to OD_{600} = 0.5–0.7 and protein expression was induced with IPTG (1 mM) for 3–4 h. Cells were collected by centrifugation at 5000*g* for 10 min and frozen at −80°C. The cell pellet was thawed on ice for 15 min and resuspended in sonication buffer (50 mM NaH_2PO_4, pH 7.5; 300 mM NaCl; 10 mM imidazole). Lysozyme was added to 1 mg/ml and the suspension was incubated on ice for 30 min, sonicated on ice until 80% of the cells were disrupted, and then centrifuged at 4000*g* for 20 min at 4°C. The supernatant fraction was incubated on a rotating mixer for 1 h at 4°C with 0.5 ml of Ni-agarose that had been preequilibrated with sonication buffer and then loaded onto a polyprep chromatography column (Bio-Rad). The column was washed with 4 ml of wash buffer (50 mM NaH_2PO_4, pH 7.5; 300 mM NaCl; 20 mM imidazole) twice. Protein was eluted with 0.5 ml of elution buffer (50 mM NaH_2PO_4, pH 7.5; 300 mM NaCl; 250 mM imidazole) four times. All samples were subjected to SDS–PAGE and examined by Coomassie blue staining. For antigen preparation, purified ICAD was subjected to SDS–PAGE, and then the gel was washed in distilled water three times for 10 min each, stained with aqueous Coomassie blue (0.1%) for 1 h, and rinsed with water until the induced protein band became obvious. The band was excised, frozen at −80°C, and then ground to a fine powder under N_2 (l) with a mortar and pestle. This powder was resuspended in PBS buffer and used to immunize two rabbits at the Scottish Antibody Production Unit (Carluke, Lanarkshire).

Construction of GFP–ICAD. The ICAD cDNA in pBluescript (Stratagene) was digested with *Hin*dIII, blunt-ended with T4 DNA polymerase (New England Biolabs) plus 100 μM dNTPs, and digested with *Xba*I (New England Biolabs). The resulting fragment was ligated into a vector containing enhanced GFP with a flexible linker (gift of Larry M. Karnitz, Mayo Research Foundation, Rochester, MN) in pCDNA3 (Invitrogen) that had been digested with *Not*I (New England Biolabs), blunt-ended with T4 DNA polymerase, and digested with *Xba*I.

Subcellular fractionation. HeLa cells were maintained in RPMI 1640 medium containing 5% (v/v) calf serum. Cells were collected by trypsinization and centrifuged at 1400*g* for 5 min at room temperature. Cell pellets washed once in PBS and once in nuclei solution (10 mM Pipes, pH 7.0, 10 mM KCl, 1.5 mM $MgCl_2$, 1 mM DTT, 100 μM PMSF, 10 μM cytochalasin B, plus 1 μM each of antipain, chymostatin, pepstatin A, and leupeptin) and resuspended into 200 μl of nuclei solution. This suspension was incubated on ice with occasional agitation and then lysed by passage through a 21-gauge needle. The lysate was fractionated into crude nuclei and cytosol by centrifugation at 2400*g* for 10 min at 4°C. The supernatant and pellet were immediately resuspended into SDS sample buffer, boiled for 5 min, and subjected to SDS–PAGE [19].

Induction of apoptosis. Apoptosis was induced in cells 20–24 h after they were electroporated either with a construct expressing GFP–ICAD or in the absence of added DNA (mock transfection). Cells were either treated with 68 μM etoposide for 1 h and kept in drug-free medium for a subsequent 6–7 h or treated with 1 μM staurosporine for 16–24 h. To examine GFP–ICAD cleavage, both floating cells and attached cells were collected, resuspended into sample buffer and subjected to SDS–PAGE.

Microscopy. Chicken DU249 cells and LLCPK cells were cultured in RPMI 1640 medium containing 10% (v/v) fetal bovine serum. After electroporation with a construct expressing GFP–ICAD, cells were grown on coverslips. These coverslips were rinsed with PBS/EDTA, fixed in a 4 % formaldehyde solution for 5 min, rinsed with PBS/EDTA, and mounted with Vectashield (Vector) containing DAPI (2 μg/ml). Images were acquired on a Zeiss Axioplan II epifluorescence

icroscope equipped with a Princeton Instruments Micromax cooled CD camera, driven by IP Lab Spectrum software.

RESULTS AND DISCUSSION

ICAD/DFF is nuclear in growing cells: The initial vidence that ICAD/DFF is a nuclear protein in a va- iety of cell types was obtained when we constructed a usion protein between murine ICAD and the *Aequoria ictoria* green fluorescent protein (GFP). Although GF- -ICAD expressed in *E. coli* was relatively insoluble, his protein was able to inhibit the CAD-mediated leavage of plasmid DNA, indicating that this molecule emains competent to interact with CAD (data not hown). Following transient transfection, this GFP– CAD fusion protein was detected solely in the nucleus f healthy human, pig, and chicken cells (Fig. 1). The GFP–ICAD fusion protein was excluded from nucleoli. Otherwise this protein showed a relatively homoge- eous distribution throughout the nuclei. GFP on its wn does not target to the nucleus ([20] and data not hown).

Although the nuclear localization of GFP–ICAD usion protein was extremely reproducible, being de- ected in all transfected cells, it was nevertheless mportant to demonstrate that these results reflect he distribution of the endogenous ICAD/DFF, par- icularly since both ICAD and DFF were originally solated from cytoplasmic lysates [15, 17]. We there- ore subcloned murine ICAD into a vector that ex- ressed the protein in *E. coli* as a fusion with a exa-histidine tag. This protein was expressed in *E. oli,* purified to homogeneity by nickel chelate chro- natography, and used to immunize two rabbits. The esultant sera recognize both murine and human CAD in immunoblots (Fig. 2).

The specificity of one of these ICAD antisera is dem- nstrated in Fig. 2A. The serum recognized a single olypeptide of ca. 45 kDa in nuclei isolated from HeLa ells (lane n). As expected [14], this endogenous olypeptide was cleaved when untransfected cells were nduced to undergo apoptosis in the presence of 1 μM taurosporine (data not shown). When nuclei were iso- ated from HeLa cells transfected with GFP–ICAD, the ntibody recognized both the endogenous human CAD/DFF and the 75-kDa GFP–ICAD fusion protein lane n′). The antiserum did not recognize any polypep- ides in a clarified cytosolic fraction prepared by sedi- nenting a postnuclear supernatant at 85,000*g* for 1 h lane c). This antiserum did not give a reproducible ignal above background in indirect immunofluores- ence.

The localization of endogenous ICAD in nuclei was onfirmed in subsequent experiments in which HeLa ells were lysed and subjected to a single centrifuga- tion at 2400*g* for 10 min (Fig. 2B). This fractionates cells into a crude nuclear pellet and total cytosol. The efficacy of this fractionation was confirmed by immunoblotting with antibodies to DNA topoisomerase I, a nuclear protein, and β-tubulin, a cytoplasmic protein. As expected, topoisomerase I was found predominantly in nuclei (lane n), with a small proportion of the protein being found in the crude cytosol (lane c). This cytosolic material may arise from low levels of nuclear breakage during cell lysis. When cells were fractionated by this method, β-tubulin was found solely in the cytosol.

The distribution of ICAD in two independent fractionation experiments is also shown in Fig. 2B. In both experiments, the endogenous ICAD was found to be predominantly nuclear, with a trace amount of the antigen being detected in crude cytosol. Given the presence of low levels of topoisomerase I in the cytoplasm in these experiments, we feel it likely that some or all of the cytoplasmic ICAD is likely to derive from nuclear breakage. This would be consistent with the absence of detectable ICAD in clarified cytosol (Fig. 2A). However, the presence of a small pool of cytoplasmic ICAD cannot be excluded by these experiments. Presumably ICAD/DFF was isolated from cytosol in previous experiments because the protein leaked from nuclei during extract preparation [14, 17].

GFP–ICAD Can Remain Associated with DNA in Apoptotic Cells

Current models of ICAD/DFF function assume that the protein is cytoplasmic, and experiments reveal that the protein is destroyed at the onset of apoptotic execution [14, 17]. Given our observation that ICAD/DFF is predominantly nuclear, we wished to confirm that the protein is in fact processed normally during apoptosis. In addition we wished to follow the fate of the GFP moiety during apoptosis. If GFP remains intact during apoptosis, then the GFP derived from GFP–ICAD might serve as a marker of nuclear integrity during apoptotic execution.

In order to follow the fate of GFP–ICAD during apoptosis, HeLa cultures transfected with constructs expressing the chimeric protein were induced to enter apoptosis by exposure to either etoposide or staurosporine. Six hours after a 1-h exposure to etoposide $\approx$10% of transfected HeLa cells had an apoptotic morphology. Following exposure to staurosporine for 24 h all cells had an abnormal morphology, with the great majority of these cells looking frankly apoptotic. Following induction of apoptosis, cells were harvested and lysed by passage through a needle, and a crude nuclear fraction was prepared by centrifugation at 2400*g* for 10 min. The integrity of the GFP–ICAD in this fraction

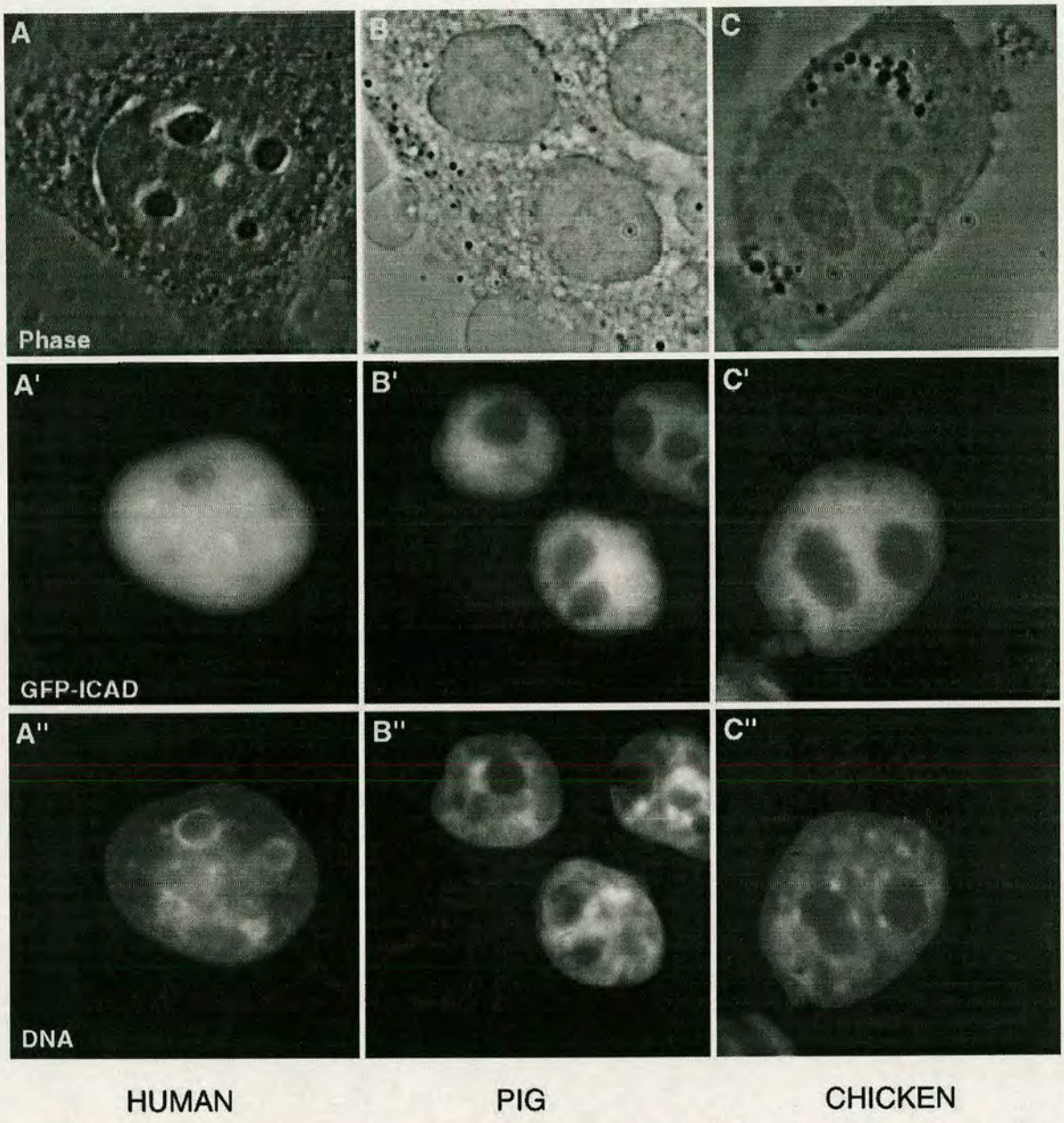

FIG. 1. GFP–ICAD is a nuclear protein. *Aequoria victoria* green fluorescent protein (GFP) was fused in-frame to murine ICAD and expressed by transient transfection in (A) human (HeLa), (B) pig (LLCPK), and (C) chicken (DU249) cells. The expressed protein was observed solely in cell nuclei. (A–C) Phase contrast. (A′–C′) GFP fluorescence. (A″– C″) DNA stained with DAPI.

was then followed by immunoblotting with a monoclonal antibody to GFP (gift of Ilan Davis). These experiments revealed that GFP–ICAD is cleaved as expected in apoptotic HeLa cells (Fig. 2C). GFP is not degraded, at least during the early stages of apoptotic execution. This experiment shows that although the chimeric protein is predominantly located in the cell nucleus, it remains accessible to the caspases that target ICAD during apoptosis.

We have used fluorescence microscopy to follow the fate of the GFP moiety derived from GFP–ICAD following induction of apoptosis in HeLa cells. In many apoptotic cells, GFP remained in close association with the chromatin, in both condensed and noncondensed regions (Fig. 3A). In other apoptotic cells, much of the GFP signal appeared to be no longer associated with the DNA (Fig. 3C). Both classes of cells could be seen to have at least two classes of cytoplasmic blebs, some of which contained both DNA and GFP, and others that were negative for both.

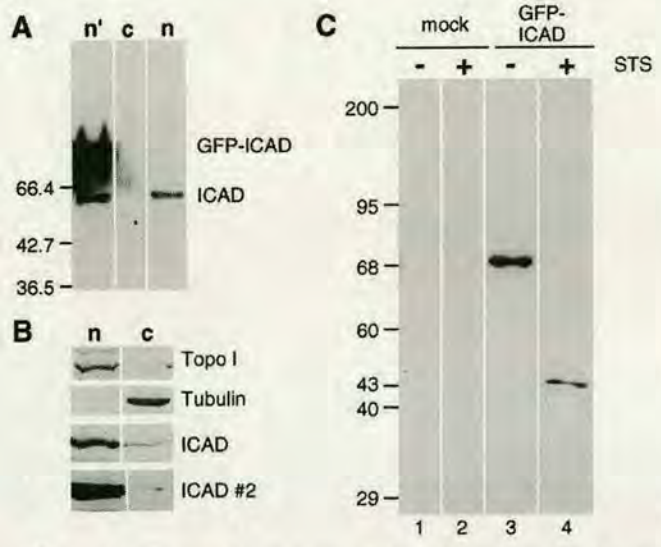

FIG. 2. Subcellular fractionation confirms that ICAD is a nuclear protein. (A) Confirmation of the specificity of the ICAD antibody. Anti-ICAD recognizes endogenous human ICAD in a crude nuclear fraction prepared by centrifugation of HeLa whole-cell extract at 2400*g* for 10 min (lane n). ICAD is not detected in clarified cytosol (85,000*g* for 1 h, lane c). Anti-ICAD recognizes GFP–ICAD in a similar fractionation of transfected cells (lane n'). (B) Confirmation that ICAD is highly enriched in nuclei and detected at only trace amounts in crude cytosol (lysates were centrifuged at 2400*g* for 10 min yielding nuclei, lane n, and cytosol, lane c). (B and C) Immunoblots of fractionated HeLa cells. (C) GFP–ICAD is cleaved in transfected cells following induction of apoptosis by exposure of cells to staurosporine. Mock-transfected cells (lanes 1 and 2) or cells transfected with a construct expressing GFP–ICAD (lanes 3 and 4) were cultured as normal (lanes 1 and 3) or exposed to 1 μM staurosporine for 24 h (lanes 2 and 4), lysed, and subjected to SDS–PAGE and immunoblotting. Detection was with a monoclonal antibody to GFP (gift of Ilan Davis).

Because GFP expressed on its own is distributed evenly throughout the cytoplasm of transfected cells [20], the fluorescence signal would be expected to diffuse relatively freely following caspase cleavage of the ICAD. Therefore, since GFP–ICAD is completely cleaved in these apoptotic cells (Fig. 2), we suggest that the nuclear envelope is likely to remain intact in those cells where the GFP stayed in close association with the condensed chromatin. This is consistent with the observation of apparently intact nuclear envelopes in apoptotic cells examined by electron microscopy [21]. Cells with a more widespread distribution of GFP are likely to represent those in which apoptotic execution was accompanied by a loss of nuclear envelope integrity. Blebs in these cells that lack detectable GFP (arrows, Fig. 3C) may have formed and been sealed off prior to the loss of nuclear envelope integrity. In other studies, we have directly observed lysis of the nuclear envelope in time-lapse movies of late-stage apoptotic HeLa cells expressing a GFP–lamin A chimera (L. M. Martins, K. Samejima, and W. C. Earnshaw, unpublished results).

Conclusions

It has previously been proposed that ICAD/DFF is a cytoplasmic factor that is cleaved upon caspase activation and then either enters the nucleus to activate nucleases [17] or releases an inactive cytoplasmic nuclease which subsequently enters the nucleus and degrades the cellular DNA [15]. The studies described above are inconsistent with both such models, since they have shown that ICAD/DFF is primarily located in the nuclei of growing and apoptotic HeLa cells. Thus, it is unlikely that the protein functions primarily in the cytoplasm, either as an anchor [15] or as a latent "trigger" waiting to enter the nucleus at the onset of apoptotic execution [17]. Instead, our data suggest that ICAD/DFF most likely functions in the nucleus.

How does ICAD gain access to the nucleus? Many studies have shown that GFP does not possess an intrinsic nuclear localization sequence (NLS), and inspection of the ICAD sequence led Enari *et al.* to conclude that ICAD also is unlikely to possess an autonomous NLS [15]. This suggests that the nuclear ICAD may be transported into the nucleus in a complex with another factor that does possess a functional NLS. This second factor could be CAD or it could be another as yet unidentified factor that interacts with ICAD. Candidates for such factors include the proapoptotic molecules CIDE A and B [22]. It is important to recognize that the cellular location of CAD remains to be determined. If CAD and ICAD are of relatively similar abundance, then our results would suggest that CAD must be nuclear, since the great majority of ICAD is nuclear. However, if CAD is considerably less abundant than ICAD, it is possible that CAD is indeed sequestered in the cytoplasm of nonapoptotic cells, where it could be complexed with the trace levels of ICAD that we did observe in crude cytosolic fractions. In the absence of antibody to CAD, these questions of abundance and localization are impossible to address at present. However, it is worth noting that the fractionation protocol used in the original identification of DFF yielded complexes in which DFF45/ICAD and DFF40/CPAN/CAD were present in roughly equimolar amounts [17].

Our results suggest that ICAD likely functions within the cell nucleus. ICAD could act as a direct inhibitor of a putative pool of nuclear CAD, or its function might be mediated by interactions with other proapoptotic factors. In either case, caspase inactivation of ICAD would occur within the nucleus following activation of one or more intranuclear

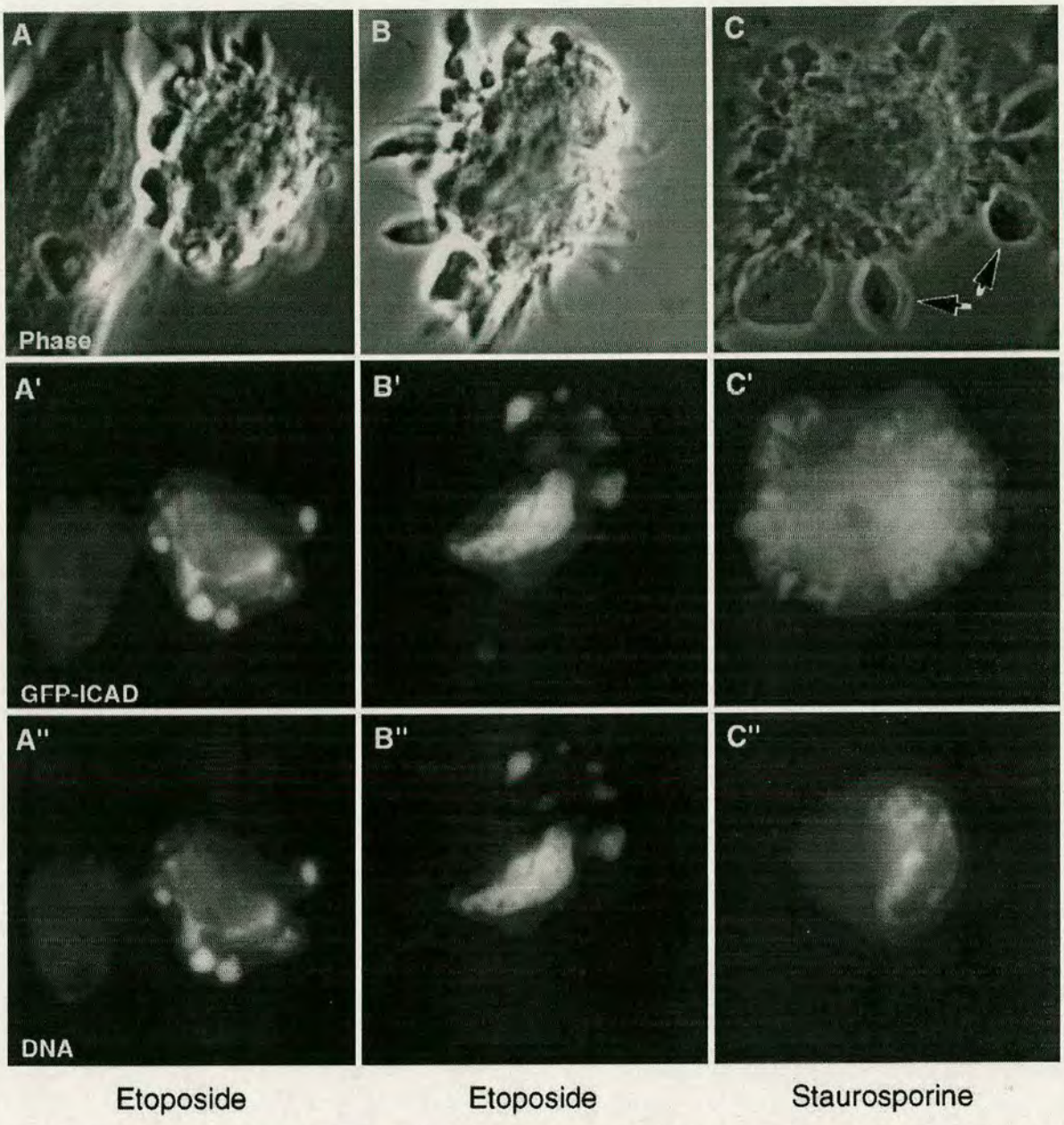

FIG. 3. Distribution of the GFP moiety of GFP–ICAD fusion protein in apoptotic HeLa cells. Cells transiently transfected with a construct expressing GFP–ICAD were exposed to (A, B) etoposide or (C) staurosporine to induce apoptosis. The expressed protein was observed in association with the DNA or in certain cases throughout the entire cytoplasm. In the case in which the GFP was cytoplasmic, not all prominent surface blebs were observed to contain the GFP fragment (arrows in C). (A–C) Phase contrast. (A′–C′) GFP fluorescence. (A″–C″) DNA stained with DAPI.

caspases and cleavage of ICAD. Consistent with this model, intranuclear forms of active caspases have been detected in both HL-60 and K562 cells undergoing drug-induced apoptosis [23, 24]. It is also possible that ICAD may function in a more general role than previously assumed, perhaps as a chaperone or storage factor for other proapoptotic activities. The further characterization of the factor or factors associated with nuclear ICAD is an important goal for future research.

We thank Masato Enari, Hideki Sakahira, and Shigekazu Nagata (Department of Genetics, Osaka University Medical School) for the gift of clones for murine CAD and ICAD, Ilan Davis (ICMB, Edinburgh) and Skip Binder (Chicago) for gifts of antibodies, and Drs. Françoise Durrieu, Pascal Villa, Jeff Craig, and Anca Petruti-Mot (all from the University of Edinburgh) for comments on the

anuscript. This work was supported by the Wellcome Trust. Kumiko Samejima was supported by NIH Grant CA69008 (to Scott H. Kaufmann and W. C. Earnshaw). W. C. Earnshaw is a Principal Research Fellow of the Wellcome Trust.

REFERENCES

1. Villa, P., Kaufmann, S. H., and Earnshaw, W. C. (1997). Caspases and caspase inhibitors. *Trends Biochem. Sci.* **22,** 388–393.
2. Cohen, G. M. (1997). Caspases: The executioners of apoptosis. *Biochem. J.* **326,** 1–16.
3. Thornberry, N. A., Rosen, A., and Nicholson, D. W. (1997). Control of apoptosis by proteases. *Adv. Pharmacol.* **41,** 155–177.
4. Wyllie, A. H. (1980). Glucocorticoid-induced thymocyte apoptosis is associated with endogenous endonuclease activation. *Nature* **284,** 555–556.
5. Peitsch, M. C., Polzar, B., Stephan, H., Crompton, T., R., M. H., Mannherz, H. G., and Tschopp, J. (1993). Characterization of the endogenous deoxyribonuclease involved in nuclear DNA degradation during apoptosis (programmed cell death). *EMBO J.* **12,** 371–377.
6. Barry, M. A., and Eastman, A. (1993). Identification of deoxyribonuclease II as an endonuclease involved in apoptosis. *Arch. Biochem. Biophys.* **300,** 440–450.
7. Alnemri, E. S., and Litwack, G. (1990). Activation of internucleosomal DNA cleavage in human CEM lymphocytes by glucocorticoid and novobiocin. Evidence for a non-$Ca^{2=}$ requiring mechanism(s). *J. Biol. Chem.* **265,** 17323–17333.
8. Shiokawa, D., Ohyama, H., Yamada, T., Takahashi, K., and Tanuma, S. (1994). Identification of an endonuclease responsible for apoptosis in rat thymocytes. *Eur. J. Biochem.* **226,** 23–30.
9. Didenko, V. V., and Hornsby, P. J. (1996). Presence of double-strand breaks with single-base 3′ overhangs in cells undergoing apoptosis but not necrosis. *J. Cell Biol.* **135,** 1369–1376.
10. Montague, J. W., Gaido, M. L., Frye, C., and Cidlowski, J. A. (1994). A calcium-dependent nuclease from apoptotic rat thymocytes is homologous with cyclophilin. *J. Biol. Chem.* **269,** 18877–18880.
11. Ucker, D. S., Obermiller, P. S., Eckhart, W., Apgar, J. R., Berger, N. A., and Meyers, J. (1992). Genome digestion is a dispensible consequence of physiological cell death mediated by cytotoxic T lymphocytes. *Mol. Cell. Biol.* **12,** 3060–3069.
12. Cohen, G. M., Sun, X.-M., Snowden, R. T., Dinsdale, D., and Skilleter, D. N. (1992). Key morphological features of apoptosis may occur in the absence of internucleosomal DNA fragmentation. *Biochem. J.* **286,** 331–334.
13. Oberhammer, F., Wilson, J. W., C., D., Morris, I. D., Hickman, J. A., Wakeling, A. E., Walker, P. R., and Sikorska, M. (1993). Apoptotic death in epithelial cells: Cleavage of DNA to 300 and/or 50 kb fragments prior to or in the absence of internucleosomal fragmentation. *EMBO J.* **12,** 3679–3684.
14. Sakahira, H., Enari, M., and Nagata, S. (1998). Cleavage of CAD inhibitor in CAD activation and DNA degradation during apoptosis. *Nature* **391,** 96–99.
15. Enari, M., Sakahira, H., Yokoyama, H., Okawa, K., Iwamatsu, A., and Nagata, S. (1998). A caspase-activated DNase that degrades DNA during apoptosis, and its inhibitor ICAD. *Nature* **391,** 43–50.
16. Halenbeck, R., MacDonald, H., Roulston, A., Chen, T. T., Conroy, L., and Williams, L. T. (1998). CPAN, a human nuclease regulated by the caspase-sensitive inhibitor DFF-45. *Curr. Biol.* **8,** 537–540.
17. Liu, X., Zou, H., Slaughter, C., and Wang, X. (1997). DFF, a heterodimeric protein that functions downstream of caspase-3 to trigger DNA fragmentation during apoptosis. *Cell* **89,** 175–184.
18. Shero, J. H., Bordwell, B., Rothfield, N. F., and Earnshaw, W. C. (1986). High titers of autoantibodies to topoisomerase I (Scl-70) in sera from scleroderma patients. *Science* **231,** 737–740.
19. Laemmli, U. K. (1970). Cleavage of structural proteins during the assembly of the head of the head of bacteriophage T4. *Nature* **227,** 680–685.
20. Rizzuto, R., Brini, M., Pizzo, P., Murgia, M., and Pozzan, T. (1995). Chimeric green fluorescent protein as a tool for visualizing subcellular organelles in living cells. *Curr. Biol.* **5,** 635–642.
21. Wyllie, A. H., Kerr, J. F. R., and Currie, A. R. (1980). Cell death: The significance of apoptosis. *Int. Rev. Cytol.* **68,** 251–305.
22. Inohara, N., Koseki, T., Chen, S., Wu, X., and Núnez, G. (1998). CIDE, a novel family of cell death activators with homology for the 45 kDa subunit of the DNA fragmentation factor. *EMBO J.* **17,** 2526–2533.
23. Martins, L. M., Kottke, T., Mesner, P. W., Basi, G. S., Sinha, S., Frigon, N. J., Tatar, E., Tung, J. S., Bryant, K., Takahashi, A., Svingen, P. A., Madden, B. J., McCormick, D. J., Earnshaw, W. C., and Kaufmann, S. H. (1997). Activation of multiple interleukin-1b converting enzyme homologues in cytosol and nuclei of HL-60 human leukemia cells during etoposide-induced apoptosis. *J. Biol. Chem.* **272,** 7421–7430.
24. Martins, L. M., Mesner, P. W., Kottke, T. J., Basi, G. S., Sinha, S., Tung, J. S., Svingen, P. A., Madden, B. J., Takahashi, A., McCormick, D. J., Earnshaw, W. C., and Kaufmann, S. H. (1997). Comparison of caspase activation and subcellular localization in HL-60 and K562 cells undergoing etoposide-induced apoptosis. *Blood* **90,** 4283–4296.

Received June 23, 1998
Revised version received July 9, 1998

Experimental Cell Research **255,** 314–320 (2000)
doi:10.1006/excr.2000.4801, available online at http://www.idealibrary.com on IDEAL®

RAPID COMMUNICATION

Differential Localization of ICAD-L and ICAD-S in Cells Due to Removal of a C-Terminal NLS from ICAD-L by Alternative Splicing

Kumiko Samejima and William C. Earnshaw[1]

Institute of Cell and Molecular Biology, University of Edinburgh, Edinburgh EH9 3JR, Scotland, United Kingdom

CAD/CPAN/DFF40 is an apoptotic nuclease that is associated with the regulatory subunit ICAD/DFF in healthy cells. ICAD has two forms, ICAD-L/DFF45 and ICAD-S/DFF35, which are transcribed from a single gene by alternative splicing. They differ at the C-terminus: 70 amino acids of ICAD-L are replaced by 4 different amino acids in ICAD-S. We previously showed that both transfected and endogenous ICAD-L are nuclear; however, the localization of ICAD and CAD remains controversial and an important issue to clarify. Here we present the evidence that ICAD-L is nuclear due to the presence of an autonomous nuclear localization signal located in the C-terminal 20 amino acids. This NLS is missing from ICAD-S, which is distributed throughout the cell. We also showed that a GFP:CAD fusion protein is located in the nucleus of transfected cells. © 2000 Academic Press

Key Words: **apoptosis; ICAD-L; ICAD-S; CAD.**

INTRODUCTION

One aspect of the regulation of apoptotic execution that has recently attracted considerable study is the movement of apoptotic factors from one intracellular compartment to another. The best studied example of this involves movement of factors, including cytochrome *c*, AIF, and caspases from the mitochondrial intermembrane space into the cytosol at the onset of apoptotic execution [1–3]. Less well understood is a requirement for nuclear transport of proteins, which is essential for the onset of apoptotic execution following the induction of apoptosis by Fas/CD95 [4]. The identity of the essential factors that must enter the nucleus is not known; however, the apoptotic nuclease CAD/CPAN/DFF40 [5–8] remains one attractive possibility, together with the recently discovered protein acinus [9].

In healthy cells, CAD/CPAN/DFF40 exists in a complex with its inhibitory chaperone ICAD-L/DFF-45. ICAD-L, after functioning as a folding chaperone for CAD during translation [5], then remains bound to the nuclease, keeping it in inactive form. The absolute requirement for ICAD-L as a folding chaperone is revealed by the phenotype of DFF-45 knockout mice, whose cells undergo apoptosis in the absence of detectible DNA cleavage despite the continued presence of CAD [10]. At the onset of apoptosis, caspases with specificities characteristic of caspases -3 and -7 cleave ICAD-L at two sites [11, 12]. This relieves the inhibition of CAD and initiates the fragmentation of the chromosomal DNA during apoptosis [12]. CAD activation is observed after diverse apoptotic stimuli in a variety of cultured cells [13], as well as in animals, in which CAD may play a role after traumatic brain injury [14].

The location of CAD/CPAN/DFF40 in cells remains controversial, with the original claims that the protein is located in the cytoplasm [5] being challenged by other results suggesting that expressed exogenous protein is in the nucleus [7, 15]. In general, studies that have examined the location of expressed ICAD-L/DFF45 in transfected cells have found the protein in the nucleus [7, 15], whereas subcellular fractionation studies have found the protein to be cytoplasmic to a greater or lesser extent [14, 16, 17]. Our own subcellular fractionation study using HeLa cells found the endogenous protein to be predominantly nuclear when steps were taken to minimize leakage from nuclei [15]. Apart from methodological differences, it is, of course, possible that the localization of these proteins could vary in differing cell types.

The localization of CAD/CPAN/DFF40 and ICAD/DFF45 in healthy cells is an important issue to clarify, as one possible mechanism for the inhibition of CAD by ICAD-L [5, 18, 19] has been suggested to involve ICAD-L binding to CAD and occluding the CAD nuclear localization signal (NLS). In the original descriptions of DFF45/ICAD-L, no obvious NLS was noted,

[1] To whom correspondence and reprint requests should be addressed. Fax: (0131) 650-7100. E-mail: bill.earnshaw@ed.ac.uk.

0014-4827/00 $35.00

and it was suggested that the protein (and therefore the complex of ICAD with CAD) was cytoplasmic [5, 11]. This model was questioned by our subsequent demonstration that both an exogenous GFP:ICAD-L fusion protein and an endogenous ICAD-L were nuclear in human (HeLa), pig (LLCPK), and chicken (DU249) cells [15].

The purpose of the present study was to determine the mechanism of ICAD-L entry into the nucleus and, in particular, whether ICAD-L enters the nucleus as a consequence of the function of an NLS that was not recognized in previous studies or whether the protein must enter the nucleus in a complex with another NLS-bearing protein or proteins. The data presented here clearly indicate that the C-terminus of ICAD-L functions as an autonomous NLS that is able to direct the entry of a GFP fusion protein into the nucleus.

MATERIALS AND METHODS

Materials. DAPI (4,4-diamidino-2-phenylindole) was obtained from Sigma. All restriction enzymes were obtained from New England Biolabs.

Construction of GFP:ICAD-L$^{1\text{-}311}$. The C-terminus of ICAD-L lacking 20 amino acids was obtained by PCR using primer (5′-CTGCTGTCAGAAGAGGACCTC-3′) and primer (5′-GCCCAAGCTTCTAGAATTCTTATGCTGATAG-3′) and then digested with *Hin*cII and *Hin*dIII. The resulting fragment was ligated into vector pRSET A (Invitrogen) containing full-length ICAD-L$^{1\text{-}331}$ which had been digested with *Hin*cII and *Hin*dIII. Next, pRSET A ICAD-L$^{1\text{-}311}$ was digested with *Xho*I and *Xba*I and the resulting fragment was ligated into vector pCDNA GFP:ICAD-L [15] which had been digested with *Xho*I and *Xba*I.

Construction of GFP:ICAD-S$^{1\text{-}265}$. The C-terminus of ICAD-S was obtained by PCR using primer (5′-CTGCTGTCAGAAGAGGACCTC-3′) and primer (5′-TAGGGCCCTTAGTTCTTGCCCACCTCCAAATCCTG-3′) and then digested with *Xcm*I and *Apa*I. The resulting fragment was ligated into vector pCDNA GFP:ICAD-L which had been digested with *Xcm*I and *Apa*I.

Construction of GFP:ICAD-S$^{1\text{-}261}$. The C-terminus of ICAD-S$^{1\text{-}261}$ lacking four amino acids was obtained by PCR using primer (5′-CTGCTGTCAGAAGAGGACCTC-3′) and primer (5′-GCCCAAGCTTCTAGAATTCTTACTCCAAATC-3′) and then digested with *Hin*cII and *Hin*dIII. The resulting fragment was ligated into vector pRSET A ICAD-L (Invitrogen) which had been digested with *Hin*cII and *Hin*dIII. Next, this pRSET A ICAD-S$^{1\text{-}261}$ was digested with *Xho*I and *Xba*I. The resulting fragment was ligated into vector pCDNA GFP:ICAD-L which had been digested with *Xho*I and *Xba*I.

Construction of Zeo GFP:ICAD-L, Zeo GFP:ICAD-L$^{1\text{-}311}$, Zeo GFP:ICAD-S, and Zeo GFP:ICAD-S$^{1\text{-}261}$. GFP:ICAD-L, GFP:ICAD-L$^{1\text{-}311}$, GFP:ICAD-S, and GFP:ICAD-S$^{1\text{-}261}$ in pCDNA3 (Invitrogen) were digested with *Hin*dIII and *Apa*I. The resulting fragments were ligated into vector pZeo SV2+ (Invitrogen) which had been digested with *Hin*dIII and *Apa*I.

Construction of Zeo GFP:CAD. First, CAD in pBluescript KS (Stratagene) was digested with *Not*I and *Xho*I. The resulting fragment was ligated into vector pCDNA3 GFP linearized by digestion of the multiple cloning site (MCS) with *Not*I and *Xho*I. This GFP:CAD was digested with *Hin*dIII and ligated into vector pZeo SV2+ which had been digested with *Hin*dIII.

Construction of pCDNA3 GFP with MCS. pBluescript KS was digested with *Not*I and *Apa*I. The resulting fragment, a part of the multiple cloning site, was ligated into pCDNA3 (Invitrogen) containing enhanced GFP with a flexible linker (gift of Larry M. Karnitz, Mayo Research Foundation, Rochester, MN) which had been digested with *Not*I and *Apa*I.

Construction of pCDNA3 GFP:ICAD-L$^{312\text{-}331}$ from ICAD-L. The C-terminal 20 amino acids of ICAD-L were obtained by PCR using primer (5′-CATAGCGGCCGCAGGAGGAGCCCAC-3′) and primer (5′-GCACCTTCCAGGGTCAAG-3′) and then digested with *Not*I and *Apa*I. The resulting fragment was ligated into pCDNA3 GFP linearized by digestion of the MCS with *Not*I and *Apa*I.

Microscopy. HeLa cells were cultured in RPMI 1640 medium containing 5% (v/v) calf serum. After electroporation with various constructs [20], cells were grown on coverslips overnight. These coverslips were rinsed with PBS, fixed in a 4% formaldehyde solution for 5 min, stained with DAPI (2 μg/ml) for 5 min, rinsed with PBS, and mounted with Vectashield (Vector). Images were acquired on a Zeiss Axioplan II epifluorescence microscope equipped with a Princeton Instruments Micromax cooled CCD camera, driven by IP Lab Spectrum software.

RESULTS AND DISCUSSION

The C-Terminus Determines the Nuclear Localization of ICAD-L/DFF45

In a previous publication [15], we showed that both endogenous and transfected ICAD-L/DFF45 are nuclear in growing cells. To investigate the mechanisms underlying the subcellular localization of ICAD-L and ICAD-S, we constructed a fusion protein between murine ICAD and the *Aequoria victoria* green fluorescent protein (GFP). Following transient transfection, this GFP:ICAD-L fusion protein was detected solely in the nucleus of healthy human epithelial and chicken hepatoma cells (Fig. 1, panels A). In contrast, a GFP:ICAD-S fusion protein was located diffusely throughout the cell (Fig. 1, panels B).

The transcripts encoding ICAD-L/DFF45 and ICAD-S/DFF35 arise by alternative splicing of a single precursor transcript. The two proteins are identical except for their C-terminal regions, in which the 70 C-terminal residues of ICAD-L are replaced by 4 different residues in ICAD-S. It therefore appeared likely that the different localization of ICAD-L and ICAD-S might be due to the differing C-termini of these proteins. We have considered two hypotheses explaining the differential localization of the two proteins. First, a nuclear localization signal might be present in the 70 residues of ICAD-L that are missing from ICAD-S. Second, the four different amino acids at the C-terminus of ICAD-S might function as part of a cytoplasmic retention or nuclear export signal.

To test the latter hypothesis, we constructed a GFP:ICAD-S fusion that lacks the four novel C-terminal amino acids (GFP:ICAD-S$^{1\text{-}261}$). When expressed by transient transfection, GFP:ICAD-S$^{1\text{-}261}$ was distributed diffusely throughout the cell, appearing indistinguishable from the GFP:ICAD-S protein (Fig. 1, Panels C). This indicated that the C-terminus of ICAD-S does

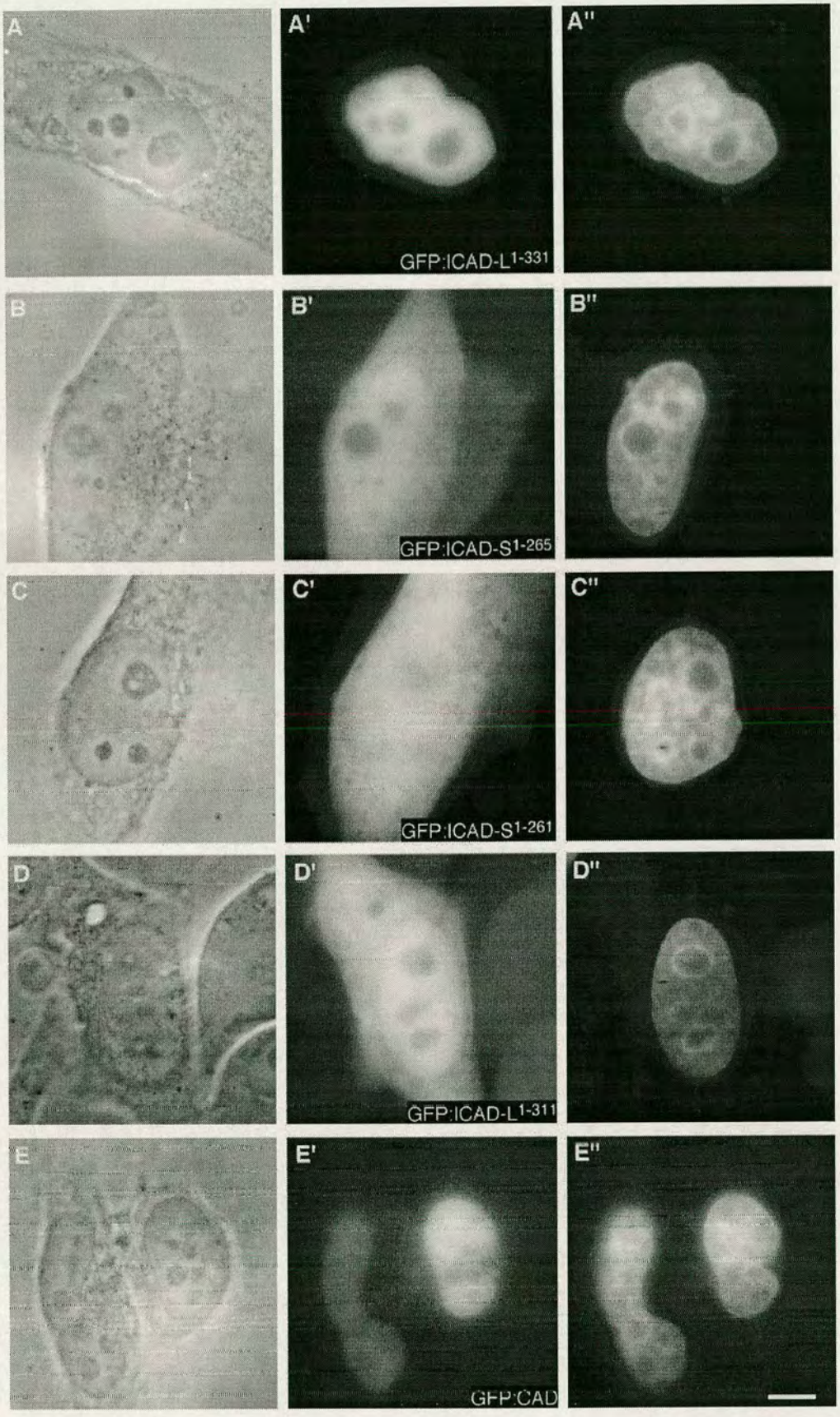
A
A'
A''
GFP:ICAD-L1-331
B
B'
B''
GFP:ICAD-S1-265
C
C'
C''
GFP:ICAD-S1-261
D
D'
D''
GFP:ICAD-L1-311
E
E'
E''
GFP:CAD

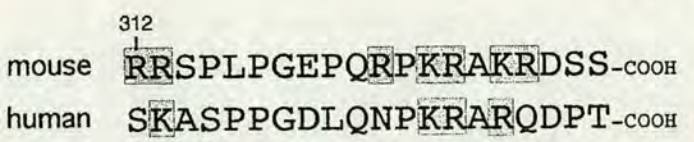

FIG. 2. A possible bipartite NLS in the C-terminal 20 amino acid residues of ICAD-L is conserved between mouse and human. Basic residues are shadowed.

not specify the cytoplasmic localization of this protein. It therefore seemed much more likely that the C-terminal region of ICAD-L contains a nuclear localization signal.

Identification of a Nuclear Localization Signal at the C-Terminus of ICAD-L

The nuclear localization of ICAD-L/DFF45 could be explained by the protein having its own nuclear localization signal or by an interaction with other proteins, such as CAD/CPAN/DFF40. We suspected that the nuclear localization of ICAD-L was unlikely to be due to the protein being transported into the nucleus in a complex with a carrier protein, such as CAD, since the GFP:ICAD-L protein was detected almost solely in the nucleus, even in cells in which the transfected protein was highly overexpressed.

Previous descriptions of the sequence of ICAD-L/DFF45 have not described a putative nuclear localization signal within the molecule. Nonetheless, upon examination of the ICAD-L deduced amino acid sequence, we noticed a cluster of basic residues in the C-terminal 20 amino acids that might possibly function as a bipartite nuclear localization signal (Fig. 2) [21]. To test the possibility that this region functions as a nuclear localization sequence, we constructed a fusion protein between GFP and ICAD-L from which these 20 amino acids had been removed (GFP:ICAD-$L^{1\text{-}311}$). Following transient transfection, GFP:ICAD-$L^{1\text{-}311}$ was localized diffusely throughout the cell, thus confirming that this region of ICAD-L is essential for the nuclear localization of the protein (Fig. 1, Panels D). It is worth noting that these 20 amino acids do not include the region which has been proposed to be necessary for interaction between ICAD and CAD [19, 22].

To confirm that the C-terminal 20 amino acids of ICAD-L possess autonomous NLS function, we constructed a vector encoding a fusion between GFP and this 20-amino-acid-peptide (GFP:ICAD-$L^{312\text{-}331}$). In control experiments, GFP on its own did not target to the nucleus (Fig. 3, panels B). However, following transient transfection, GFP:ICAD-$L^{312\text{-}331}$ was predominantly nuclear (Fig. 3, panels A). This result strongly supports the hypothesis that ICAD-L localizes in the nucleus due to the action of a C-terminal nuclear localization signal.

CAD Is also a Nuclear Protein

It has been proposed that CAD/CPAN/DFF40 exists as a 1 to 1 complex with ICAD-L/DFF45 in healthy cells [5, 11], although it has not proven possible to detect significant complexes between CAD and ICAD-S/DFF35 in cells [18]. Furthermore, it has been claimed that CAD contains a nuclear localization signal near its C-terminus (CAD: amino acid residues 331–345) [5]. To confirm the localization of CAD within cells, we constructed a plasmid encoding a GFP:CAD fusion protein. Following transient transfection, this fusion protein was detected almost solely in the nucleus of human epithelial and chicken hepatoma cells (Fig. 1, panels E). To exclude the possibility that the nuclear localization of GFP:CAD was due to its overexpression and failure to form a complex with ICAD, we also cotransfected HeLa cells with plasmids expressing GFP:CAD plus HA-tagged ICAD-L. Both proteins were highly concentrated in the nucleus of human epithelial cells (data not shown). In addition, endogenous CAD was detected in the nuclear fraction following subcellular fractionation and immunoblotting (K.S. and S. Kandels-Lewis, preliminary observations).

The CAD:ICAD-L Complex Is Stored within Nuclei

These data reveal that both CAD and its inhibitory chaperone ICAD-L possess autonomous nuclear localization sequences. This is consistent with prior observations both from ourselves [15] and from others [7] indicating that both CAD and ICAD-L are stored in the nucleus of healthy cells. It has previously been shown using a model for the induction of apoptosis by Fas/CD95 that nuclear transport of proteins is essential for cells to enter apoptotic execution [4]. Our results suggest that activated CAD is unlikely to be the key factor that must translocate into the nucleus.

The nature of the translocating factor is unknown. Likely candidates include apoptosis inducing factor

FIG. 1. The C-terminal 20 amino acids (aa) of ICAD-L are required for localization of the protein in cell nuclei. *Aequoria victoria* green fluorescent protein (GFP) was fused in flame to murine ICAD-L, ICAD-S, and CAD and expressed by transient transfection in human (HeLa) cells. (Panels A) The expressed GFP:ICAD-$L^{1\text{-}331}$ (full length ICAD-L) was solely observed in nuclei. In contrast, GFP:ICAD-$S^{1\text{-}265}$ (full length ICAD-S) (panels B), GFP:ICAD-$S^{1\text{-}261}$ (panels C), and GFP:ICAD-$L^{1\text{-}311}$ (panels D) were all found to be distributed throughout the cell in both nucleus and cytoplasm. (Panels E) GFP:CAD was highly concentrated in nuclei. Panels A–E, phase contrast; Panels A′–E′, detection of GFP fluorescence; Panels A″–E″, DAPI fluorescence of cellular DNA. The bar shows 10 micrometers.

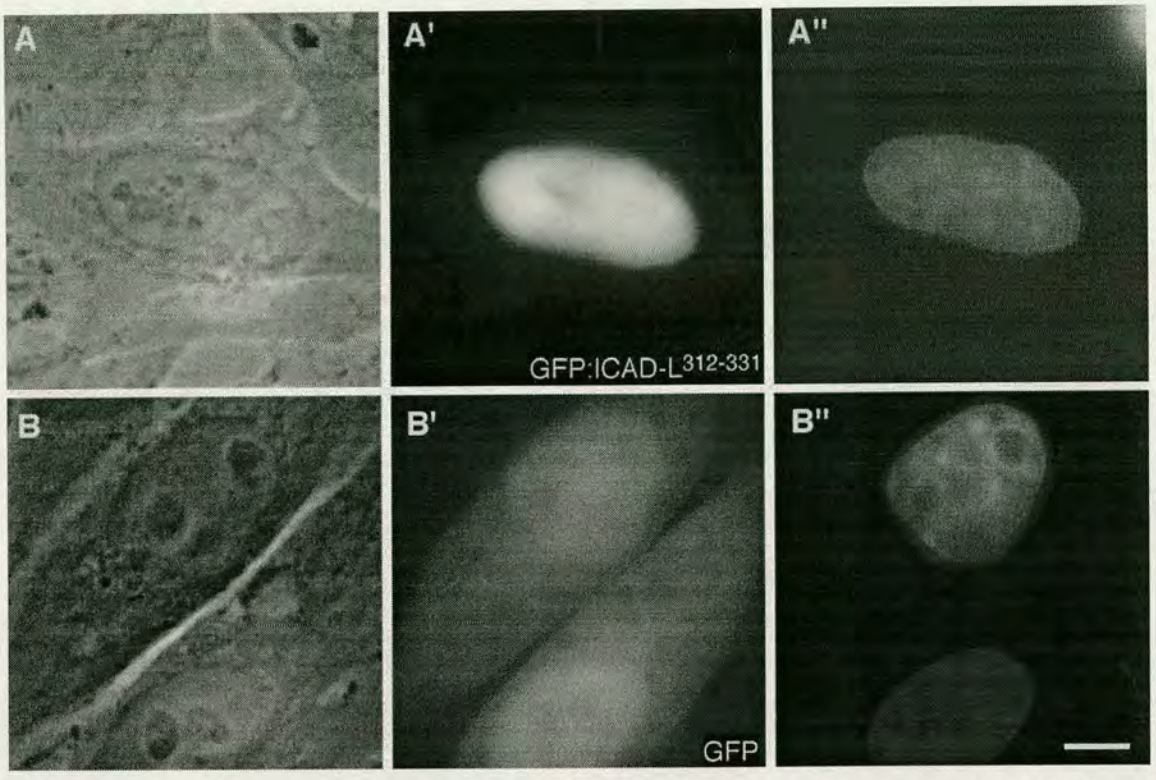

FIG. 3. The C-terminal 20 aa of ICAD-L functions as an autonomous nuclear localization sequence capable of targeting GFP to the cell nucleus. *Aequoria victoria* green fluorescent protein (GFP) was fused in flame to a peptide comprising the C-terminal 20 amino acids from murine ICAD-L and expressed by transient transfection in HeLa cells. (Panels A) The expressed GFP:ICAD-$L^{312-331}$ was highly concentrated in nuclei. (Panels B) GFP expressed on its own is distributed throughout the cell in both nucleus and cytoplasm. Panels A and B, phase contrast; Panels A′ and B′, detection of GFP fluorescence; Panels A″ and B″, DAPI fluorescence of cellular DNA. The bar shows 10 micrometers.

AIF [23], Acinus [9], and in view of the results described here, activated caspase-3 and possibly caspase-7, since these enzymes appear to be responsible for the activation of CAD in cells [24–29]. The intracellular localization and translocation of caspases during apoptosis is still under investigation; however, we previously detected an activity comigrating with activated caspase-3 in the nucleus by activity labeling and two-dimensional gel analysis [30]. It has recently been reported that, following cleavage of procaspase-3, which exists primarily in the cytoplasm and mitochondria [31, 32], active caspase-3 is found in the nuclear, mitochondrial, and cytosolic fractions [17, 33]. In contrast, caspase-7 shifts quantitatively from the cytosol to the microsomal fraction following activation [17].

What Is the Role of ICAD-S?

The levels of expression of ICAD-L/DFF-45 and ICAD-S/DFF35 are similar at least in mouse WR19L and human Jurkat T lymphoma cells [18]. It has been suggested that ICAD-S might function as a safety device for preventing the mistaken activation of CAD in healthy cells [19]. Promoter analysis of the murine ICAD and CAD genes suggests that expression of these genes is regulated by different mechanisms [34]. Alternative splicing of the ICAD pre-mRNA could serve as a mechanism for regulating the level of ICAD-L in response to the expression level of functional CAD. Changes in the efficiency of alternative splicing of the ICAD pre-mRNA would alter the ratio of ICAD-L to ICAD-S without necessitating changes in the transcription of the gene.

Although ICAD-S/DFF35 cannot act as a folding chaperone to enable the synthesis of functional CAD/CPAN/DFF40, *in vitro* it can bind to active CAD/DFF40 and inhibit its nuclease activity [18, 19]. This is because amino acid residues 101–180 of DFF35/45 mediate the binding to DFF40, whereas residues 23–100 are implicated in the inhibition of the nuclease *in vitro* [19]. Despite the fact that ICAD-S can inhibit CAD in cells [12, 19], ICAD-S exists primarily in free form *in vivo* [18]. Our data suggest that this may be because much of ICAD-S is cytoplasmic, whereas CAD is nuclear. Whether ICAD-S has a distinct cytoplasmic function in addition to interaction with CAD is not currently known. A preliminary yeast two-hybrid study

suggested an association of ICAD with cytoskeletal components (K.S. unpublished data), possibly indicative of unknown functions for ICAD in the cytoplasm, either during apoptosis or in healthy cells.

CONCLUSIONS

Cells contain two forms of ICAD, ICAD-L and ICAD-S, which differ at their C-termini (ICAD-S replaces the C-terminal 70 residues of ICAD-L with a stretch of 4 different residues). Because the region of ICAD-L that is missing from ICAD-S is precisely the region containing the NLS, these two splice forms occupy very different cellular locations. ICAD-S is found in both the nucleus and the cytoplasm, whereas ICAD-L is almost exclusively nuclear. Interestingly, these two forms of ICAD are functionally distinct [18, 19]. Whether ICAD-S has a distinct function in the cytoplasm is not currently known, and it is not known whether the cytoplasmic pool of ICAD-S is associated with CAD. All in all, current results are consistent with models in which the primary location of CAD in growing cells is nuclear, making it unlikely that regulation of CAD entry into the nucleus is a critical factor in the control of the onset of apoptotic execution.

REFERENCES

1. Liu, X., Kim, C. N., Yang, J., Jemmerson, R., and Wang, X. (1996) Induction of apoptotic program in cell-free extracts: Requirement for dATP and cytochrome C. *Cell* **86,** 147–157.
2. Susin, S. A., Zamzami, N., Castedo, M., Hirsch, T., Marchetti, P., Macho, A., Daugas, E., Geuskens, M., and Kroemer, G. (1996) Bcl-2 inhibits the mitochondrial release of an apoptogenic protease. *J. Exp. Med.* **184,** 1331–1342.
3. Susin, S. A., Lorenzo, H. K., Zamzami, N., Marzo, I., Brenner, C., Larochette, N., Prevost, M. C., Alzari, P. M., and Kroemer, G. (1999) Mitochondrial release of caspase-2 and -9 during the apoptotic process. *J. Exp. Med.* **189,** 381–394.
4. Yasuhara, N., Eguchi, Y., Tachibana, T., Imamoto, N., Yoneda, Y., and Tsujimoto, Y. (1997) Essential role of active nuclear transport in apoptosis. *Genes Cells* **2,** 55–64.
5. Enari, M., Sakahira, H., Yokoyama, H., Okawa, K., Iwamatsu, A., and Nagata, S. (1998) A caspase-activated DNase that degrades DNA during apoptosis, and its inhibitor ICAD. *Nature* **391,** 43–50.
6. Halenbeck, R., MacDonald, H., Roulston, A., Chen, T. T., Conroy, L., and Williams, L. T. (1998) CPAN, a human nuclease regulated by the caspase-sensitive inhibitor DFF-45. *Curr. Biol.* **8,** 537–540.
7. Liu, X., Li, P., Widlak, P., Zou, H., Luo, X., Garrard, W. T., and Wang, X. (1998) The 40-kDa subunit of DNA fragmentation factor induces DNA fragmentation and chromatin condensation during apoptosis. *Proc. Natl. Acad. Sci. USA* **95,** 8461–8466.
8. Mukae, N., Enari, M., Sakahira, H., Fukuda, Y., Inazawa, J., Toh, H., and Nagata, S. (1998) Molecular cloning and characterization of human caspase-activated DNase. *Proc. Natl. Acad. Sci. USA* **95,** 9123–9128.
9. Sahara, S., Aoto, M., Eguchi, Y., Imamoto, N., Yoneda, Y., and Tsujimoto, Y. (1999) Acinus is a caspase-3-activated protein required for apoptotic chromatin condensation. *Nature* **401,** 168–173.
10. Zhang, J., Liu, X., Scherer, D. C., van Kaer, L., Wang, X., and Xu, M. (1998) Resistance to DNA fragmentation and chromatin condensation in mice lacking the DNA fragmentation factor 45. *Proc. Natl. Acad. Sci. USA* **95,** 12480–12485.
11. Liu, X., Zou, H., Slaughter, C., and Wang, X. (1997) DFF, a heterodimeric protein that functions downstream of caspase-3 to trigger DNA fragmentation during apoptosis. *Cell* **89,** 175–184.
12. Sakahira, H., Enari, M., and Nagata, S. (1998) Cleavage of CAD inhibitor in CAD activation and DNA degradation during apoptosis. *Nature* **391,** 96–99.
13. McIlroy, D., Sakahira, H., Talanian, R. V., and Nagata, S. (1999) Involvement of caspase 3-activated DNase in internucleosomal DNA cleavage induced by diverse apoptotic stimuli. *Oncogene* **18,** 4401–4408.
14. Zhang, C., Raghupathi, R., Saatman, K. E., LaPlaca, M. C., and McIntosh, T. K. (1999) Regional and temporal alterations in DNA fragmentation factor (DFF)-like proteins following experimental brain trauma in the rat. *J. Neurochem.* **73,** 1650–1659.
15. Samejima, K., and Earnshaw, W. C. (1998) ICAD/DFF regulator of apoptotic nuclease is nuclear. *Exp. Cell Res.* **243,** 453–459.
16. Sabol, S. L., Li, R., Lee, T. Y., and Abdul-Khalek, R. (1998) Inhibition of apoptosis-associated DNA fragmentation activity in nonapoptotic cells: The role of DNA fragmentation factor-45 (DFF45/ICAD). *Biochem. Biophys. Res. Commun.* **253,** 151–158.
17. Zhivotovsky, B., Samali, A., Gahm, A., and Orrenius, S. (1999) Caspases: Their intracellular localization and translocation during apoptosis. *Cell Death Differ.* **6,** 644–651.
18. Sakahira, H., Enari, M., and Nagata, S. (1999) Functional differences of two forms of the inhibitor of caspase-activated DNase, ICAD-L, and ICAD-S. *J. Biol. Chem.* **274,** 15740–15744.
19. Gu, J., Dong, R. P., Zhang, C., McLaughlin, D. F., Wu, M. X., and Schlossman, S. F. (1999) Functional interaction of DFF35 and DFF45 with caspase-activated DNA fragmentation nuclease DFF40. *J. Biol. Chem.* **274,** 20759–20762.
20. Mackay, A. M., Eckley, D. M., Chue, C., and Earnshaw, W. C. (1993) Molecular analysis of the INCENPs (Inner Centromere Proteins): Separate domains are required for association with microtubules during interphase and with the central spindle during anaphase. *J. Cell Biol.* **123,** 373–385.
21. Robbins, J., Dilworth, S. M., Laskey, R. A., and Dingwall, C. (1991) Two interdependent basic domains in nucleoplasmin nuclear targeting sequence: Identification of a class of bipartite nuclear targeting sequence. *Cell* **64,** 615–623.
22. Inohara, N., Koseki, T., Chen, S., Benedict, M. A., and Nunez, G. (1999) Identification of regulatory and catalytic domains in the apoptosis nuclease DFF40/CAD. *J. Biol. Chem.* **274,** 270–274.
23. Susin, S. A., Lorenzo, H. K., Zamzami, N., Marzo, I., Snow, B. E., Brothers, G. M., Mangion, J., Jacotot, E., Constantini, P., Loeffler, M., Larochette, N., Goodlett, D. R., Aebersold, R., Siderovski, D. P., Penninger, J. M., and Kroemer, G. (1999) Molecular characterisation of mitochondrial apoptosis-inducing factor (AIF). *Nature* **397,** 441–446.
24. Zheng, T. S., Schlosser, S. F., Dao, T., Hingorani, R., Crispe, I. N., Boyer, J. L., and Flavell, R. A. (1998). Caspase-3 controls both cytoplasmic and nuclear events associated with Fas-mediated apoptosis in vivo. *Proc. Natl. Acad. Sci. USA* **95,** 13618–13623.

25. Tang, D., and Kidd, V. J. (1998) Cleavage of DFF-45/ICAD by multiple caspases is essential for its function during apoptosis. *J. Biol. Chem.* **273,** 28549–28552.

26. Jänicke, R. U., Ng, P., Sprengart, M. L., and Porter, A. G. (1998) Caspase-3 is required for alpha-fodrin cleavage but dispensable for cleavage of other death substrates in apoptosis. *J. Biol. Chem.* **273,** 15540–15545.

27. Mitamura, S., Ikawa, H., Mizuno, N., Kaziro, Y., and Itoh, H. (1998) Cytosolic nuclease activated by caspase-3 and inhibited by DFF-45. *Biochem. Biophys. Res. Commun.* **243,** 480–484.

28. Liu, X., Zou, H., Widlak, P., Garrard, W., and Wang, X. (1999) Activation of the apoptotic endonuclease DFF40 (caspase-activated DNase or nuclease): Oligomerization and direct interaction with histone H1. *J. Biol. Chem.* **274,** 13836–13840.

29. Wolf, B. B., Schuler, M., Echeverri, F., and Green, D. R. (1999) Caspase-3 is the primary activator of apoptotic DNA fragmentation via DNA fragmentation factor-45/Inhibitor of caspase-activated DNase inactivation. *J. Biol. Chem.* **274,** 30651–30656.

30. Martins, L. M., Mesner, P. W., Kottke, T. J., Basi, G. S., Sinha, S., Tung, J. S., Svingen, P. A., Madden, B. J., Takahashi, A., McCormick, D. J., Earnshaw, W. C., and Kaufmann, S. H. (1997) Comparison of caspase activation and subcellular localization in HL-60 and K562 cells undergoing etoposide-induced apoptosis. *Blood* **90,** 4283–4296.

31. Mancini, M., Nicholson, D. W., Roy, S., Thornberry, N. A., Peterson, E. P., Casciola-Rosen, L. A., and Rosen, A. (1998) The caspase-3 precursor has a cytosolic and mitochondrial distribution: Implications for apoptotic signaling. *J. Cell Biol.* **140,** 1485–1495.

32. Samali, A., Zhivotovsky, B., Jones, D. P., and Orrenius, S. (1998) Detection of pro-caspase-3 in cytosol and mitochondria of various tissues. *FEBS Lett.* **431,** 167–169.

33. Chandler, J. M., Cohen, G. M., and MacFarlane, M. (1998) Different subcellular distribution of caspase-3 and caspase-7 following Fas-induced apoptosis in mouse liver. *J. Biol. Chem.* **273,** 10815–10818.

34. Kawane, K., Fukuyama, H., Adachi, M. H. S., Copeland, N. G., Gilbert, D. J., Jenkin, N. A., and Nagata, S. (1999) Structure and promoter analysis of murine CAD and ICAD genes. *Cell Death Differ.* **6,** 745–752.

Received November 22, 1999

DNA topoisomerase IIα interacts with CAD nuclease and is involved in chromatin condensation during apoptotic execution

Françoise Durrieu*†, Kumiko Samejima*†, John M. Fortune‡, Stefanie Kandels-Lewis*, Neil Osheroff‡ and William C. Earnshaw*

Apoptotic execution is characterized by dramatic changes in nuclear structure accompanied by cleavage of nuclear proteins by caspases (reviewed in [1]). Cell-free extracts have proved useful for the identification and functional characterization of activities involved in apoptotic execution [2–4] and for the identification of proteins cleaved by caspases [5]. More recent studies have suggested that nuclear disassembly is driven largely by factors activated downstream of caspases [6]. One such factor, the caspase-activated DNase, CAD/CPAN/DFF40 [4,7,8] (CAD) can induce apoptotic chromatin condensation in isolated HeLa cell nuclei in the absence of other cytosolic factors [6,8]. As chromatin condensation occurs even when CAD activity is inhibited, however, CAD cannot be the sole morphogenetic factor triggered by caspases [6]. Here we show that DNA topoisomerase IIα (Topo IIα), which is essential for both condensation and segregation of daughter chromosomes in mitosis [9], also functions during apoptotic execution. Simultaneous inhibition of Topo IIα and caspases completely abolishes apoptotic chromatin condensation. In addition, we show that CAD binds to Topo IIα, and that their association enhances the decatenation activity of Topo IIα *in vitro*.

Addresses: *Institute of Cell and Molecular Biology, University of Edinburgh, Edinburgh EH9 3JR, UK. ‡Department of Biochemistry, Vanderbilt University School of Medicine, Nashville, Tennessee 37232-0146, USA.

†These authors contributed equally to this manuscript.

Correspondence: William C. Earnshaw
E-mail: bill.earnshaw@ed.ac.uk

Received: **15 May 2000**
Revised: **7 June 2000**
Accepted: **7 June 2000**

Published: **21 July 2000**

Current Biology 2000, 10:923–926

0960-9822/00/$ – see front matter

Results and discussion

HeLa nuclei incubated in E/X extracts underwent chromatin condensation in two stages: condensation against the nuclear rim was followed by the formation of discrete apoptotic bodies (Figure 1b). The rim-condensation also occurred when caspase activity was inhibited with the peptide–fluoromethylketone inhibitor DEVD–fmk (Figure 1c) [6]. A similar phenotype was observed when nuclei were preincubated with the highly specific Topo II inhibitors ICRF-159, ICRF-187 or etoposide (VP16) for 30 minutes before addition of E/X extracts (Figure 1d–f). Simultaneous inhibition of caspase and Topo II activity completely abolished apoptotic chromatin condensation (Figure 1d′–f′). This was not simply a kinetic effect, as nuclei retained this normal appearance for at least 6 hours at 37°C (data not shown). This inhibition of apoptotic chromatin condensation was unlikely to arise from global changes in the accessibility of chromatin to condensation factors, as simultaneous inhibition of caspases and Topo IIα had no effect on the ability of CAD nuclease to cleave nuclear DNA into an oligonucleosomal ladder (Figure 2e). These experiments provide the first evidence that Topo IIα has a role in chromatin condensation during apoptosis.

The abolition of apoptotic chromatin condensation following simultaneous inhibition of Topo IIα and caspases was seen with three different Topo II inhibitors, suggesting that the effect is due to the action of the drugs on Topo IIα. In a further control, apoptotic chromatin condensation was restored when highly purified human Topo IIα [10] (Figure 2d) was added to nuclei in E/X extract in the presence of Topo II and caspase inhibitors (Figure 1d″–f″). This rescue was abrogated when the purified Topo IIα was pretreated with monospecific anti-Topo IIα antibodies (Figure 2b, and data not shown). Topo IIα alone had no effect on the morphology of nuclei in buffer after 2 hours (Figure 2a). Finally, simultaneous inhibition of Topo I and caspases had no effect on chromatin condensation induced by E/X extracts (Figure 2c). These controls strongly support the conclusion that both Topo IIα and caspases act in pathways that promote apoptotic chromatin condensation. The rescue by purified Topo IIα in the presence of inhibitors raises the possibility that Topo IIα could be functioning in a non-enzymatic role, either as a structural or targeting factor, as has been proposed for its role in mitotic chromosome condensation [11].

Simultaneous inhibition of caspases and CAD (by addition of the CAD-inhibitory chaperone ICAD-L) also blocked chromatin condensation in E/X extracts (Figure 1h). This confirmed our previous results suggesting that CAD and caspases act in parallel pathways of apoptotic chromatin condensation [6]. Surprisingly, inhibition of chromatin condensation could be reversed upon addition of purified human Topo IIα (Figure 1i), suggesting that Topo IIα

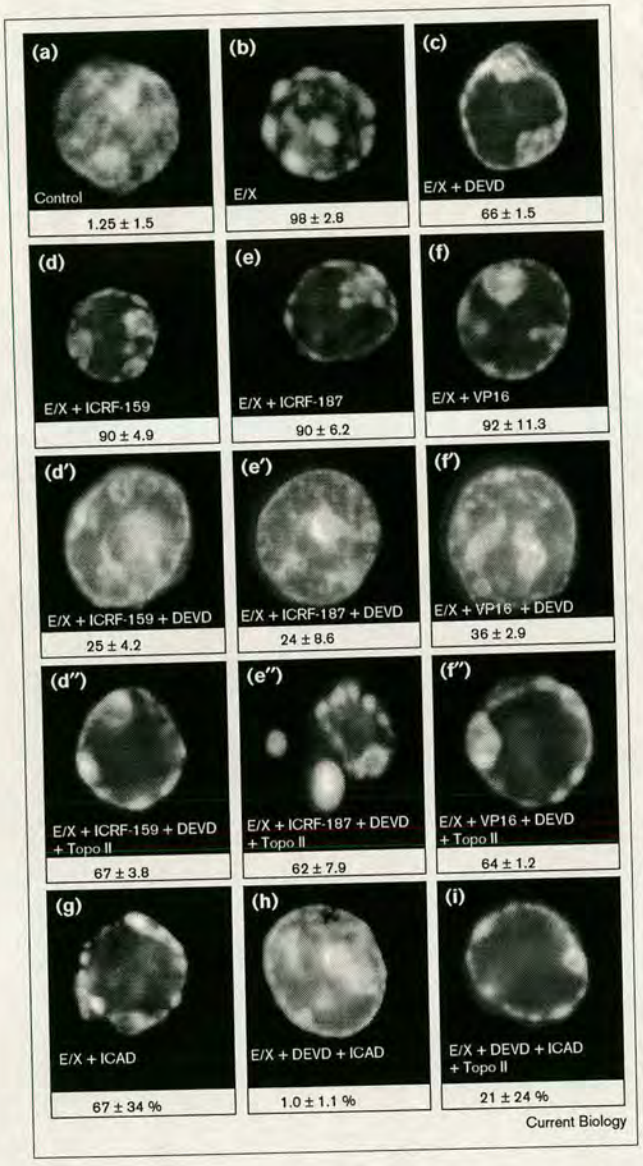

Figure 1

Topo IIα is required for apoptotic chromatin condensation in the absence of caspase activity. Isolated HeLa cell nuclei were preincubated with **(a–c)** diluent alone or with **(d)** 50 μg/ml ICRF-159, **(e)** 50 μg/ml ICRF-187 or **(f)** 100 μM etoposide (VP16). The nuclei were then added to (a) buffer or (b–f) apoptotic E/X extract [6] and incubated for 2 h at 37°C. (d–f) Inhibition of Topo IIα alone only partly inhibited apoptotic chromatin condensation. **(d'–f')** Inhibition of Topo IIα plus caspases (with 100 μM DEVD–fmk) abolished chromatin condensation. **(d"–f")** This block was reversed if 1 μg (2.9 pM) purified human Topo IIα was added at the start of the 37°C incubation. **(g)** Inhibition of CAD with 160 ng of the uncleavable mutant DM-ICAD-L does not block apoptotic chromatin condensation. **(h)** Simultaneous inhibition of CAD plus caspases blocks morphological apoptosis. **(i)** Added Topo IIα (1.5 μg) rescues apoptotic morphology after inhibition of CAD plus caspases. The percentage of apoptotic cells scored in the microscope is indicated below each micrograph.

acts downstream of CAD or promotes condensation in a pathway parallel to the CAD pathway. It was also possible, however, that the added Topo IIα might interfere with the interaction between CAD and the exogenous ICAD added in these reactions as a CAD inhibitor.

Physical and functional interactions between Topo IIα and CAD were readily detected both *in vitro* and in cell extracts. Purified Topo IIα bound quantitatively to GST–CAD on glutathione–sepharose, but not to GST alone, GST–ICAD-L, GST–BubR1, GST–AIRK2, or GST–β tubulin (data not shown), or sepharose alone (Figure 3a). As a control, purified poly(ADP-ribose) polymerase (PARP) added to the mix did not bind to any protein (Figure 3a). Similar Topo IIα binding was also observed with Intein–CAD (data not shown).

To confirm that Topo IIα can bind CAD in cell extracts, we made stable sublines of chicken MSB-1 cells expressing green fluorescent protein (GFP) fused to histidine (His) and haemagglutinin (HA) tags (His–HA–GFP) or very low levels of His–HA–CAD. The expressed CAD was immunoprecipitated from lysates using anti-HA antibody. These immunoprecipitates reproducibly contained Topo IIα, which was not seen in immunoprecipitates of the much more highly expressed control protein, His–HA–GFP (Figure 3b). This shows that CAD can interact with Topo IIα in cell extracts. It is not surprising that only a fraction of Topo IIα was bound to CAD, as Topo IIα is abundant in MSB-1 cells, and is presumably present in vast excess over CAD.

The interaction between Topo IIα and CAD appears to be functionally significant. In a quantitative assay for DNA decatenation, purified GST–CAD, either on its own or as a complex with His–ICAD-L, stimulated the decatenation activity of Topo IIα two to threefold, whereas buffer, GST or GST–ICAD-L had no effect (Figure 3c). Under these conditions CAD is enzymatically inactive, and does not interfere with the Topo II assay (which measures the release of intact minicircles from kinetoplast networks, see Supplementary material). In other experiments, we could not detect an effect of Topo IIα inhibition or addition on CAD activity against nuclear chromatin (Figure 2e, and data not shown).

It is widely accepted that Topo IIα is nuclear [9], and that CAD must be nuclear during apoptotic execution [4]. The localization of CAD in non-apoptotic cells has, however, been more controversial. DFF [3], and then CAD/ICAD [4] were first identified in cytoplasmic extracts. The first evidence that the CAD/ICAD complex might be nuclear was the observation that exogenous ICAD expressed in a variety of cell types was nuclear [6,8]. Also, our subcellular fractionation experiments confirmed that endogenous ICAD is predominantly nuclear [6]. Consistent with this,

we have identified an autonomous nuclear localization sequence at the carboxyl terminus of ICAD-L [12]. Here we address the localization of the CAD nuclease itself.

GFP–CAD is exclusively nuclear when expressed at low to moderate levels in cultured cells (Figure 4a, panel 2; see also [12]), and is distributed throughout the nucleus in a micropunctate pattern that largely follows the DNA distribution. Endogenous Topo IIα is similarly distributed in interphase cell nuclei (Figure 4a, panel 3), and in a merged image (Figure 4a, panel 4), the CAD and Topo IIα signals superimpose as a yellow signal distributed throughout the nucleus. To confirm the nuclear localization of endogenous CAD, we used a rabbit antiserum to cloned murine CAD in subcellular fractionation experiments (Figure 4b). A substantial portion of the CAD is revealed in the nuclear fraction. Although it is possible that some CAD is normally resident in the cytoplasm, our results show that much of this protein is nuclear, and would therefore be available to interact with Topo IIα.

Our results are consistent with models in which CAD and Topo IIα act in independent pathways in E/X extracts, but both are modulated by caspases. Several other proteins that appear to induce apoptotic chromatin condensation in nuclei have been identified. These include the mitochondrial flavoprotein AIF (apoptosis-inducing factor) [13], L-DNase II [14] and Acinus [15]. The experiments reported here suggest that, in the absence of caspases, none of these activities is sufficient to induce apoptotic chromatin condensation unless either CAD or Topo IIα is also present and functional.

Figure 2

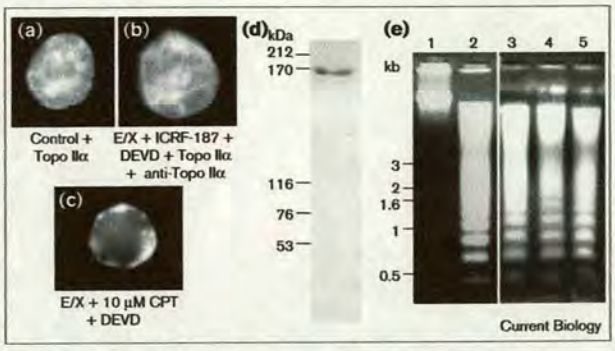

Control experiments for the involvement of Topo IIα in apoptotic chromatin condensation. **(a)** Purified human Topo IIα (1 μg is 2.9 pM) did not induce chromatin condensation in nuclei in buffer. **(b)** Purified human Topo IIα immunoadsorbed with the anti-Topo IIα antibody Ki-S1 does not reverse the block to apoptotic chromatin condensation imposed by simultaneous inhibition of Topo IIα and caspases. **(c)** Inhibition of caspases and Topo I (with 10 μM camptothecin (CPT)) had no effect on apoptotic chromatin condensation beyond that seen when caspases alone were inhibited. **(d)** Protein purity was verified by SDS–PAGE of the Topo IIα preparation in a 10% gel and silver stained. **(e)** Inhibition of Topo IIα plus caspases did not affect the digestion of chromosomal DNA by CAD. Nuclei (5×10^5 per loading) were incubated for 2 h in (1) buffer, (2) E/X extract, (3) E/X extract plus DEVD–fmk plus ICRF-159, (4) ICRF-187, or (5) etoposide. Nuclear DNA was isolated and electrophoresed in a 1% gel containing 0.5 mg/ml ethidium bromide.

Figure 3

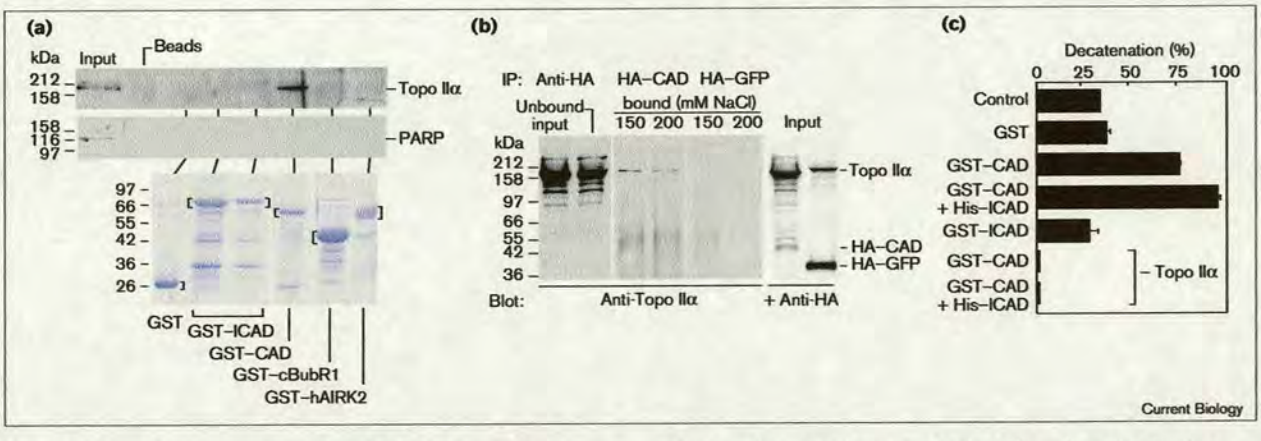

Functional interaction between Topo IIα and CAD *in vivo* and *in vitro*. **(a)** Human Topo IIα binds *in vitro* to GST–CAD, but not to GST, GST–ICAD-L, GST–cBubR1 or GST–hAIRK2. PARP tested as a control does not bind (see Supplementary material). The Coomassie Blue-stained gel shows the relative amount of each protein on the beads. **(b)** A subfraction of endogenous Topo IIα associates with tagged CAD *in vivo*. HA-tagged proteins were immunoprecipitated from stable transfectants expressing His–HA–CAD or His–HA–GFP and subjected to SDS–PAGE. Left, blot with anti-Topo IIα showing the input and unbound fractions (equivalent to 8×10^5 cells), and the fractions bound to the beads (5×10^6 cells for His–HA–CAD and 1×10^6 cells for His–HA–GFP). Right, blot with anti-HA showing the input and unbound fractions (equivalent to 8×10^5 cells for His–HA–CAD and 1.6×10^5 cells for His–HA–GFP). We estimate that His–HA–GFP is expressed roughly 25–100-fold more abundantly than His–HA–CAD in these cells. **(c)** GST–CAD stimulates Topo IIα activity measured using a kinetoplast minicircle decatenation assay (see Supplementary material). The error bars represent SEM for two independent assays.

Figure 4

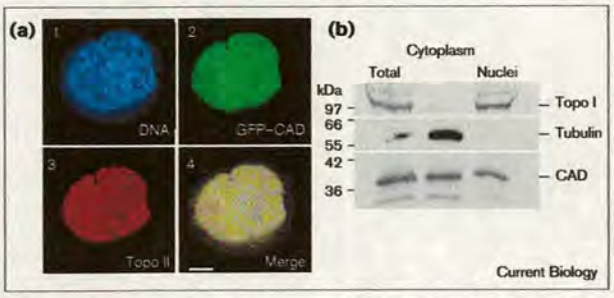

(a) Topo IIα and GFP–CAD co-localize in healthy cell nuclei. Chicken DU249 cells were transfected with constructs expressing GFP–CAD and stained for endogenous Topo IIα. The two proteins were distributed in the nucleus in an overlapping micropunctate pattern. A single deconvolved optical section is shown. The scale bar represents 5 μm. **(b)** A significant portion of endogenous CAD is nuclear. HeLa S3 cells were fractionated into nucleus and cytoplasm [6] and immunoblotted with rabbit anti-mouse CAD, mouse anti-tubulin, and human autoantibody against Topo I.

Although a role for Topo IIα in apoptotic execution has been controversial [16,17], its involvement in generating high-molecular-weight DNA fragments following oxidative stress has recently been demonstrated [18]. In addition, Topo IIα has been shown to stimulate the activity of CAD against a naked DNA substrate approximately eight-fold, although the cleavage of chromatin was essentially unaffected [19]. The direct interaction between Topo IIα and CAD we show here might result in targeting of CAD to sites occupied by Topo IIα at the base of chromosomal loop domains. At those sites, CAD might initially stimulate Topo IIα activity and then subsequently, upon cleavage of ICAD-L by caspases, it might commence the wholesale digestion of DNA characteristic of apoptosis, possibly being further stimulated by interactions with Topo IIα. Our results predict that CAD cleavage might initiate at or near Topo IIα-binding sites.

Supplementary material

Supplementary material, including a full description of the methods with references, is available at http://current-biology.com/supmat/supmatin.htm.

Acknowledgements

We thank A. Imondi for ICRF-159 and -187, S. Nagata for the CAD and ICAD-L cDNAs, S. Kaufmann for the anti-Topo IIα antibody and purified PARP, and J. Brown for the anti-HA antibody. We thank Sally Wheatley-Dempsey for advice in reorganising the manuscript, and R. Adams, M. Carmena, I. Davis, S. Ruchaud, and P. Villa for comments. This work was supported by the Wellcome Trust (WCE), NIH grant CA69008 to Scott Kaufmann and W.C.E. and NIH grant GM33944 to N.O. W.C.E. is a Principal Research Fellow of the Wellcome Trust.

References

1. Earnshaw WC, Martins LM, Kaufmann SH: **Mammalian caspases: structure, activation, substrates and functions during apoptosis.** *Annu Rev Biochem* 1999, **68**:383-424.
2. Lazebnik YA, Cole S, Cooke CA, Nelson WG, Earnshaw WC: **Nuclear events of apoptosis *in vitro* in cell-free mitotic extracts: a model system for analysis of the active phase of apoptosis.** *J Cell Biol* 1993, **123**:7-22.
3. Liu X, Zou H, Slaughter C, Wang X: **DFF, a heterodimeric protein that functions downstream of caspase-3 to trigger DNA fragmentation during apoptosis.** *Cell* 1997, **89**:175-184.
4. Enari M, Sakahira H, Yokoyama H, Okawa K, Iwamatsu A, Nagata S: **A caspase-activated DNase that degrades DNA during apoptosis, and its inhibitor ICAD.** *Nature* 1998, **391**:43-50.
5. Lazebnik YA, Kaufmann SH, Desnoyers S, Poirier GG, Earnshaw WC: **Cleavage of poly(ADP-ribose) polymerase by a protease with properties like ICE.** *Nature* 1994, **371**:346-347.
6. Samejima K, Ton S, Kottke TJ, Enari M, Sakahira H, Cooke CA, *et al.*: **Transition from caspase-dependent to caspase-independent mechanisms at the onset of apoptotic execution.** *J Cell Biol* 1998, **143**:225-239.
7. Halenbeck R, MacDonald H, Roulston A, Chen TT, Conroy L, Williams LT: **CPAN, a human nuclease regulated by the caspase-sensitive inhibitor DFF-45.** *Curr Biol* 1998, **8**:537-540.
8. Liu X, Li P, Widlak P, Zou H, Luo X, Garrard WT, *et al.*: **The 40 kDa subunit of DNA fragmentation factor induces DNA fragmentation and chromatin condensation during apoptosis.** *Proc Natl Acad Sci USA* 1998, **95**:8461-8466.
9. Wang JC: **DNA topoisomerases.** *Annu Rev Biochem* 1996, **65**:635-692.
10. Kingma PS, Greider CA, Osheroff N: **Spontaneous DNA lesions poison human topoisomerase IIα and stimulate cleavage proximal to leukemic 11q23 chromosomal breakpoints.** *Biochemistry* 1997, **36**:5934-5939.
11. Adachi Y, Luke M, Laemmli UK: **Chromosome assembly *in vitro*: topoisomerase II is required for condensation.** *Cell* 1991, **64**:137-148.
12. Samejima K, Earnshaw WC: **Differential localisation of ICAD-L and ICAD-S in cells due to removal of a C-terminal NLS from ICAD-L by alternative splicing.** *Exp Cell Res* 2000, **255**:314-320.
13. Susin SA, Lorenzo HK, Zamzami N, Marzo I, Snow BE, Brothers GM, *et al.*: **Molecular characterisation of mitochondrial apoptosis-inducing factor (AIF).** *Nature* 1999, **397**:441-446.
14. Torriglia A, Perani P, Brossas JY, Chaudun E, Treton J, Courtois Y, *et al.*: **L-DNase II, a molecule that links proteases and endonucleases in apoptosis, derives from the ubiquitous serpin leukocyte elastase inhibitor.** *Mol Cell Biol* 1998, **18**:3612-3619.
15. Sahara S, Aoto M, Eguchi Y, Imamoto N, Yoneda Y, Tsujimoto Y: **Acinus is a caspase-3-activated protein required for apoptotic chromatin condensation.** *Nature* 1999, **401**:168-173.
16. Lagarkova MA, Iarovaia OV, Razin SV: **Large-scale fragmentation of mammalian DNA in the course of apoptosis proceeds via excision of chromosomal DNA loops and their oligomers.** *J Biol Chem* 1995, **270**:20239-20241.
17. Beere HM, Chresta CM, Hickman JA: **Selective inhibition of topoisomerase II by ICRF-193 does not support a role for topoisomerase II activity in the fragmentation of chromatin during apoptosis of human leukemia cells.** *Mol Pharmacol* 1996, **49**:842-851.
18. Li TK, Chen AY, Yu C, Mao Y, Wang H, Liu LF: **Activation of topoisomerase II-mediated excision of chromosomal DNA loops during oxidative stress.** *Genes Dev* 1999, **13**:1553-1560.
19. Widlak P, Li P, Wang X, Garrard WT: **Cleavage preferences of the apoptotic endonuclease DFF40 (caspase-activated DNase or nuclease) on naked DNA and chromatin substrates.** *J Biol Chem* 2000, **275**:8226-8232.
20. Hoffmann A, Heck MMS, Bordwell BJ, Rothfield NF, Earnshaw WC: **Human autoantibody to topoisomerase II.** *Exp Cell Res* 1989, **180**:409-418.

Supplementary material

DNA topoisomerase IIα interacts with CAD nuclease and is involved in chromatin condensation during apoptotic execution

Françoise Durrieu, Kumiko Samejima, John M. Fortune, Stefanie Kandels-Lewis, Neil Osheroff and William C. Earnshaw

Current Biology 21 July 2000, **10**:923–926

Figure S1

The kinetoplast minicircle decatenation assay. **(a)** Experiment. All samples contained: 5 nM kinetoplast-DNA, 1 mM ATP and 10 nM Topo II (except where indicated) in 50 mM Tris pH 7.9, 100 mM KCl, 10 mM $MgCl_2$, 0.5 mM NaEDTA pH 8.0, 2.5% glycerol. The positions of the kinetoplast network (substrate), released minicircles (Topo II reaction product) and linear DNA (product of cleavage by CAD) are indicated. Less than 3% of the kinetoplast DNA minicircles are cleaved. Because decatenation is determined by quantifying released DNA minicircles (and not by disappearance of the kinetoplast DNA substrate), any CAD-mediated DNA cleavage would deplete the Topo II decatenation substrate and thus decrease (not increase) observed levels of decatenation. **(b)** Controls. This experiment is the same as in (a), except that Topo II was omitted from all GST, GST–CAD, GST–CAD/His–ICAD, and GST–ICAD samples. That is, the only sample that contained Topo II is that labelled Topo II.

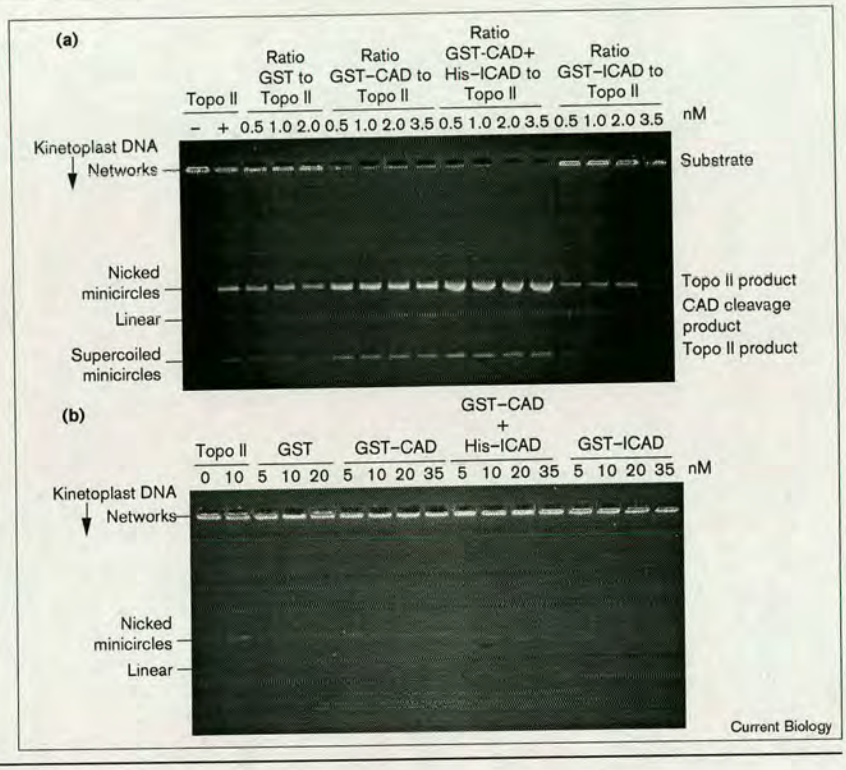

Supplementary materials and methods

Preparation of apoptotic extracts and in vitro *apoptosis reaction*

Apoptotic (E/X) extracts [S1] were prepared from chicken DU249 cells treated for 12 h with 0.5 μM staurosporine (Sigma). Cells were washed in KPM buffer (50 mM PIPES-KOH pH 7.0, 50 mM KCl, 10 mM EGTA, 2 mM $MgCl_2$, 20 mM cytochalasin B (Sigma), 1 mM DTT, 0.1 mM PMSF, 1 μg/ml each of chymostatin, leupeptin, antipain, pepstatin A) [S2], subjected to several cycles of freezing and thawing and further disrupted by mild sonication. The cell lysate was then centrifuged at 139,000*g* for 2 h, yielding clear cytosolic extracts with a protein concentration of 20–30 mg/ml (measured by the Bradford assay [3]).

HeLa nuclei (10^6 per incubation) were preincubated for 30 min at 37°C with either the Topo IIα inhibitors ICRF-159, ICRF-187 (50 μg/ml, both gifts of A. Imondi, Pharmacia) or etoposide (VP-16, 100 μM, Sigma), or the Topo I inhibitor camptothecin (0.1, 1 or 10 μM, Calbiochem), or diluent. For CAD inhibition, E/X extracts were preincubated with ICAD-L or CAD buffer (10 mM HEPES pH 7.4, 50 mM NaCl, 5 mM EGTA, 2 mM $MgCl_2$, 1 mM DTT) for 15 min at 37°C. For caspase inhibition, E/X extracts were preincubated with DEVD–fmk (100 μM, Calbiochem) or diluent for 15 min at 37°C. Nuclei were then added (up to 10^6 nuclei per 20 μl of extract) and incubated at 37°C for up to 6 h in the presence of an ATP regeneration system [S2]. In certain experiments, 1 or 1.5 μg of purified human Topo IIα expressed in *Saccharomyces cerevisiae* [S4,S5] was added to the incubation. This corresponds to 2.9 pmol dimer, a ~3× physiological level of 1.7×10^6 molecules per nucleus [S6]. Nuclei were subsequently stained with DAPI to observe chromatin condensation, solubilized in SDS–sample buffer for protein analysis, or lysed for analysis of DNA ladder formation.

Construction of clones

For construction of intein–ICAD, mouse full-length ICAD-L [S7] (gift of S. Nagata, Osaka) was cloned into the *Nco*I/*Sma*I cloning sites of pTYB4 (New England BioLabs Inc.). *GST–CAD* was prepared by cloning full-length murine CAD into the pGEX 4T-1 (Pharmacia Biotech) *Eco*RI and *Xho*I cloning site. To make the plasmid encoding the GST–CAD His_6-tagged ICAD combination (GST–CAD/His–ICAD), His–ICAD in pRSETB [S1] was obtained by PCR with primer (5′-TGAGACGTC-TAATACGACTCAC-3′) and primer (5′-GTCGACGTCAGCAAAAAAC-CCC-3′) and cloned into the *Aat*II site of pGEX 4T-1 containing GST–CAD. To make the Zeo–His–HA vector, first a His tag was constructed by ligation of oligonucleotides (5′-CTAGCATGCATCATCATCATCATCAC-CGCGGA-3′) and (5′-AGCTTCCGCGGTGATGATGATGATGATG-CATG-3′). The resulting fragment was ligated into vector pZeoSV2+ (Invitrogen) that had been digested with *Nhe*I and *Hin*dIII. The HA tag in

pBluescript KS (Stratagene) was digested with *Sac*II and blunt-ended with T4 DNA polymerase plus 100 μM dNTPs, and digested with *Eco*R I. The resulting fragment was ligated into vector pZeo–His that had been digested with *Kpn*I and blunt-ended with T4 DNA polymerase plus 100 μM dNTPs, and digested with *Eco*R I. To make Zeo–His–HA–CAD and Zeo–His–HA–GFP, the CAD ORF was obtained by PCR from a plasmid containing the full-length CAD cDNA (gift of S. Nagata), cloned into pBluescript KS (Stratagene) and digested with *Eco*RI and *Xho*I. GFP was obtained by PCR using primer T7 and primer (5′-CCGCTCGAGTACTTGTACAGC-3′) from an enhanced GFP–lamin A in pCDNA 3 (gift of Larry M. Karnitz, Mayo Research Foundation), then digested with *Eco*RI and *Xho*I. The resulting fragments were ligated into vector Zeo–His–HA that had been digested with *Eco*RI and *Xho*I.

Expression and purification of GST–ICAD, GST–CAD, GST–CAD/His–ICAD and GST

Plasmids encoding the glutathione-*S*-transferase (GST) fusion proteins GST–ICAD, GST–CAD, GST–CAD/His–ICAD, GST–BubR1, GST–hAIRK2 and GST alone transformed into *E. coli* BL21(DE3)Lys S cells were grown to $OD_{600} = 0.5–0.7$, and protein expression was induced with isopropylthiogalactoside (IPTG; 0.3–0.5 mM) for 3–5 h. Cells were collected by centrifugation at 5000*g* for 10 min and frozen at −80°C.

GST–CAD/His–ICAD was first purified with 0.5 ml Ni–agarose (Qiagen) as described previously for the purification of His_6–ICAD purification [S1]. Protein eluted from the column was diluted 20-fold into GST wash buffer (PBS, 5 mM EDTA, 5 mM DTT, 1% Triton X-100), and then purified a second time over glutathione–sepharose as described below.

Pellets of *E. coli* expressing GST–ICAD, GST–CAD or GST were thawed on ice and resuspended in lysis buffer (PBS, 5 mM EDTA, 5 mM DTT) with lysozyme (final concentration 1 mg/ml) and incubated on ice for 30 min. After sonication, Triton X-100 was added to 1% and the lysate was centrifuged at 4000*g* for 20 min. The supernatant was mixed with glutathione–sepharose 4B (Pharmacia Biotech) which had been equilibrated with PBS and incubated on a rotating mixer for 1 h at 4°C. The sepharose beads were washed in batch three times with wash buffer. GST–ICAD and GST were eluted with elution buffer 1 (10 mM glutathione, 50 mM Tris-HCl pH 8.0). GST–CAD, and GST–CAD/His–ICAD were eluted with elution buffer 2 (20 mM glutathione, 100 mM Tris-HCl pH 8.0, 120 mM NaCl). The eluted proteins were dialysed for at least 3 h against two changes of CAD buffer (10 mM HEPES pH 7.4, 50 mM NaCl, 5 mM EGTA, 2 mM $MgCl_2$, 1 mM DTT), aliquoted, and frozen in liquid nitrogen.

Expression and purification of intein–ICAD

Intein–ICAD encoded by pTYB4/ICAD-L was expressed in *E. coli* ER2566 and purified using the IMPACT™ T7 system (New England BioLabs Inc.) following the manufacturer's instructions. Intein–ICAD bound to chitin beads was left at 4°C overnight in cleavage buffer (20 mM Tris-HCl pH 8.0, 50 mM NaCl, 0.1 mM EDTA, 30 mM DTT). The protein was eluted with cleavage buffer without DTT. The eluted protein was dialysed for at least 3 h against two changes of CAD buffer (10 mM HEPES pH 7.4, 50 mM NaCl, 5 mM EGTA, 2 mM $MgCl_2$, 1 mM DTT) aliquoted and frozen in liquid nitrogen.

Binding of Topo IIα to GST fusion proteins in vitro

Purified Topo IIα (125 ng) and 53.3 ng purified PARP (in PBS + 5 mM DTT, 10 mM EDTA, 1% Triton X-100) was incubated with glutathione–sepharose beads either alone, or with bound GST, GST–ICAD-L, GST–CAD, GST–cBubR1 or GST–hAIRK2. The bound fraction was resolved by SDS–PAGE (10% gel), and Topo IIα was detected by immunoblotting with monoclonal antibody Ki-S1. PARP was detected by immunoblotting with monoclonal antibody C2-10.

Immunoprecipitation of HA-tagged CAD and GFP from stable cell lines

Stable lines of MSB-1 chicken lymphoblastoid cells expressing His–HA–CAD and His–HA–GFP were obtained by electroporation with Zeo–His–HA–CAD and Zeo–His–HA–GFP (310 V 975 μF (BioRad Gene-Pulser with 0.4 mm cuvettes), selected with 400 μg/ml Zeosin (Invitrogen) and confirmed by immunoblotting with anti-HA tag antibody. For immunoprecipitation, cells were harvested, washed twice with PBS/EDTA and lysed by sonication in IPP150 (10 mM Tris pH 8.0, 150 mM NaCl, 0.1% NP-40), and insoluble material removed by centrifugation for 5 min at 8161*g* at 4°C. HA-conjugated proteins were immunoadsorbed using monoclonal antibody 12CA5 preloaded onto Affi-Prep Protein A Support beads (BioRad). After incubation for 1 h at 4°C the beads were washed three times for 5 min with 25 bed volumes of either IPP150, IPP200 (200 mM NaCl) or IPP300 (300 mM NaCl). Bound proteins were subjected to SDS–PAGE in 10% Prosieve 50 Acrylamide gels (FMC), transferred to Hybond C nitrocellulose (Amersham), and detected by enhanced chemiluminescence. Topo IIα was detected with Rabbit G [S8] diluted 1:1000. HA–CAD was detected with mouse monoclonal 12CA5 diluted 1:1000.

Kinetoplast minicircle decatenation assay

Kinetoplast DNA (0.3 μg) was incubated with 10 nM purified human Topo IIα plus 10 nM GST–CAD, GST–ICAD, GST–CAD + GST–ICAD, or GST alone for 10 min at 37°C [S9]. The reaction was stopped by addition of DNA loading buffer, heated at 65°C for 10 min, loaded onto a 1% agarose gel containing 0.5 mg/ml ethidium bromide and run at 90 V for 2 h (Figure S1), and the minicircles released by decatenation were quantified. No detectable intact minicircles were released in incubations with GST–CAD or GST–CAD + His–ICAD-L in the absence of Topo IIα. Under these conditions, the GST–CAD is catalytically inactive and does not interfere with the assay.

Supplementary references

S1. Samejima K, Toné S, Kottke TJ, Enari M, Sakahira H, Cooke CA, *et al.*: **Transition from caspase-dependent to caspase-independent mechanisms at the onset of apoptotic execution.** *J Cell Biol* 1998, **143:**225-239.

S2. Lazebnik YA, Cole S, Cooke CA, Nelson WG, Earnshaw WC: **Nuclear events of apoptosis *in vitro* in cell-free mitotic extracts: a model system for analysis of the active phase of apoptosis.** *J Cell Biol* 1993, **123:**7-22.

S3. Bradford MM: **A rapid and sensitive method for the quantitation of microgram quantities of protein utilizing the principle of protein-dye binding.** *Anal Biochem* 1976, **72:**248-254.

S4. Kingma PS, Greider CA, Osheroff N: **Spontaneous DNA lesions poison human topoisomerase IIα and stimulate cleavage proximal to leukemic 11q23 chromosomal breakpoints.** *Biochemistry* 1997, **36:**5934-5939.

S5. Wasserman RA, Austin CA, Fisher LM, Wang JC: **Use of yeast in the study of anticancer drugs targeting DNA topoisomerases: expression of a functional recombinant human DNA topoisomerase II alpha in yeast.** *Cancer Res* 1993, **53:**3591-3596.

S6. Heck MMS, Earnshaw WC: **Topoisomerase II: a specific marker for proliferating cells.** *J Cell Biol* 1986, **103:**2569-2581.

S7. Sakahira H, Enari M, Nagata S: **Cleavage of CAD inhibitor in CAD activation and DNA degradation during apoptosis.** *Nature* 1998, **391:**96-99.

S8. Hoffmann A, Heck MMS, Bordwell BJ, Rothfield NF, Earnshaw WC: **Human autoantibody to topoisomerase II.** *Exp Cell Res* 1989, **180:**409-418.

S9. Miller KG, Liu LF, Englund PT: **A homogeneous type II DNA topoisomerase from HeLa cell nuclei.** *J Biol Chem* 1981, **256:**9334-9339.